ERDC/CHL TR-06-7

US Army Corps of Engineers ®
Engineer Research and Development Center

Coastal Inlets Research Program

Matagorda Ship Channel, Texas: Jetty Stability Study

Nicholas C. Kraus, Lihwa Lin,
Brian K. Batten, and Gary L. Brown

August 2006

Coastal and Hydraulics Laboratory

Coastal Inlets Research Program

ERDC/CHL TR-06-7
August 2006

Matagorda Ship Channel, Texas: Jetty Stability Study

Nicholas C. Kraus, Lihwa Lin, Brian K. Batten, and Gary L. Brown

Coastal and Hydraulics Laboratory
U.S. Army Engineer Research and Development Center
3909 Halls Ferry Road
Vicksburg, MS 39180-6199

Final Report

Approved for public release; distribution is unlimited

Prepared for U.S. Army Engineer District, Galveston
2000 Fort Pint Road
Galveston, TX 77550

and U.S. Army Corps of Engineers
Washington, DC 20314-1000

ABSTRACT: The entrance of the Matagorda Ship Channel, connecting the Gulf of Mexico to Matagorda Bay, Texas, has experienced a strong currents since its construction in 1963-1964. Strong currents had been predicted in physical model experiments performed during design to determine the optimal location of the new inlet cut through Matagorda Peninsula and entrance configurations. The current has produced a large area of scour on the bay side of the inlet adjacent to the west jetty, and vessels encountering a strong along-channel and cross-channel current at the entrance experience difficulty in navigation. This study was performed to understand the hydrodynamics of the existing condition and evaluate alternatives for stabilizing the jetties to reduce the current velocity, thereby reducing the scour and improving navigation reliability. The interaction between the entrance and Pass Cavallo, the natural inlet to Matagorda Bay located southwest of the Matagorda Ship Channel entrance, was also examined in a regional approach. The study proceeded by review of the engineering and scientific literature, analysis of regional and local trends in the shoreline change at the entrance and at Pass Cavallo, field measurements of the water level and current, bathymetry surveys, and hydrodynamic numerical modeling of tidal circulation, including wind forcing and river discharges to the bay. Alternative configurations of the jetties were investigated with the hydrodynamic model. A frequency-of-occurrence methodology based on the current velocity magnitude was introduced to evaluate the alternatives. Possible changes in salinity were also investigated.

Contents

Conversion Factors, Non-SI to SI Units of Measurements xi

Preface xii

1—History and Status of Matagorda Ship Channel Entrance 1

Overview of Coastal Processes at Matagorda Bay 1
Morphology and sediment 3
Wind 5
Astronomical tide 6
Waves 6
Littoral drift 7
Tropical storms 7
History of Matagorda Ship Channel 9
Pass Cavallo 9
Matagorda Ship Channel design 13
Alternatives for Jetty Stability 20
Regional Processes 21
Report Contents 22

2—Shoreline Dynamics at Matagorda Ship Channel and Pass Cavallo 23

Introduction 23
Relative sea-level rise 23
Historical shoreline change 24
Shoreline Analysis Methods 26
Shoreline definition 26
Data sources 27
Aerial imagery 27
Shoreline digitizing 27
Shoreline change rate analysis 29
Shoreline Change at Matagorda Ship Channel 30
Gulf of Mexico shoreline 30
Matagorda Bay shoreline change 41
Pass Cavallo 51
Spit growth 51
Inlet width 54
Summary 56

3—Dredged Volume and Sediment Accumulation 58

Dredging Data and Analysis 58
Bathymetric Survey Data and Analysis 60
Summary 65

4—Hydrodynamics and Evaluation of Alternatives 66

Numerical Model of Flow 66
Boundary Conditions 68
Model Verification 69
Evaluation of Alternatives 77
Calculations with Pass Cavallo Closed 102
Summary 105

5—Discussion and Conclusions 107

Current Velocity and Jetty Stability 108
Regional Processes 109
Monitoring Recommendations 110

References 111

Appendix A: Aerial Photographs, Matagorda Ship Channel Entrance A1

Appendix B: Aerial Photographs, Pass Cavallo B1

Appendix C: Response of Salinity and Residence Time to MSC Alternatives .. C1

Purpose of Study C1
Background of Model C1
Numerical Model C2
Model Results C2
Mesh modifications and verification check C2
Model runs C3
Salinity C3
Residence Time C3
Conclusions C5

List of Figures

Figure 1. Location map for Matagorda Bay and federal coastal inlets 2

Figure 2. Detail map for Matagorda Bay and East Matagorda Bay 4

Figure 3. MSC and Pass Cavallo area, based on 1995 shoreline 10

Figure 4. Time evolution of tidal prisms at Pass Cavallo and MSC 12
Figure 5. Alternative routes tested 14
Figure 6. MSC entrance design 17
Figure 7. MSC entrance, September 2002 19
Figure 8. Sketch of jetty stability alternatives 21
Figure 9. Project area Gulf of Mexico shoreline change baseline 31
Figure 10. Shoreline position and change rate, 1963 to 1965 32
Figure 11. Shoreline position and change rate, 1965 to 1968 33
Figure 12. Shoreline position and change rate, 1968 to 1974 34
Figure 13. Shoreline position and change rate, 1974 to 1978 35
Figure 14. June 1974 and November 1978 aerial photographs of the Matagorda Peninsula spit 35
Figure 15. Shoreline position and change rate, 1978 to 1982 36
Figure 16. Shoreline position and change rate, 1982 to 1986 37
Figure 17. Shoreline position and change rate, 1986 to 1988 38
Figure 18. Shoreline position and change rate, 1988 to 1995 38
Figure 19. Shoreline position and change rate, 1995 to 2000 39
Figure 20. Shoreline position, end-point and linear regression change rates between 1963 and 2000 41
Figure 21. Baseline for Matagorda Bay shoreline change analysis 42
Figure 22. Shoreline position and change rate, 1956 to 1963 43
Figure 23. Dredged material placement, bay side of the MSC, October 1965 44
Figure 24. Shoreline position and change rate, 1963 to 1965 44
Figure 25. Shoreline position and change rate, 1965 to 1968 45
Figure 26. Shoreline position and change rate, 1968 to 1978 46
Figure 27. Shoreline position and change rate, 1978 to 1982 46
Figure 28. Shoreline position and change rate, 1982 to 1986 47
Figure 29. Shoreline position and change rate, 1986 to 1995 48
Figure 30. Shoreline position and change rate, 1995 to 2002 49
Figure 31. Long-term shoreline position and change rate, pre-MSC (1956) to 2002 50
Figure 32. Long-term shoreline position and change rate, 1963 (post-MSC) to 2002 51
Figure 33. Spit growth baselines for Matagorda Island and Matagorda Peninsula 52

Figure 34. Growth of Matagorda Peninsula, 1930 to 2001 53
Figure 35. Growth of Matagorda Island, 1956 to 2000 54
Figure 36. Inlet width at Pass Cavallo, 1856 to 2003 55
Figure 37. Map of stations for dredging records 59
Figure 38. Bottom topography map, March 2000 survey 61
Figure 39. Bottom topography map, September 2002 survey 62
Figure 40. Bottom topography map, November 2004 survey 62
Figure 41. Bathymetry change between March 2000 and September 2002 surveys 63
Figure 42. Bathymetry change between September 2002 and November 2004 surveys 64
Figure 43. Regional ADCIRC grid 67
Figure 44. Detail of circulation model grid at MSC 68
Figure 45. Location of CHL water level gauges and TCOON stations 69
Figure 46. Depth-averaged current vectors from ADCP measurements during the peak ebbing cycle of 17 November 2004 70
Figure 47. Vertical distributions of current speed on bay side of MSC entrance 71
Figure 48. Measured water levels, surface winds, and river discharges for model input boundary conditions 72
Figure 49. Calculated and measured water levels at Port Lavaca and Port O'Connor 73
Figure 50. Calculated and measured water levels at MSC-CM20, Palacios Harbor, and LCRDC 74
Figure 51. Calculated ebbing current field at 1600 GMT, 17 November 2004 75
Figure 52. Calculated and measured current vectors along three transects at bay entrance of bottleneck 76
Figure 53. Comparison of calculated and measured discharges 76
Figure 54. Ship channel geometry and bathymetry for existing and three alternative configurations 77
Figure 55. Model Cross Section A-A' for existing configuration and three alternatives 78
Figure 56. Wind information collected at EMATGC and PTOCON for January and 10 July to 10 August 2004 79
Figure 57. Water level measured at Bob Hall Pier for January and 10 July to 10 August 2004 80
Figure 58. River flow rates from Colorado River and San Bernard River for January and 10 July to 10 August 2004 80

Figure 59. Calculated maximum current speed during flood at 2100 GMT, 20 January 2004....82
Figure 60. Calculated maximum current speed during ebb at 1300 GMT, 22 January 2004....83
Figure 61. Calculated maximum current speed during flood at 0800 GMT, 30 July 2004....84
Figure 62. Calculated maximum current speed during ebb at 0200 GMT, 2 August 2004....85
Figure 63. Locations of comparison sta a to f....86
Figure 64. Estimated cross section of MSC entrance near gulfward end for Alt 3 based on assumed scour....89
Figure 65a. Maximum current speed along center of MSC entrance for existing condition and alternatives....90
Figure 65b. Maximum current speed along center of MSC entrance for existing condition and Alt 3a....90
Figure 66. Percent exceedance diagrams for sta a, b, and c for January 2004....91
Figure 67. Percent exceedance diagrams for sta d, e, and f for January 2004....92
Figure 68. Percent exceedance diagrams for sta a, b, and c for 12 July to 10 August 2004....93
Figure 69. Percent exceedance diagrams at sta d, e, and f for 12 July to 10 August 2004....94
Figure 70. Percent exceedance diagrams for sta a, b, and c for January 2004, comparing Alt 3 and Alt 3a with existing condition....95
Figure 71. Percent exceedance diagrams for sta d, e, and f for January 2004, comparing Alt 3 and Alt 3a with existing condition....96
Figure 72. Current magnitude percent occurrence pie charts for sta c for January 2004....97
Figure 73. Current magnitude percent occurrence pie charts for sta e for January 2004, comparing Alt 1, Alt 2, and Alt 3a with existing condition....98
Figure 74. Calculated maximum current speed during flood at 2100 GMT, 20 January, for Alt 2b....101
Figure A1. Matagorda Ship Channel Entrance, 4 October 1963....A1
Figure A2. Matagorda Ship Channel Entrance, 22 October 1965....A2
Figure A3. Matagorda Ship Channel Entrance, 17 January 1968....A2
Figure A4. Matagorda Ship Channel Entrance, 20 November 1974....A3
Figure A5. Matagorda Ship Channel Entrance, 30 November 1978....A3
Figure A6. Matagorda Ship Channel Entrance, 10 April 1984....A4

Figure A7. Matagorda Ship Channel Entrance, 17 October 1986 ..... A4
Figure A8. Matagorda Ship Channel Entrance, 24 August 1988..... A5
Figure A9. Matagorda Ship Channel Entrance, 1 March 1991..... A5
Figure A10. Matagorda Ship Channel Entrance, 20 February 1995..... A6
Figure A11. Matagorda Ship Channel Entrance, 26 September 2002 ..... A6
Figure A12. Matagorda Ship Channel Entrance, 7 August 2003..... A7
Figure B1. Pass Cavallo, Circa 1930 ..... B1
Figure B2. Pass Cavallo, 16 October 1943..... B2
Figure B3. Pass Cavallo, Circa 1953 ..... B2
Figure B4. Pass Cavallo, 18 September 1961..... B3
Figure B5. Pass Cavallo, 4 October 1963..... B3
Figure B6. Pass Cavallo, 22 October 1965..... B4
Figure B7. Pass Cavallo, 17 January 1968 ..... B4
Figure B8. Pass Cavallo, 20 November 1974..... B5
Figure B9. Pass Cavallo, 30 November 1978..... B5
Figure B10. Pass Cavallo, Circa 1982 ..... B6
Figure B11. Pass Cavallo, 10 April 1984 ..... B6
Figure B12. Pass Cavallo, 14 April 1985 ..... B7
Figure B13. Pass Cavallo, 17 October 1986..... B7
Figure B14. Pass Cavallo, 24 August 1988 ..... B8
Figure B15. Pass Cavallo, 20 February 1995 ..... B8
Figure B16. Pass Cavallo, 13 December 1999 ..... B9
Figure B17. Pass Cavallo, 26 September 2002..... B9
Figure B18. Pass Cavallo, 26 August 2003 ..... B10
Figure C1. Entire model mesh C6
Figure C2. Model mesh at the MSC entrance..... C6
Figure C3. Data collection stations for original Mouth of Colorado Study.... C7
Figure C4. Salinity verification check of rms error C8
Figure C5. Salinity verification check of index of agreement C8
Figure C6. Flood tide currents for existing configuration C9
Figure C7. Flood tide currents for Alt 1 ..... C9
Figure C8. Flood tide currents for Alt 2 ..... C10
Figure C9. Flood tide currents for Alt 3 ..... C10
Figure C10. Design year flows for Colorado River..... C11
Figure C11. Design year flows for LaVaca River C11

Figure C12. Design year flows for Tres Palacios River C12
Figure C13. Annual average salinity for existing configuration, low flow scenario C12
Figure C14. Annual average salinity difference for Alt 1, low flow scenario C13
Figure C15. Annual average salinity difference for Alt 2, low flow scenario C13
Figure C16. Annual average salinity difference for Alt 3, low flow scenario C14
Figure C17. Annual average salinity for existing configuration, medium flow scenario C14
Figure C18. Annual average salinity difference for Alt 1, medium flow scenario C15
Figure C19. Annual average salinity difference for Alt 2, medium flow scenario C15
Figure C20. Annual average salinity difference for Alt 3, medium flow scenario C16
Figure C21. Annual average salinity for existing configuration, high flow scenario C16
Figure C22. Annual average salinity difference for Alt 1, high flow scenario C17
Figure C23. Annual average salinity difference for Alt 2, high flow scenario C17
Figure C24. Annual average salinity difference for Alt 3, high flow scenario C18
Figure C25. Residence time found by average flux method C18
Figure C26. Residence time found by tracer method C19

List of Tables

Table 1. Tropical Storms at Northwest Gulf of Mexico, 1851 to 2004 8
Table 2. Definition of Alternatives 20
Table 3. Estimated Shoreline Recession Due to Sea-Level Rise, Matagorda Peninsula 24
Table 4. Shoreline Inventory 28
Table 5. Aerial Photograph Inventory for Pass Cavallo and MSC 29
Table 6. Selected Gulf of Mexico Shorelines 31

Table 7. Selected Matagorda Bay Shorelines 42
Table 8. Dredged Volumes at Matagorda Ship Channel 60
Table 9. Average Depth Change and Sediment Volume Accretion/Erosion ..65
Table 10. Water Surface Elevation Bias, RMS Error, and Percent Error, 20 November 2004 to 10 January 2005 74
Table 11. Bias and RMS Error of Flow Discharge During Peak Ebbing Cycle at MSC, 1500 – 2100 GMT, 17 November 2004 77
Table 12. Coordinates of Comparison Stations 86
Table 13. Maximum Flood Current Speed for January 2004, at 2100 GMT....86
Table 14. Maximum Ebb Current Speed for January 2004, at 1300 GMT....87
Table 15. Maximum Flood Current Speed for12 July to 10 August 2004, at 0800 GMT....87
Table 16. Maximum Ebb Current Speed for 12 July to 10 August 2004, at 0200 GMT....87
Table 17. Flood Current Speed at 20 Percent Exceedance, January 2004....99
Table 18. Ebb Current Speed at 20 Percent Exceedance, January 2004....99
Table 19. Flood Current Speed at 20 Percent Exceedance, 12 July to 10 August 2004....99
Table 20. Ebb Current Speed at 20 Percent Exceedance, 12 July to 10 August 2004....100
Table 21. Calculated Mean Discharge, January 2004....100
Table 22. Calculated Mean Discharge, 12 July to 10 August 2004....100
Table 23. Maximum Flood Current Speed for Existing Condition and Alts 3, 4, and 5 at 2100 GMT, 20 January 2004....103
Table 24. Maximum Ebb Current Speed for Existing Condition and Alts 3, 4, and 5 at 1300 GMT, 22 January 2004....103
Table 25. Maximum Flood Current Speed for Existing Condition and Alts 3, 4, and 5 at 0800 GMT, 30 July 2004....103
Table 26. Maximum Ebb Current Speed for Existing Condition and Alts 3, 4, and 5 at 2:00 GMT, 2 August 2004 104
Table 27. Calculated Mean Discharge for Existing Condition and Alts 3, 4, and 5, January 2004 104
Table 28. Calculated Mean Discharge for Existing Condition, Alts 3, 4, and 5, 12 July to 10 August 2004 104

Conversion Factors, Non-SI to SI Units of Measurement

Non-SI units of measurement used in this report can be converted to SI units as follows:

Multiply	By	To Obtain
acres	4,046.873	square meters
acre-feet	1,233.489	cubic meters
cubic feet	0.02831	cubic meters
cubic yards	0.7645549	cubic meters
feet	0.3048	meters
knots	0.5144444	meters per second
miles (U.S. nautical)	1.852	kilometers
miles (U.S. statute)	1.609347	kilometers
square feet	0.09290304	square meters
square miles	2.589988×10^{6}	square meters

Preface

This report documents a study performed to examine alternatives for jetty stability at the entrance to the Matagorda Ship Channel, which connects the Gulf of Mexico to Matagorda Bay, Calhoun County, Texas. The current through the jetties is frequently strong, raising concern about scour at the jetties and navigation reliability. The analysis of alternatives was performed for the U.S. Army Engineer District, Galveston (SWG) and is intended to provide quantitative information to reduce the strength of the current. The study was performed in the context of the acting regional coastal processes and responses.

This study was performed by the U.S. Army Engineer Research and Development Center (ERDC), Coastal and Hydraulics Laboratory (CHL). Mr. Volker E. Schmidt was the SWG study Project Manager. Ms. Joanne B. Williams was the SWG Planning lead, and Mr. Ishaq Syed was the SWG Hydrology and Hydraulics engineer. Assistance in previous related studies and the present study by Mr. Ronnie G. Barcak of SWG Operations Division is acknowledged. The main text and Appendices A and B of this report were written by Dr. Nicholas C. Kraus, Senior Scientists Group, CHL, and by Dr. Lihwa Lin and Dr. Brian K. Batten, Coastal Engineering Branch (CEB), Navigation Division (ND), CHL. Appendix C was written by Mr. Gary L. Brown, Estuarine Engineering Branch, ND. Ms. J. Holley Messing, CEB, completed final formatting of the report, and Mr. David Cate was the Information Technology Laboratory editor. Work was performed under the general administrative supervision of Dr. Rose M. Kress, Chief, ND; Dr. William D. Martin, Deputy Director, CHL; and Mr. Thomas W. Richardson, Director, CHL.

This hydrodynamics portion of this study concerned application of models and interface developed under the Coastal Inlets Research Program (CIRP) administered by Headquarters, U.S. Army Corps of Engineers (USACE). Dr. Sandra K. Knight and Mr. James E. Clausner, CHL, are the Technical Director and Associate Director, respectively, for the Navigation Systems Program. Dr. Kraus is the CIRP Program Manager. The mission of the CIRP is to conduct applied research to improve USACE capability to manage federally maintained inlets, which are present on all coasts of the United States, covering the Atlantic Ocean, Gulf of Mexico, Pacific Ocean, Great Lakes, and U.S. territories. CIRP objectives are to advance knowledge and provide quantitative predictive tools (a) to make management of coastal inlet navigation projects, principally the design, maintenance, and operation of channels and jetties, more effective to reduce the cost of dredging, and (b) to preserve the adjacent beaches in a systems approach that treats the inlet and beach together. To achieve these objectives, the CIRP is organized in work units conducting research and

development in hydrodynamic, sediment transport and morphology change modeling; navigation channels and adjacent beaches; inlet structures and scour; laboratory and field investigations; and technology transfer.

COL Richard B. Jenkins was Commander and Executive Director.
Dr. James R. Houston was Director of ERDC.

1 History and Status of Matagorda Ship Channel Entrance

This study was performed for the U.S. Army Engineer District, Galveston (hereafter, Galveston District) by the U.S. Army Engineer Research and Development Center, Coastal and Hydraulics Laboratory (CHL). The purpose of the study was to develop and evaluate alternatives for reducing the current velocity through the entrance of the Matagorda Ship Channel (MSC). The MSC carries approximately 5.7 million tons of commerce annually. Presently, the current velocity through the entrance exceeds 5 knots[1] on occasion and 3 knots commonly, causing scour in the bay near the south jetty and raising concern for navigation. The channel cross section of Pass Cavallo, the natural inlet and other main connection of Matagorda Bay to the Gulf of Mexico, is becoming smaller, and any further reduction will increase the current velocity through the MSC.

Overview of Coastal Processes at Matagorda Bay

This section gives the background of hydrodynamic and meteorological forcing at the site. The geomorphic setting, sediment grain size characteristics, and littoral processes are also reviewed. Long-term relative sea-level rise is discussed in Chapter 2.

Matagorda Bay is located on the north-central coast of Texas, and navigation through it is served by the deep-draft MSC as one of eight federally maintained inlets on the Texas Gulf of Mexico coast (Figure 1). Matagorda Bay, among the largest of seven major estuarine systems along the coast of Texas (Mathews and Mueller 1987), is located about 80 miles northeast of Corpus Christi and 125 miles southwest of Galveston. As shown in Figure 2, the MSC cuts through Matagorda Peninsula and is composed of deep-draft and shallow-draft navigation channels in Matagorda Bay that connect local ports to the Gulf of Mexico and the Gulf Intracoastal Waterway (GIWW). Major ports are Port O'Connor to the west, Port Lavaca and Point Comfort to the northwest in Lavaca Bay, and Port of

[1] This study involves analysis of historic and recent engineering documents with values expressed in American customary (non-SI) units. To maintain continuity with the existing body of work and to provide the most utility to engineering and navigation interests, the original units are retained in their context. Oceanographic measurements and calculations made as part of the present study are expressed in SI units if there is no connection with previous data and uses. A table of factors for converting non-SI units of measurement to SI units is presented on page xi.

Palacios on the north-central side of Matagorda Bay. The deep-draft channel of the MSC crosses Matagorda Bay for about 22 miles. The authorized dimensions of the MSC entrance channel through Matagorda Peninsula is 300 ft wide at the bottom, 38 ft deep at the entrance bar, and 36 ft deep through the jetties, referenced to the local Galveston District navigation datum mean low tide (mlt).

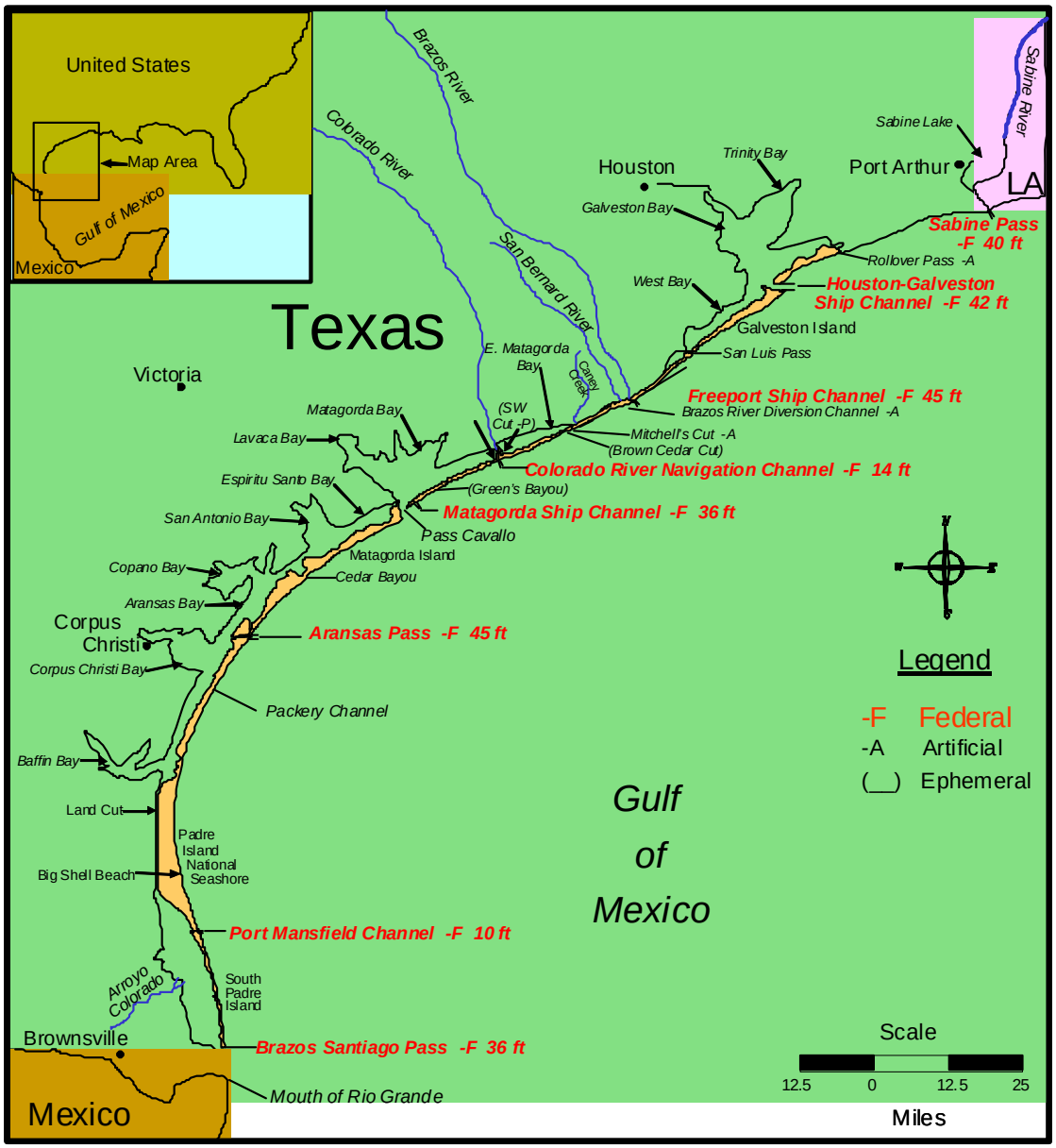

Figure 1. Location map for Matagorda Bay and federal coastal inlets

Matagorda Bay possesses five entrances that support either commercial or recreational navigation (Figure 2). These are (a) the GIWW, which connects to the locks at the Colorado River on the northeast side; (b) the Colorado River Diversion Channel, which enters on the northeast corner, accessible by very shallow-drafting recreational boats; (c) Port O'Conner, through which the GIWW traverses on the west side; (d) Pass Cavallo, a natural inlet in the southwest corner of the bay that is accessible by shallow-drafting recreational boats; and (e) the MSC, which is located about 3.4 miles northeast of Pass Cavallo. The GIWW is 125 ft wide across the bottom and 12 ft deep mlt, indicating that the channel cross sections at the ends of the bay are small compared to those of the two gulf inlets of Pass Cavallo and the MSC.

Matagorda Bay has a surface area of approximately 1.01×10^{10} sq ft, or 360 square miles. The bay receives water from the Colorado River through a diversion channel opened in March 1995 and from the Lavaca River. Although of substantial ecological significance, the freshwater discharge is typically less than 10 percent of the daily tidal exchange; therefore, an increase in bay volume by river flow is of minor importance in the control of the geomorphology of the two gulf entrances. Tidal prisms of Texas bays tend to be relatively large because of the large bay surface areas, despite having modest tidal range.

Morphology and sediment

Regional sediment budgets have identified three sources of sediments along Matagorda Peninsula: (a) erosion of the Brazos-Colorado Headland, (b) the Colorado River, and (c) relict offshore sediment (Paine and Morton 1989). The Brazos-Colorado headland supplies sediment by erosion from relict Holocene deposits and by new sediment transported down the Brazos and San Bernard Rivers. Mean annual discharge by the Colorado River is estimated at 1,776,684 acre-ft/year, producing 1,350 acre-ft/year in suspended load and approximately 300 acre-ft in bedload transport (Paine and Morton 1989). A large magnitude of sediment discharge from the Colorado River was observed in 1929, when removal of a log jam caused rapid progradation of the Colorado River delta across Matagorda Bay. Despite the progradation of the Colorado delta across Matagorda Peninsula and the large sediment loads, shorelines adjacent to the mouth of the Colorado River receded in the years following the opening of the river to the Gulf of Mexico. Morton (1977a) identifies riverine supply as a significant historical source of sediments but notes that natural decreases in sediment supply, reduction in peak discharge, and river basin development have reduced the sand supply to the coast.

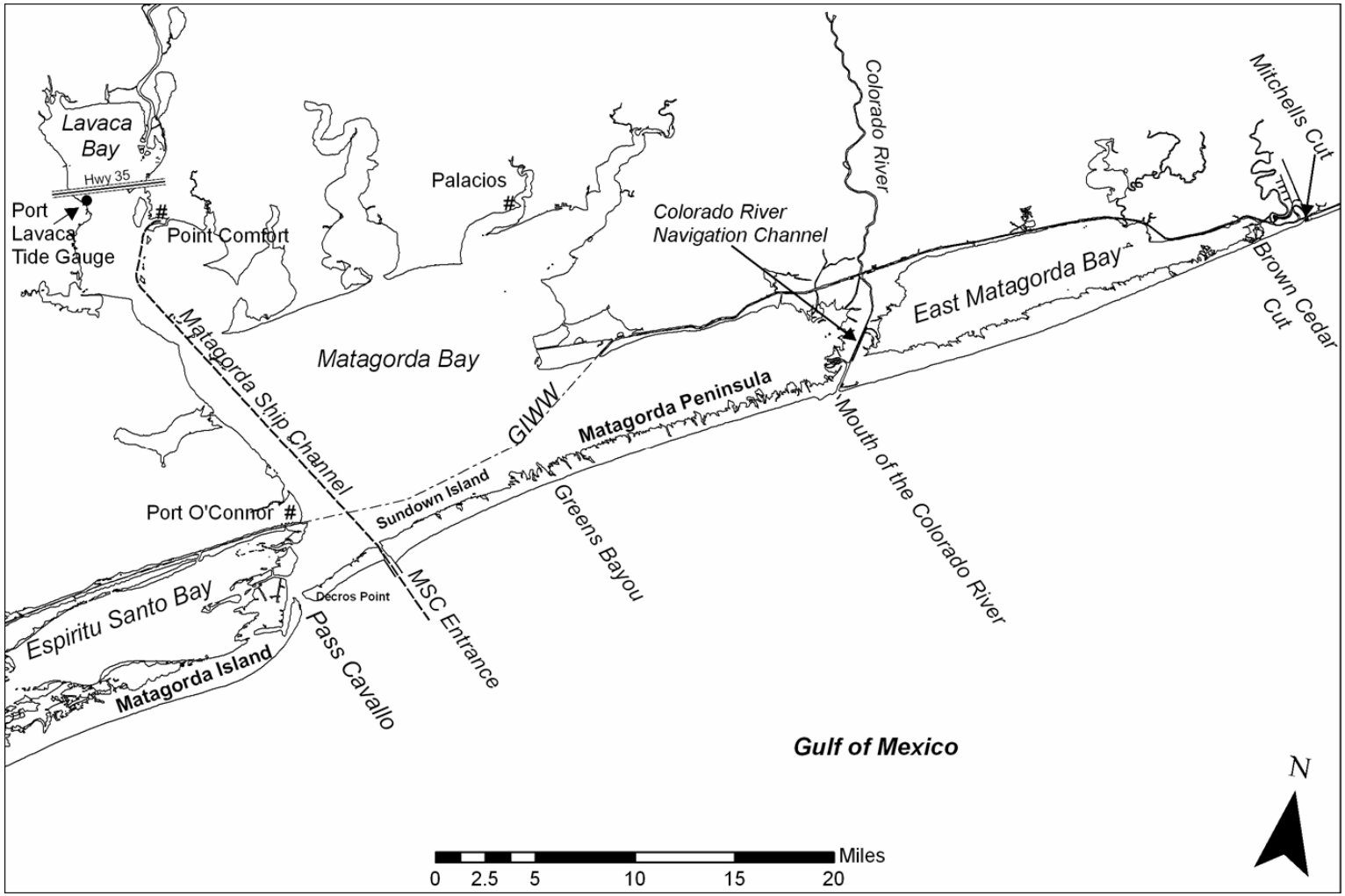

Figure 2. Detail map for Matagorda Bay and East Matagorda Bay

Offshore shelf sediments are considered to be the primary source for littoral material for the Matagorda Peninsula sediment budget (Morton et al. 1976). These sediments are composed of Pleistocene and early Holocene deltaic deposits. Landward transport of these deposits has been a historically significant source of material, although Morton (1977a) speculates that these sources have diminished as the inner shelf has equilibrated to present sea level.

Sediments within the study area are composed primarily of fine-grained sand, in addition to mixed sand, shell, and shell gravel associated with washover deposits (Gibeaut et al. 2000). The primary agents of morphologic change along the Texas coast are waves, wind, and storms. High waves generated by the frequent passage and landfall of tropical storms result in large-scale morphologic change to the coast (Morton et al. 1976, 2004; Paine and Morton 1989; Gibeaut et al. 2000). In general, the low relief of Matagorda Peninsula subjects the barrier to channelized washover, inundation, and breaching in response to tropical storms. Periods of strong northerly wind fronts generate erosive wave conditions for north- and west-facing (bay) shorelines (McGowen and Brewton 1975). Harwood (1973) discusses the long-term geomorphic background of the area. The fine sand along the Texas coast is easily transported by the strong wind there, creating dunes and also potentially contributing to inlet channel infilling (Kraus and Heilman 1997).

Extensive sediment samples and deep sediment cores were obtained in preparation for cutting of the MSC entrance (Galveston District 1962; Weiser and Armstrong 1963). Bay surface sediment samples taken from 2,000 to 14,000 ft from Matagorda Peninsula had a median grain size of 0.059 to 0.092 mm. On the Gulf of Mexico side, west of Pass Cavallo, the median grain size varied from 0.092 to 0.12 mm at 6-ft depth to finer sands in the range of 0.09 to 0.72 mm at various locations in 12- and 18-ft depths. In the fall of 1961, 24 deep borings were made in the area of the then-proposed jetties and channel. The entrance was subsequently moved slightly to the north. Foundation material for the jetties consisted of medium to very dense fine sand to a depth of about 60-65 ft below mlt. Thin seams of soft clay were encountered in some borings at depths varying from 20 to 40 ft below mlt. Medium-to-stiff red clay (of the Beaumont Clay formation of the Pleistocene age) is encountered below the sand (Galveston District 1962).

Wind

The water level and current in the shallow coastal bays and lagoons of Texas are frequently dominated by wind (meteorological tide dominating the astronomical tide). For this and other reasons, including recognition of the large seasonal variation in water level with respect to the tide range, the Galveston District established the navigation datum of mlt. This datum lies below mean lower low water and accounts for water set down by wind (Kraus et al. 1997). Strong wind mixes the water vertically, indicating that depth-averaged circulation models as applied in this study (Chapter 4) are applicable except where the water body might be sheltered. Strong wind can create steep, large waves in large bays such as Matagorda Bay, resuspending fine sediment and posing a hazard to small craft.

In warm climates, sea breeze can introduce substantial diurnal motion in water bodies (Kraus and Militello 2001). This situation is common along the coast of Texas, where the strong predominant southeast wind and sea breeze can dominate the tide in producing setup and setdown in its numerous shallow estuaries and bays (Collier and Hedgpeth 1950). Wind fronts from the north that pass through the area every 5 or 6 days from mid-September through May also cause significant setup and setdown across the bays. Kraus and Militello (1996, 1999) document along-axis oscillations in water level exceeding 0.6 m in response to periodic fronts passing East Matagorda Bay.

Wind direction is defined as the direction from which it blows. The annual wind rose for 1995 at East Matagorda Bay (where local wind records were available) shows that the wind is incident predominantly from the southeast and east-southeast (120 to 150 deg) and that strong winds (>9 m/sec) can also blow from the east-northeast and northeast (45 to 75 deg) and from the north and north-northwest (335 to 360 deg). Wind rarely blows from the west at the study site. For the shallow-water bays of Texas, wind with speeds greater than about 9 m/sec generates a current that can dominate the tidally forced circulation (Kraus and Militello 1996; Brown and Kraus 1997). Because of the approximate east-west orientation of Matagorda Bay, wind with an easterly component will drive water from the eastern side to the western side of the bay.

Astronomical tide

The mean tidal range on the northwest side of the bay as measured at Port Lavaca[1] is 0.84 ft, approximately 64 percent that of the Gulf of Mexico at the entrance (1.31 ft, measured at the Bob Hall Pier near Port Aransas). The tide in the Gulf of Mexico at Matagorda Bay is strongly mixed and is usually classified as diurnal. The seasonal variation in water elevation (which does not enter computation of tidal datums, which are based on phase of tide) on the Texas Gulf coast can exceed the daily change in tide (Kraus et al. 1997). Typically, there are two monthly maxima, centered on May and October, and two minima, centered on January and July (Lyle et al. 1988). Plots of measured and calculated water levels are contained in Chapter 4.

Waves

The Wave Information Study (WIS) performed a 20-year hindcast of wave climate for a location 40 km (24.8 miles) southeast of the Colorado River Entrance at a depth of 26 m (Hubertz and Brooks 1989). Mean significant wave height H_s was 1.0 m, with a mean peak spectral wave period T_p of 5.7 sec. The hindcast showed that H_s peaked in April at 1.2 m, with a mean of 1.1 m from November to March. Conditions were found to be milder in August, when H_s averaged 0.8 m. The predominant wave direction was from the southeast (64 percent). Waves from this quadrant had the highest mean H_s (1.1 m) and a mean T_p of 6.1 sec.

[1] Port Lavaca, Texas Coastal Ocean Observation Network (TCOON) sta 033 (NOAA sta 87732591); Bob Hall Pier, TCOON sta 014 (NOAA sta 87758701). Mean tide range is defined as mean high water (mhw) minus mean low water (mlw).

Waves dissipate as they travel across the shelf, and wave hindcasts are difficult for the restricted fetch and strong winds of the Gulf of Mexico. There have been relatively few nearshore measurements of waves. King and Prickett (1998) report wave measurements made from 1991 to 1993 about 3.2 km offshore in 10-m depth of the entrance to the Colorado River. They obtained a mean significant wave height of 0.6 m and a mean peak period of 5.9 sec.

Littoral drift

Because the southeast wind and waves dominate in the study area, the predominant direction of littoral drift is from the northeast to the southwest along Matagorda Peninsula. Temporary reversals in transport occur during southerly winds and during some storms (Paine and Morton 1989). The net longshore transport rate along Matagorda Peninsula was estimated from wave energy flux calculations at 84,000 cu yd/year, and the gross longshore transport rate was estimated at 325,000 cu yd/year (Galveston District 1985). These rates were verified by impoundment volumes updrift of the MSC and the Colorado River entrance (Gibeaut et al. 2000).

Tropical storms

Tropical storms are frequent along the Texas coast and can alter the geomorphology by increasing the shoaling rate in navigation channels, translating the shoreline landward, and causing overwash and breaching. Elevated water level or surge, precipitation in bays, and strong wind can drive a stronger current through inlets than can the astronomical tide, thereby increasing channel depth. Storms with increased forces of large waves and stronger-than-normal currents can also damage jetties. Morton et al. (1976) document changes in the morphology of Matagorda Peninsula and Pass Cavallo after the passage of Hurricane Carla in 1961.

Records of tropical storms were reviewed in this study to compile major storms that made landfall or passed near Matagorda Bay. Eighty-seven storms were identified, listed in Table 1. Tropical storms were selected if they had a wind speed greater than 35 knots (40 mph) and passed through the area between latitude 27.5 to 29°N and longitude 95 to 97.5°W. Hurricanes were selected if the wind speed was greater than 65 knots (75 mph) and the eye passed through the larger area of latitude 27.5 to 29°N and longitude 91.5 to 97.5°W.

Table 1
Tropical Storms in Northwest Gulf of Mexico, 1851 to 2004

Storm No.	Year/Month*	Name
1	1851/June*	None
2	1854/September*	None
3	1860/September*	None
4	1863/September	None
5	1865/September*	None
6	1866/July*	None
7	1867/October*	None
8	1869/August*	None
9	1871/June	None
10	1871/September*	None
11	1874/July	None
12	1875/September*	None
13	1877/September*	None
14	1879/August*	None
15	1879/August*	None
16	1880/June	None
17	1881/August	None
18	1882/September*	None
19	1885/September*	None
20	1886/June*	None
21	1886/August*	None
22	1886/September*	None
23	1886/October*	None
24	1888/June*	None
25	1888/July	None
26	1889/September*	None
27	1891/July*	None
28	1893/September*	None
29	1895/October	None
30	1900/August	None
31	1901/July	None
32	1902/June*	None
33	1909/July*	None
34	1912/October*	None
35	1915/August*	None
36	1918/August*	None
37	1921/June*	None
38	1929/June*	None
39	1932/August*	None
40	1933/July	None
41	1934/July	None
42	1934/August*	None
43	1936/June*	None
44	1938/August*	None
45	1938/October	None
46	1940/August	None
47	1940/September	None
48	1941/September*	None

* Hurricanes are marked by asterisk.

Table 1 (Continued)		
Storm No.	**Year/Month***	**Name**
49	1942/August*	None
50	1942/August*	None
51	1943/July*	None
52	1943/September*	None
53	1945/July	None
54	1945/August*	None
55	1947/August*	None
56	1949/September*	None
57	1957/June*	Audrey
58	1958/August*	Ella
59	1959/July*	Debra
60	1960/June	None
61	1961/September*	Carla
62	1963/September*	Cindy
63	1964/August	Abby
64	1964/September*	Hilda
65	1968/June	Candy
66	1970/July*	Celia
67	1971/September*	Edith
68	1971/September*	Fern
69	1973/September	Delia
70	1979/August	Elena
71	1983/August*	Alicia
72	1985/August*	Danny
73	1985/October*	Juan
74	1986/June*	Bonnie
75	1989/June	Allison
76	1989/July*	Chantal
77	1989/October*	Jerry
78	1998/August	Charley
79	1998/September	Frances
80	2001/June	Allison
81	2002/July	Bertha
82	2002/September	Fay
83	2002/September*	Lili
84	2003/July*	Claudette
85	2003/August	Grace
86	2004/September*	Ivan
87	2004/October	Matthew

History of Matagorda Ship Channel

The history of the MSC is closely connected with Pass Cavallo, the natural pass to Matagorda Bay (Figure 3).

Pass Cavallo

Prior to construction of the MSC entrance from 1962 to 1966, Matagorda Bay was connected to the Gulf of Mexico through a single natural inlet, Pass Cavallo. The French explorer LaSalle entered Pass Cavallo in January 1686, almost 320 years ago, mistaking it for a western arm of the Mississippi River

(LaRoi 1997). Price (1952) noted that the bays and lagoons of Texas tend to possess a stable inlet to the Gulf of Mexico situated in their southwest corners because of the wind setup generated by the daily sea breeze from the southeast and by the strong wind fronts blowing out of the northeast during autumn and winter (see also Price and Parker 1979). Thus, as a "southwest corner pass," Pass Cavallo has probably been in existence for at least 2,600 years (Harwood 1973) or longer (Price and Parker 1979).

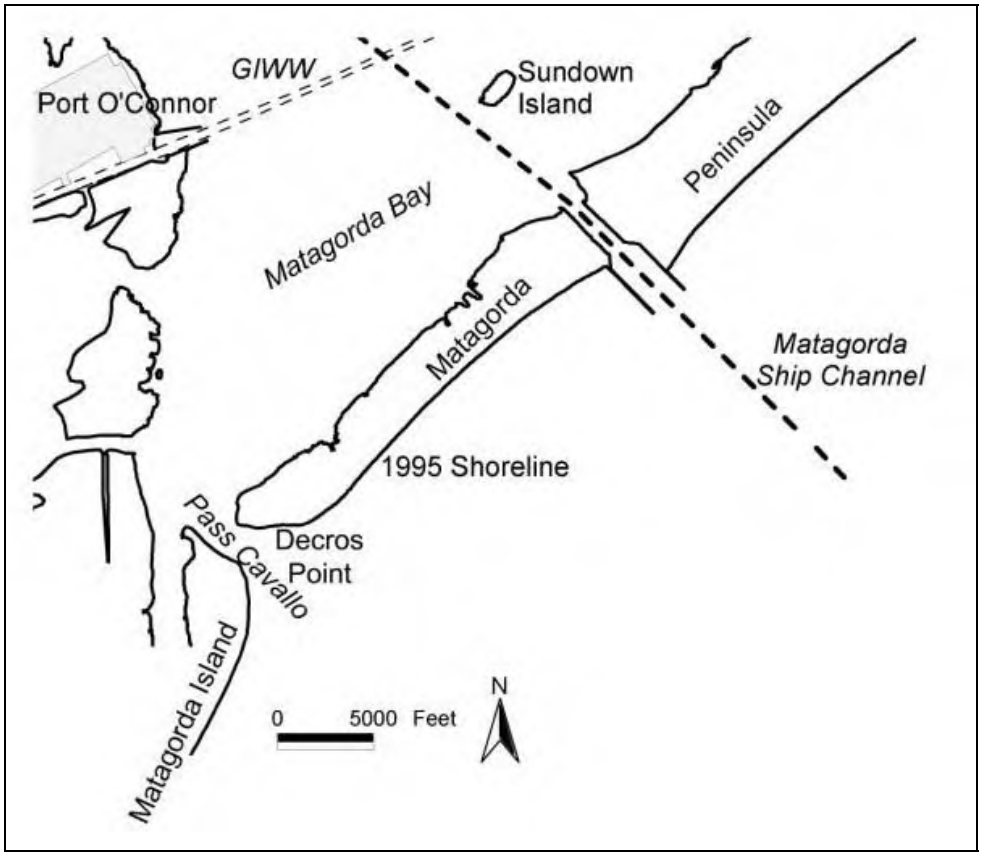

Figure 3. MSC and Pass Cavallo area, based on 1995 shoreline

Pass Cavallo was one the first inlets in Texas serving commercial navigation. The city of Indianola, located on the northwest bay shore, competed with Galveston as a center of commerce for the Texas coast during the 19th century. Indianola was destroyed by the powerful 1875 and 1886 hurricanes, two of several major hurricanes that struck the area from 1874 to 1886 (Price 1956). Morton et al. (1976) state that in the 1800s, the shipping industry considered Pass Cavallo as second only to Galveston as a natural navigable pass on the Texas coast. In that era, local interests and the Galveston District attempted to stabilize Pass Cavallo. "To secure a 12-ft-channel depth across the bar, a single jetty was begun in 1881 at the south side of the pass, designed to extend 7,600 ft from Matagorda Island" (Galveston District 1992). Construction proceeded over the next 5 years, with the jetty reaching 5,253 ft into the Gulf of Mexico. This jetty evidently subsided and can no longer be found. In 1888, the attempt to improve

Pass Cavallo was abandoned because of the destruction of Indianola, which would have been the main interest for navigation commerce. Morton et al. (1976) discuss general changes to Pass Cavallo in response to storms and document nine U.S. Army Corps of Engineers reports on possible navigation improvements and depth surveys starting as early as 1854 and continuing to 1888.

An 1886 U.S. Coast and Geodetic Survey map of Pass Cavallo shows an entrance width of approximately 9,200 ft (Chapter 2), with a deep channel approximately 1,000 ft wide running along its western side, adjacent to Matagorda Island. The westward location of such a trough is consistent with the concept of strong, wind-generated ebb flows originating from the body of the bay to the northeast and the setup that would drive water toward the southwestern shore. Release of a large log raft by dredging in 1929 that had blocked the Colorado River on the north shore of Matagorda Bay caused progradation of a delta that isolated what is now called East Matagorda Bay from Matagorda Bay by 1935 (Wadsworth 1966; Bouma and Bryant 1969). According to National Oceanographic and Atmospheric Administration (NOAA) shoreline position files, upon which the perimeter of the circulation model described in Chapter 4 is based, removal of East Matagorda Bay waters decreased the bay area of the total system by 14 percent (the present Matagorda Bay area is 1.01×10^{10} sq ft; the East Matagorda Bay surface area is 1.63×10^{9} sq ft).

The tidal prism P is the volume of water that flows into an inlet at flood tide or out of the inlet at ebb tide. This volume can be estimated as the product of the tidal range in the bay and the surface area of the bay. Typically, either the spring tidal range or the mean tidal range defines the tidal prism. Based on consideration of tidal circulation, Jarrett (1976) derived an empirical formula relating the cross-sectional channel area A_C of an inlet below mean sea level and the spring tidal prism for inlets without jetties on the Gulf of Mexico coast:

$$A_C = 3.51 \times 10^{-4} P^{0.86} \quad (1)$$

where A_C is expressed in square feet and tidal prism P is in cubic feet. By this formula, a 14 percent reduction in tidal prism is expected to decrease the cross sectional area of Pass Cavallo by 12 percent. This estimate does not include consideration of the wind-generated current, but a similar reduction would be expected because the length of Matagorda Bay over which wind blows was reduced by the Colorado River delta.

The cross-sectional area of an inlet is expected to gradually decrease to a smaller dynamic equilibrium value over perhaps decades because of the reduced tidal prism, although this is just one factor among many controlling inlet cross-sectional area. Estimated tidal prisms available in the literature [1856, 1934, 1965, and 1973 from Harwood (1973) and 1951, 1972, 1975, and 1976 from Ward (1982)], plotted together with calculations from the present study (Chapter 4), show that the discharge through Pass Cavallo has been decreasing, while flow through the MSC has been increasing (Figure 4).

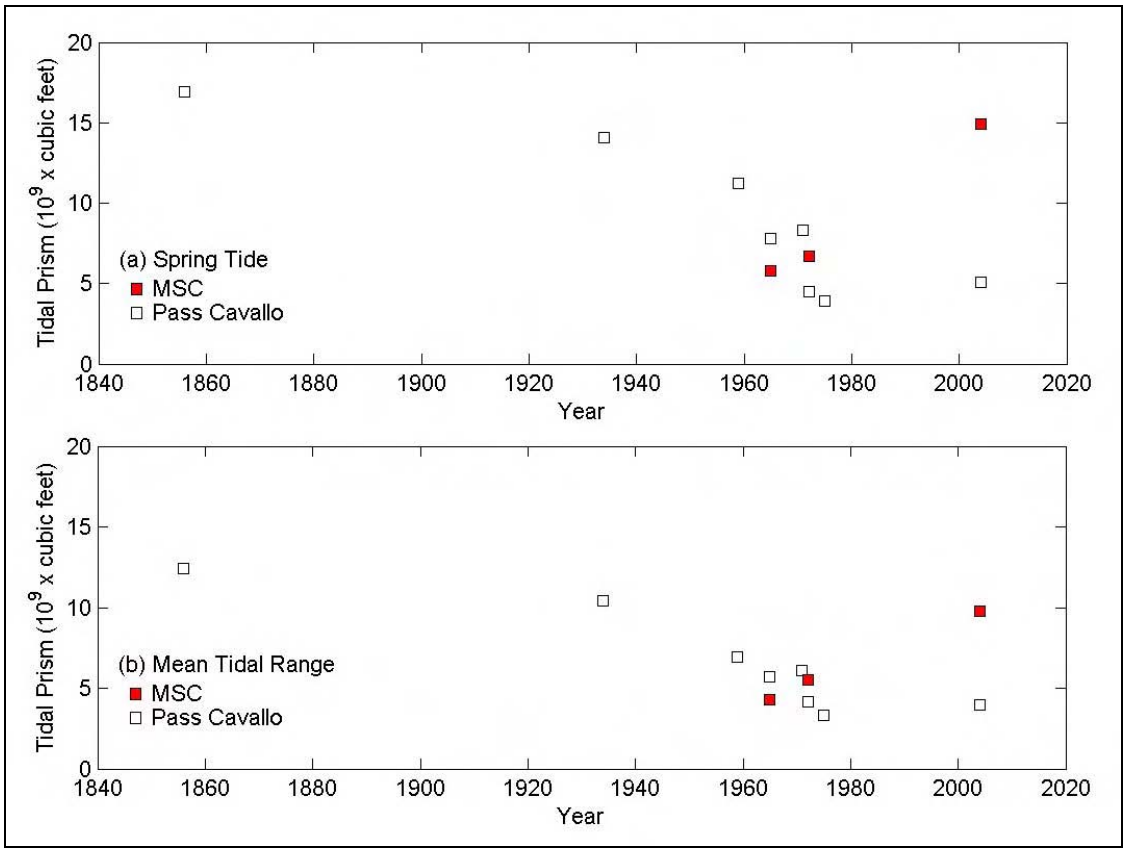

Figure 4. Time evolution of tidal prisms at Pass Cavallo and MSC

The tidal prism at Pass Cavallo appears to have decreased by approximately half from the 1856 estimate to the late 1950s and early 1960s, prior to the cutting of the MSC. This decrease is due in part to reduction in bay area by growth of the Colorado River delta in 1935, and also perhaps to the influence of storms (either the lack of precipitation and strong wind that would tend to open the pass or the presence of strong longshore sediment transport that would tend to fill the pass).

By 1949, navigation across the outer bar of Pass Cavallo by even small fishing and oil exploration vessels proved difficult. Passage could only be accomplished in calm sea conditions by boats drafting less than 6 ft (Galveston District 1992). As an emergency measure, the Galveston District cut a 3,000-ft-long channel 17 ft deep and 135 ft wide through the pass, completed in September 1949. The channel shoaled rapidly, attributed primarily to sedimentation during a hurricane in November 1949. By March 1952, the channel depth had decreased to 8 ft, and no further attempts were made to dredge Pass Cavallo.

Chapter 2 contains an analysis of shoreline change at Pass Cavallo and the MSC entrance, based on available photographs. The width of Pass Cavallo has decreased from some 9,000 ft in 1856 to about 1,000 ft at the present time, although at some times in the past the width exceeded 9,000 ft. The decrease in

width and channel cross-sectional area has been caused in part by cutting of the MSC, as pointed out by Ward (1982) and explored analytically by van de Kreeke (1985). Based on a linear stability analysis and certain assumptions such as constant rise and fall of the water surface over the entire bay, van de Kreeke (1990a, 1990b) concluded that two inlets cannot serve the same bay system. The more efficient inlet is expected to dominate, capturing the tidal prism or discharge, thereby closing the other inlet. However, the analysis neglects the "southwest corner" wind discharge as observed by Price (1952), and so it is not a certainty that Pass Cavallo will close because of the presence of the MSC.

Matagorda Ship Channel design

The MSC was authorized by the River and Harbor Act of 3 July 1958, as described in House Document No. 131, 84th Congress, 1st Session and House Document No. 388, 84th Congress, 2nd Session (Weiser and Armstrong 1963). The latter includes possible plans for a reliable deep-draft navigation channel from the Gulf of Mexico to Point Comfort, TX.

Initially, the recommended entrance was through Pass Cavallo, but concerns were raised regarding the feasibility of maintenance of a deep-draft channel in a wide inlet, with an indirect route northward to Lavaca Bay, and close proximity to Port O'Connor and the GIWW. Other routes were subsequently identified, and those initially considered were:

a. Pass Cavallo.

b. Greens Bayou (ephemeral inlet on northeast side of Matagorda Bay).

c. Mouth of the Colorado River.

d. An artificial inlet through Matagorda Peninsula.

Comprehensive hydraulic physical model tests (Rhodes and Boland 1963; Simmons and Rhodes 1966) were performed to evaluate three possible routes or plans (Figure 5). Route A was through Pass Cavallo; Route B cut through Matagorda Peninsula about 12,000 ft northeast of Pass Cavallo; and Route C was a land cut similar to that of Route B, but 18,000 ft northeast of Pass Cavallo. The hydraulic physical model was calibrated by comparison to extensive field measurements of water level made throughout the bay and in the Gulf of Mexico. The model also represented changes in salinity and qualitative movement of sediment tracer, not discussed here. The three routes were tested with and without jetties.

Based on the hydraulic model tests and engineering considerations, Route C with dual jetties was selected, which is the present location of the MSC. As a summary of considerations, a land cut through Matagorda Peninsula would provide a shorter and straighter entrance, shorter jetties, a shorter length of channel in which the current was expected to be strong, and reduced maintenance by dredging as compared to an entrance located at Pass Cavallo.

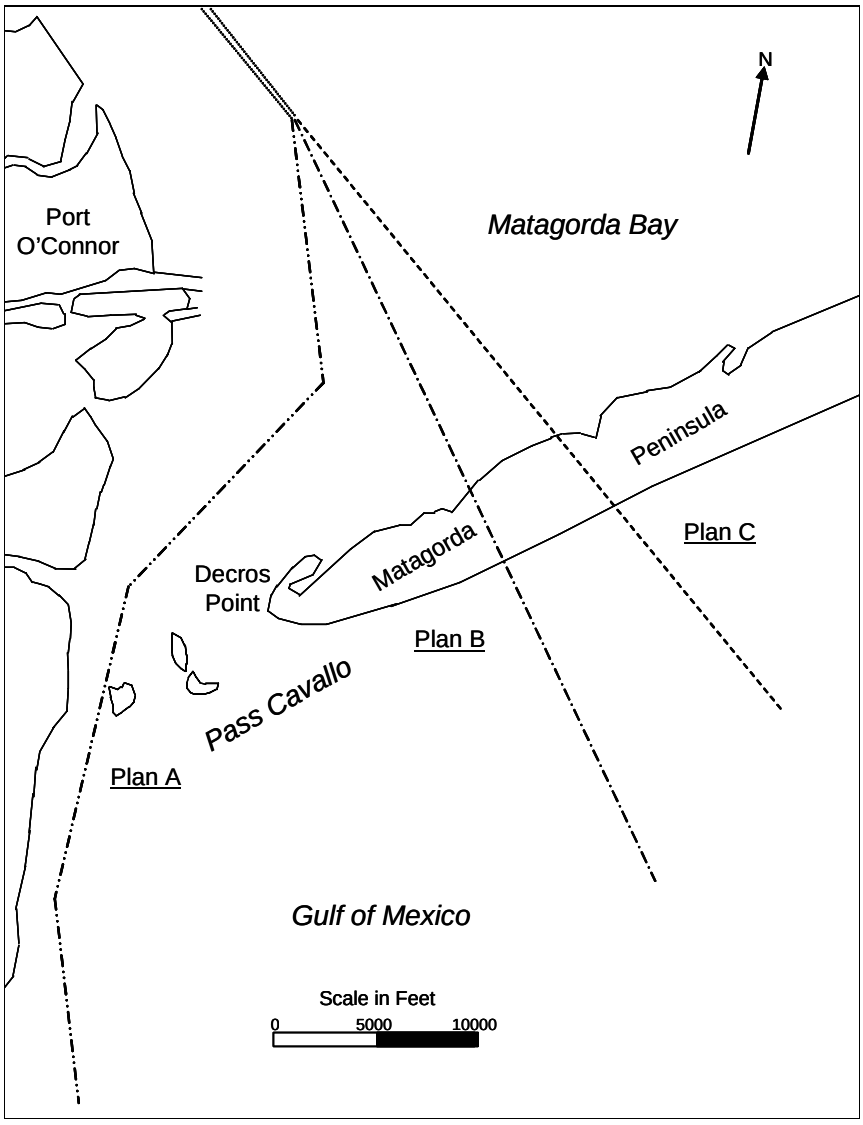

Figure 5. Alternative routes tested (modified from Simmons and Rhodes 1966)

The following is a slightly edited version of salient conclusions of the physical model study (Rhodes and Boland 1963; Weiser and Armstrong 1963; Simmons and Rhodes 1966), as taken from Simmons and Rhodes (1966):

a. Entrance Plan C was considered superior to Plan A because of the shorter and straighter entrance channel, the much reduced length of jetties required, the shorter length of channel in which the current would be relatively strong, and estimation of less maintenance dredging.

b. Entrance Plan C was considered superior to Plan B because of the straighter entrance channel and reduced cross current in that portion of the channel between Matagorda Peninsula and the GIWW crossing Matagorda Bay.

c. Dikes or islands of dredged material extending approximately 1,000 ft into Matagorda Bay on both sides of the Plan C entrance are required to prevent undesirable cross currents in the bay end of the land cut across Matagorda Peninsula. Even with such dikes, the cross current is anticipated to be such that serious erosion of the west side of the land cut, and less but significant erosion of the east side, would probably occur unless the sides of the channel are protected by revetment.

d. Material removed from the channel during initial dredging should be placed on the east side of the channel through Matagorda Bay, with gaps between elevated banks to permit tidal circulation. In the reach between Matagorda Peninsula and the GIWW, the dikes should be oriented to conform to the alignment of the flood and ebb tidal currents, and the spacing between adjacent banks should be sufficient to prevent erosion of the banks and reduce cross-current velocity in the navigation channel to acceptable levels.

e. Jetties extending to about the 24-ft depth contour into the Gulf of Mexico on both sides of the Plan C entrance are required to protect the entrance from wave action and to prevent rapid shoaling of the entrance channel by littoral drift.

f. The final design of the Plan C entrance and interior channels will have no adverse effect on the hydraulic, flushing, or salinity regimens of Matagorda Bay. Salinities in the navigation channel, at depths greater than those in the adjacent portions of the bay, will be appreciably higher than now occur in the bay system, but salinities outside the navigation channel will not change significantly.

g. Increasing the dimensions of the Plan C entrance channel to 500-ft width and 43-ft depth, and those of the channel to Point Comfort to 400-ft width and 42-ft depth, in consideration of future expected navigation requirements, would increase current velocities slightly in the land cut across Matagorda Peninsula.

h. Complete closure of Pass Cavallo, after construction of the ship channel and appurtenant works, would reduce the tidal prism of the bay system, reduce vertical mixing of salt and fresh water caused by tidal current action, and probably reduce the flushing time of the entire bay complex.

i. Breaches in Matagorda Peninsula by storm action, such as those caused by Hurricane Carla, would increase the tidal prism of the bay system as well as the mean salinity of the bay system. However, based on past experience, it appears that such breaches would soon be closed by littoral action, and thus their effects would be temporary.

j. During flood stages on the Colorado River, large inflows of fresh water to Matagorda Bay can raise water levels by 0.1 to 0.2 ft, increase slightly the maximum ebb current velocities in natural and artificial channels connecting the bay and the Gulf of Mexico, and temporarily reduce the mean salinity of the bay as much as 4 ppt.

k. Extreme tide ranges in the Gulf of Mexico, on the order of 4 ft, would significantly increase the tidal prism of the bay and would produce maximum current velocities in the Plan C entrance of about 8.0 ft/sec

during flood and 7.7 ft/sec during ebb. Under these same conditions, maximum current velocities in Pass Cavallo would be on the order of 10.9 ft/sec during flood and 6.3 ft/sec during ebb.

After the physical model tests, dredging was initiated in July 1962, and construction of the jetties began in 1963. The channel was cut across the approximately 1-mile-wide Matagorda Peninsula and completed on 24 September 1963 (Committee on Tidal Hydraulics (CTH) 1964). Dredging of the inner portion of the entrance channel and construction of the south jetty were completed early in 1966. Dredging on the outer portion of the entrance channel and construction of the north jetty were completed in October 1966. The north jetty is 5,900 ft long, and the south jetty is 6,000 ft long (Galveston District 1992).

Construction plans called for the jetties to be built simultaneously such that the length of one jetty would not exceed the length of the other by more than 50 ft at any time (Galveston District 1962). However, as stated in the preceding paragraph, this was not the case. Upon opening the entrance in 1963, the current proved strong and caused rapid scouring and expansion of the cut. The Galveston District requested assistance from the CTH to address this and other identified problems, but because widening of the cut was extremely rapid, "…a decision was reached several days before the Committee meeting (held 28-30 January 1964) to revet both sides of the complete length of the land cut through the peninsula as rapidly as possible…." "The physical model had indicated that serious bank erosion was probable," so "…materials to revet one or both sides of the land cut were stockpiled in the area while dredging of the channel was in progress" (CTH 1964). Complication in construction of the MSC entrance resulted in litigation between the contracted dredger and the Galveston District, which likely also delayed completion of construction.

All Galveston District design drawings and specifications for the MSC entrance that could be located for this study call for two jetties spaced 2,000 ft apart but are ambiguous about the width of the land cut. Figure 6 is an example. Construction with dredged material of banks on the north and south sides was conceived to shelter the bay side of the channel from cross currents (Simmons and Rhodes 1966; Galveston District 1962; CTH 1964). The use of material dredged during the entrance opening for protecting the bay side portion of the channel is likely the origin of Sundown Island and a high plateau in bathymetry located northeast of the bay entrance (Chapters 3 and 4).

Initial tests involving jetties in the physical model for Plan C (and Plan B) employed jetties spaced 2,400 ft apart and extending 6,000 ft into the Gulf of Mexico with the same orientation as the MSC in Matagorda Bay. In addition, the channel width in the cut through Matagorda Peninsula was only 200 ft (at the bottom, with channel banks rising to the surface with 1-on-5 side slopes). Refinement of Plan C in Tests 20, 20A, 20B, and 29 changed such parameters as the distance between jetties to 2,000 ft and the channel width at the bottom to 300 ft.

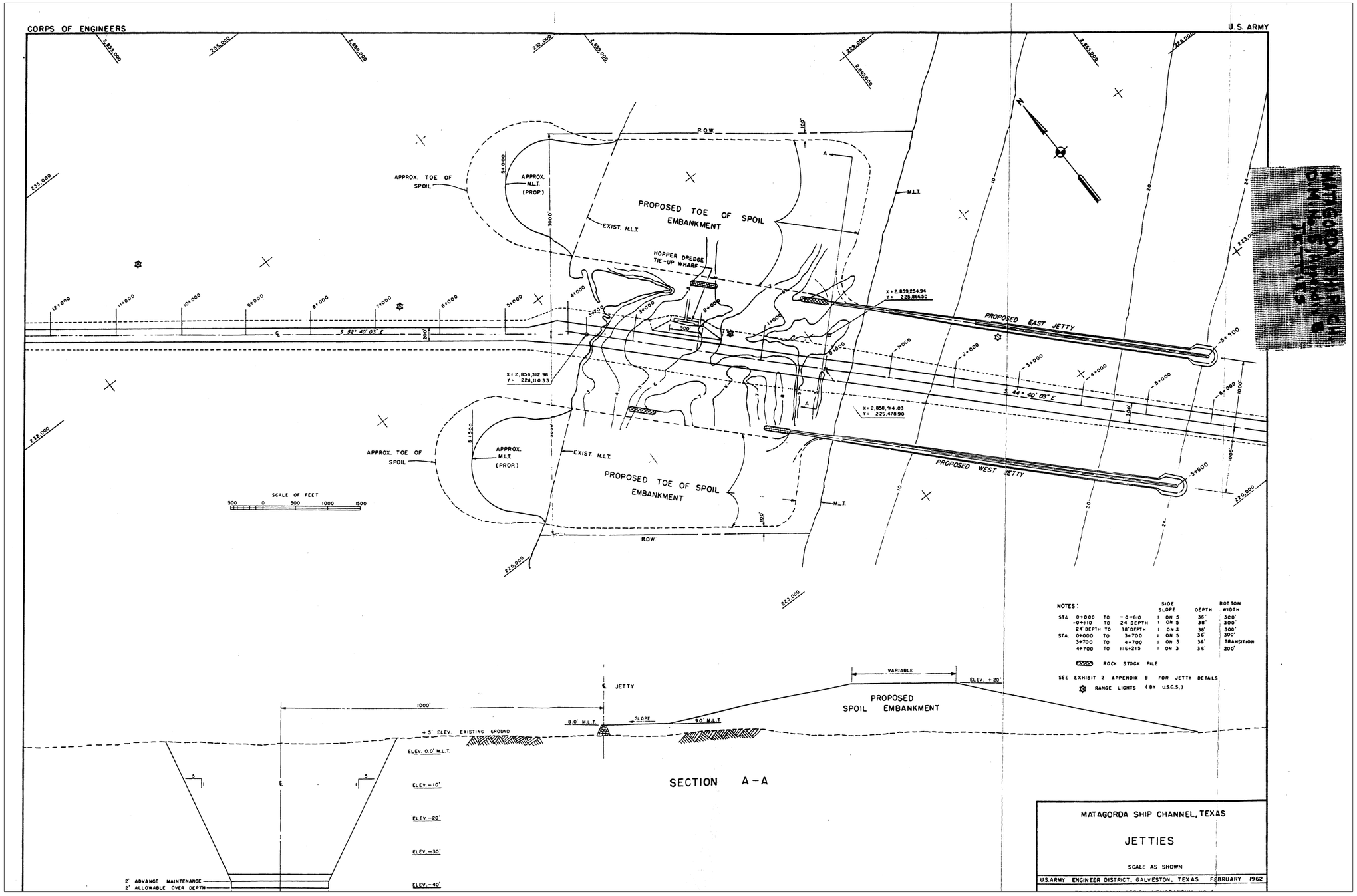

Figure 6. MSC entrance design (from Galveston District 1962)

The physical model tests, therefore, did not maintain a 2,000-ft width in the land cut as between the jetties. It is not known why the land cut channel section was specified to be narrower than the distance between jetties, but it is surmised that the tests were done under the assumption that a narrower cut would reduce dredging costs. After the cut was dredged in the prototype and rapid bank erosion occurred, revetting of the land cut banks as performed by the Galveston District was qualitatively consistent with the physical model tests. The narrow planform area of the MSC entrance is called the "bottleneck." The bottleneck constricts the flow, increasing current velocity (Chapter 4).

Figure 7 is an aerial photograph showing the jetties and the bottleneck, which has a minimum width of 950 ft. This photograph indicates an ebb current flowing from the eastern portion of Matagorda Bay and focused toward the north (bay) side of the north jetty. Deterioration of the bottleneck revetment (a series of sandy beach coves in the revetments) can also be observed. Impoundment at the north jetty was rapid (Morton 1977b) (Chapter 2), and the rate of shoreline advance has decreased. The recession rate of the shoreline on the south side has also decreased over the years (Chapter 2).

Figure 7. MSC entrance, September 2002

Alternatives for Jetty Stability

In preliminary work of this study, several alternatives were investigated with the numerical circulation model to assess relative performance for reducing the current velocity through the MSC entrance. Based on this initial work, the Galveston District Project Delivery Team, accounting for such factors as constructability, cost, and environmental consequences, identified three alternatives for full study (Table 2). These alternatives are sketched in Figure 8 and are investigated in Chapter 4.

Table 2
Definition of Alternatives

Alternative	Definition	Comments
Existing Condition	Present situation if no action is taken.	--
Alt 1	Remove south bottleneck.	Remove south bottleneck revetment and extend south jetty northward approximately 5,000 ft. Moves south bottleneck away from scour area.
Alt 2	Remove north and south bottlenecks.	Remove north and south bottleneck revetments and extend both jetties northward approximately 5,000 ft.
Alt 3	Remove north and south bottlenecks and flange bay entrance.	Same as Alt 2, but flange the bay entrance to train the ebb flow toward the center of the channel. Moves south bottleneck away from scour area.

All alternatives increase the width of the bottleneck as a necessary condition for reducing the current velocity through the MSC entrance. Alt 3 also provides a revetment flange on both sides of the bay entrance to train the ebb current, which has produced a large scour hole near the north side of the west revetment of the bottleneck (Chapters 3 and 4). The flange would guide the ebb flow toward the center of the channel and away from the structures. Removing the south bottleneck increases the distance between the existing scour hole and the revetted entrance shoreline.

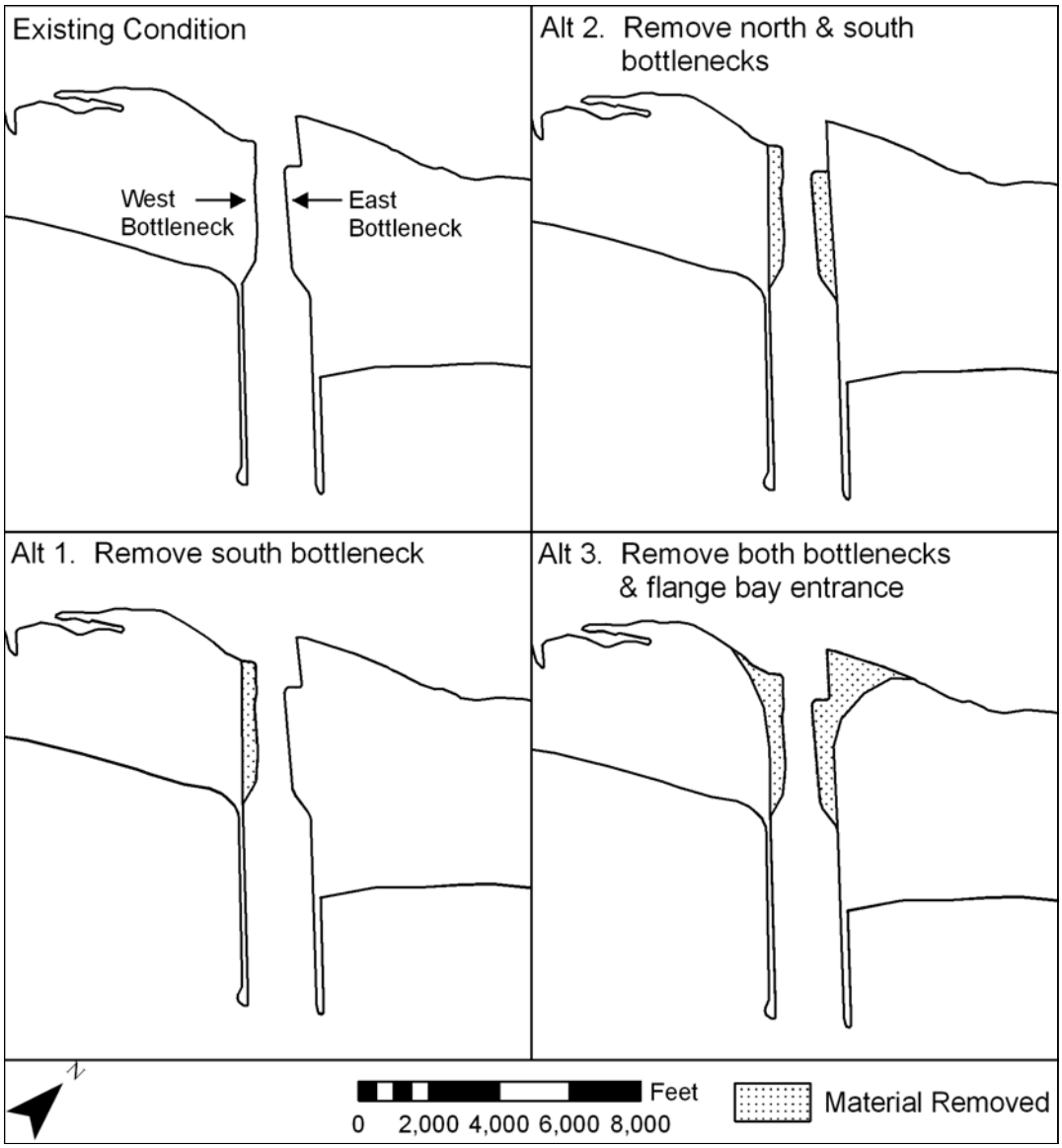

Figure 8. Sketch of jetty stability alternatives

Regional Processes

The U.S. Army Corps of Engineers (USACE) constructs, maintains, and operates federal navigation projects within a regional sediment management (RSM) context. RSM recognizes that the consequences of navigation projects, intended and unintended, may extend beyond authorized physical limits. Martin and Rosati (2003) compiled civil works authorities and policies supporting implementation of RSM. Among these policies, pursuant to Section 5 of the River and Harbor Act of 1935, "…each investigation on navigation improvements potentially affecting adjacent shorelines must include analysis of the probable effects on shoreline configurations. A distance of not less than 10 miles on either side of the improvement should be analyzed" [USACE 2000;

paragraph E-14(b)]. An RSM approach was followed in this study in consideration of the shoreline west of the MSC entrance and Pass Cavallo. In addition, any reduction in the flood current at the bay side of the MSC entrance will contribute to reducing erosion of Sundown Island (Figure 3) and maintenance dredging of the GIWW in its vicinity (Kraus et al. 2000).

Report Contents

Chapter 1 gives the problem statement of the study, an overview of the physical processes in Matagorda Bay, and the history and present state of the MSC entrance and Pass Cavallo. Alternatives evaluated in this study for the jetties are defined in Chapter 1. Chapter 2 describes results of analysis of historical and recent shoreline behavior on both the Gulf of Mexico and bay sides of the MSC entrance and at Pass Cavallo. Chapter 3 presents and analyzes bathymetric survey data and channel survey data at the MSC entrance, identifying shoaling and scouring patterns.

Chapter 4 contains an analysis of the hydrodynamics, principally for the depth-averaged current through the entrance, and evaluation of the alternatives. A methodology is introduced for comparing the alternatives through frequency of occurrence of current speed in the MSC entrance. Main results and conclusions of this study are contained in Chapter 4 for evaluation of the alternatives, supplemented by regional morphological results from Chapter 2. Chapter 5 is a compilation of conclusions of this study. Appendix A and Appendix B display aerial photographs consulted in this study for the MSC entrance and for Pass Cavallo, respectively. Appendix C describes numerical simulations of salinity change in response to the proposed alternatives.

2 Shoreline Dynamics at Matagorda Ship Channel and Pass Cavallo

This chapter evaluates historical shoreline change in response to the construction of the MSC entrance. The chapter is composed of five sections: an introduction, methods, shoreline change rates for the Gulf of Mexico and Matagorda Bay shorelines near the MSC entrance, spit growth and inlet width at Pass Cavallo, and a summary.

Introduction

A review of relative sea-level rise in the vicinity of the MSC and summary of previous work on historic shoreline change along Matagorda Peninsula is given.

Relative sea-level rise

Shoreline evolution is influenced by sediment transport processes and, if applicable, the long-term trend in relative sea-level change. This study concerns time scales of coastal change over which a rise in sea level relative to land is relevant. The National Ocean Service (NOS) reports mean sea level trends for Rockport, TX (NOS sta 8774770, approximately 45 miles southwest of the MSC), and Freeport, TX (NOS sta 8772440, approximately 80 miles northeast of the MSC). Both stations exhibit a long-term trend of sea-level rise. Between 1948 and 1999, the mean sea-level trends at Rockport (1948-1999) and Freeport (1954-1999) were relative sea-level rises of 1.51 ft/century (4.6 mm/year) and 1.93 ft/century (5.87 mm/year), respectively.

Although long-term tidal records document relative sea-level rise, they do not differentiate between rise of the sea and subsidence. Morton (1977a) provides a thorough review of relative sea level, attributing compactional subsidence and secular sea-level variations as the primary factors in relative sea-level rise along the Texas coast. Concerns of land surface subsidence due to oil and water extraction were also discussed; however, these were not considered to be a primary factor for relative sea-level changes in the vicinity of the MSC. Estimated land losses due to relative sea-level rise for Matagorda Peninsula over time are given in Table 3.

Table 3
Estimated Shoreline Recession Due to Sea-Level Rise, Matagorda Peninsula[1]

Interval, year	Recession, ft
1	1
5	6
10	11
25	29
50	57
75	86
100	115

[1] Assumed foreshore slope of 0.015 and rate of sea-level rise of 1.72 ft/century.

Historical shoreline change

Historical shoreline change analysis along the Matagorda Peninsula Gulf of Mexico coast has been conducted by McGowen and Brewton (1975), Morton et al. (1976), Galveston District (1971), Paine and Morton (1989), Gibeaut et al. (2000), and, most recently, by the U.S. Geologic Survey (USGS) (Morton et al. 2004). All but McGowen and Brewton (1975) were larger studies encompassing the entire gulf shoreline of Texas. Results from these studies are reviewed in this section.

McGowen and Brewton (1975) studied historical shoreline change for Matagorda Peninsula along both the Gulf of Mexico and Matagorda Bay shorelines for the period 1856/57 to 1971/72. Results indicated that shoreline recession was the dominant trend. It was estimated that approximately 8,450 acres of land were lost from Matagorda Peninsula due to recession of the gulf and bay shorelines. Gulf shorelines receded at an average rate of 5 ft/year, while bay shorelines receded at an average rate of 4 ft/year. At the northeast end of the barrier, in the vicinity of Brown Cedar Cut, shoreline change rates varied from station to station, ranging from 14 ft/year of recession to 8 ft/year of advance. Brown Cedar Cut is an ephemeral inlet to the Gulf of Mexico located on the northern end of East Matagorda Bay (Mason and Sorensen 1971). Midway between Brown Cedar Cut and the mouth of the Colorado River, the shoreline advanced at rates between 3 and 5 ft/year. The shoreline was stable towards the mouth of the Colorado River. Southwest of the Colorado River, shoreline change rates were consistently recessional, with exception of a single station directly downdrift of the Colorado River entrance. Shoreline recession rates in this area ranged from 2 to 20 ft/year. A recession rate of 16 ft/year was reported downdrift of the MSC entrance. Rates were not reported directly updrift of the MSC or at the tip of Matagorda Peninsula. Volumetric gains and losses due to updrift impoundment and downdrift erosion were estimated. It was calculated that approximately 1.66 million cu yd of sand was trapped by the north jetty at the MSC, and 1.91 million cu yd of sand was eroded from the downdrift beach between 1964 and 1971.

McGowen and Brewton (1975) also calculated shoreline change rates for the Matagorda Bay shoreline from southwest of Greens Bayou to Pass Cavallo. Directly southwest of Greens Bayou, the bay shoreline advanced or was stable. Farther west, shoreline recession was the dominant trend, although two of the five stations exhibited no change. Bay shoreline recession rates ranged from 2 to 3 ft/year.

For the period 1855/57 to 1974, Morton et al. (1976) reported a net recessional shoreline trend along Matagorda Peninsula. The only exception to this trend was at four stations updrift of the MSC. Two stations of shoreline advance occurred 5 and 10 miles updrift of the MSC, prior to opening (1856-1937). The other two stations were directly updrift of the MSC and represent sediment impoundment by the north jetty. The first two stations updrift of the MSC experienced shoreline advance rates of 1.7 and 5.1 ft/year. On average, the net rate of shoreline change was small, about 3 ft/year. Two areas with higher recession rates were noted, one 6 miles downdrift of Brown Cedar Cut (10 ft/year) and the other at the southern end of Matagorda Peninsula between the MSC and Decros Point at Pass Cavallo (1.9 to 11.5 ft/year).

Paine and Morton (1989) described shoreline change rates from 1974 to 1982. During this period, Matagorda Peninsula experienced minor (less than 5 ft/year) to moderate (5 to 15 ft/year) shoreline recession rates. Overall, rates were lower than during the previous period (1930 to 1974). Five distinct zones of shoreline change were identified along Matagorda Peninsula:

a. Shoreline recession was observed southwest of Brown Cedar Cut, with change rates ranging from 5.5 to 15.8 ft/year.

b. A 13-mile reach of stable shoreline, from northeast of the mouth of the Colorado River to Greens Bayou, exhibited mixed accretion and erosion, with shoreline change rates between 8.7 ft/year of advance and 15.8 ft/year of recession.

c. Shoreline advance occurred between Greens Bayou and the MSC. Advance rates in this area were between 6.9 and 39 ft/year, with rates diminishing with distance from the north jetty. The updrift extent of the impoundment fillet had lengthened by at least 1 mile as compared to previous intervals (2 miles, 1965 to 1974).

d. The largest shoreline change rates in the interval were downdrift of the MSC. Directly downdrift of the MSC, the shoreline receded at a maximum rate of 36.7 ft/year.

e. At Decros Point, the shoreline advanced at a rate of 113 ft/year as a result of spit progradation and accretion at the tip of Matagorda Peninsula. Paine and Morton (1989) noted that the southwest end of Matagorda Peninsula was becoming longer and narrower during this interval.

Gibeaut et al. (2000) determined long-term shoreline change rates by analyzing shoreline data from 1930 to 2000 for the Gulf of Mexico shoreline between the Brazos River and Pass Cavallo. Data prior to 1974 were excluded for rates calculated between Greens Bayou and Pass Cavallo to provide an accurate assessment of processes in the modern sediment budget. The dominant long-term trend for Matagorda Peninsula during this period was recession.

Beginning at the northeast extent of the peninsula, shoreline recession rates decreased more or less linearly from 14 ft/year at Brown Cedar Cut to an area of stability beginning 9 miles west of the mouth of the Colorado River. From this point southwest to Greens Bayou, the shoreline experienced lower rates of recession (1.6 to 6.5 ft/year). The highest observed recession rate along Matagorda Peninsula was 16 ft/year, directly downdrift of the MSC. Shoreline advance was observed in three locations: directly downdrift of the mouth of the Colorado River (6.5 to 9.8 ft/year), southwest of Greens Bayou to the MSC (3 to 26 ft/year), and at the southwestern tip of Matagorda Peninsula (peak of 82 ft/year). Over this period, the impoundment fillet extended approximately 6 miles updrift of the MSC.

Shoreline Analysis Methods

The following section describes methodologies applied to the shoreline rate change analysis. Subsections on shoreline definition, data sources, aerial imagery and rectification, shoreline digitizing, and shoreline change rate analysis are included.

Shoreline definition

In the simplest description, a shoreline is defined as the boundary where a body of water comes in contact with dry land. Changing conditions in the marine and terrestrial environments modify the position of the shoreline in time spans from seconds to decades, resulting in numerous fluctuations of the shoreline position from inches to hundreds of feet. To accurately compare successive shoreline positions at a site, a consistent shoreline definition must be established (Kraus and Rosati 1997). For this study, the analyzed shoreline is the high water line (hwl).

The hwl is defined as "the intersection of land with the water surface at an elevation of high water," which can be interpreted by a continuous line of deposition of debris on the foreshore [National Oceanographic and Atmospheric Administration (NOAA) 2000]. The hwl is an interpreted shoreline, as opposed to the mean high water line (mhwl), which is determined through the measurement and analysis of water levels at a site (Kraus and Rosati 1997). The hwl is the most commonly used shoreline indicator in the United States because of ease of interpretation in the field and on aerial photography (Leatherman 2003). Early NOS topographic sheets (T-sheets) identified the shoreline as the hwl, as described by Shalowitz (1964):

> "From the standpoint of the surveyor, the high-water line is the only line of contact between land and water that is identifiable on the ground at all times and does not require the topographer being there at a specified time during the tidal cycle, or the running of levels. The high-water line can generally be closely approximated by noting the vegetation, driftwood, discoloration of rocks, or other visible signs of high tides. The mean high-water line must not be confused with the storm high-water line, which is usually marked by driftwood and the edge of considerable vegetation."

The hwl is identified in aerial photographs through the same method. This definition becomes problematic if interpreting historical aerial photographs, which are sometimes of poor quality, either under- or overexposed, resulting in a washing out of the sub-aerial beach. The hwl is interpreted from historical photographs by a difference in color tone on the subaerial beach. This interpretation is not to be confused with the water-saturated zone, which occurs close to the water line (Leatherman 2003). Specialized experience and manipulation of the digital image are employed to identify these features and create an accurate representation of the shoreline. Modern aerial photography and orthophotographs are of much higher resolution and allow distinction of the hwl with less manipulation of the digital data.

Data sources

Shoreline data analyzed in this study originate from four sources: NOS vector shorelines (NOS 2005), Texas Bureau of Economic Geology (BEG) (BEG 2004) vector shorelines, USGS vector shorelines (Morton et al. 2004), and digitized shorelines from aerial photography. In total, 27 shorelines were available from 25 unique dates between 1856 and 2003. Data are summarized in Table 4. Shoreline dates that are denoted CHL were digitized in-house from rectified aerial photography.

Aerial imagery

Aerial photographs were available for this study in both digital and 9- by 9-in. print format, sourced primarily from CHL archives. An inventory of available images is given in Table 5. Images from the MSC are located in Appendix A, and images from Pass Cavallo are located in Appendix B. Print photographs were scanned on a UMAX 2100XL flatbed scanner at a resolution of 600 dpi and saved in tagged image file (tif) format. Selected photographs were then rectified to 1995 1-m-resolution digital orthophotograph quarter quadrangles (DOQQ) available from the Texas Natural Resources Information System (TNRIS) (TNRIS 1995). This photo set provided a high-accuracy (National Map Accuracy Standards; see Anders and Byrnes 1991), high-resolution (1 m or 3.28 ft pixel) base for rectification.

The study area has few control points useful for image rectification. Control points were improvised from geomorphologic features and vegetation. A typical rectification consisted of 7 to 10 control points. Because of lack of control, the majority of the imagery was rectified with a first-order polynomial transformation. Images with 15 or more control points were rectified with a second-order polynomial transformation. Rectification quality was evaluated by the goodness-of-fit of the output image to the TNRIS DOQQs. Uncertainty of ground positions from the rectified imagery is estimated at 20 to 60 ft. Images having gross positioning errors were excluded from the study.

Shoreline digitizing

If not readily apparent, the position of the hwl was enhanced by applying standard deviation and histogram stretching techniques prior to digitizing.

Viewer scale was set according to image resolution to maximize the accuracy of the digitized line. For example, higher-resolution images were digitized at a lower scale than low-resolution images. Image scale was held constant as the shoreline was digitized across each image or series of images.

Table 4
Shoreline Inventory[1]

Year	Date	Source	Coverage			
			Pass Cavallo		MSC	
			West	East	Gulf of Mexico	Matagorda Bay
1856	1 Apr	NOS	x	x	x	x
1930	circa	CHL		x	x	x
1933	23 Nov	NOS	x	x	x	x
1937	4 Mar	BEG	x	x	x	
1943	16 Oct	CHL		x		
1953	circa	CHL		x		
1956	9 Sep	BEG		x	x	x
1957	Nov/Dec	BEG	x			
1961	18 Sep	CHL	x	x		
1963	4 Oct	CHL		x	x	x
1965	15 Jun	BEG	x	x	x	
1965	15 Oct	CHL	x	x	x	x
1968	17 Jan	CHL		x	x	x
1974	15 Jun	BEG/USGS	x	x	x	
1974	20 Nov	CHL	x	x	partial	x
1978	30 Nov	CHL		x	x	x
1982	10 Jun	CHL	x	x	x	x
1984	10 Apr	CHL	x	x		
1985	14 Apr	CHL	x	x		
1986	17 Oct	CHL	x	x	partial	x
1988	24 Aug	CHL	x	x	partial	x
1991	1 Mar	BEG		x	x	
1995	20 Feb	CHL/BEG	x	x	x	x
2000	29 May	BEG	x	x	x	
2001	1 Jan	USGS	x	x	x	
2002	6 Aug	CHL	x	partial		
2003	26 Sep	CHL	x	partial		

[1] USGS and BEG shorelines are Gulf of Mexico shore only; NOS and CHL shorelines include Matagorda Bay shoreline.

Digitization began at the west end of Matagorda Peninsula and ended at the east end for the Gulf of Mexico shoreline. The MSC was the origin for Matagorda Bay shorelines (digitized to the east and west). During digitizing across a series of images, shorelines were annotated towards the center of each image in an effort to minimize positioning errors associated with distortion

towards the image edges (Anders and Byrnes 1991). This practice improves overall image-to-image fit of the shoreline. Point density was varied as necessary to capture alongshore variations in shoreline position. Once the shoreline was complete, the digitized line was reviewed and individual points or sections adjusted as needed. Few photo sets documented the full length of the project area. As a result, several shorelines digitized from the available imagery cover only a portion of the study area. Shoreline coverage is documented in Table 4.

Table 5
Aerial Photograph Inventory for Pass Cavallo and MSC

Year	Coverage		Georeferenced
	Pass Cavallo	MSC	
1930	X		X
1943	X		X
1953	X		X
1961	X		X
1963	X	X	X
1965	X	X	X
1966	X	X	
1967	X	X	
1968	X	X	X
1974	X	X	X
1977	X	X	
1978	X	X	X
1979	X	X	
1980	X	X	
1982	X	X	X
1984	X	X	
1985	X	X	X
1986	X	X	X
1987	X	X	
1988	X	X	X
1991	X	X	
1995[1]	X		X
1999		X	X
2002	X	X	X
2003	X	X	X

[1] TNRIS DOQQs (reference set).

Shoreline change rate analysis

Shoreline change rates were calculated by both the end-point and the linear regression methods. Calculation of the end-point rate is direct; the distance between two shorelines at a known point is measured, with the result divided by

the time interval to give the change rate. The end-point rate is easily applied to data series and is commonly used; however, there are some disadvantages. Results are controlled by the accuracy of individual shorelines, and the rate does not represent processes occurring between the two data points (Dolan et al. 1991).

The method of linear regression is an accepted alternative to the end-point method (Dolan et al. 1991; Foster and Savage 1989). This method incorporates a least-squares solution to determine a change rate from a series of shoreline positions, with no weight given to time intervals. The resulting rate represents intermediate shorelines, but is sensitive to the temporal spacing of the data. The linear regression method is best suited for application across an entire data series and is often employed to show intermediate trends in a data set excluded by the end-point rate.

For this study, the end-point rate was employed to quantify changes between each selected time interval. These intervals typically span 10 or fewer years with no intermediate shorelines. The end-point method was also applied to quantify rates between end-member shoreline dates. Although intermediate shoreline movements are of value for understanding processes at the site, net changes are best represented by the end-point method. The linear regression method was applied in conjunction with the end-point method to present intermediate processes in long-term intervals.

Shoreline positions were generated at an interval of 50 ft using the ArcView 3.2 extension BeachTools (Hoeke et al. 2001) from a baseline established parallel to the local shoreline orientation. BeachTools measures shoreline distance by generating transects perpendicular to a baseline at a user-specified interval. Shoreline change transects were evaluated for overlap after initial generation. If transect overlapping occurred, the transect having the best fit to the local shoreline orientation was retained. Shoreline distances relative to the baseline were exported from the ArcView GIS and change rates were calculated in Matlab®. A low-pass filter was applied to the change rates to remove high-frequency noise induced by the dense spatial sampling of the shorelines.

Shoreline Change at Matagorda Ship Channel

This section discusses shoreline change rates along the Gulf of Mexico and Matagorda Bay shorelines in the vicinity of the MSC. Progradation of Matagorda Peninsula and northeastern spit growth of Matagorda Island into Pass Cavallo are quantified together with inlet width through time.

The Texas coast experiences seasonal variations in water level (discussed in Chapter 1). Water level is typically at its lowest during January and July and at its highest during May and October. When possible, shorelines from dates during similar seasonal water levels were chosen for analysis.

Gulf of Mexico shoreline

Shoreline change along the Gulf of Mexico shoreline in the vicinity of the MSC was evaluated for the interval 1963 to 2000. On average, the available data

covered the shoreline northeast (updrift) of the MSC for 3 to 5 miles and for approximately 5 miles southwest of the MSC (downdrift) to Pass Cavallo. Shoreline change was evaluated from a baseline established along the axial orientation of Matagorda Peninsula on the landward side of the shoreline (Figure 9). Ten shoreline dates were chosen to represent short-term change in response to the MSC (Table 6). Short-term shoreline change rates were evaluated for each interval via the end-point method. Rates of shoreline advance due to spit progradation were precluded from the analysis. Successive intervals are discussed first, and then long-term change rates follow.

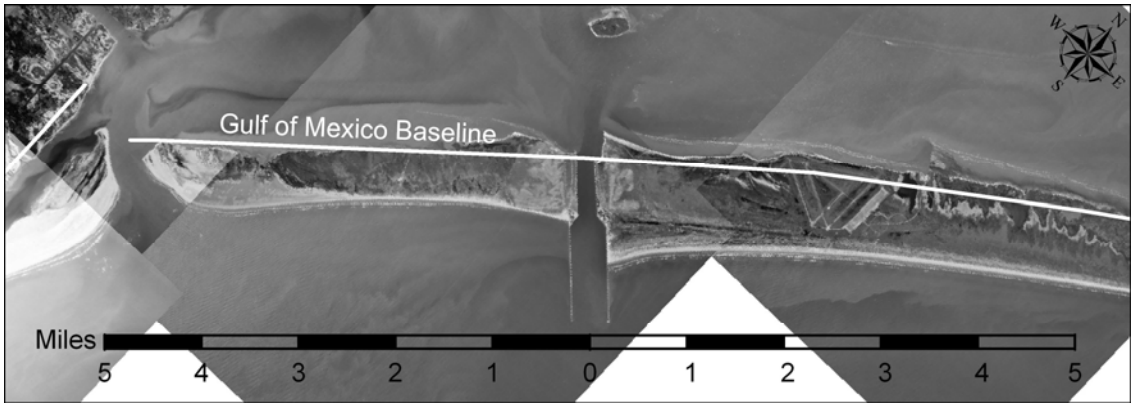

Figure 9. Project area Gulf of Mexico shoreline change baseline

Table 6
Selected Gulf of Mexico Shorelines

Year	Date
1963	4 October
1965	15 October
1968	17 January
1974	15 June
1978	30 November
1982	10 June
1986	17 October
1988	24 August
1995	20 February
2000	29 May

Interval 1: 1963 to 1965 (2.0 years). Updrift shoreline response to the construction of the MSC was immediate, as observed in the 2-year interval following completion in 1963. Figure 10 shows the shoreline position of each date (upper frame) and the shoreline change between the dates (lower frame). The Gulf of Mexico is located towards the bottom of each frame. Shoreline advance rates updrift of the north jetty averaged 86 ft/year (maximum of 360 ft/year). The impoundment fillet extends approximately 1.5 miles to the northeast. Maximum net shoreline advance of the north jetty was 741 ft.

Downdrift of the MSC, the shoreline response was mixed. A small impoundment fillet was observed adjacent to the south jetty, followed by an area of shoreline advance to the southeast. Shoreline advance rates in this area ranged from 10 to 60 ft/year. This accretion was likely supported by material discharged from the MSC during construction.

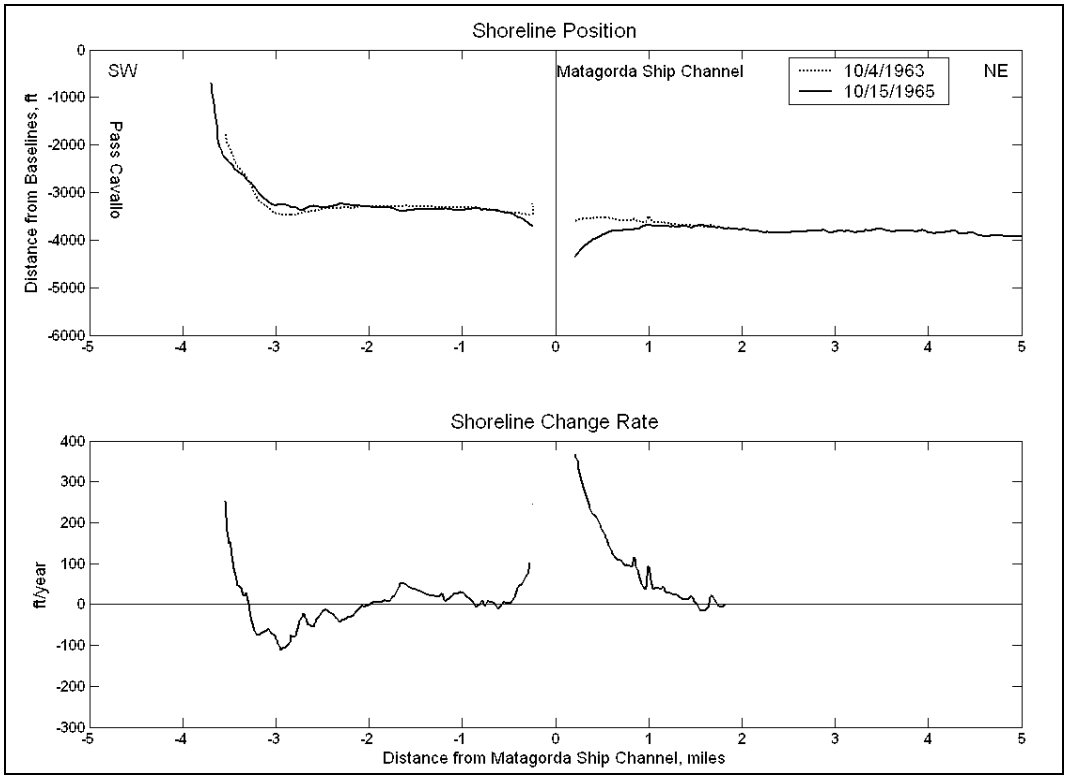

Figure 10. Shoreline position and change rate, 1963 to 1965

A 1.5-mile zone of shoreline recession is apparent, beginning 2 miles southwest of the MSC. High rates of recession were observed in this area, ranging from 40 to 110 ft/year. In 1963, the Matagorda Peninsula shoreline extended southwest for 3.5 miles downdrift of the MSC. By 1965, the length of the downdrift shoreline had increased due to spit growth at the southwest tip of Matagorda Peninsula. This growth appears to have been supported by shoreline recession updrift of the tip and downdrift of the MSC. The average shoreline change trend during this interval was an advance of 29 ft/year.

Interval 2: 1965-1968 (2.2 years). Large advances of the shoreline both updrift and downdrift of the MSC were observed during this interval (Figure 11). Net shoreline advance totaled 320 ft directly adjacent to the north jetty. The alongshore extent of the impoundment fillet appears to have remained unchanged, although compared to the previous interval, a 0.5-mile extension of shoreline advance is apparent. This reach of shoreline appears isolated and is likely not related to impoundment. Downdrift of the MSC, the small impoundment fillet adjacent to the south jetty advanced an additional 321 ft. The reach of shoreline recession noted in the 1963 to 1965 interval migrated 1 mile northeast, and the linear extent decreased by 0.5 mile. Recession rates in this

reach ranged from 20 to 50 ft/year. Towards the tip of Matagorda Peninsula, a subaerial sand flat emerged, resulting in high (maximum 290 ft/year) shoreline advance rates. On average, the shoreline advanced at a rate of 59 ft/year during this interval. It is hypothesized that material comprising this accretion was derived from scouring of the MSC as the flow through the inlet began to increase.

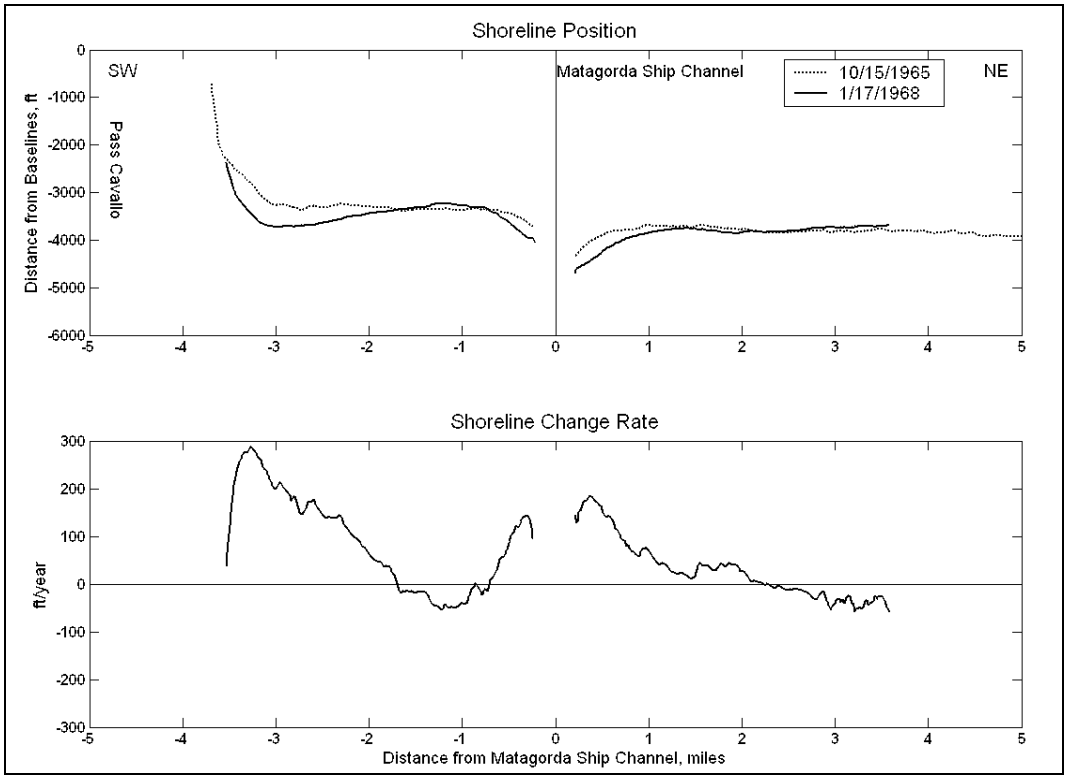

Figure 11. Shoreline position and change rate, 1965 to 1968

Interval 3: 1968 to 1974 (6.4 years). The average shoreline change rate during this interval was a recession of 29 ft/year. Shoreline advance occurred updrift of the MSC and at the tip of Matagorda Peninsula (spit progradation). Recession was observed between the MSC and the southwest tip of Matagorda Peninsula (Figure 12). Recession rates averaged 79 ft/year (maximum of 175 ft/year) and occurred primarily in the form of removal of the subaerial sand flat observed in the previous interval. During this interval, material removed from this flat was transported and deposited at the southwest terminus of Matagorda Peninsula. Aerial photographs from this period show that the spit morphology matured from an ephemeral inter- to supra-tidal sand flat in 1968 to an elongated spit with a developing vegetated dune field in 1974.

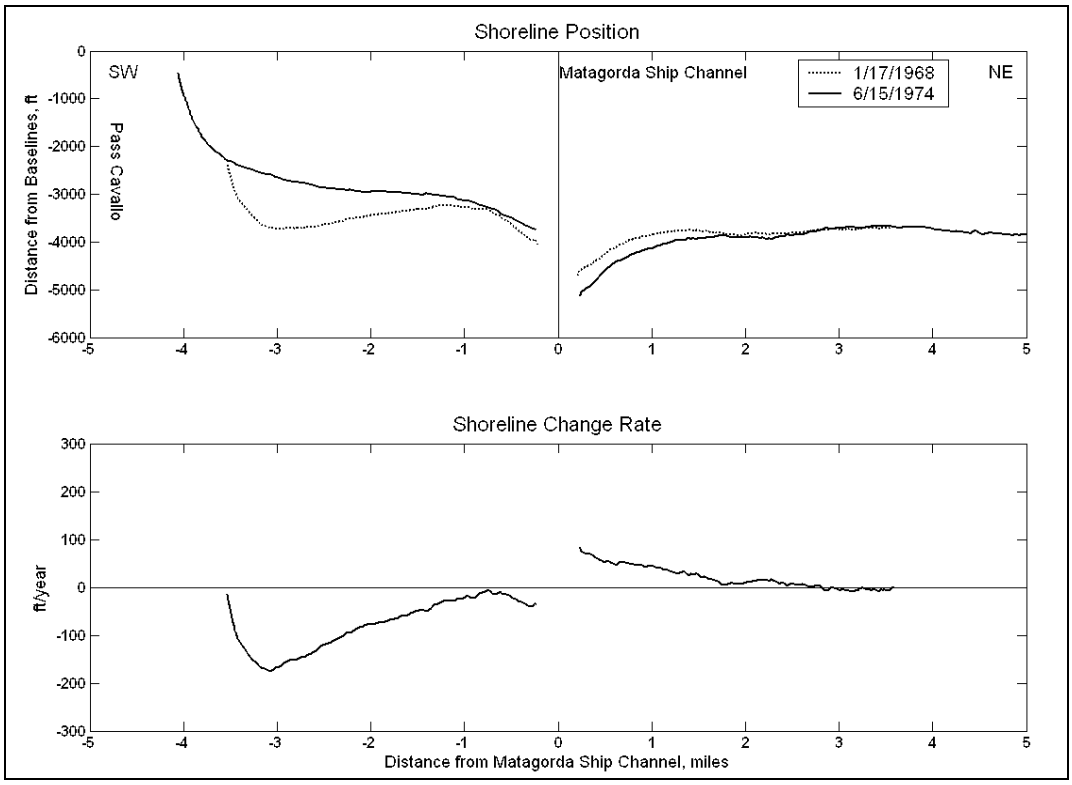

Figure 12. Shoreline position and change rate, 1968 to 1974

Interval 4, 1974 to 1978 (4.5 years). Between 1974 and 1978, the magnitude of shoreline change updrift and downdrift of the MSC decreased from rates observed in previous intervals (Figure 13). Updrift of the MSC, the shoreline adjacent to the north jetty advanced 109 ft, about one-quarter of the change observed during the previous interval. Shoreline advance rates updrift of the north jetty averaged 28 ft/year. Shoreline recession occurred for 2.5 miles downdrift of the MSC at an average rate of 20 ft/year (maximum of 34 ft/year). The southwestern 2 miles of Matagorda Peninsula experienced high rates of shoreline advance, with rates averaging 125 ft/year.

The Matagorda Peninsula spit appears to have experienced overwash between 1974 and 1978. In contrast to the vegetated developing dune field apparent in the 1974 image, the spit appears to have lower elevation and greater width (Figure 14). It is possible that a portion of the shoreline advance observed at the tip of Matagorda Peninsula during this interval was caused by flattening and spreading of the spit dune field by washover.

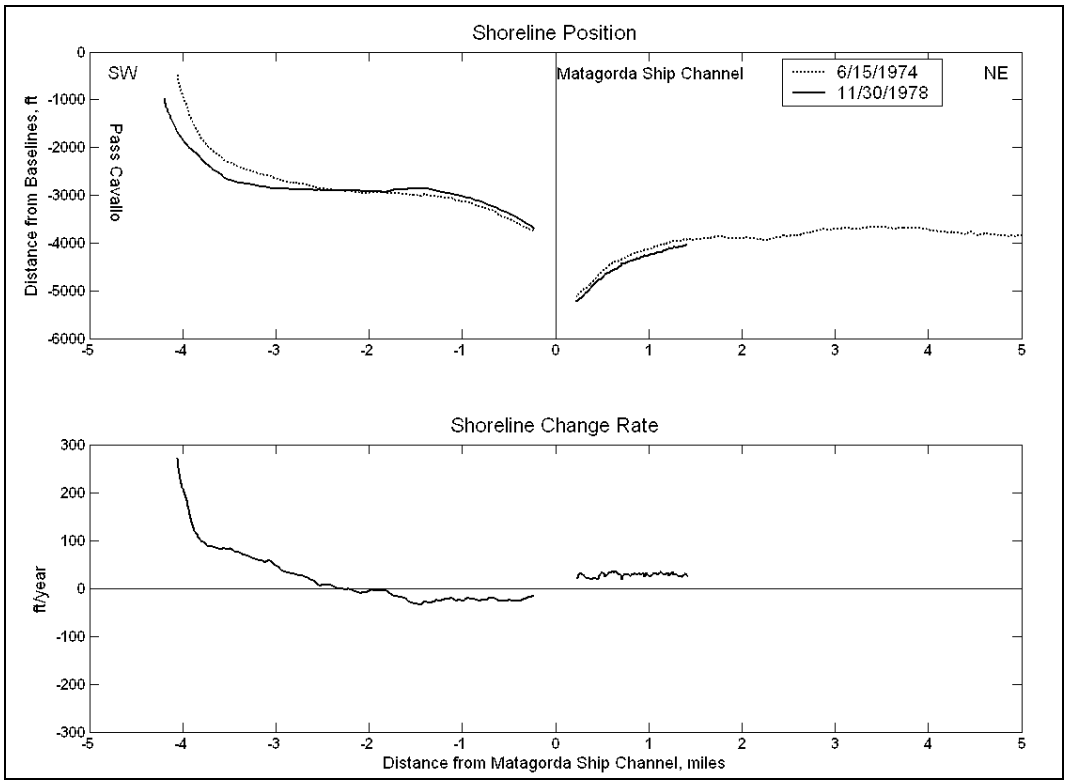

Figure 13. Shoreline position and change rate, 1974 to 1978

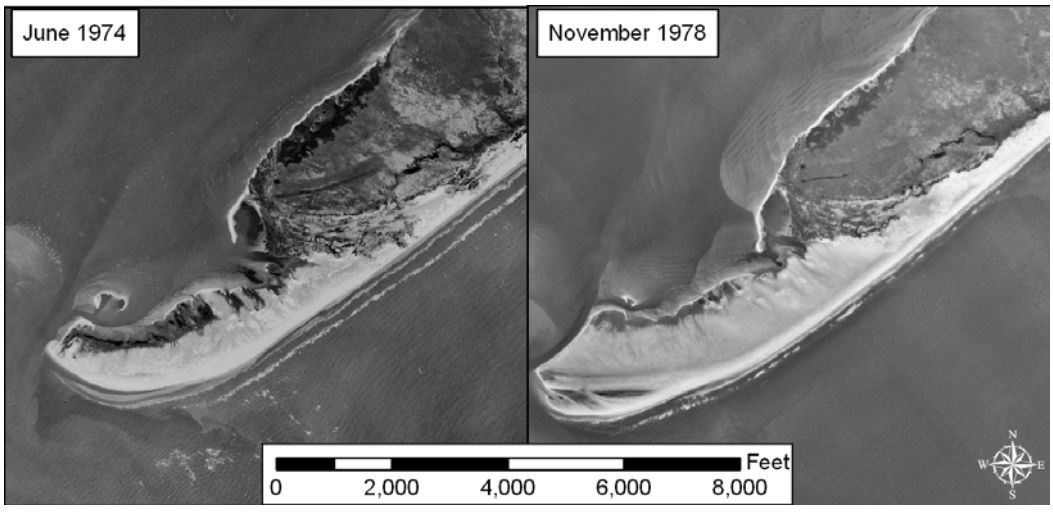

Figure 14. June 1974 and November 1978 aerial photographs of the Matagorda Peninsula Spit

Interval 5: 1978 to 1982 (3.5 years). Between 1978 and 1982, the recession area downdrift of the MSC lengthened by about 1 mile, for a total length of 3.5 miles (Figure 15). The average rate of shoreline recession in this area was 25 ft/year, with a maximum recession rate of 46 ft/year. Shoreline change rates updrift of the MSC increased to an average of 46 ft/year, with a peak rate of 66 ft/year. Net shoreline advance adjacent to the north jetty was 232 ft. Spit progradation and net shoreline advance at the tip of Matagorda Peninsula continued during this interval. Shoreline advance rates at the tip of Matagorda Peninsula averaged 125 ft/year, with a maximum rate of 217 ft/year.

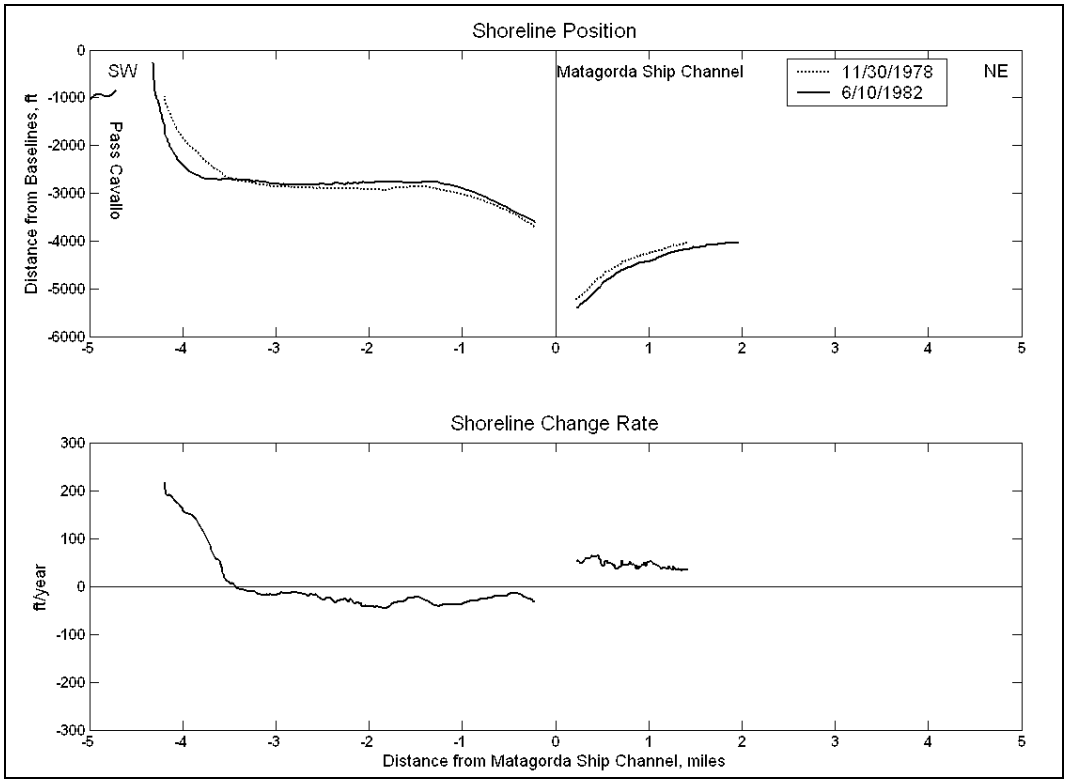

Figure 15. Shoreline position and change rate, 1978 to 1982

Interval 6: 1982 to 1986 (4.4 years). Coverage for this interval was limited to shorelines directly adjacent to the MSC and the southwest tip of Matagorda Peninsula (Figure 16). The shoreline updrift of the MSC continued to advance, but at a lower rate than previously observed (averaging 18 ft/year). Net shoreline advance adjacent to the north jetty was 39 ft. Spit progradation combined with shoreline advance continued at the southwest tip of Matagorda Peninsula during this interval. Rates of shoreline advance averaged 202 ft/year for the spit area during this interval.

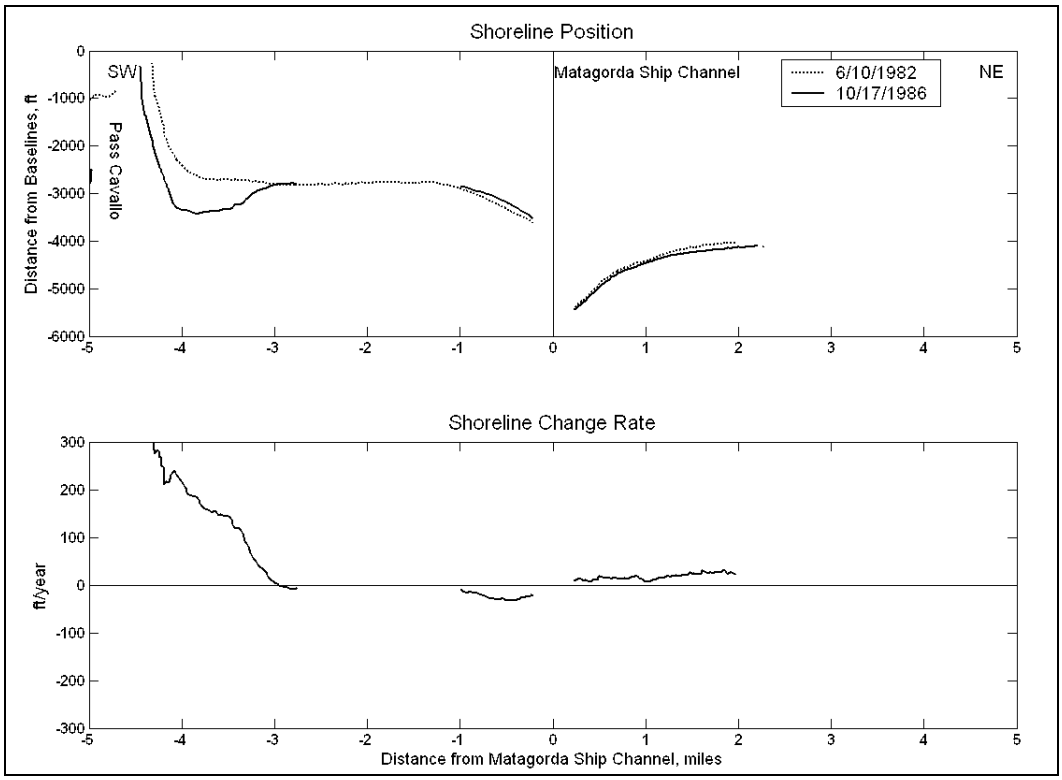

Figure 16. Shoreline position and change rate, 1982 to 1986

Interval 7: 1986 to 1988 (1.9 years). The 1986 to 1988 interval is notable for limited progradation of the spit at the tip of Matagorda Peninsula (Figure 17) although high rates of shoreline advance persisted in the spit area (averaging 160 ft/year). Shoreline advance rates updrift of the north jetty continued the trend of lower rates observed in the previous interval. The average rate of shoreline advance updrift of the north jetty was 24 ft/year, and net shoreline advance adjacent to the jetty was 64 ft.

Interval 8: 1988 to 1995 (6.5 years). This interval exhibited mixed shoreline change downdrift of the MSC and continued relatively lower rates of accretion updrift (Figure 18). Downdrift of the MSC, shoreline change rates ranged from 15 ft/year of recession to 33 ft/year of advance. On average, the shoreline within the 3.5 miles reach downdrift of the MSC advanced at a rate of 6 ft/year. Updrift of the MSC, shoreline advance rates averaged 25 ft/year (maximum 30 ft/year); net shoreline advance was 177 ft. Similar to the prior interval, progradation of the southwest tip of Matagorda Peninsula was limited. The rate of shoreline advance in the area of historical spit progradation beginning 3.5 miles southwest of the MSC was much lower than during any previous intervals, averaging 17 ft/year. This is a large departure from the average advance rates previously observed (magnitude <100 ft/year). Maximum rates of change remained high, with the maximum rate at the tip of the peninsula reaching 190 ft/year.

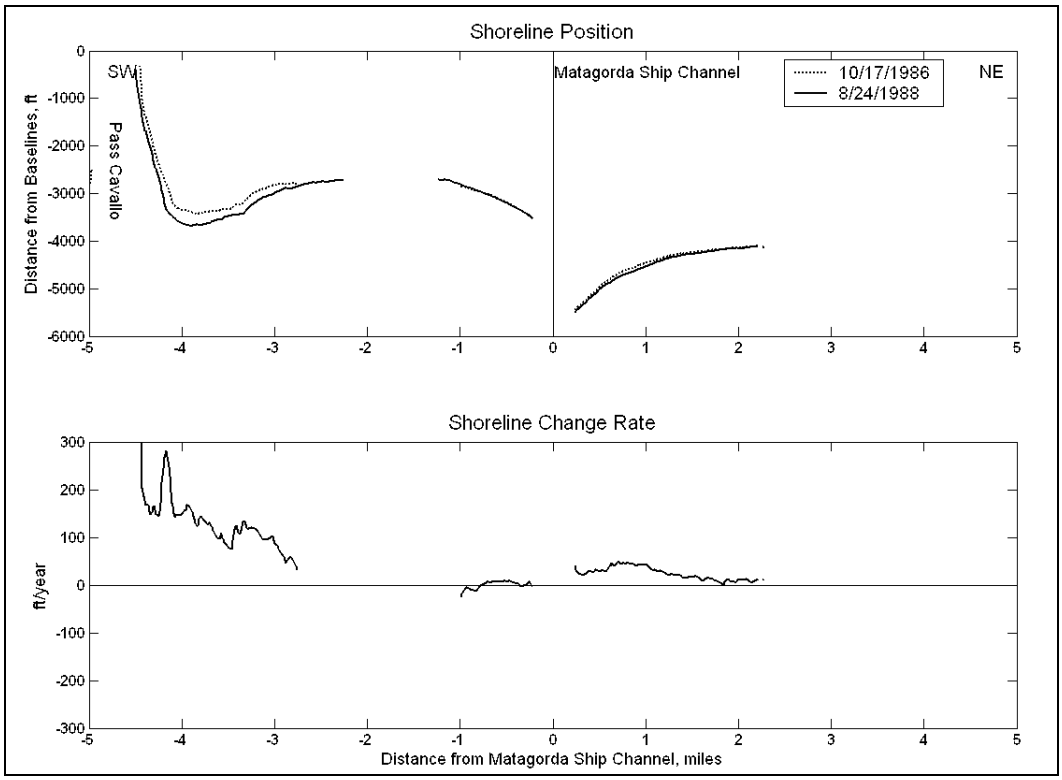

Figure 17. Shoreline position and change rate, 1986 to 1988

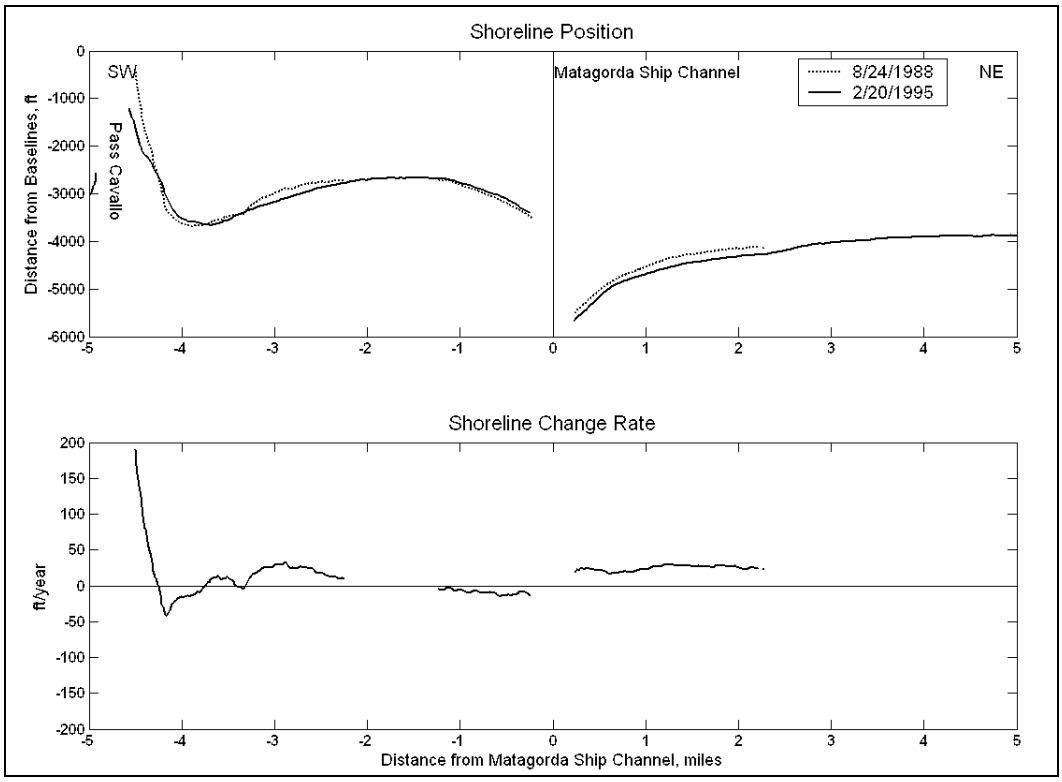

Figure 18. Shoreline position and change rate, 1988 to 1995

Interval 9: 1995 to 2000 (5.3 years). The 1995 to 2000 interval offered greater coverage of the updrift shoreline. (The horizontal axis of Figure 19 extended by 1 mile further updrift than for previous intervals to display this coverage.) Shoreline change during this interval indicates that the impoundment fillet had extended to reach approximately 5 miles updrift of the MSC, an increase of 2 miles from 1974. Shoreline advance rates within this reach averaged 10 ft/year and generally increased toward the north jetty. Compared to shoreline change rates for previous intervals, the maximum rates (22 ft/year) during this interval were similar to the average rates for the 1988 to 1995 interval (25 ft/year).

Downdrift of the MSC, the shoreline exhibited recession, with some isolated pockets of advance. Downdrift of the south jetty to the extent of the 1963 shoreline (3.5 miles), the average rate of shoreline recession was 4 ft/year. Mixed erosion and accretion are observed within the area of the historical spit (3.5 miles southwest of the MSC to the southwest tip of Matagorda Peninsula). Of note and contrary to prior trends, spit growth ceased, and the tip of Matagorda Peninsula transgressed to the northeast. The average change rate in this reach was a shoreline advance of 50 ft/year, with maximum rates of 100 ft/year.

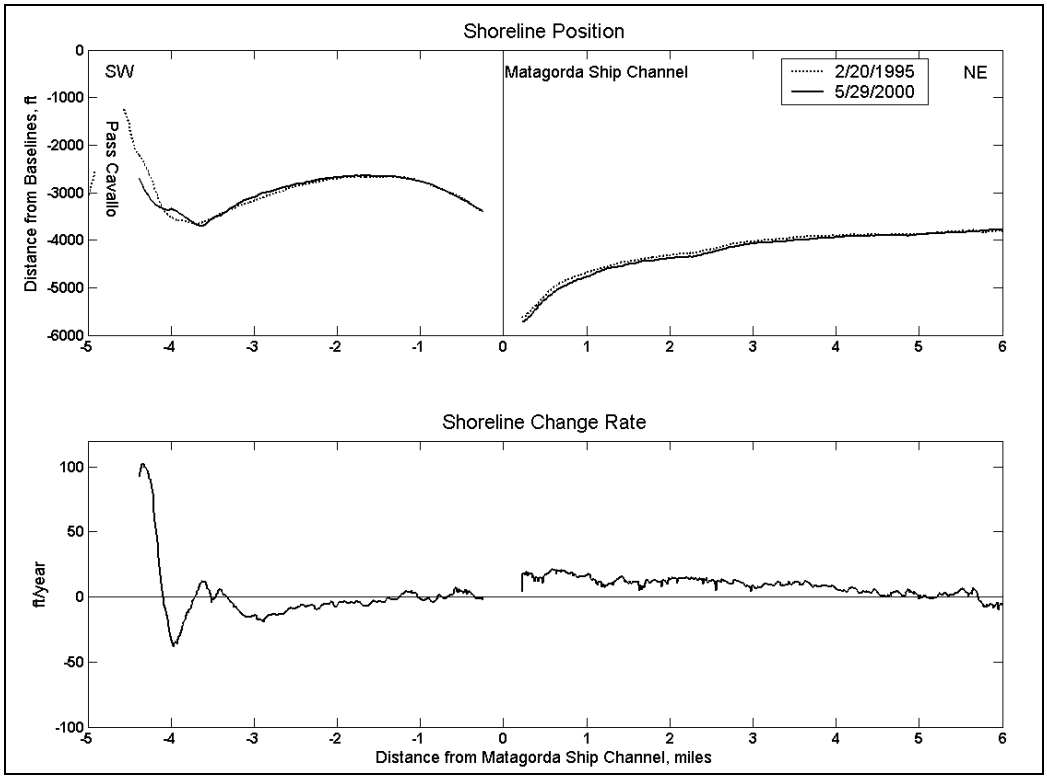

Figure 19. Shoreline position and change rate, 1995 to 2000

Long-term shoreline change: 1963 to 2000 (36.7 years). Long-term change was evaluated between the 1963 and 2000 shorelines. Both end-point and linear regression change rates were calculated for this interval (Figure 20). Shoreline change rates in the area of spit progradation at the tip of Matagorda Peninsula were calculated by using the 1995 bay-side shoreline (farthest extent of growth) of the spit as a proxy to define new growth and advance of the Gulf of Mexico shoreline.

Long-term shoreline advance rates updrift of the MSC averaged 34 ft/year for the available extent of shoreline, with a maximum rate of 58 ft/year adjacent to the north jetty. Within the impoundment fillet, shoreline advance rates increased approaching the MSC north jetty. Average rates of shoreline advance in this area would be lower if the entire 5-mile impoundment reach were included. Comparison of the 1968 and 2000 (not shown) shorelines indicated an average rate of shoreline advance of 15 ft/year within an impoundment zone extending for 4.5 miles northeast of the MSC. The lower-magnitude long-term rate of shoreline advance indicated by the linear regression rate reflects the tendency towards lower rates subsequent to 1982. Net shoreline advance adjacent to the north jetty at the MSC was 2,080 ft.

Long-term rates indicate shoreline recession downdrift of the MSC. The average rate of shoreline recession was 9 ft/year in the area updrift of spit progradation. Because of data constraints, calculation of a long-term linear regression rate in the downdrift area was limited; however, the results suggest higher intermediate rates of recession than indicated by the end-point method. Comparison of 1968 and 2000 shorelines indicate that the southwest terminus of Matagorda Peninsula prograded by approximately 0.8 miles. Shoreline advance rates in the area of progradation averaged 82 ft/year, with a maximum rate of 89 ft/year.

Spit progradation and shoreline advance at the tip of Matagorda Peninsula did not appear to be supported by recession of the shoreline downdrift of the MSC. Morton (1977b) noted excess material in the downdrift compartment, described the source as “problematic,” and suggested bank and channel erosion as potential sources. These sources are inadequate to account for the observed long-term spit growth. It is hypothesized here that sediments from offshore deposits are also contributing to growth at the tip of Matagorda Peninsula. One likely source is partial collapse of the ebb-tidal shoal at Pass Cavallo. Because the tidal prism has been reduced since growth of the Colorado River delta in 1935 and completion of the MSC jetties in 1966, much of the existing ebb-tidal shoal would have migrated onshore.

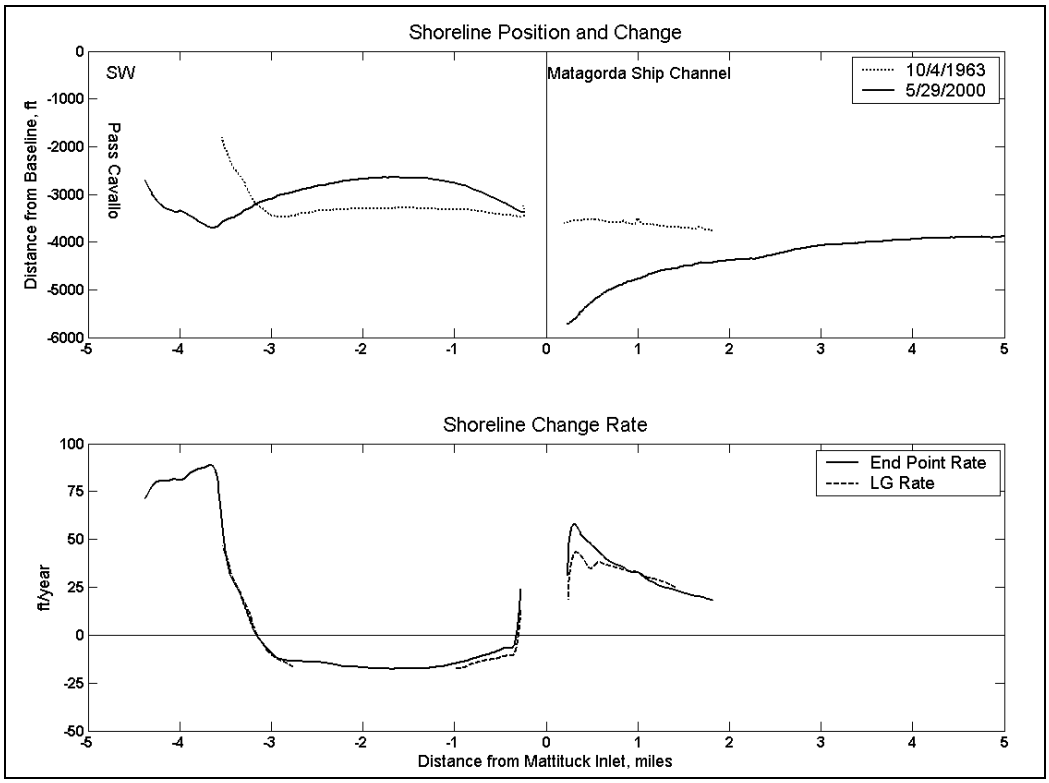

Figure 20. Shoreline position, end-point, and linear regression (LG) change rates between 1963 and 2000

Matagorda Bay shoreline change

Shoreline change along the bay shore of Matagorda Peninsula in the vicinity of the MSC was evaluated for the interval 1956 to 2002. Available shoreline data typically extended for 1.5 miles northeast and southwest of the MSC. Shoreline change was evaluated from a baseline established on the bay side of the shoreline following the general orientation of Matagorda Peninsula (Figure 21).

Nine shorelines were chosen to represent bay shoreline response to the construction of the MSC (Table 7). Similar to the Gulf of Mexico shoreline analysis, short-term shoreline change rates were evaluated for each interval via the end-point method, and both the end-point and linear-regression methods were applied to determine long-term rates. Two end-member intervals were calculated for the bay shorelines; 1956 to 2003, and 1963 to 2003. As the MSC was dredged, material was pumped to each side of the channel, and large deposits were placed along the bay shoreline to protect the channel from wave action (discussed in Chapter 1). The 1956 shoreline is the latest available date before construction of the channel. The 1963 shoreline captures the placement of this material and provides a basis to investigate post-construction shoreline evolution. Successive intervals are discussed first, and then long-term change rates follow.

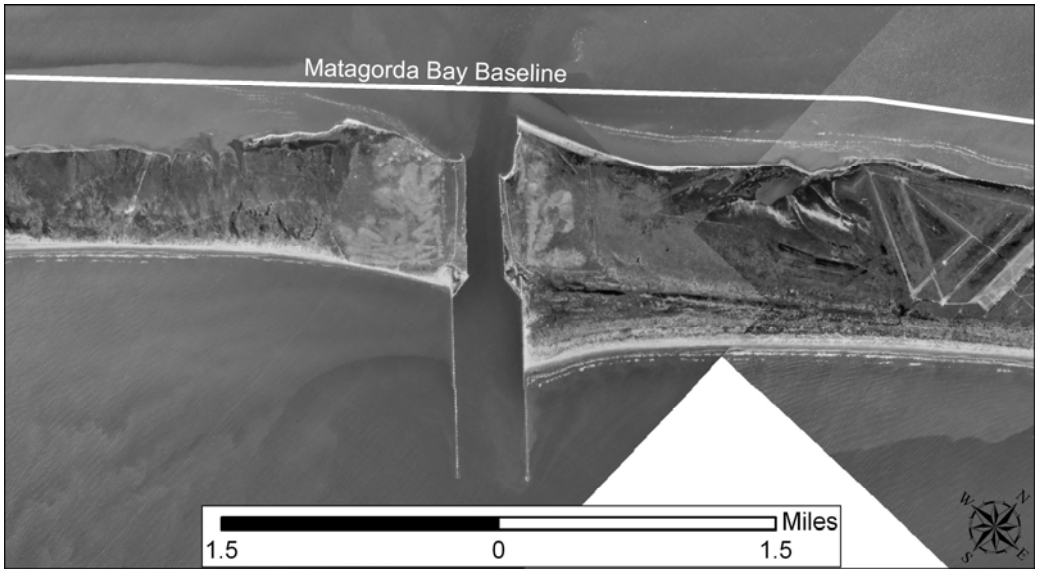

Figure 21. Baseline for Matagorda Bay shoreline change analysis

Table 7
Selected Matagorda Bay Shorelines

Year	Date
1956	9 September
1963	4 October
1965	15 October
1968	17 January
1978	30 November
1982	10 June
1986	17 October
1995	20 February
2002	6 August

Interval 1: 1956 to 1963 (7.1 years). Changes for this interval were dominated by advance of the bay shoreline on both sides of the MSC bay entrance by placement of dredged material (Figure 22). As discussed in Chapter 1, material dredged out of the channel was placed along the bay shoreline on either side of the channel to protect the construction from wave action. Figure 23 shows the placement areas adjacent to the completed channel. Placement of material advanced the shoreline as much as 1,500 ft to the southwest and 900 ft to the northeast. The area of shoreline advance beginning 1.25 miles northeast of the MSC is caused by spit migration along the bay shoreline.

Interval 2: 1963 to 1965 (2.0 years). This interval spans ongoing construction at the MSC entrance. A small jetty was constructed at the southwest edge of the navigation channel by June 1964 (south bay jetty), and another small jetty was constructed by November 1964 on the northeast bay shoreline (north bay jetty). Shoreline change during this interval shows rapid recession of both areas of dredged material placement (Figure 24). The spit located to the northeast migrated 0.25 mile to the southwest during this interval, resulting in an isolated maximum of the shoreline change rate 1 mile updrift of the channel.

Interval 3: 1965 to 1968 (2.3 years). Shoreline change during the 1965 to 1968 interval is shown in Figure 25. Northeast of the MSC, sediment began to impound updrift of the north bay jetty, resulting in a smoothing of the shoreline. The spit described in the two previous intervals continued to migrate southwest, which occurred at a slightly higher rate during this interval. Southwest of the channel, the dredged material placement area continued to experience high rates of shoreline recession. The planform of this feature appears to have rotated around the south bay jetty.

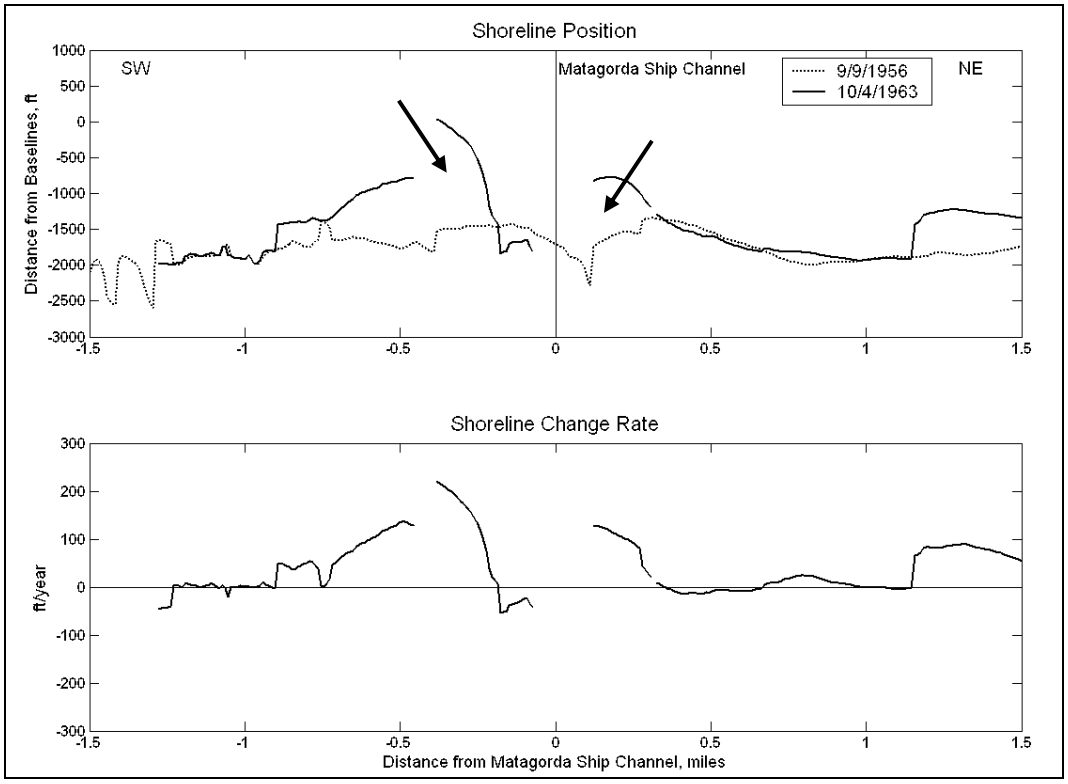

Figure 22. Shoreline position and change rate, 1956 to 1963. Arrows indicate areas of dredged material disposal

Figure 23. Dredged material placement, bay side of the MSC, October 1965

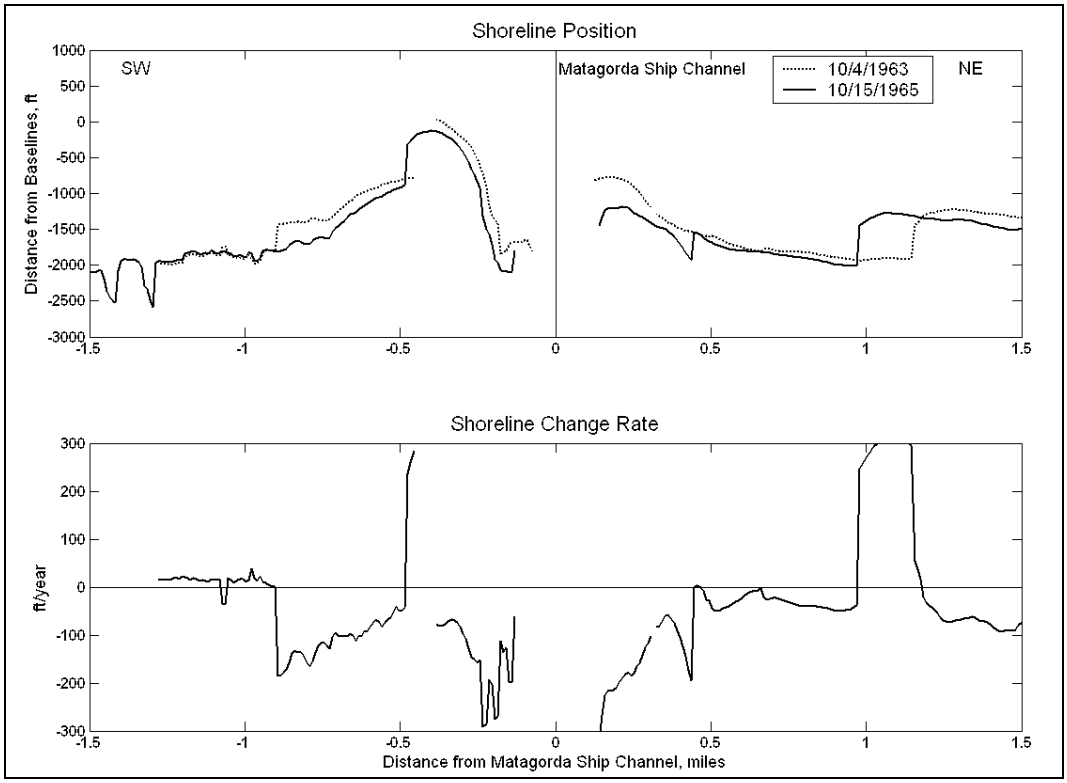

Figure 24. Shoreline position and change rate, 1963 to 1965

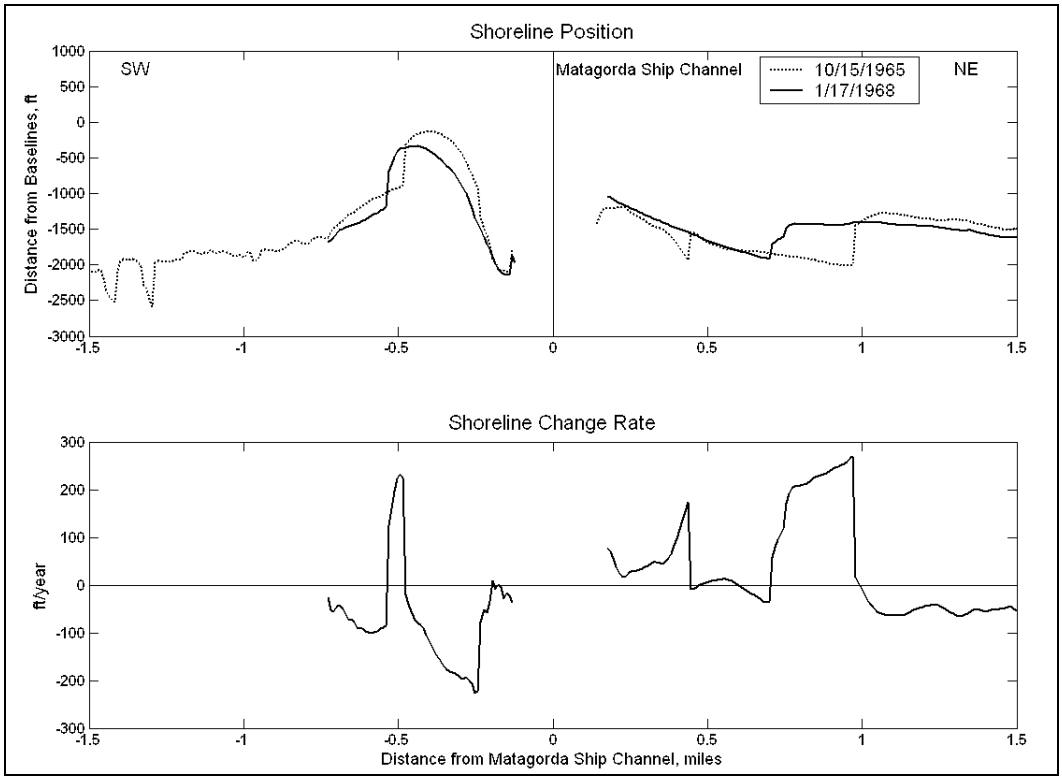

Figure 25. Shoreline position and change rate, 1965 to 1968

Interval 4: 1968 to 1978 (10.9 years). The southwest shoreline continued to recede and rotate around the south bay jetty during this interval. Material eroded from the disposal area was dispersed to the southwest, resulting in shoreline advance (Figure 26). Mixed shoreline recession and advance occurred to the northeast. Material supplied by erosion of the spit supported the high rates of shoreline advance observed northeast of the channel during this interval.

Interval 5: 1978 to 1982 (3.5 years). During this interval, the northeast shoreline continued to experience mixed recession and advance, while the southwest shoreline receded and dispersed (Figure 27). Sediment impoundment northeast of the channel resulted in shoreline advance rates of as much as 10 ft/year. Farther to the northeast, shoreline recession rates were 15 to 25 ft/year. Southwest of the channel, the shoreline receded in the dredged material placement area. Recession rates increased with distance away from the channel. Material placed into transport by this recession dispersed to the southwest, resulting in an isolated maximum of shoreline advance 1 mile southwest of the channel.

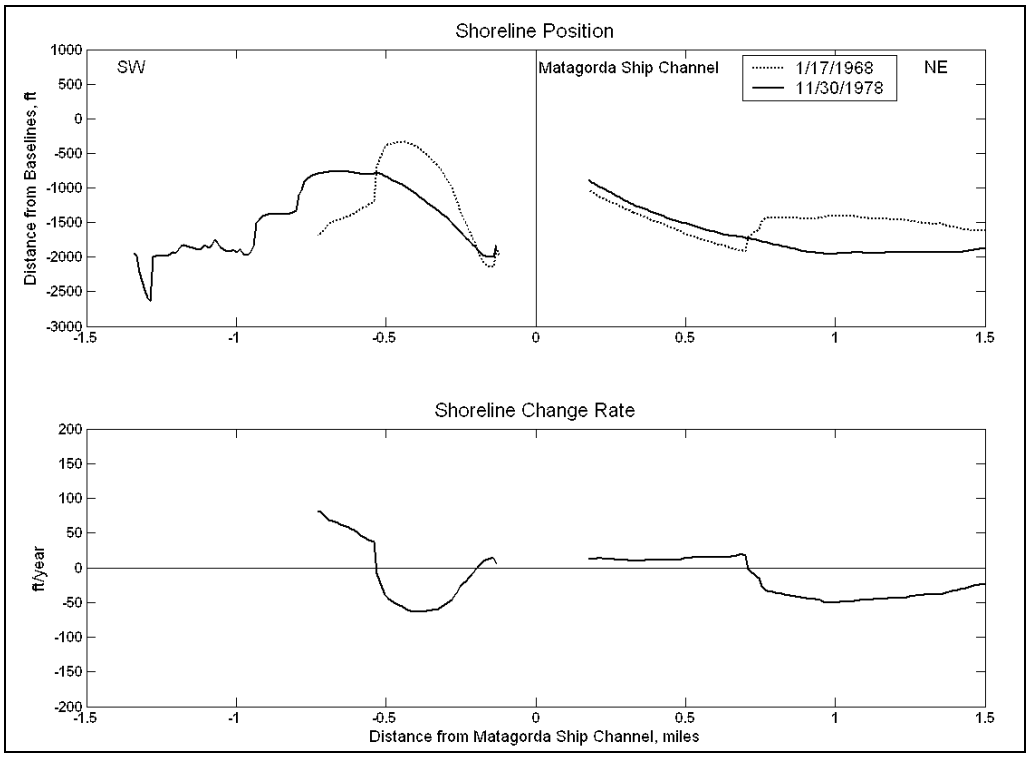

Figure 26. Shoreline position and change rate, 1968 to 1978

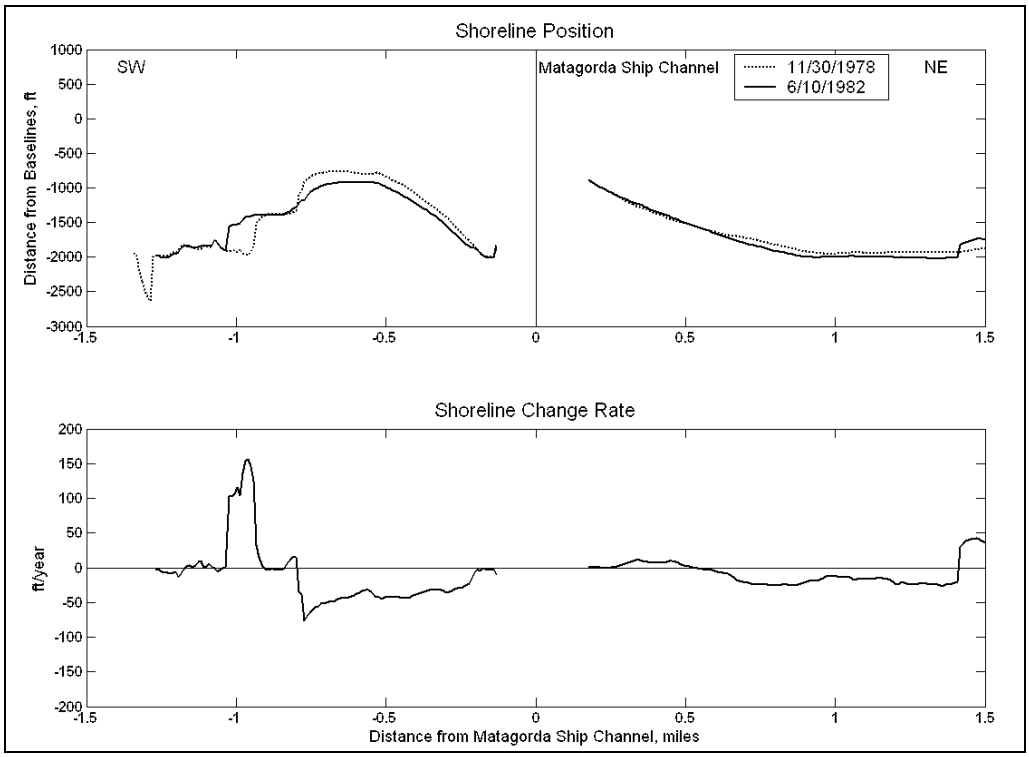

Figure 27. Shoreline position and change rate, 1978 to 1982

Interval 6: 1982 to 1986 (4.4 years). Shoreline changes during this interval were similar to Interval 5. Shoreline change rates varied between 35 ft/year of recession and 38 ft/year of advance (Figure 28). The lower magnitude of change rates implies that the shoreline had begun to approach an equilibrium condition.

Interval 7: 1986 to 1995 (8.35 years). The 1986 to 1995 interval exhibits shoreline change trends similar to the prior two. The northeast shoreline experienced mixed accretion and erosion, while the southwest shoreline experienced further recession and dispersion of material (Figure 29). Recession rates along the southwest shoreline remained steady for about a mile, in contrast to the earlier intervals, where recession rates became greater with increasing distance from the channel.

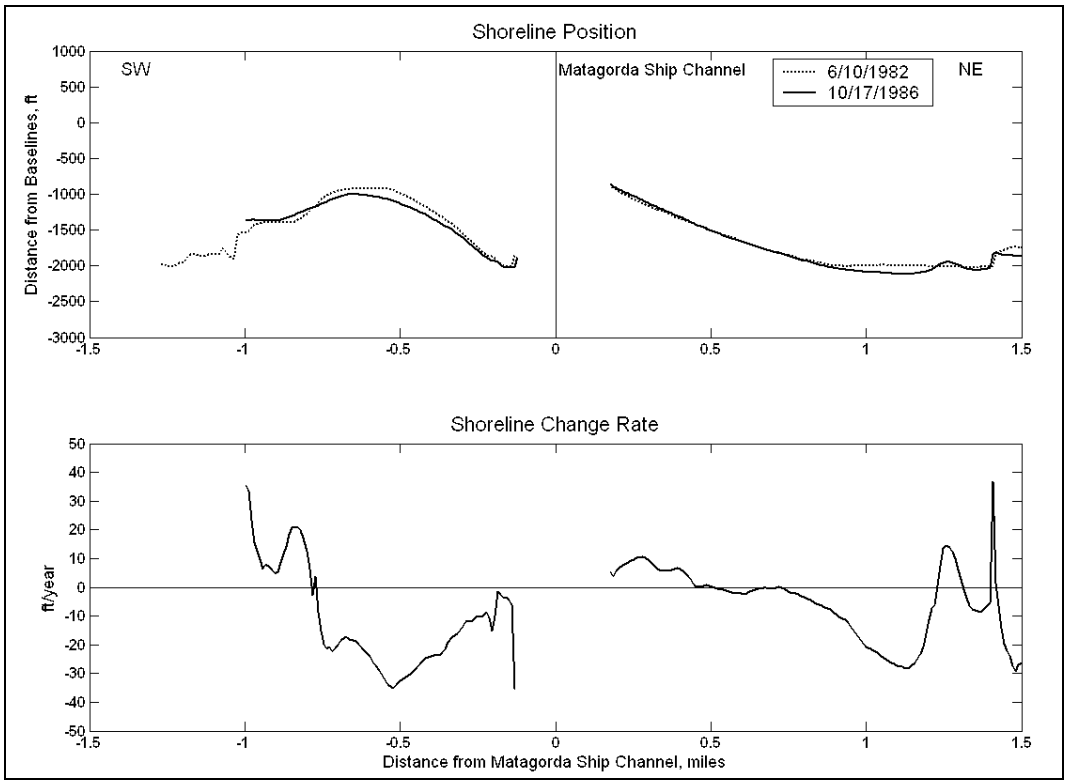

Figure 28. Shoreline position and change rate, 1982 to 1986

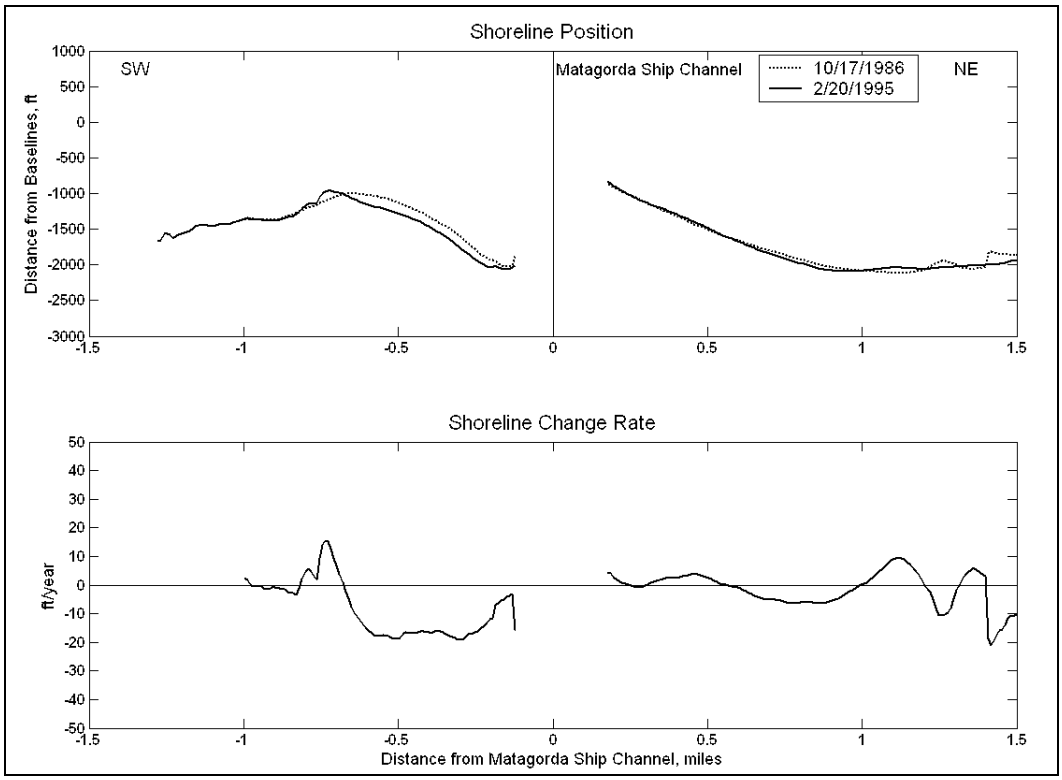

Figure 29. Shoreline positon and change rate, 1986 to 1995

Interval 8: 1995 to 2002 (7.46 years). The final interval exhibits trends similar to those observed subsequent to 1978. Mixed shoreline advance and recession are apparent to the northeast, although the trend was towards recession for this interval (Figure 30). A pocket of recession with rates approaching 30 ft/year appeared 1 mile northeast of the channel. To the southwest, the shoreline continued to recede and disperse in the area of dredged material placement. Recession rates in the placement area tended to be lower than in previous intervals, ranging between 4 and 16 ft/year. These rates are of similar magnitude to those observed 1.25 to 1.5 miles northeast of the MSC.

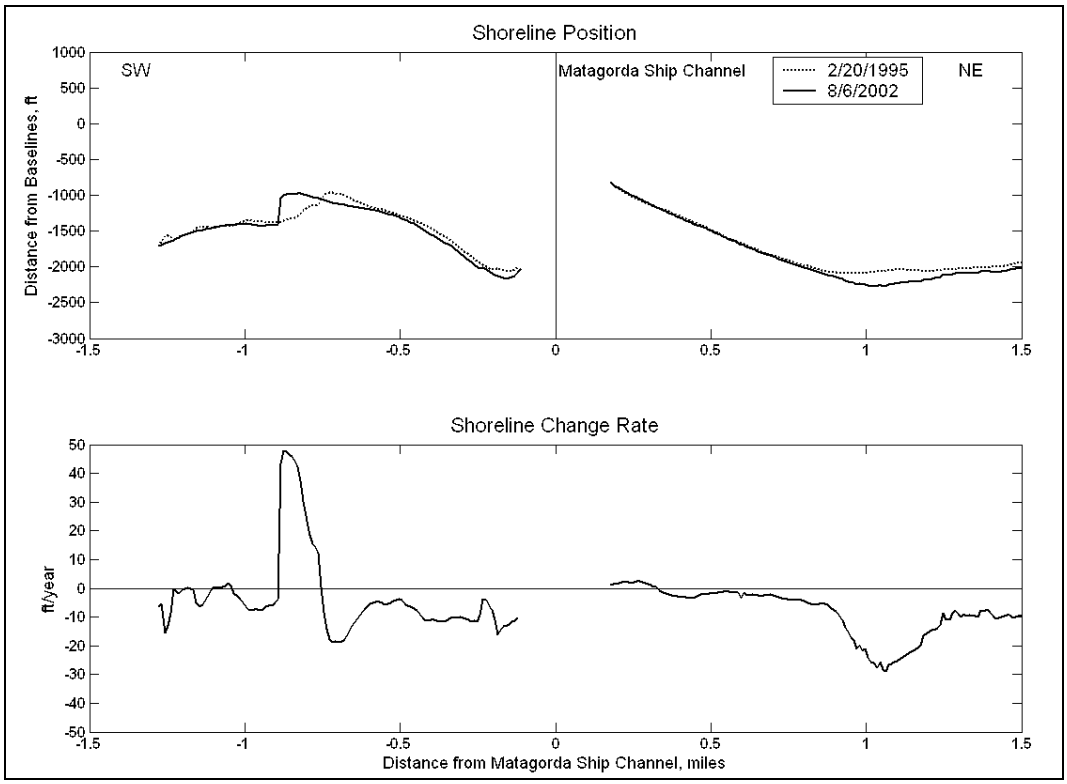

Figure 30. Shoreline position and change rate, 1995 and 2002

Long-term change. Two intervals were selected for the calculation of long-term shoreline change rates along the bay shoreline: 1956 to 2002 (45.9 years) and 1963 to 2002 (38.9 years). Pre-construction (1956) and modern (2002) shoreline configurations and shoreline change are shown in Figure 31. Three areas of shoreline change attributable to the construction of the MSC can be identified: (a) shoreline advance 0.75 to 1.25 miles to the southwest, (b) shoreline recession for 0.25 mile southwest, and (c) shoreline advance due to impoundment for 0.7 mile to the northeast (Figure 31). Southwest of the MSC, net shoreline advance occurred over a greater area than shoreline recession. Shoreline advance in the area was enhanced by the placement of dredged material along the bay shoreline during channel construction, represented in the calculated linear regression rate of change for this time period. Shoreline recession rates 1.25 miles and further northeast from the MSC are likely representative of the local long-term natural recession rate for the bay shoreline. These recession rates range from 5 to 8 ft/year and are approximately twice the magnitude of those observed by McGowen and Brewton (1975) for the period 1946 to 1972.

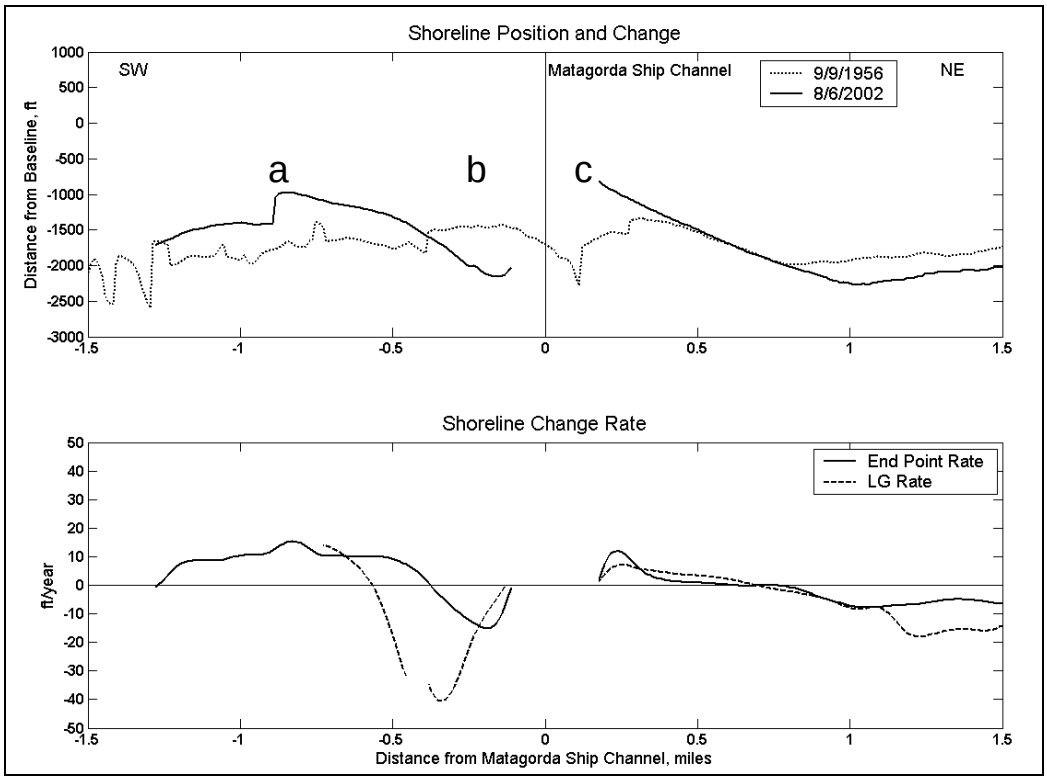

Figure 31. Long-term shoreline position and change rate, 1956 (pre-MSC) to 2002. The letters a, b, and c refer to areas of shoreline change attributable to the construction of the MSC

The post-construction (1963) and modern (2002) shorelines are compared in Figure 32. The 1963 shoreline shows the placement of dredged material along the bay shoreline. By 2002, this material had eroded and dispersed to the southwest. Shoreline change northeast of the MSC was similar to that shown in the 1956 to 2002 analysis.

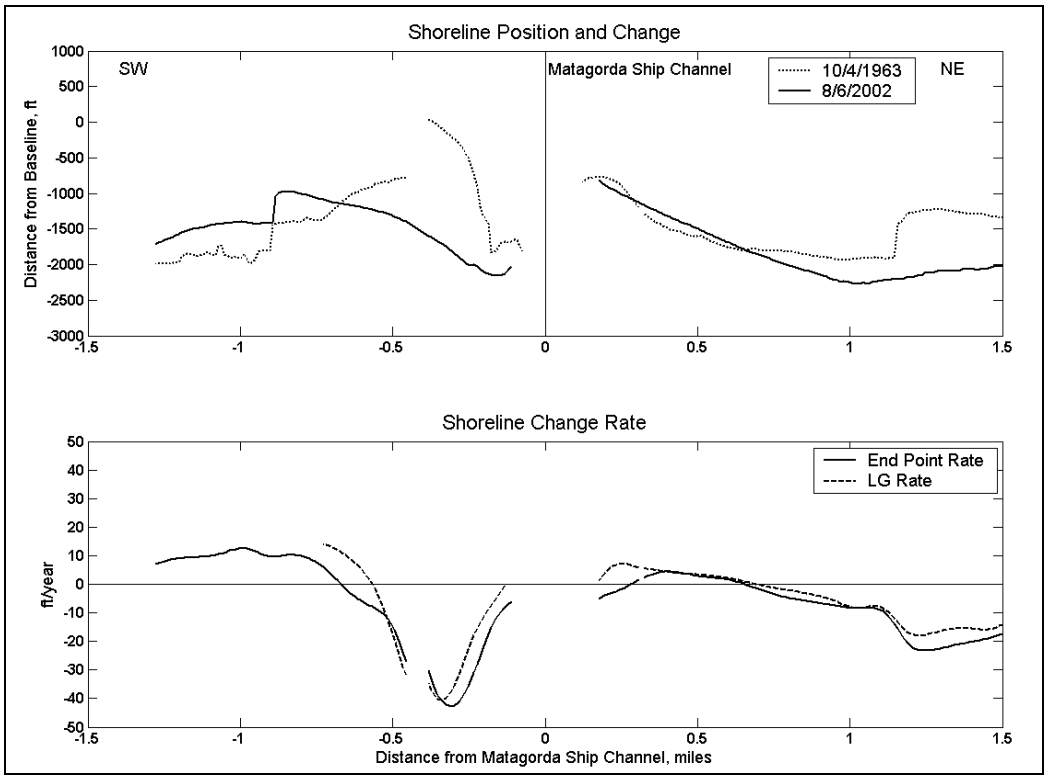

Figure 32. Long-term shoreline position and change rate, 1963 (post-MSC) to 2002

Pass Cavallo

This section discusses spit growth and encroachment of Pass Cavallo by Matagorda Peninsula and Matagorda Island.

Spit growth

The tidal prism at Pass Cavallo decreased as the Colorado River delta progradated across Matagorda Bay (1929 to 1935) and later when the MSC opened in 1963 (Chapter 1). The opening of the MSC resulted in additional shoaling and spit growth into Pass Cavallo from both Matagorda Peninsula and Matagorda Island. Spit growth of Matagorda Peninsula and Matagorda Island in response to the construction of the MSC entrance is evaluated in this section.

Spit growth was evaluated by establishing two baselines fronting the Gulf of Mexico shorelines of Matagorda Peninsula and Matagorda Island (Figure 33). For Matagorda Peninsula, the baseline originated at the south jetty of the MSC. The origin of the Matagorda Island baseline was placed at the observed origin of the Matagorda Island spit. Spit growth along each baseline was measured in the GIS environment using BeachTools (see Shoreline change rate analysis, this chapter). Perpendicular transects were generated by BeachTools along the baseline at 10-ft intervals. The distance of the last transect to intersect the spit shoreline was recorded for each date.

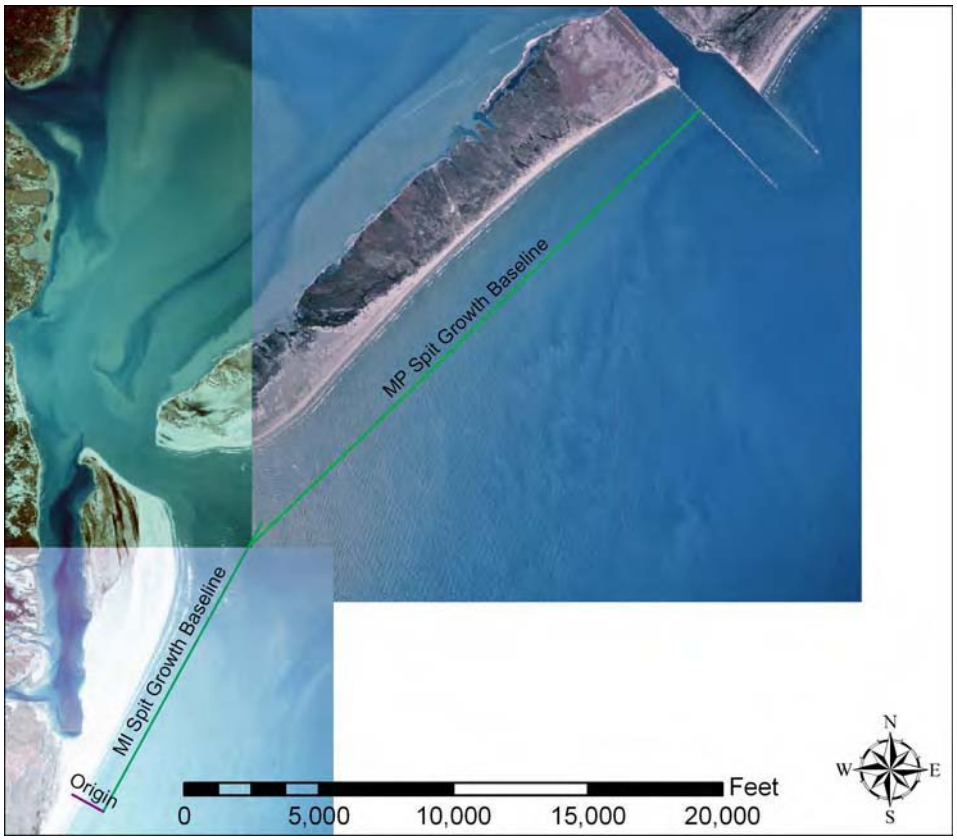

Figure 33. Spit growth baselines for Matagorda Island and Matagorda Peninsula

The evolution of Matagorda Peninsula and Matagorda Island can be generalized into three eras of morphologic behavior: (a) relative stability prior to 1963, (b) rapid growth from 1963 to the late 1980s, and (c) relative stability subsequent to 1990. During the first era, Matagorda Peninsula and Matagorda Island appear dynamically stable, as shown in Figure 34 and Figure 35. The only emergent feature was a small island between Matagorda Peninsula and Matagorda Island that first appeared in 1952. Although spit growth was minimal, significant shoaling of the inlet was observed during this era (Harwood 1973). For Era 1, Matagorda Peninsula receded approximately 290 ft, while Matagorda Island remained unchanged.

Era 2 is characterized by southwestward growth of Matagorda Peninsula that occurred in rapid, step-wise fashion. Periods of rapid growth were followed by periods of retarded growth and relative inactivity (Figure 34). Net progradation of Matagorda Peninsula between 1963 and 1988 was about 5,000 ft. A recurved spit emerged from Matagorda Island and rapidly prograded at a high, linear rate between 1978 and 1982. During these 4 years, the spit grew by about 8,200 ft. This high rate of growth continued through 1986, when the total spit length reached approximately 11,400 ft. The southwest tip of Matagorda Island and a portion of the shoreline experienced erosion through this period (Paine and Morton 1989); this material likely supported growth of the spit during this time. As it extended, the Matagorda Island spit prograded in a north-northeast direction and recurved towards Matagorda Island; therefore, growth should not be

interpreted as being directed only across the mouth of Pass Cavallo. The inlet channel at Pass Cavallo has historically migrated westward (Harwood 1973). Growth of the Matagorda Island spit into the inlet pushed the channel eastward, a reversal of the historical trend.

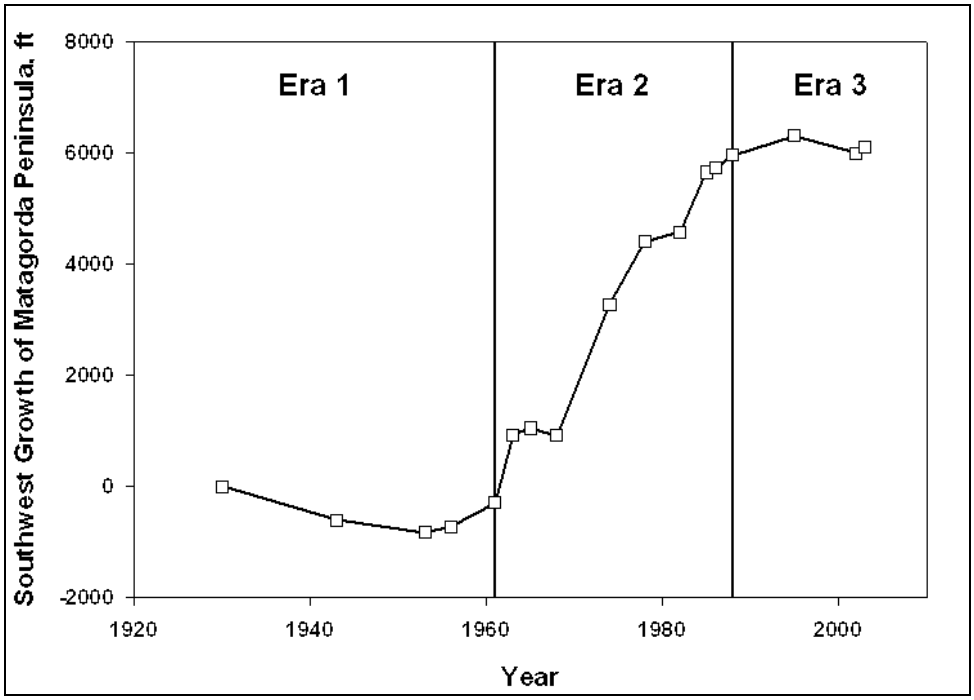

Figure 34. Growth of Matagorda Peninsula, 1930 to 2001

Era 3 represents a maturation of the system, as spit growth reached an apparent dynamic equilibrium with tidal forcing through Pass Cavallo in the late 1980s (Figure 34 and Figure 35). Between 1988 and 2003, growth rates of Matagorda Peninsula and Matagorda Island decreased. During this time, Matagorda Peninsula prograded 140 ft, while the Matagorda Island spit receded westward by 40 ft (1986-2003). In total, Matagorda Peninsula prograded by approximately 5,200 ft from 1963 to 2003, and the spit at Matagorda Island prograded by about 11,400 ft between 1974 and 2003. During the same period, the inlet width at Pass Cavallo decreased by approximately 9,300 ft.

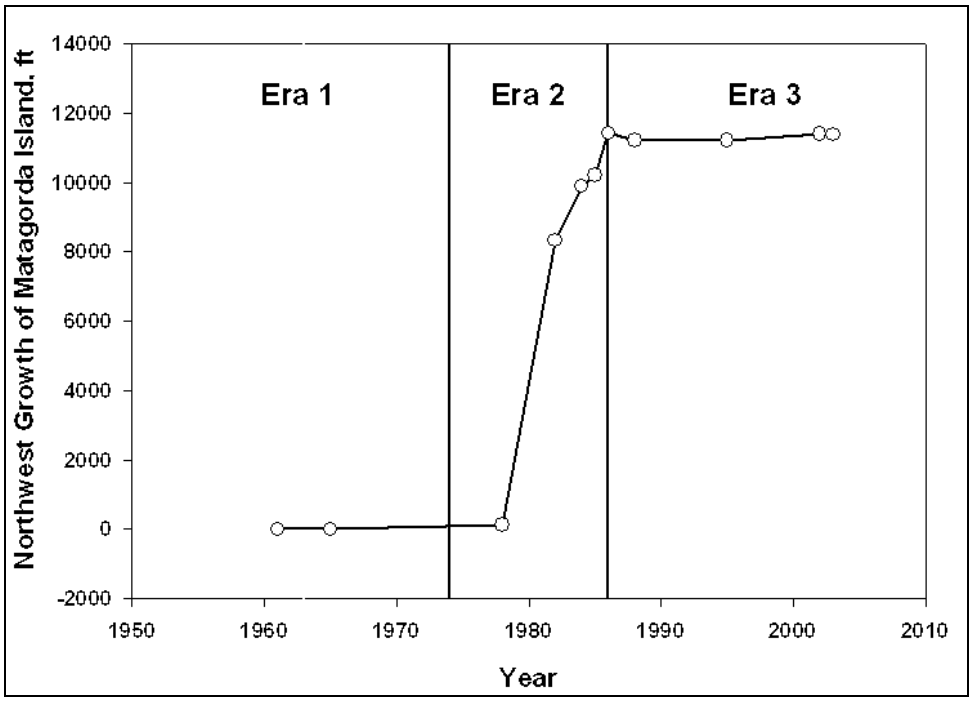

Figure 35. Growth of Matagorda Island, 1956 to 2000

Inlet width

The width of Pass Cavallo was measured from available shoreline data between 1856 and 1995. Measurement was limited to shoreline data that extended into the channel from both sides of the inlet. The inlet width was evaluated in ArcMap 8.3 GIS from the westernmost extent of Matagorda Peninsula to the easternmost extent of Matagorda Island. Each measurement was recorded along a reference line aligned to the axial orientation of Matagorda Peninsula. This line was positioned at the narrowest section of Pass Cavallo, and then the distance across the inlet was measured. Results are shown in Figure 36.

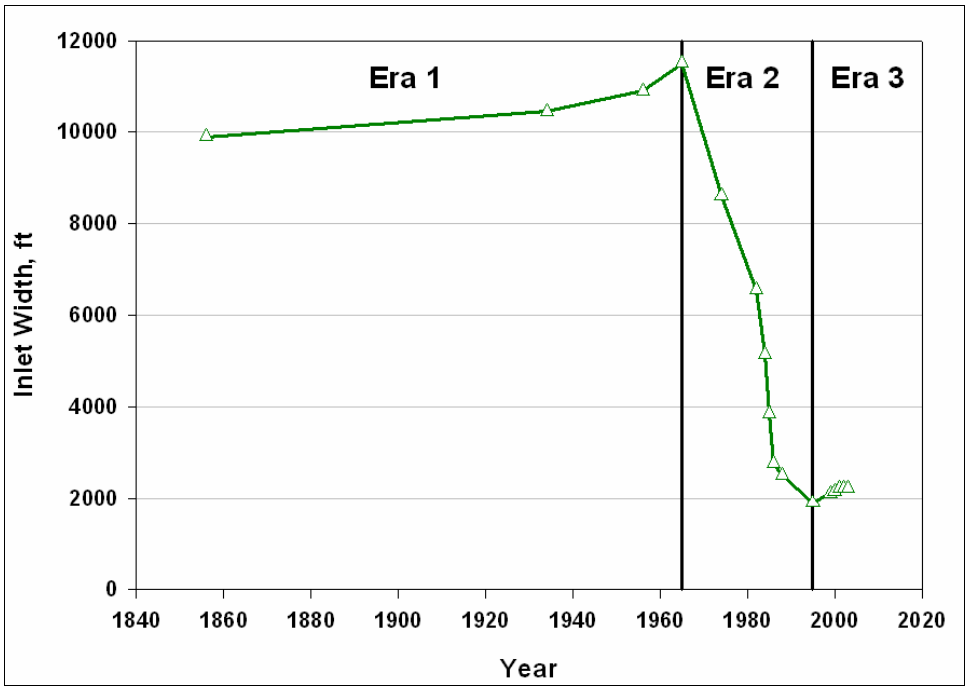

Figure 36. Inlet width at Pass Cavallo, 1856 and 2003

Pass Cavallo maintained a width near to or greater than 10,000 ft between 1856 and 1965 (Era 1). Although the overall width of the inlet was large during this time, a review of the literature indicates that the inlet was shallow. Harwood (1973) observed that the eastern portion of Pass Cavallo, previously a secondary tidal channel, shoaled between 1934 and 1952. Shoreline coverage during this period typically shows a sub-aerial island (Pelican Island) in the entrance, though the area was variable through time. A second sub-aerial island appeared after 1952, a sign of additional shoaling in the inlet (Harwood 1973). Inlet width increased slightly until the mid-1960s, reaching a maximum measured width of 11,500 ft in 1965. In 1961, Hurricane Carla made landfall at Pass Cavallo with an estimated maximum surge elevation of 12.1 ft. Extreme conditions associated with this hurricane created 32 washovers along Matagorda Peninsula (Morton et al. 1976) and presumably transported sediment out of Pass Cavallo to create the maximum width observed in 1965.

The loss of flow to the MSC in 1963 reduced the tidal discharge through Pass Cavallo. This resulted in increased sediment deposition in the channel. In response, inlet width decreased rapidly from 1965 to 1986 (Era 2). During this 21-year period, inlet width decreased by about 8,800 ft at a rate of approximately 417 ft/year. After 1986, the rate of inlet closure decreased. The minimum width of Pass Cavallo is observed at 2,100 ft in 1999. From 1999 to 2003, inlet width increased by about 130 ft. During Era 3, inlet width decreased by about 520 ft (31 ft/year).

Evolution of the tidal prism through Pass Cavallo and the MSC is discussed in Chapter 1 (Figure 4). The tidal prism through Pass Cavallo decreased rapidly after the construction of the MSC, reaching a minimum value in the late 1970s. Subsequently, the tidal prism has remained nearly constant, slightly increasing by

around 2004. The time history of the inlet width and spit growth at Pass Cavallo indicate that the morphologic system lagged behind stabilization of the tidal prism, requiring an additional 10 years to equilibrate. The decrease of inlet closure rates in the late 1980s and the stabilization of inlet width from the mid-1990s through 2003 suggest that Pass Cavallo is in, or near, dynamic equilibrium with the smaller tidal prism and wind-setup ebb current.

Summary

Review of the literature determined that Matagorda Peninsula has historically experienced shoreline recession (McGowen and Brewton 1975; Morton et al. 1976, 2004; Morton 1977a; Paine and Morton 1989; Gibeaut et al. 2000). Construction of the MSC resulted in shoreline advance through impoundment of sediment updrift, and downdrift shoreline recession due to sediment restriction by the jetties and channel. For shorelines adjacent to the MSC, the literature reports long-term advance rates reaching 26 ft/year updrift and recession rates of 16 ft/year downdrift. Rates of shoreline advance in the area of spit growth approach 82 ft/year (1974-2000) (Gibeaut et al. 2000).

Shoreline change rate analysis for the Gulf of Mexico shorelines adjacent to Matagorda Ship channel revealed trends and rates similar to those reported in the literature. Specific areas of updrift accretion, downdrift erosion, and spit progradation were identified and delineated. Impoundment was found to extend approximately 5 miles updrift of the MSC. The most reliable long-term average rate of shoreline advance for this reach was 15 ft/year. Average rates increase to 58 ft/year directly adjacent to the north jetty. Downdrift of the MSC, shoreline recession extends for 3.5 miles to the southwest terminus of the 1963 shoreline. An average long-term recession rate of 9 ft/year was calculated for this reach. Southwest spit progradation of Matagorda Peninsula occurred in response to the decrease in tidal exchange through Pass Cavallo. Average long-term rates of shoreline advance were calculated at 82 ft/year for the spit-progradation reach.

Matagorda Bay shoreline position in the vicinity of the MSC was evaluated for response to construction of the MSC entrance and net change. During construction, large amounts of dredged material were placed on the northeast and southwest sides of the channel, advancing the shorelines as much as 900 and 1,500 ft, respectively. Initially, the southwest area experienced high rates of recession, while the northeast area was stabilized by construction of a small groin intended to prevent material from entering the channel (north bay jetty). Shoreline change trends allowed the delineation of an impoundment fillet extending approximately 1 mile northeast of the MSC. Within this reach, long-term shoreline advance rates were 5 to 10 ft/year. Farther to the northeast, change rates indicated mixed shoreline advance and recession, with a dominant trend of recession. Southwest of the MSC, the bay shoreline experienced high long-term recession rates over a 0.7-mile reach. High rates of recession within this reach indicate erosion of the dredged material placed southwest of the channel during construction. Farther southwest, recession rates peak, then rapidly decrease by 0.7 mile southwest of the MSC. At this point, the long-term trend reverses, and advance rates are observed for the next mile southwest. Shoreline advance in this reach was directly supplied by dispersion of dredged material placed along the southwest bay shoreline. In comparison to the 1956

pre-construction shorelines, the shoreline response as recession extends for a 0.25-mile reach, while a positive response of advance extends for 1 mile southwest of the recession area. Overall, the construction of the entrance channel has benefited the bay shoreline to the southwest.

Progradation of Matagorda Peninsula and spit growth from Matagorda Island into Pass Cavallo were evaluated for their response to the construction of the MSC. The southwest growth of Matagorda Peninsula totaled 5,170 ft from 1963 to 2003, while the spit at Matagorda Island prograded by 11,380 ft between 1974 and 2003. During the same period, the inlet width at Pass Cavallo decreased by about 9,200 ft.

The evolution of Pass Cavallo was divided into three eras: Era 1 was defined as a period of natural stability prior to the completion of the MSC in 1965. Matagorda Peninsula and Matagorda Island grew rapidly between 1965 and the late 1980s, defining Era 2. These classifications are consistent with the analysis of Harwood (1973). Era 3 (1988-2003) is marked by maturation of the system, during which spit progradation rates decreased as the channel width stabilized. This evidence supports the conclusion that Pass Cavallo has apparently reached a new dynamic equilibrium with tidal forcing and wind-setup ebb current through the inlet. Extreme events could disturb and change this equilibrium.

3 Dredged Volume and Sediment Accumulation

This chapter summarizes the dredged volumes removed from the MSC entrance and gives estimates of the shoaling rate at the entrance and vicinity based on bathymetric surveys. The volume of sediment deposition in the navigation channel can be estimated from Galveston District dredging records. Bathymetry surveys covering the same general area made at different times allow calculation of the local erosion rate and scour depth.

Dredging Data and Analysis

The Galveston District provided initial and maintenance dredging records for the MSC dated from 1962 to 2004 listing dredging frequency and volume by stations specified at 1,000-ft spacing along the navigation channel. The station number is labeled as the distance (in feet) relative to the northern end of the north jetty (0+000) of the entrance channel. The station numbers increase (positive numbers) toward the bay and decrease (negative numbers) toward the Gulf of Mexico (Figure 37). The dredged area covers the channel from the Gulf of Mexico to Point Comfort and Port Lavaca in Lavaca Bay. The records indicate that 43 million cu yd were dredged to open the MSC entrance and the entire deep-draft channel in 1963. The authorized channel is 38 ft deep mlt and 300 ft wide on the outer bar in the Gulf of Mexico, 36 ft deep in the entrance channel, and 200 ft wide in the bay. Maintenance dredging frequency is approximately every 2 years over the available record.

According to the dredging records, the sediment consists primarily of sand between sta 0+000 and -21+000 gulfward of the entrance channel. The median grain size is 0.233 mm at sta -10+000, 0.207 mm at sta -15+000, and 0.121 mm at sta -20+000. Because the current is stronger in the entrance channel than elsewhere in the area, finer sand tends to be transported out of the entrance to settle in regions of weaker current. In the range of sta 0+000 to 15+000, from the bay entrance channel to the junction of the GIWW, more than 75 percent of the dredged sediment is sand. This sand entered the channel from the Gulf of Mexico, carried by the flood current. Based on bottom samples collected in 1991 and 1995, the median grain size is 0.18 mm at sta 15+000 (MSC-GIWW junction). Farther north across the GIWW junction, the sediment contains more silt and clay in the channel, derived from bay and river sediment. These grain sizes are consistent with those of grab samples taken prior to MSC opening

(Chapter 1) except for the appearance of coarser fine sand gulfward of the entrance channel in the dredged material.

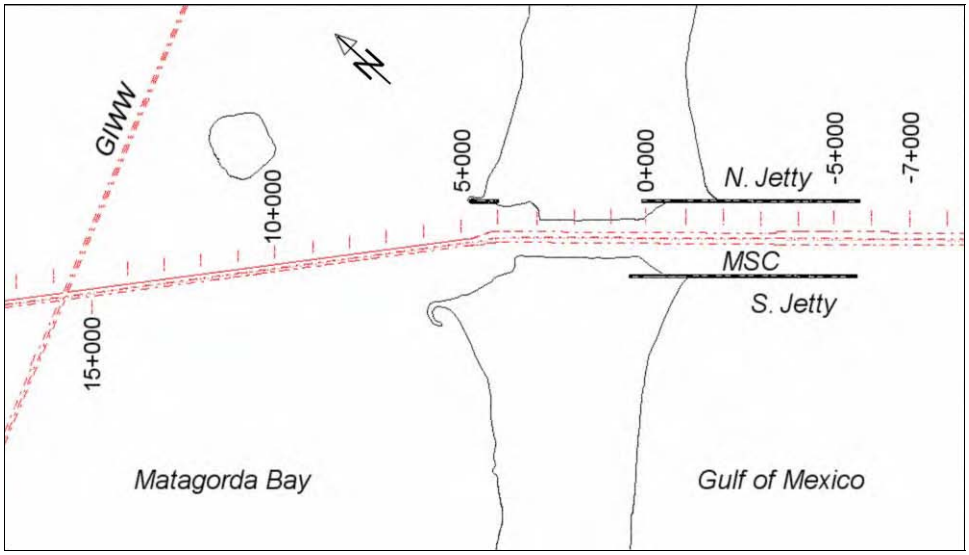

Figure 37. Map of stations for dredging records

Because the entrance channel rapidly scoured after it was opened in 1963, no dredging was required between sta 0+000 and -7+000 from 1963 to 1978. However, maintenance dredging took place in this area during the following 2 years (1979 and 1980), indicating that the wider section of the Gulf of Mexico entrance channel may have reached a state requiring regular dredging, perhaps because of updrift shoreline advance at the north jetty that would promote formation of a jetty tip shoal. For this reason, and also to investigate sediment accumulation in the entrance channel, dredged volumes were analyzed for the period 1980 to 2004 in the range of sta -21+000 to 15+000.

Table 8 presents the dredging events between 1980 and 2004, the dredged volume from each, and the average annual volume dredged in the ranges of sta 0+000 to -7+000, sta 0+000 to -21+000, and sta 0+000 to 15+000. Evidently, sand was deposited offshore of the MSC entrance as a result of littoral and inlet interaction. The average annual dredged volume between sta -7+000 and -21+000 is 155,000 cu yd/year. This volume is ten times greater than those in the Gulf of Mexico entrance between sta 0+000 and -7+000 and in the bay entrance channel between sta 0+000 and 15+000. In fact, no dredging was done in the range of sta 0+000 to 10+000 after October 1977 and in the range of sta 0+000 to -4+000 after October 1996. Because of the strong current occurring during spring tide in the entrance channel, channel scouring can be severe in this area. Estimation of local scour and shoaling rates requires analysis of bathymetric survey data, discussed next.

Table 8
Dredged Volumes at Matagorda Ship Channel (1980-2004)

Range (sta)	Date	Interval (month)	Total Volume (cu yd)	Rate (cu yd/year)
0+000/-7+000	12/80-3/84	38	73,370	24,000
	3/84-2/89	60	41,870	8,400
	2/89-9/93	54	114,515	25,000
	9/93-10/96	37	0	0
	10/96-8/99	33	4,207	1,500
	8/99-12/01	29	31,066	13,000
	12/01-2/04	25	0	0
	12/80-2/04*	**276**	**265,028**	**11,500**
0+000/-21+000	12/80-3/84	38	908,933	290,000
	3/84-2/89	60	498,040	100,000
	2/89-9/93	54	664,190	150,000
	9/93-10/96	37	488,383	160,000
	10/96-8/99	33	590,740	215,000
	8/99-12/01	29	310,655	130,000
	12/01-2/04	25	365,226	175,000
	12/80-2/04*	**276**	**3,826,167**	**166,500**
0+000/15+000	2/80-3/82	25	58,181	28,000
	3/82-11/86	55	129,112	28,000
	11/86-9/96	118	89,550	9,000
	9/96-2/04	89	95,000	13,000
	2/80-2/04*	**287**	**371,843**	**15,500**

* Total volume and the average rate of volume dredged per year.

Bathymetric Survey Data and Analysis

Four sets of bathymetric survey data were available for analysis of local scouring and shoaling in the MSC entrance channel. Three surveys were conducted (March 2000, September 2002, and November 2004) by the Galveston District. The Texas Water Development Board (TWDB) conducted a survey in the area in November 2001. Because the November 2001 survey was incomplete at the bay and gulf ends of the entrance channel, this data set was not analyzed. All the surveys were done by acoustic methods with ±1-ft elevation accuracy and ±6-ft horizontal positioning requirement (http://www.usace.army.mil/usace-docs/eng-manuals/).

Figures 38 to 40 contain bottom topography maps for the MSC from March 2000, September 2002, and November 2004 surveys, respectively. Depth is referenced to mean tide level (mtl). The tidal datum mtl is approximately equal to mean sea level and is commonly available in tide gauge records. The datum mtl should not be confused with the Galveston District navigation datum mlt. Scour holes with depths exceeding 90 ft are evident along the south bottleneck in

the bay entrance and at the two south corners of bottlenecks. Scour holes are also present near the north and south jetty tips in the gulf entrance channel. These scour holes are indicative of strong currents and can cause channel bank erosion, threatening the MSC entrance structures.

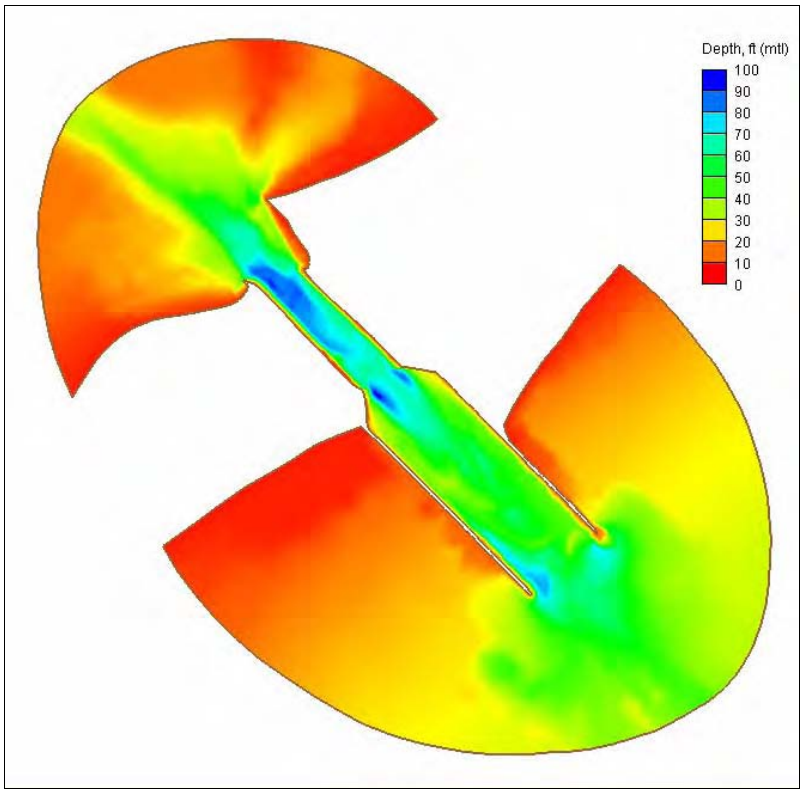

Figure 38. Bottom topography map, March 2000 survey (mtl datum)

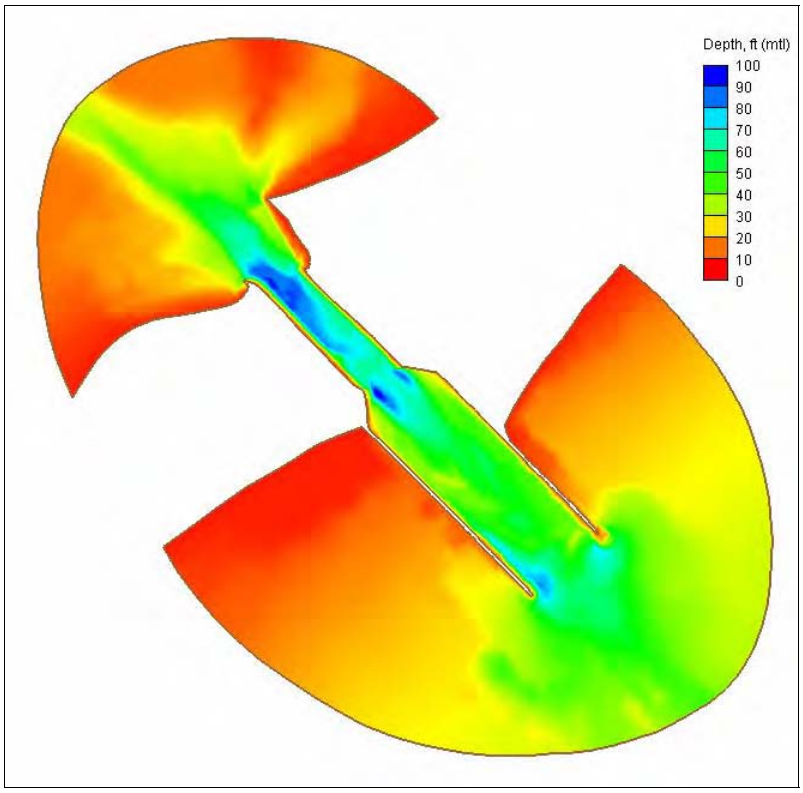

Figure 39. Bottom topography map, September 2002 survey (mtl datum)

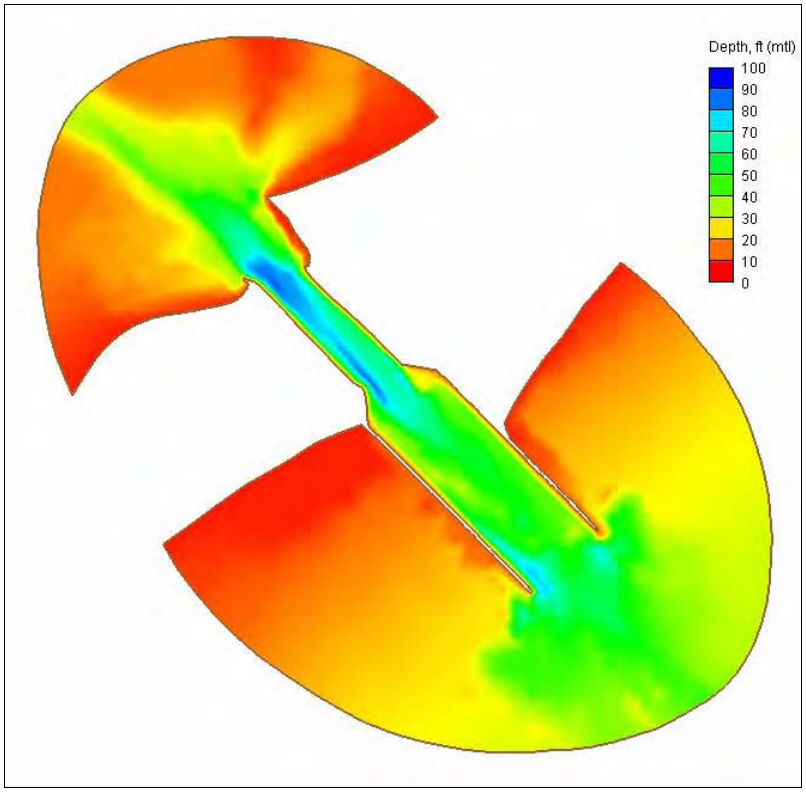

Figure 40. Bottom topography map, November 2004 survey (mtl datum)

The scour and shoaling pattern varies in time and space. Figures 41 and 42 show bottom topography change contours between the March 2000 and September 2002 surveys and between the September 2002 and November 2004 surveys, respectively. These figures indicate that bed erosion and shoaling are irregularly spaced in the channel. The bottom topography also changed more between September 2002 and November 2004 than between March 2000 and September 2002. Bottom scour increased significantly along the bank of the bottleneck section and along the inner side of the south jetty between September 2002 and November 2004. The scour rate is estimated at 4.5 ft/year in these areas, according to the last two surveys. In the same time interval, sediment shoaling appears to be extensive and covers other areas in the bottleneck and between the jetties (Figure 42).

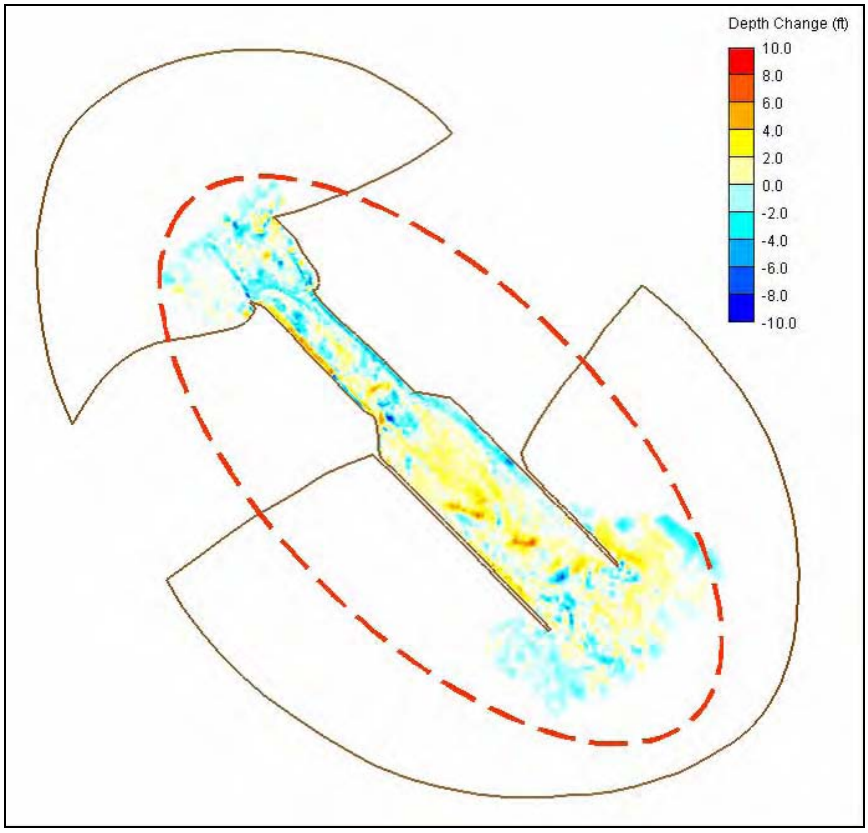

Figure 41. Bathymetry change between March 2000 and September 2002 surveys (general survey coverage within dashed circle)

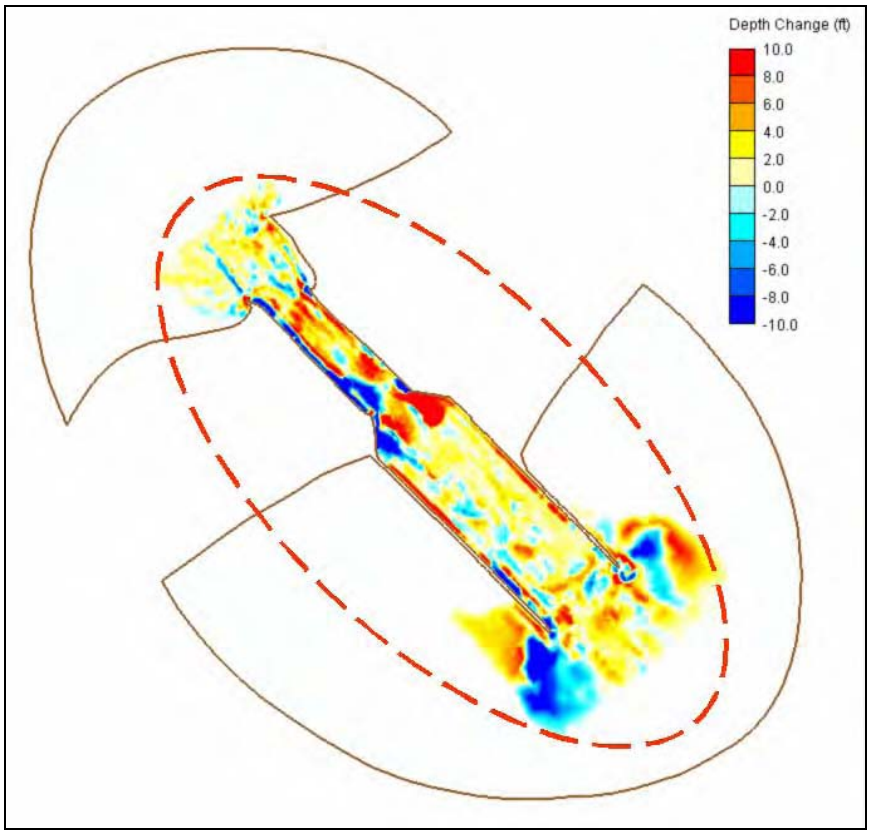

Figure 42. Bathymetry change between September 2002 and November 2004 surveys (general survey coverage within dashed circle)

Table 9 summarizes the sediment volume accretion and erosion based on the March 2000, September 2002, and November 2004 bathymetry surveys. The average depth change was calculated for the bay entrance including the bottleneck section from sta 0+000 to 6+000 and for the Gulf of Mexico entrance including the area between the jetties from sta 0+000 to –6+000. The largest average depth change was 2.2 ft (shoaling) in the wider section between jetties. This depth change is relatively small compared to the average depth of 47 ft (mtl) in the same area.

More sediment accreted between September 2002 and November 2004 than between March 2000 and September 2002. The annual rate of sediment accumulation is estimated as 0.5 million cu yd in the channel, including the bottleneck and wider channel areas from the September 2002 and November 2004 survey data sets. This large sediment accumulation may have been caused by increased tropical storm occurrence on the Texas south-central coast from September 2002 to November 2004, including Fay (2002), Lili (2002), Claudette (2003), Grace (2003), and Ivan (2004) (Table 1). Note that only one tropical storm (Bertha, in 2002) approached the study area from March 2000 to September 2002. The annual mean wave height, based on deepwater buoy data (NDBC 42019) collected offshore of the MSC, was about the same for these two time intervals: 4 ft for 2000, 2001, 2003, and 4.3 ft for 2002 and 2004.

Table 9
Average Depth Change and Sediment Volume Accretion/Erosion

Station Range*	Average Depth Change (ft)** March 2000 - September 2002	Average Depth Change (ft)** September 2002 - November 2004	Volume Change (cu yd) March 2000 - September 2002	Volume Change (cu yd) September 2002 - November 2004
0+000 to 6+000	-0.5	1.0	-100,000	220,000
0+000 to -6+000	0.5	2.2	180,000***	920,000

* Station 0+000 to 6+000 covers the bottleneck and bay entrance channel area. Station 0+000 to -6+000 covers the wider section of the entrance channel and gulf-side entrance.
** Positive values denote shoaling; negative values denote scour or erosion.
*** Excluding 31,000 cu yd dredged between sta -5+000 to -6+000 from October to December 2001.

Summary

Sediment volume distributions in the MSC were analyzed based on the new-work dredging and maintenance dredging records covering 1962 to 2004. Sediment accumulated at the MSC entrance and vicinity is primarily sand, with littoral sediments serving as a source and with finer-grained sediment transported away from the entrance by the strong tidal current. Analysis of the dredging data indicates a large amount of sediment accumulation in the outer bar gulfward of the MSC entrance. The annual dredged volume in the outer bar (sta -7+000 to -21+000) is 155,000 cu yd/year. This quantity is ten times greater than volumes dredged in the entrance channel and in the bay between the bay entrance and MSC-GIWW junction (Table 8).

Three sets of bathymetric survey data collected in March 2000, September 2002, and November 2004 were analyzed to investigate channel scour and shoaling in the entrance channel. Scour holes with depths exceeding 90 ft are located along the south bottleneck and at the two gulfward corners of the bottleneck. Deep scour holes also appear near the north and south jetty tips at the Gulf of Mexico entrance. These scour holes are growing, according to the survey data, and the growth was more significant from September 2002 to November 2004. The surveys show maximum rates of scour of 8.5 and 9.5 ft/year at the south bottleneck and near the south jetty tip, respectively. The survey data indicate that the entrance channel experienced significant shoaling between September 2002 and November 2004. The annual shoaling rate estimated for this time period is 0.5 million cu yd. This corresponds to an average depth change of 1 ft (shoaling) in the bottleneck section and 2.2 ft in the wider channel area between the jetties.

4 Hydrodynamics and Evaluation of Alternatives

Numerical modeling of tidal hydrodynamics in the MSC jetty stability study was conducted for evaluating alternatives (Chapter 1) with the ADvanced CIRCulation (ADCIRC) model (Luettich et al. 1992). ADCIRC calculates the water surface fluctuation and depth-averaged current with high resolution in areas of complex shoreline configuration and bathymetry. The model is based on a finite-element algorithm that allows for flexible spatial discretization of the computational domain. Forcing functions include time-varying water surface elevation, wind shear stress, river inflow, and wave radiation stress if operated together with a wave model.

The ADCIRC model solves either the two-dimensional (2-D), depth-integrated shallow water equations or the three-dimensional equations of motion for conservation of mass and momentum. The water is assumed to be incompressible and can inundate dry land, depending on the water surface elevation. The model can be applied to computational domains encompassing the ocean, continental shelves, coastal seas, and estuarine systems. If wave radiation stresses are included in the forcing, the model computes the wave-generated nearshore current (longshore current and rip currents). A weir jetty algorithm is included in the model (Westerink et al. 2001). The depth-averaged version of ADCIRC was applied in this study.

Numerical Model of Flow

The model grid for the study site covers a multiple-inlet system that includes the MSC and Pass Cavallo in Matagorda Bay, Mitchells Cut in East Matagorda Bay, and the mouth of the Colorado River (MCR) between the two bays. At present, the flow system associated with the MSC and Pass Cavallo is nearly isolated from the MCR, East Matagorda Bay, and the westward section of the GIWW by a pair of boat locks (Lin et al. 2001). Port O'Connor and the GIWW are also included.

Figure 43 shows the computational grid defined for the multiple-inlet flow system. The bottom topography data sets input to generate the grid were obtained from multiple sources:

a. NOAA nautical charts.

b. A bathymetry survey of the East Matagorda Bay reported by Kraus and Militello (1996).

c. A bathymetry survey of Pass Cavallo by the Galveston District (Kraus et al. 2000).

d. A bathymetry survey of the MCR and Colorado River Navigation Channel (CRNC) by CHL (January 2000, December 2001).

e. A bathymetry survey of Mitchell's Cut by CHL (December 2001).

f. A bathymetry survey of Matagorda Bay near and around the diversion channel and the junction of Colorado River and GIWW by CHL (July 2001).

g. Cross sections of the MCR and GIWW by the Galveston District (October 1999 to February 2002).

h. A bathymetry survey of the MSC by CHL and the Galveston District (October and November 2004).

i. The digital Nautical Chart (DNC) database (http://earth-info.nima.mil/dncpublic) produced by the National Imagery and Mapping Agency.

j. Aerial photographs taken periodically at the MCR, Mitchells Cut, and MSC, furnished additional information on the bay and gulf perimeters (shorelines) and configuration of the jetties.

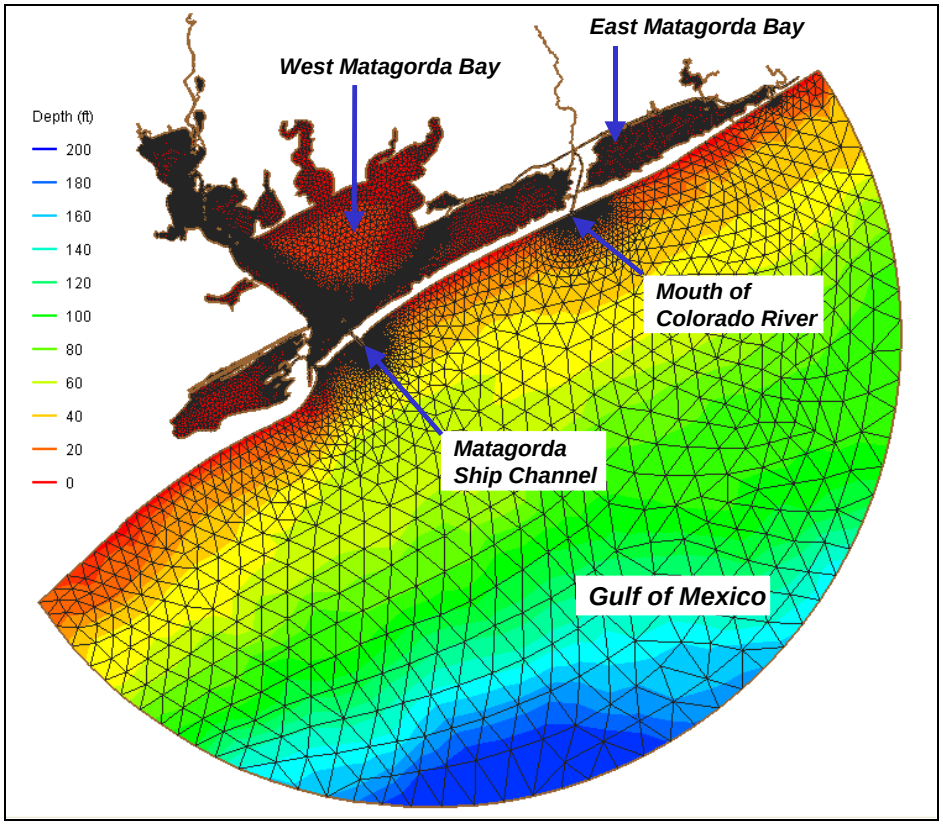

Figure 43. Regional ADCIRC grid (depths referenced to mtl)

Figure 44 shows the detail of the model grid at the MSC. The water depth defined in the grid is referenced to mtl. The average width of the MSC is 950 ft in the bottleneck section and 1,950 ft at the gulfward jetty section. At present, the average depth is approximately 75 ft in the bottleneck and 50 ft between the gulfward jetties. As a result of strong ebb and flood currents flowing through the channel, scour holes more than 90 ft deep appear along the south bank of the bottleneck section and the southwest corner (80 ft deep) of the gulf entrance (Chapter 3).

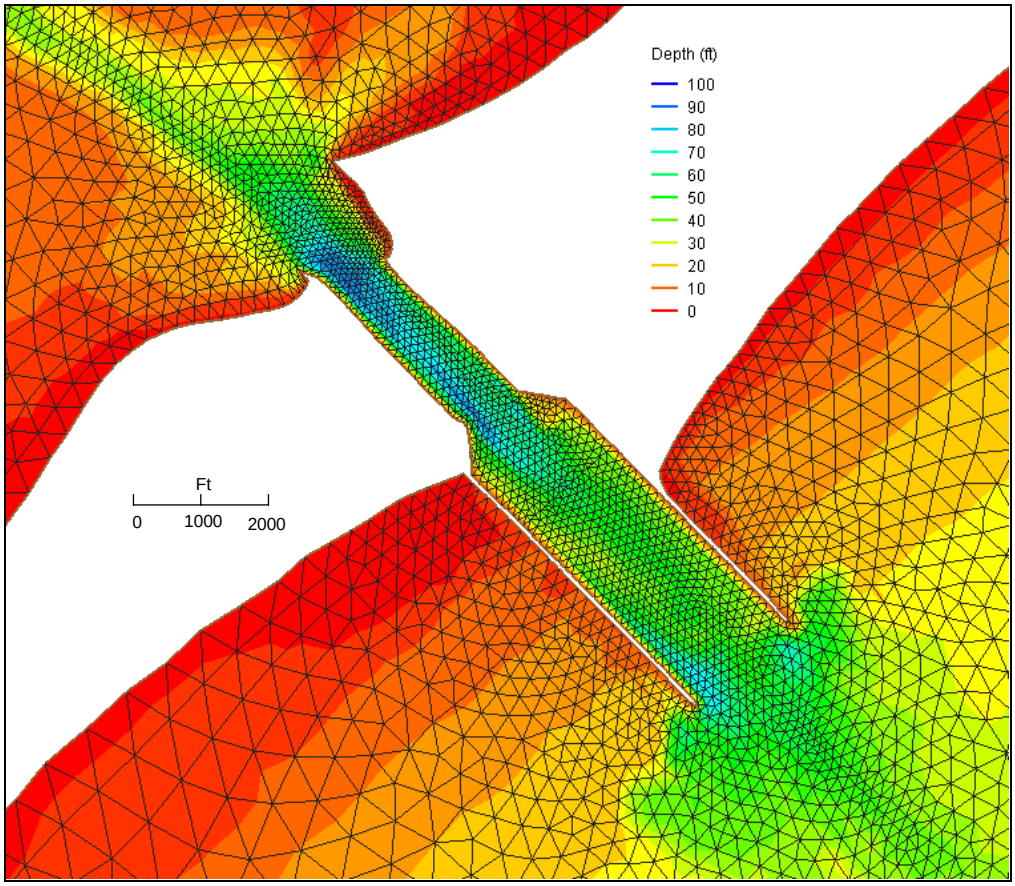

Figure 44. Detail of circulation model grid at MSC (mtl datum)

Boundary Conditions

The model was driven by wind forcing over the numerical grid domain and the tidal fluctuation in water surface elevation specified at the grid boundary in the Gulf of Mexico. Inflows of the Lavaca River, Colorado River, Caney Creek, and Live Oak Bayou were included as additional forcing to the model.

Surface wind data collected by the Texas Coastal Ocean Observation Network (TCOON) at the East Matagorda Old Gulf Cut (EMATGC, 28°42′48″N and 95°53′18″W) and Port O'Connor (PTOCON, 28°26′48″N and 96°23′48″W)

stations (Figure 45) served as sources of wind forcing to the model. ADCIRC was forced at the Gulf of Mexico with water level measurements to capture the meteorological tide as well as the astronomical tide. The water surface elevation measured at Bob Hall Pier (27°34′54″N and 97°13′W) in Corpus Christi by the TCOON was specified as the ocean boundary condition. The wind and tide level measurements are available at http://dnr.cbi.tamucc.edu.

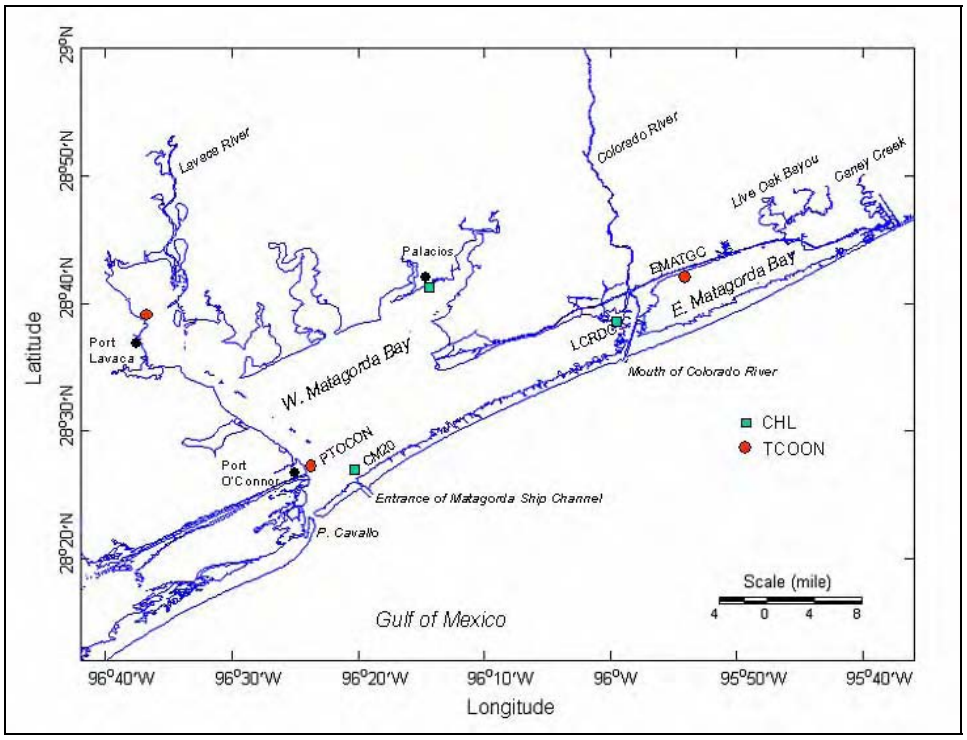

Figure 45. Location of CHL water level gauges and TCOON stations

Discharges from the Lavaca River, Colorado River, Caney Creek, and Live Oak Bayou were represented in the simulation of the hydrodynamics. The daily average river discharge information for the Colorado River is available from the USGS National Water Information System. The river discharges for Lavaca River, Caney Creek, and Oak Bayou were approximated as one-tenth (proportion of the watershed area) of the river discharge of the nearby San Bernard River. River discharge information for both the Colorado River and the San Bernard River is available at http://water.usgs.gov/data.html.

Model Verification

ADCIRC was established for a 64-day simulation from 10 November 2004 to 12 January 2005, containing two full cycles of spring and neap tides. This time period was selected because comparison water level data were available from two TCOON stations at Port Lavaca (PTLAVA, 28°38’24”N and 96°36’36”W), and Port O’Connor and three CHL tide gauges at the MSC Channel Marker 20 (MSC-CM20, 28°26’56”N and 96°21’19”W), Palacios Harbor (28°41’47”N and

96°13’36”W), and Lower Colorado River Diversion Channel (LCRDC, 28°38’29”N and 95°59’43”W) located around the perimeter of Matagorda Bay (Figure 45). Acoustic-Doppler Current Profiler (ADCP) data (velocity profile measurements along a vertical line) were made in the bottleneck and in the vicinity of the bay entrance of the MSC from 1500 to 2000 GMT, 17 November 2004, during the maximum of an ebbing cycle (Figure 46).

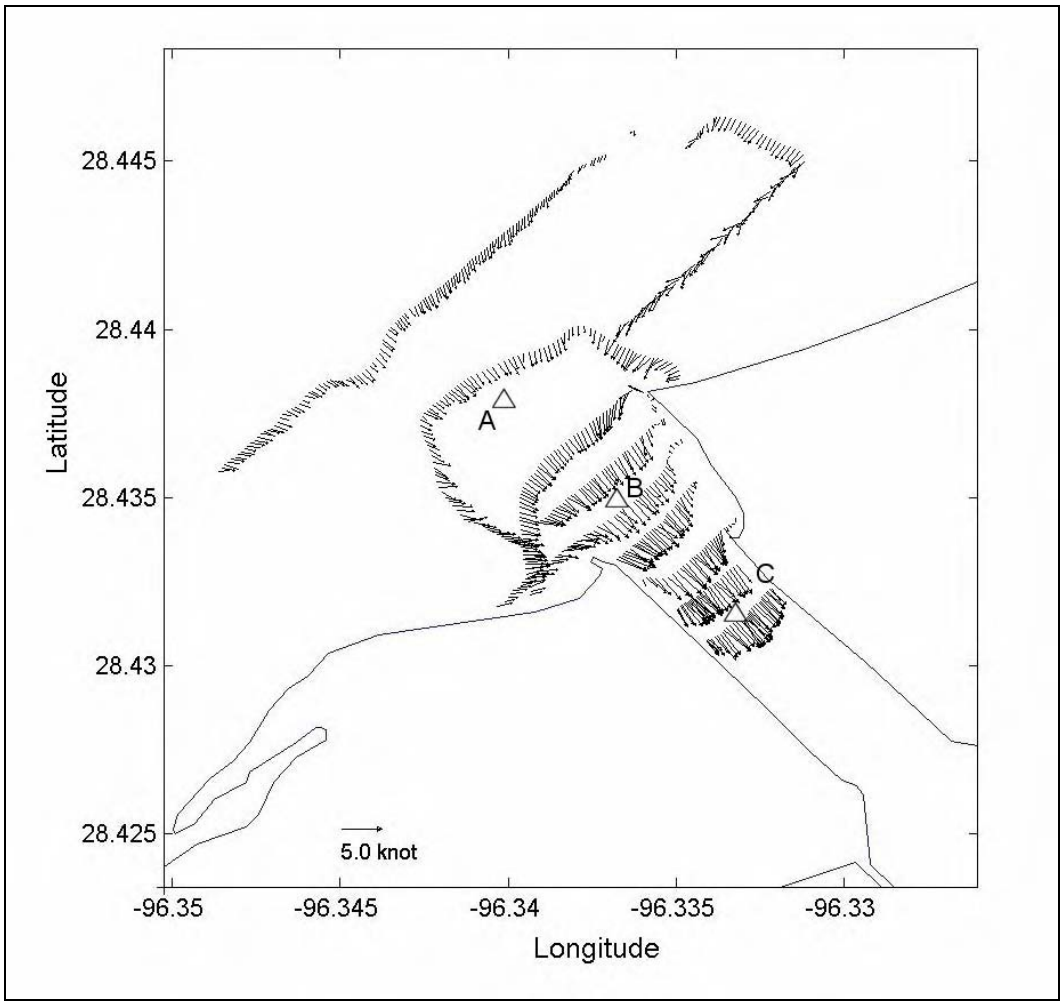

Figure 46. Depth-averaged current vectors from ADCP measurements during peak ebbing cycle of 17 November 2004

Because ADCIRC was operated in a depth-averaged, or 2-D mode, the ADCP measurements were examined for the structure of the vertical distribution of the current. The ADCP collected data in 1-m depth increments below the acoustic sensor. Plots of the vertical distribution of the current speed at locations A, B, and C, on the bay side of the entrance (Figure 46) where the ebb current is strong, are shown in Figure 47. The distributions show some randomness in structure but overall are uniform with depth. The distributions end near the channel bottom, where the current begins to decrease. Location C is

in the scour region and shows a depth exceeding 90 ft (mtl). The increase in current near the bottom at location C is not considered reliable and may be an artifact of acoustic beam reflection from the steep bottom slopes in the scoured area.

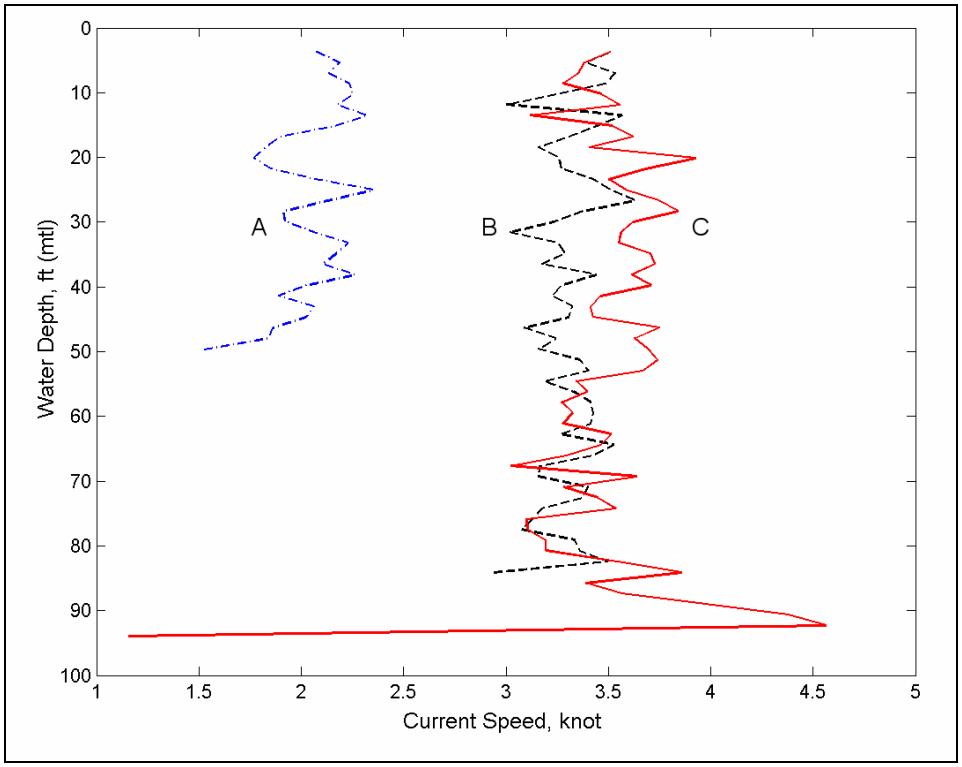

Figure 47. Vertical distributions of current speed on bay side of MSC entrance

ADCIRC was run with a 1-sec time step and default control parameters (generalized wave continuity equation weighting factor τ_o = 0.01 and bottom friction coefficient C_f = 0.0015). The input water level along the ocean boundary and surface wind information were updated hourly, whereas the river discharge boundary condition was updated daily. Figure 48 shows the ocean boundary water level data from Bob Hall Pier, the surface wind data from EMATGC and PTOCON, and the river discharges from the lower Colorado River and San Bernard River for generating the input to the simulation.

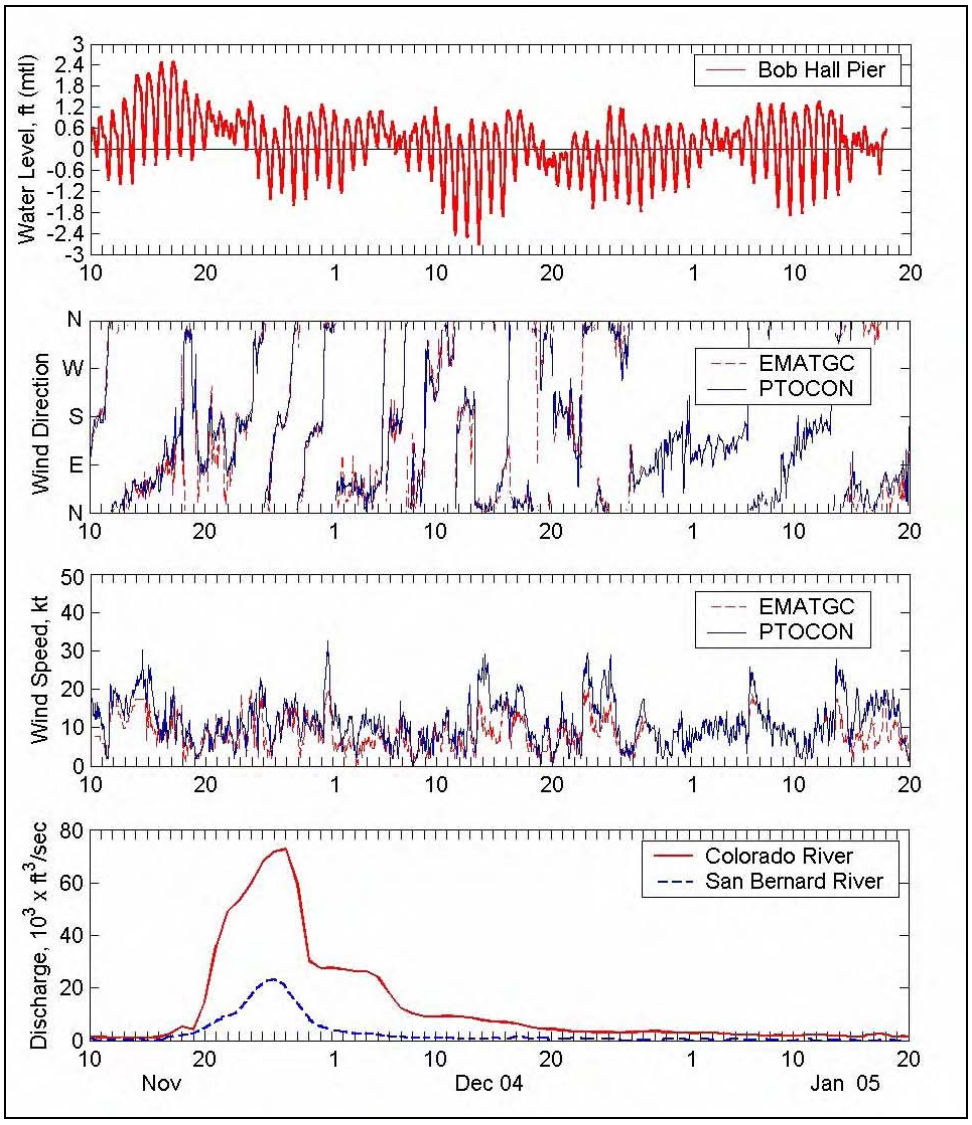

Figure 48. Measured water levels, surface winds, and river discharges for model input boundary conditions

Calculation results were saved at 1-hr intervals for comparison to the water level and velocity measurements. Figure 49 shows calculated and measured water levels at Port Lavaca and Port O'Connor. Figure 50 compares calculated and measured water levels at MSC-CM20, Palacios Harbor, and LCRDC. Calculated water levels agree well with the measurements. Comparison of calculated and measured water levels at the LCRDC shows that ADCIRC also performed well for a large river discharge in the Colorado River that occurred between 20 November and 10 December 2004. Table 10 presents the statistics comparing the calculated and measured water levels. The bias in calculated water levels is small, ranging from -0.11 to 0.05 ft. The root-mean-square (RMS) errors of the calculated water levels are also small, ranging from 0.23 to 0.34 ft (28 to 37 percent of the local tidal range, which is greatly altered by wind).

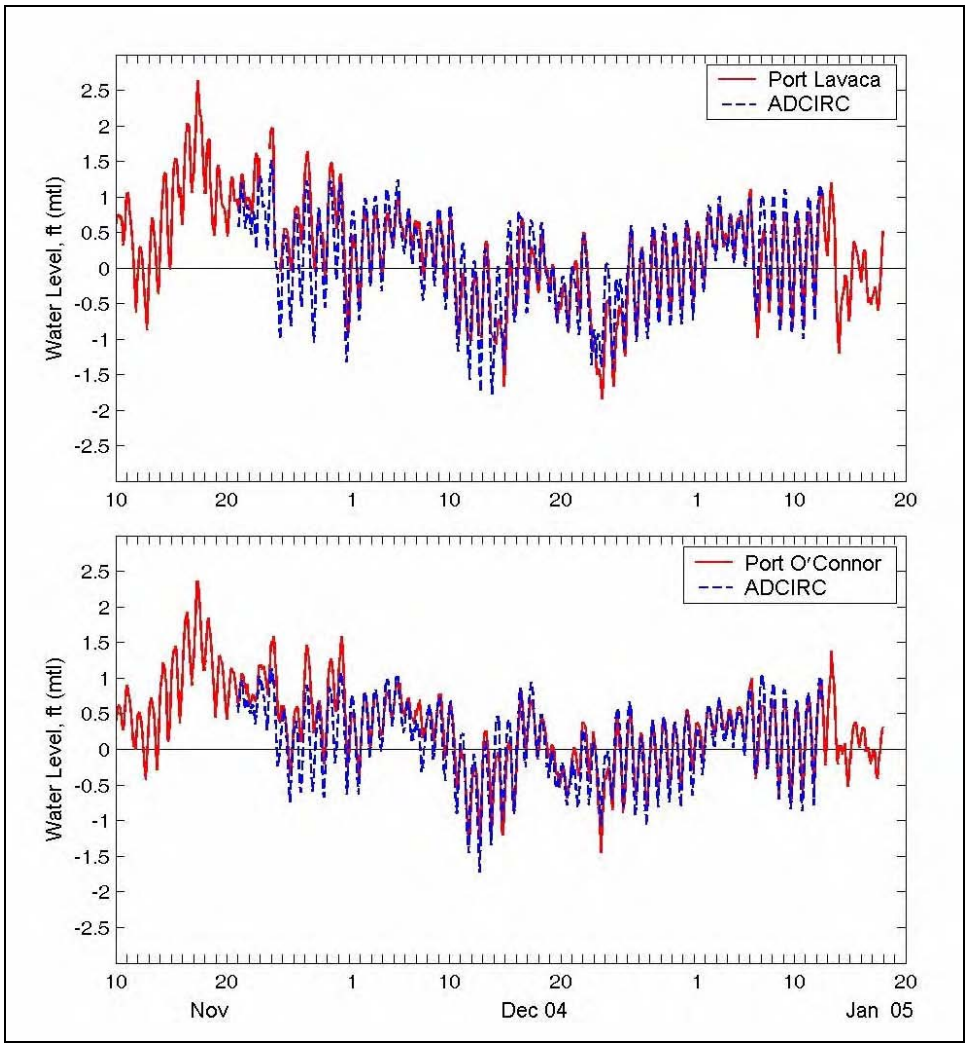

Figure 49. Calculated and measured water levels at Port Lavaca and Port O'Connor

Figure 51 illustrates the calculated current field at 1600 GMT, 17 November 2004, during the peak ebbing cycle in the bay entrance of the MSC. In this case, the calculated current agrees well with the measured current pattern (Figure 46). Both the calculated and measured velocities plotted in Figures 46 and 51 are depth-averaged quantities. Figure 52 compares calculated velocities along three transect lines where current data were collected at the bay entrance of the bottleneck. Two minor differences in calculated and measured currents are apparent. Near the shoreline, especially along the bank of the bottleneck, the model tends to overestimate the current magnitude, possibly a result of having a greater water depth in the model. In the bottleneck, the calculated maximum current magnitude (5 knots) is 11 percent greater than the measured maximum current (4.5 knots). Overall, the calculated current speed and direction are similar to the measurements at the bay entrance of the bottleneck.

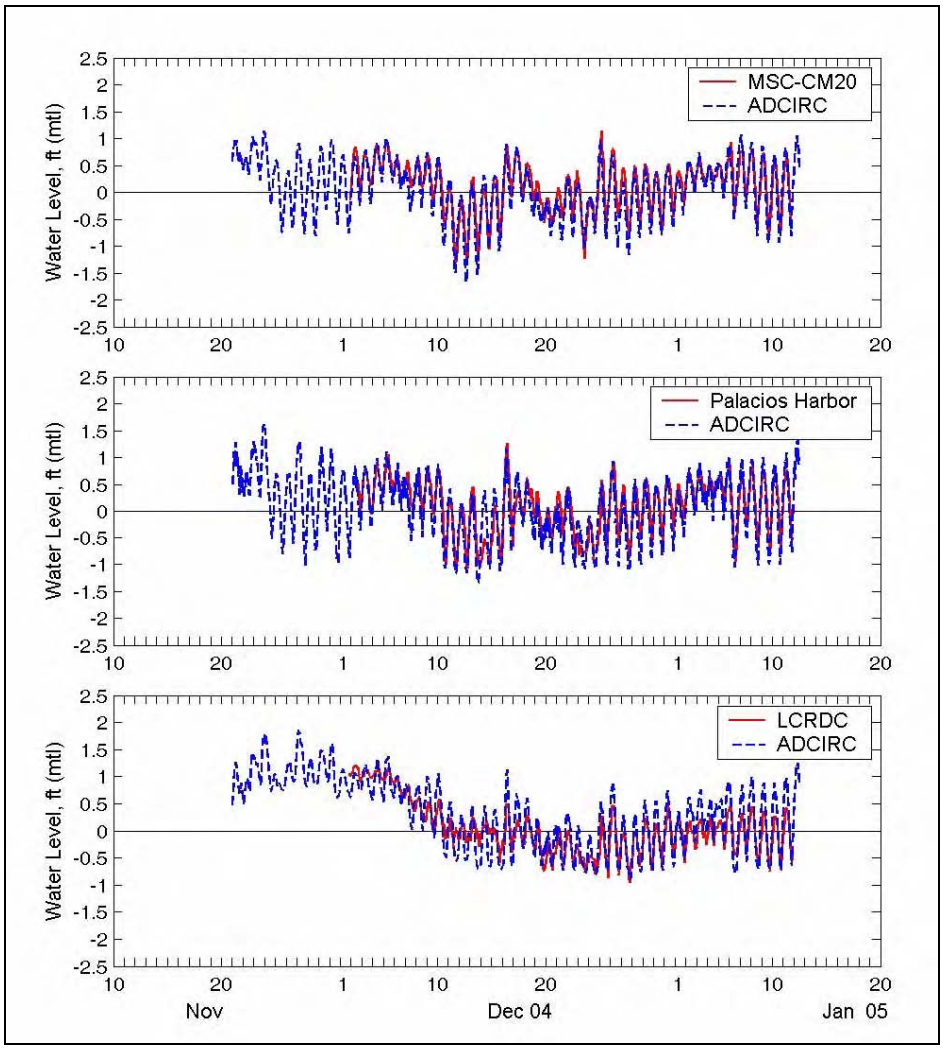

Figure 50. Calculated and measured water levels at MSC-CM20, Palacios Harbor, and LCRDC

Table 10
Water Surface Elevation Bias, RMS Error, and Percent Error, 20 November 2004 to 10 January 2005

Location	Sample Size	Bias (ft)	RMS Error (ft)	Percent Error
Port Lavaca	1228	-0.04	0.34	37
Port O'Connor	1261	-0.11	0.27	35
MSC-CM20	979	-0.10	0.23	29
Palacios Harbor	966	-0.11	0.28	28
LCRDC	989	0.05	0.29	29

Remarks: Percent Error = RMS Error / Tidal Range.
Tidal range (mean higher high water minus mean lower low water) is 0.92 ft at Port Lavaca, 0.78 ft at Port O'Connor (also used for MSC-CM20), and 1.01 ft at Palacios (also used for LCRDC).

The calculated discharge was verified by the flow rate computed from the vertical and horizontal velocity profile data (ADCP) collected on transects across the MSC during the peak ebbing cycle on 17 November 2004 (Figure 53). Figure 53 shows the calculated discharge versus the measured discharge. The calculated discharge also agrees well with the measurements. Table 11 lists statistics comparing the calculated and measured discharges. The bias of both calculated mean and maximum discharges appears to be negative, as they are greater than the measurements during the peak ebb cycle. The negative bias of the calculated ebb discharges is expected in this application because the model tends to slightly overestimate the maximum current magnitude in the bottleneck and also the current near the shoreline of the MSC, attributed to ambiguous bathymetry close to the revetments and jetties.

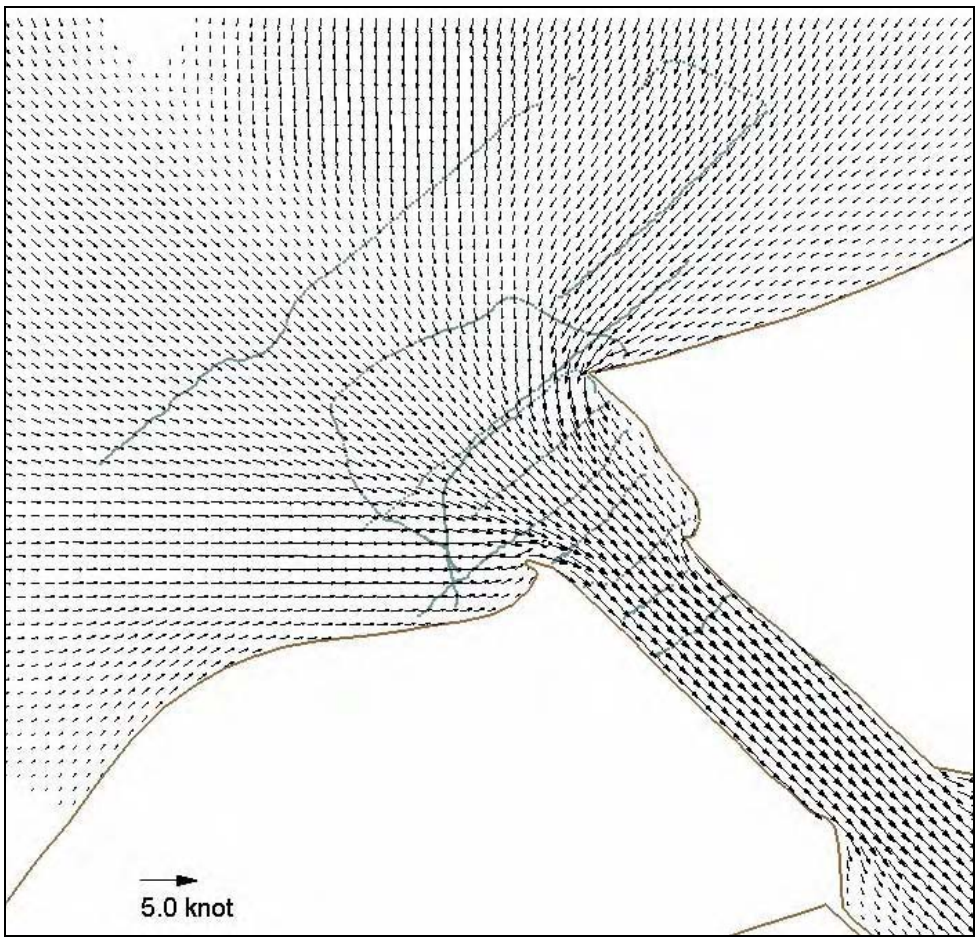

Figure 51. Calculated ebbing current field (also transect lines for ADCP measurement) at 1600 GMT, 17 November 2004

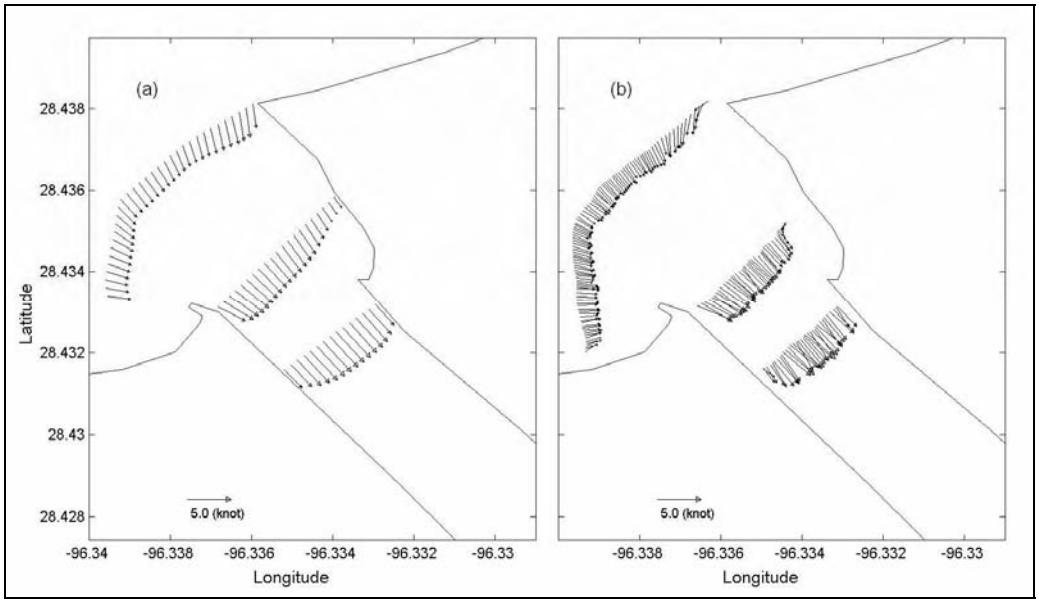

Figure 52. Calculated (a) and measured (b) current vectors along three transects at bay entrance of bottleneck

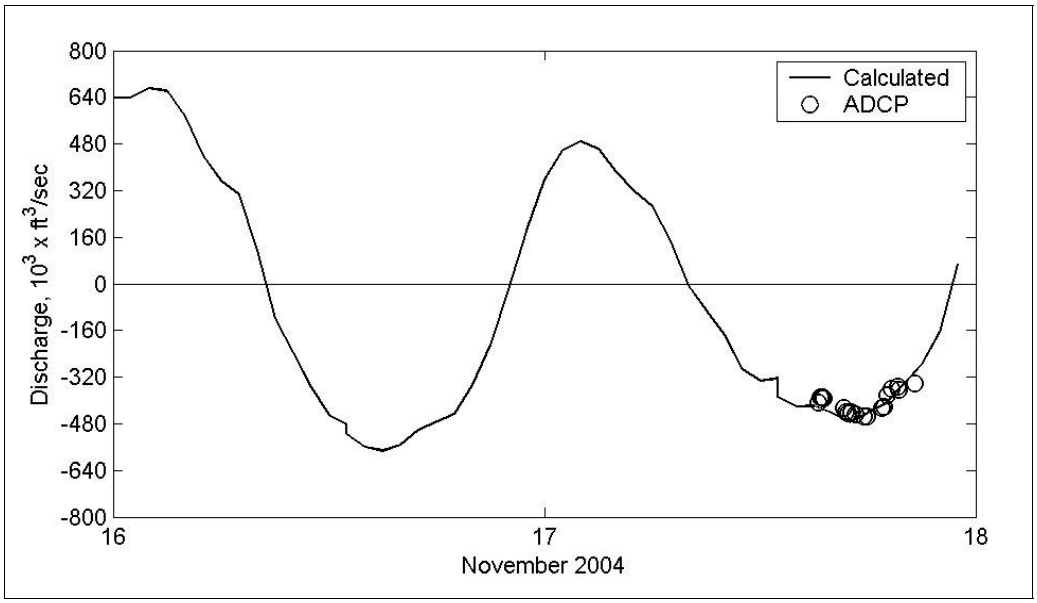

Figure 53. Comparison of calculated and measured discharges

Table 11
Bias and RMS Error of Flow Discharge During Peak Ebbing Cycle at MSC, 1500 – 2100 GMT, 17 November 2004

Location	Sample Size	Bias, Mean Discharge (ft^3/sec)	Bias, Max. Discharge (ft^3/sec)	RMS Error (ft^3/sec)	Percent Error
MSC	18	-3,620	-19,380	55,770	12.3

Remarks: Calculated maximum ebb discharge = 474,340 cu ft/sec (17 November 2004).
Measured maximum ebb discharge = 454,960 cu ft/sec.
Percent error = RMS error/measured maximum discharge.

Evaluation of Alternatives

Three alternatives were considered in this study (Chapter 1): (a) remove the south bottleneck (Alt 1), (b) remove the north and south bottlenecks (Alt 2), and (c) remove the north and south bottlenecks and flange bay entrance (Alt 3). These alternatives were evaluated by comparing model current velocities and discharges to the existing condition. The large magnitude of the current velocity in the MSC is of main interest because of concern for navigation and scouring around the jetties and revetment. Figure 54 displays the existing channel configuration and the three alternatives as represented in the circulation model grid. Figure 55 shows the model Cross Section A-A' of the existing and three alternatives. The Cross Section A-A' in Alt 1 through Alt 3 resembles that between the jetties gulfward of the bottleneck in the existing condition.

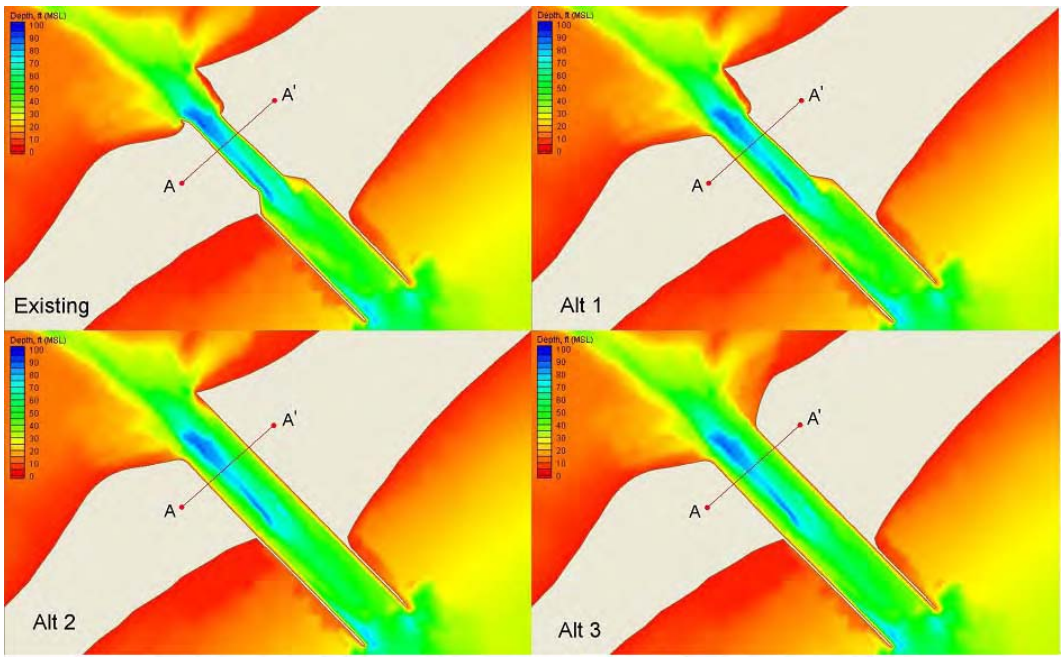

Figure 54. Ship channel geometry and bathymetry for existing and three alternative configurations

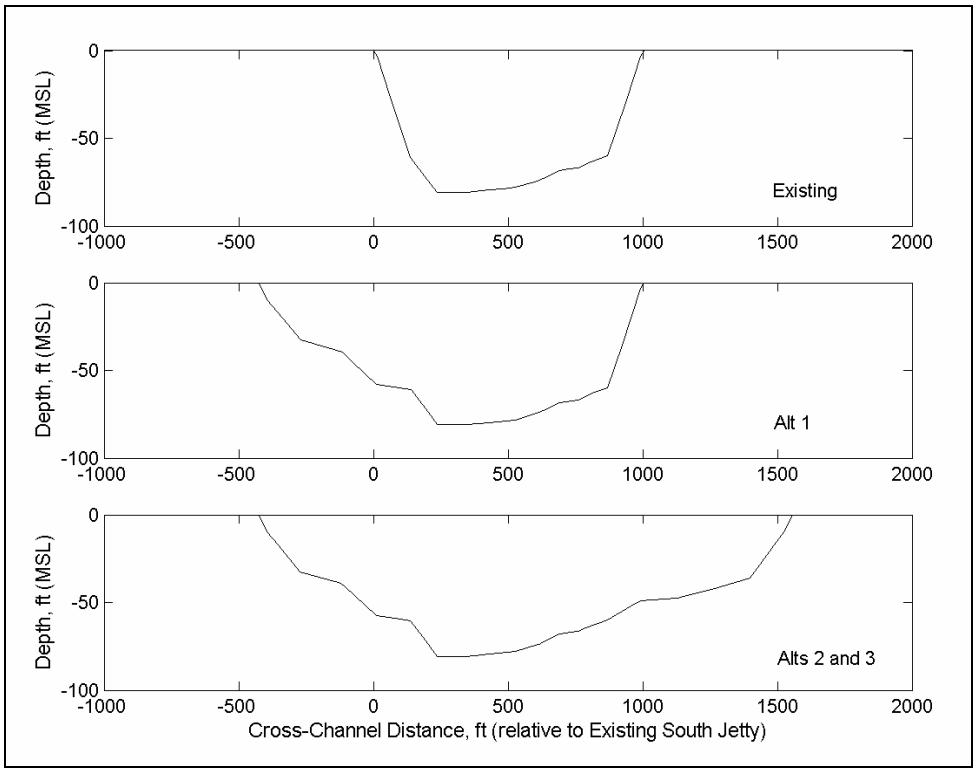

Figure 55. Model Cross Section A-A' for existing condition and three alternatives

The evaluation of alternatives was conducted for a representative winter month (January 2004) that was dominated by northerly cold fronts, and a typical summer condition (12 July to 10 August 2004) with prevalent southeasterly winds and a daily sea breeze. Wind plays a major role in controlling the water level and circulation in Matagorda Bay and other shallow coastal waters of Texas, as discussed in Chapter 1. Figure 56 displays wind input information for January 2004 and for 10 July to 10 August 2004, from EMATGC and PTOCON. As seen in Figure 56, the wind speed can be considerably greater in the winter than in the summer.

Figure 57 plots water level input information from Bob Hall Pier. The magnitudes of water level for the two simulated summer and winter durations are similar. However, the variation in water level is slightly less regular in the winter, because it is more influenced by the stronger wind. River discharges to Matagorda Bay are generally small in these months. Figure 58 plots flow rates from the Colorado River and San Bernard River used for the river boundary conditions to the model.

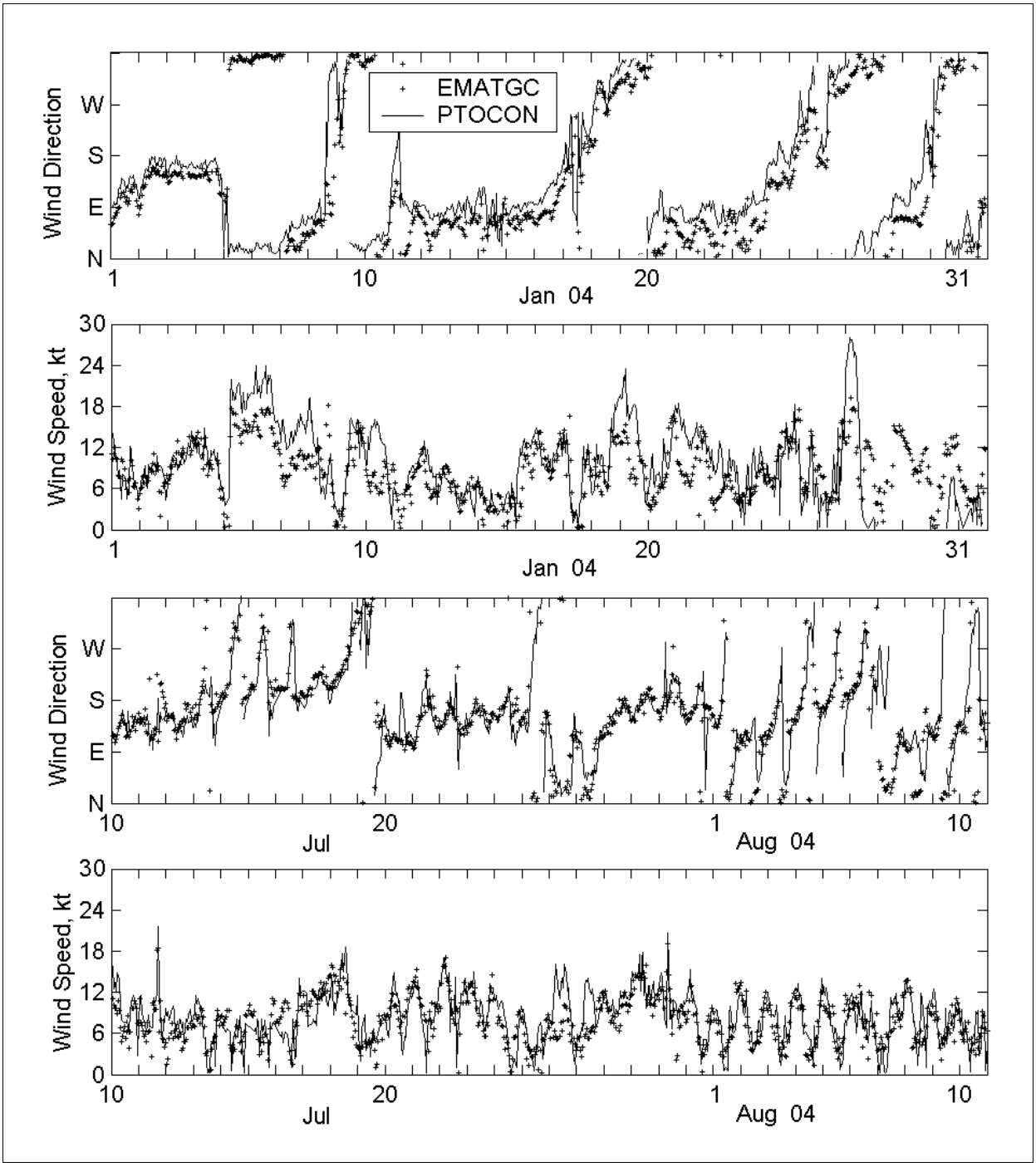

Figure 56. Wind information collected at EMATGC and PTOCON for January and 10 July to 10 August 2004

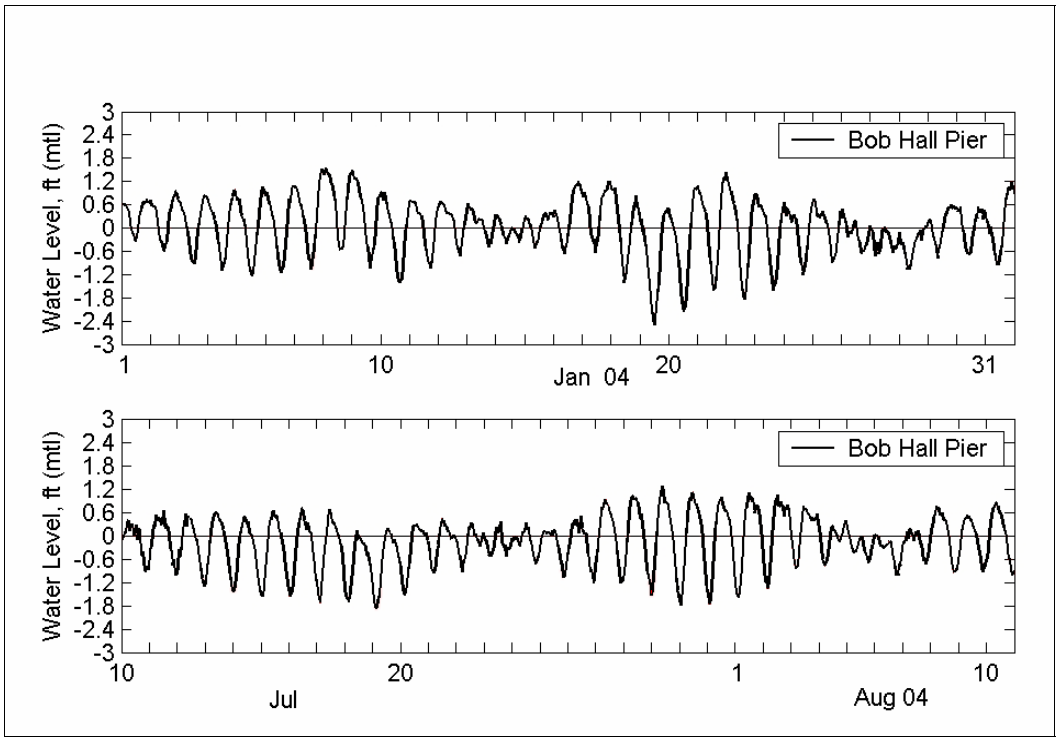

Figure 57. Water level measured at Bob Hall Pier for January and 10 July to 10 August 2004

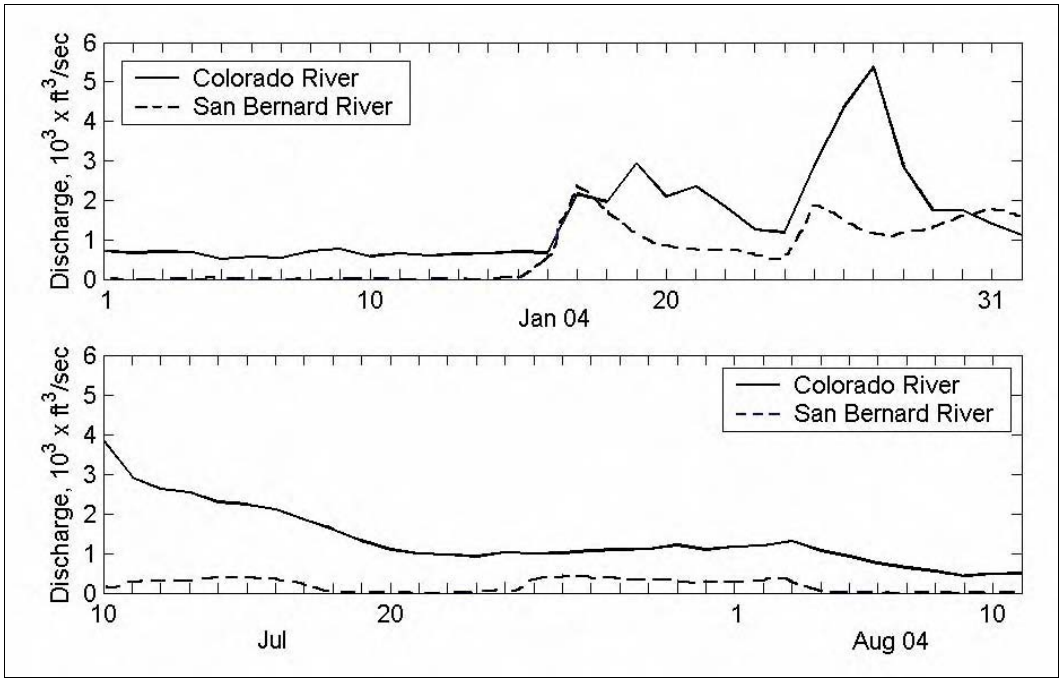

Figure 58. River flow rates from Colorado River and San Bernard River for January and 10 July to 10 August 2004

Numerical simulations conducted for the existing condition and the three alternatives reveal that the magnitude of the ebb current is slightly greater than the flood current in the same tidal cycle. An ebb bias is expected because of river inputs. The current magnitude across the entrance channel is more uniform during flood than during ebb. Calculations from the January 2004 simulation indicate that the maximum current magnitude occurred during flood at 2100 GMT, 20 January, and the maximum current magnitude occurred during ebb at 1300 GMT, 22 January. Figures 59 and 60 show calculated current fields corresponding to these maximum flood and ebb current conditions for the existing and three alternative configurations. For the simulation of 12 July to 10 August 2004, the maximum flood current speed occurred at 0800 GMT, 30 July, and the maximum ebb current occurred at 0200 GMT, 2 August. Figures 61 and 62 show calculated current fields corresponding to these conditions for the existing and alternative configurations. At the north end of bottleneck, the maximum current magnitude for the existing condition is somewhat unevenly distributed across the bay entrance channel, especially during ebb. The ebb current magnitude is also larger at the bay entrance for the existing condition than for the alternatives.

The uneven distribution of a strong current across the bay entrance tends to generate eddies and cross currents that may be hazardous to navigation. Figures 59 to 62 indicate that the three alternatives generally produce more uniform current flows across the bay entrance channel. Among them, Alt 3 produces the most uniform flow, and with a smaller current magnitude, across the bay entrance channel. Therefore, Alt 3 is expected to have weaker cross currents and eddies at the bay entrance.

Six stations were selected for comparison of calculated current magnitude. Figure 63 gives the locations of these stations in the existing condition: sta a and b are located in the bay entrance, c is in the bottleneck segment, d is in the wider jetty channel, and e and f are in the gulf-side entrance. Table 12 lists station coordinates and depth information. For the three alternatives, calculated maximum velocities within 150 ft of these stations were compared to corresponding current speeds in the existing condition. Tables 13 and 14 present calculated maximum flood and ebb current speeds, respectively, at the six stations for January 2004. Tables 15 and 16 present calculated maximum flood and ebb current magnitudes, respectively, for 12 July to 10 August 2004. Comparing maximum velocities at sta a and f indicates relatively little difference among the three alternatives and the existing condition. Current magnitudes for sta a and f, located in the bay and the Gulf of Mexico away from the jetty channel, are weaker than those of sta b to e, located inside the entrance channel between jetties.

Comparing calculated maximum velocities at sta b to e indicates that the ebb and flood current magnitudes are reduced significantly at sta b and c in the bottleneck for all three alternatives, whereas the current magnitude increases during flood at sta d and e in the gulf entrance channel between the jetties, because the flow converges more toward the center of the channel than for the existing condition. The increase in the flood current magnitude at sta d and e for the three alternatives is expected to be smaller than calculated because the channel should scour as a result of a stronger current at those locations, explored next.

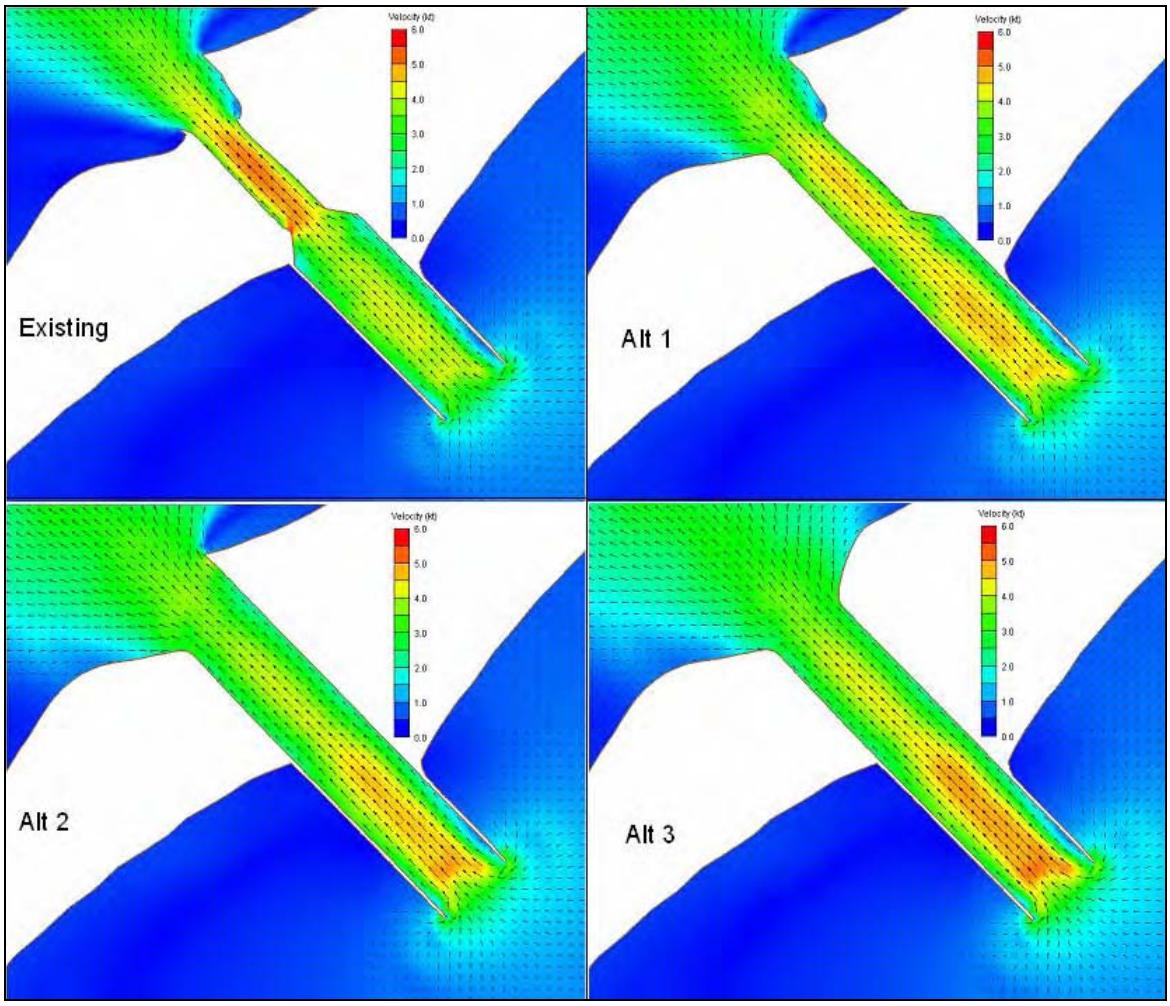

Figure 59. Calculated maximum current speed during flood at 2100 GMT, 20 January 2004

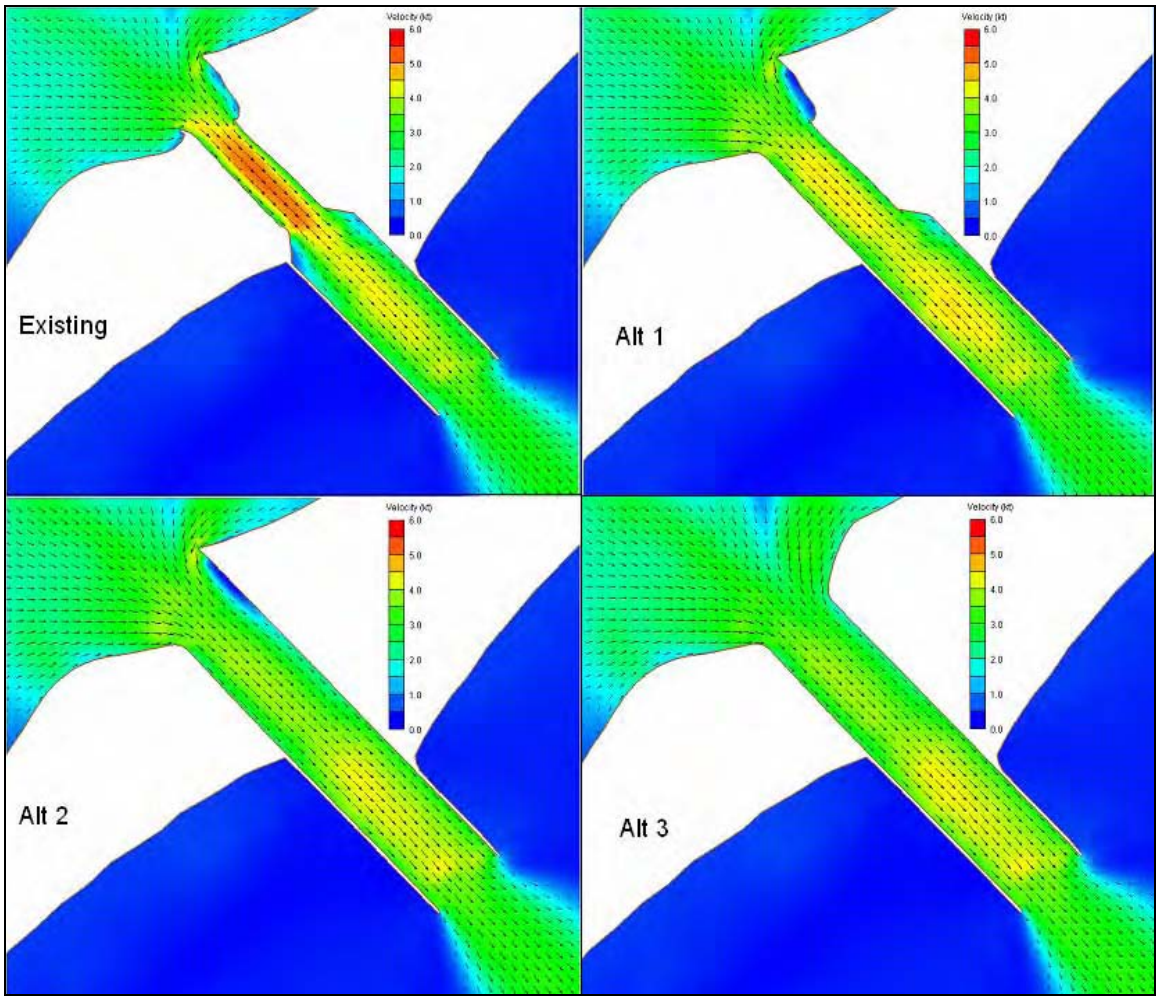

Figure 60. Calculated maximum current speed during ebb at 1300 GMT, 22 January 2004

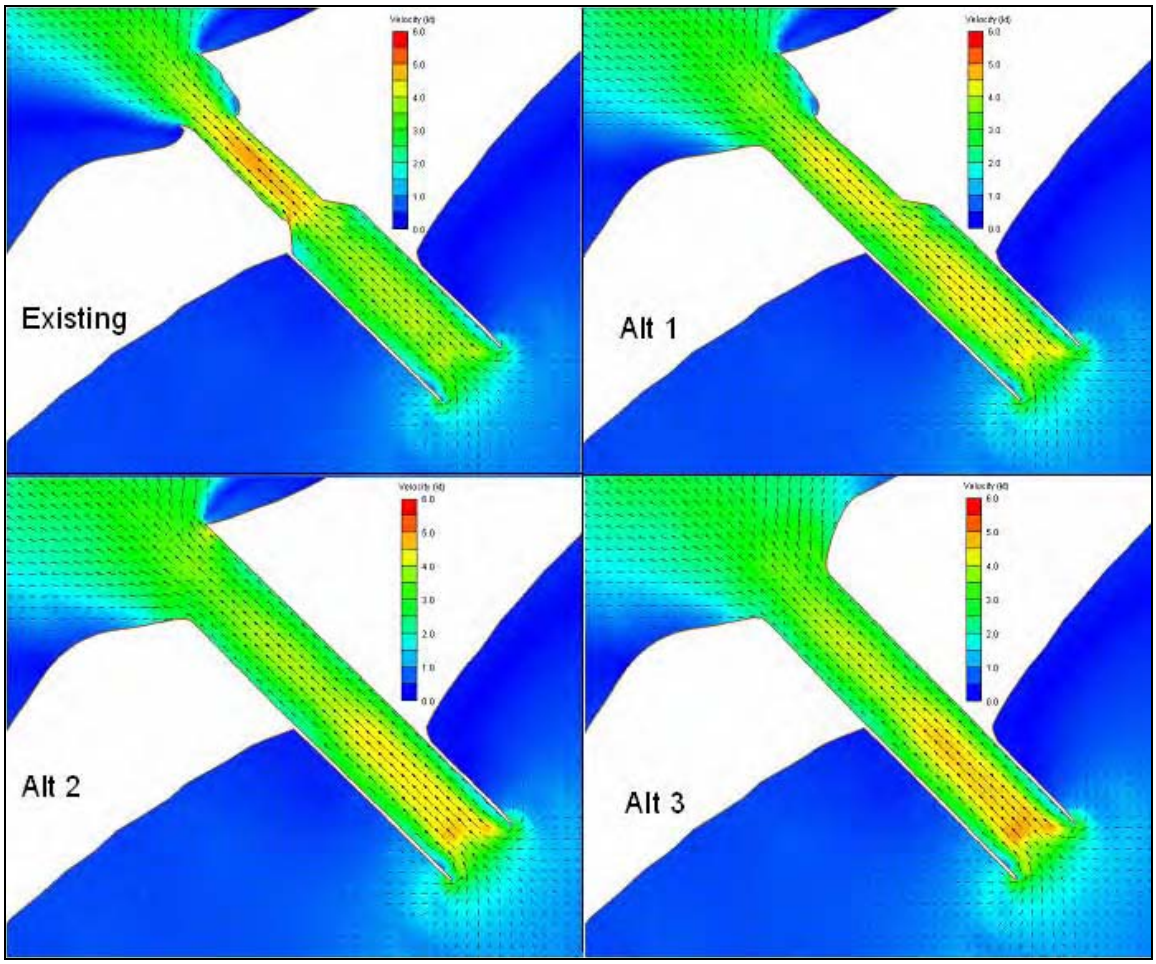

Figure 61. Calculated maximum current speed during flood at 0800 GMT, 30 July 2004

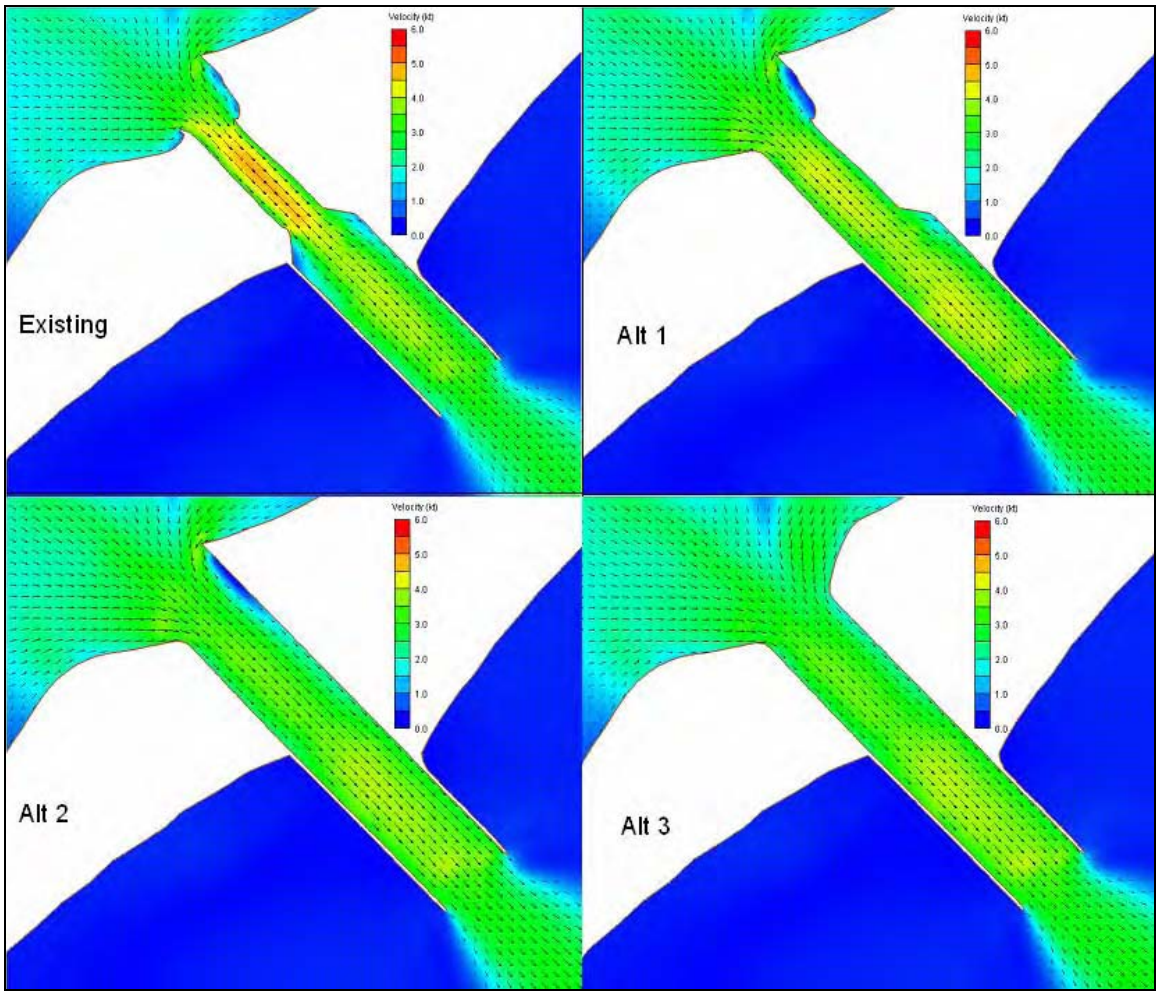

Figure 62. Calculated maximum current speed during ebb at 0200 GMT, 2 August 2004

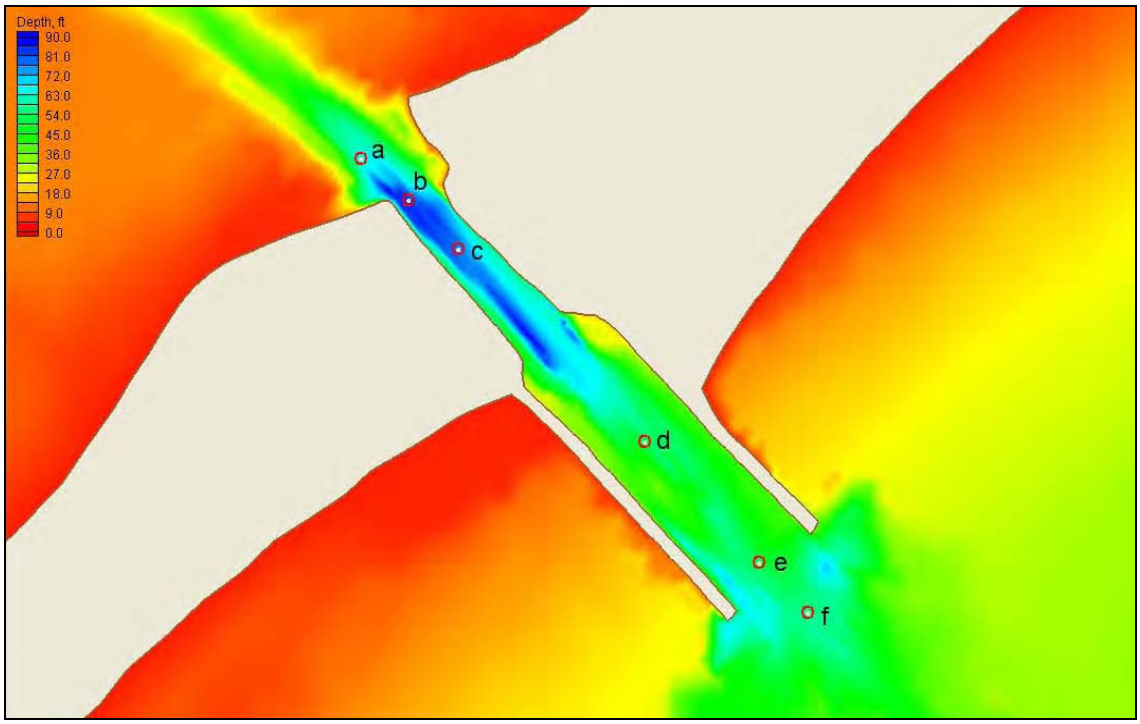

Figure 63. Locations of comparison sta a to f

Table 12
Coordinates of Comparison Stations

Station	Latitude	Longitude	Depth (ft) mtl
a	28°26′0″N	96°20′16″W	63
b	28°25′59″N	96°20′09″W	86
c	28°25′51″N	96°19′58″W	79
d	28°25′18″N	96°19′23″W	52
e	28°25′01″N	96°19′05″W	42
f	28°24′49″N	96°18′52″W	57

Table 13
Maximum Flood Current Speed (knots) for January 2004, at 2100 GMT

Station	Existing	Alt 1*	Alt 2*	Alt 3*
a	3.8	3.9 (3%)	3.7(-3%)	3.3 (-13%)
b	4.3	4.0 (-7%)	3.5 (-19%)	3.3 (-23%)
c	5.1	4.6 (-10%)	3.9 (-24%)	4.1 (-20%)
d	4.1	4.7 (14%)	4.7 (14%)	4.9 (20%)
e	4.1	4.7 (14%)	5.0 (22%)	5.2 (27%)
f	1.4	1.6 (14%)	1.7 (21%)	1.7 (21%)

* Percent difference compared to existing condition shown in parentheses. Negative values indicate reduced magnitude, and positive values indicate increased magnitude.

Table 14
Maximum Ebb Current Speed (knots) for January 2004, at 1300 GMT

Station	Existing	Alt 1*	Alt 2*	Alt 3*
a	3.4	3.6 (6%)	3.6 (6%)	3.2 (-6%)
b	4.6	3.9 (-15%)	3.6 (-22%)	3.3 (-28%)
c	5.2	4.5 (-13%)	3.8 (-27%)	3.7 (-29%)
d	4.4	4.5 (2%)	4.3 (-2%)	4.3 (-2%)
e	4.1	4.3 (5%)	4.4 (7%)	4.4 (7%)
f	3.1	3.1 (0%)	3.1 (0%)	3.1 (0%)

* Percent difference compared to existing condition shown in parentheses. Negative values indicate reduced magnitude, and positive values indicate increased magnitude.

Table 15
Maximum Flood Current Speed (knots) for 12 July to 10 August 2004, at 0800 GMT

Station	Existing	Alt 1*	Alt 2*	Alt 3*
a	3.6	3.7 (3%)	3.5 (-3%)	3.0 (-17%)
b	4.0	3.8 (-5%)	3.2 (-20%)	3.1 (-23%)
c	4.8	4.4 (-8%)	3.7 (-23%)	3.8 (-21%)
d	3.9	4.4 (12%)	4.5 (15%)	4.6 (18%)
e	3.9	4.5 (15%)	4.8 (23%)	5.0 (28%)
f	1.3	1.5 (15%)	1.6 (23%)	1.7 (31%)

* Percent difference compared to existing condition shown in parentheses. Negative values indicate reduced magnitude, and positive values indicate increased magnitude.

Table 16
Maximum Ebb Current Speed (knots) for 12 July to 10 August 2004, at 0200 GMT

Station	Existing	Alt 1*	Alt 2*	Alt 3*
a	3.1	3.3 (6%)	3.3 (6%)	2.9 (-6%)
b	4.2	3.6 (-14%)	3.3 (-21%)	3.0 (-28%)
c	4.8	4.1 (-15%)	3.5 (-27%)	3.4 (-27%)
d	4.0	4.1 (2%)	3.9 (-2%)	3.9 (-2%)
e	3.7	3.9 (5%)	4.0 (8%)	4.0 (8%)
f	2.8	2.8 (0%)	2.9 (4%)	2.9 (4%)

* Percent difference compared to existing condition shown in parentheses. Negative values indicate reduced magnitude, and positive values indicate increased magnitude.

Overall, Alt 2 and Alt 3 perform similarly reducing the current magnitude in the bottleneck at sta b and c by 19 to 27 percent for Alt 2 and by 20 to 29 percent for Alt 3. At sta b, where a scour hole has appeared, Alt 3 provides the greatest reduction in the maximum current speed compared to the other alternatives.

Alt 2 and Alt 3 reduce the current magnitude substantially on both flood and ebb at the bay side of the MSC entrance. At the gulf side of the entrance, however, the current in the middle of the channel increases substantially for both alternatives compared to the existing condition, while remaining almost the same as for the existing condition at ebb. Because the (flood) current magnitude increases along the gulf side of the entrance, scour is expected. The flow net theory of scour given by Hughes (2002) was applied to estimate the maximum expected depth on the gulf side of the channel for a symmetric flood flow. This simple scour theory gave 60-ft depth for 0.18-mm sand at the gulf side of the MSC entrance.

The ADCIRC grid was modified for Alt 3 to have 60-ft maximum depth in the channel, while retaining the greater depth in the scour area adjacent to the west jetty (Figure 64). The scoured situation for Alt 3 is denoted Alt 3a. Results of this and previous simulations are summarized in Figure 65. The current in the center of the channel decreases at sta a, b, and c for the alternatives during both ebb and flood tide. The magnitude of the current at sta d changes little among the alternatives, probably because it is near the center of the inlet and distant from both the bay and gulf ends of the MSC entrance. During flood, the current increases at sta e for the alternatives. Anticipated scour decreases the current about 12 percent at sta e during flood (compare Figures 65a and 65b). The current during both flood and ebb further decreases for Alt 3a at the bay-side stations (sta a, b, and c), because the scoured entrance broadens or spreads the flow more uniformly across the channel.

Figures 66 and 67 are percent exceedance diagrams of calculated flood and ebb current velocities at sta a, b, and c and at sta d, e, and f, respectively, for January 2004. Similarly, Figures 68 and 69 are percent exceedance diagrams of calculated current velocities at sta a, b, and c and at sta d, e, and f, respectively, for 12 July to 10 August 2004. Figures 70 and 71 compare Alt 3 and Alt 3a (assumed scour between the jetties) with the existing condition at sta a, b, and c and at sta d, e, and f, respectively, for January 2004. These figures quantify the improvement afforded by Alt 3 or Alt 3a at all stations except sta e (and excluding sta f, where the current is relatively weak). Figures 70 and 71 are percent exceedance diagrams, January 2004, of calculated current velocities at sta a, b, c and sta d, e, f, respectively, for the existing condition, Alt 3, and Alt 3a. These figures and along-channel maximum velocity plots (Figures 65a and 65b) show that both flood and ebb current velocities in Alt 3a are reduced at sta d and e compared to Alt 3. Calculated current velocities at sta a, b, c, and f are similar for Alt 3 and Alt 3a. For the current velocity at 20 percent exceedance, current magnitudes at sta d and e for Alt 3a are reduced by 4 and 11 percent, respectively, compared to Alt 3.

Figure 72 displays percent occurrence pie charts of calculated flood and ebb currents (the existing condition, Alt 1, Alt 2, and Alt 3) at sta c for January 2004. The current velocity magnitude at sta c in the bottleneck is the strongest among all the stations. For Alt 2 and Alt 3, current velocities are reduced significantly at sta b and c but increase during flood at sta d and e compared to the existing

condition. However, the increase in flood current speed at sta d and e for all three alternatives will be slightly smaller than given in these calculations because the channel bottom is expected to scour and reduce the current magnitude in those regions. Figure 73 shows percent occurrence pie charts of flood and ebb currents (the existing condition, Alt 1, Alt 2, and Alt 3a) at sta e for January 2004.

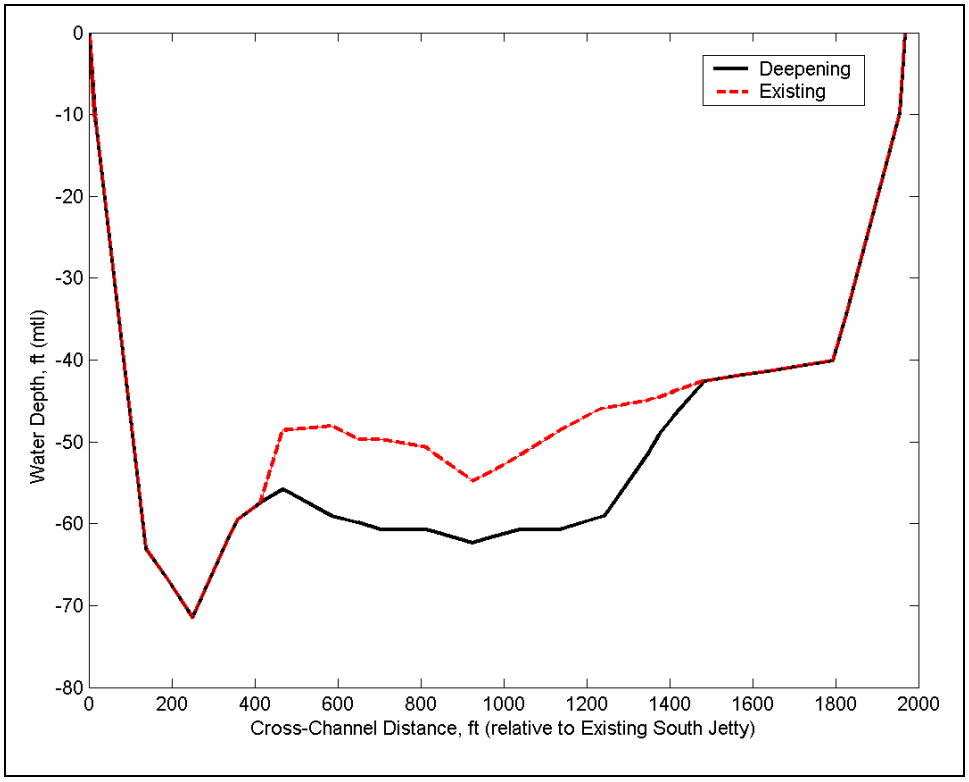

Figure 64. Estimated cross section of MSC entrance near gulfward end for Alt 3 based on assumed scour

Tables 17 to 20 present current magnitudes corresponding to 20 percent exceedance (Figures 66 to 69) for the existing condition and alternative configurations. For the current magnitude at 20 percent exceedance, Alt 2 and Alt 3 show similar and more favorable performance in reducing the current strength in the bottleneck at sta b and c by 20 to 29 percent for Alt 2, and by 22 to 31 percent for Alt 3.

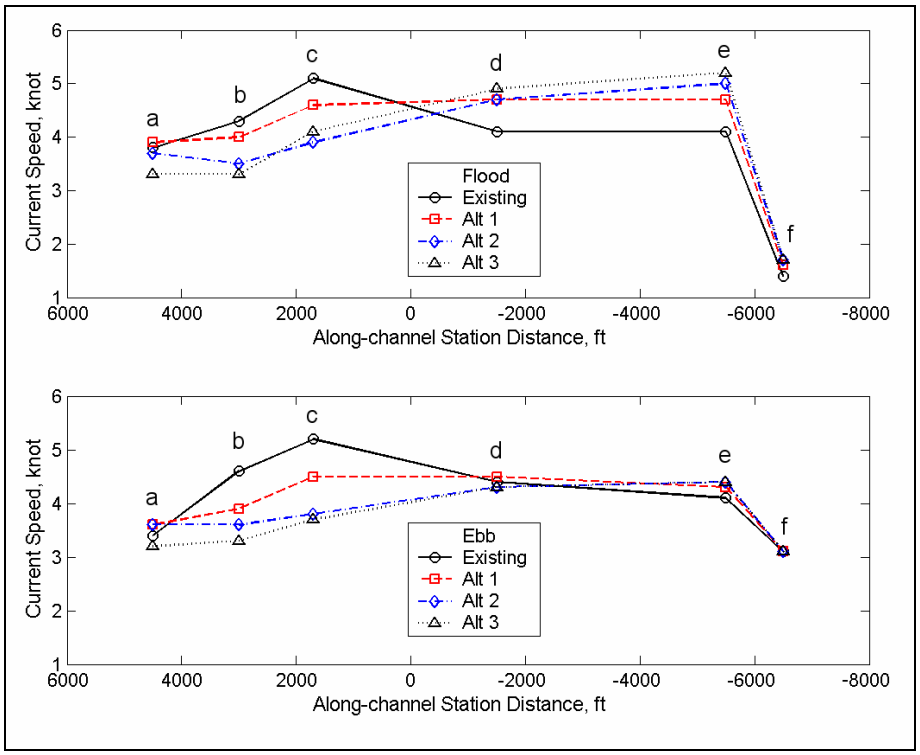

Figure 65a. Maximum current speed along center of MSC entrance for existing condition and alternatives

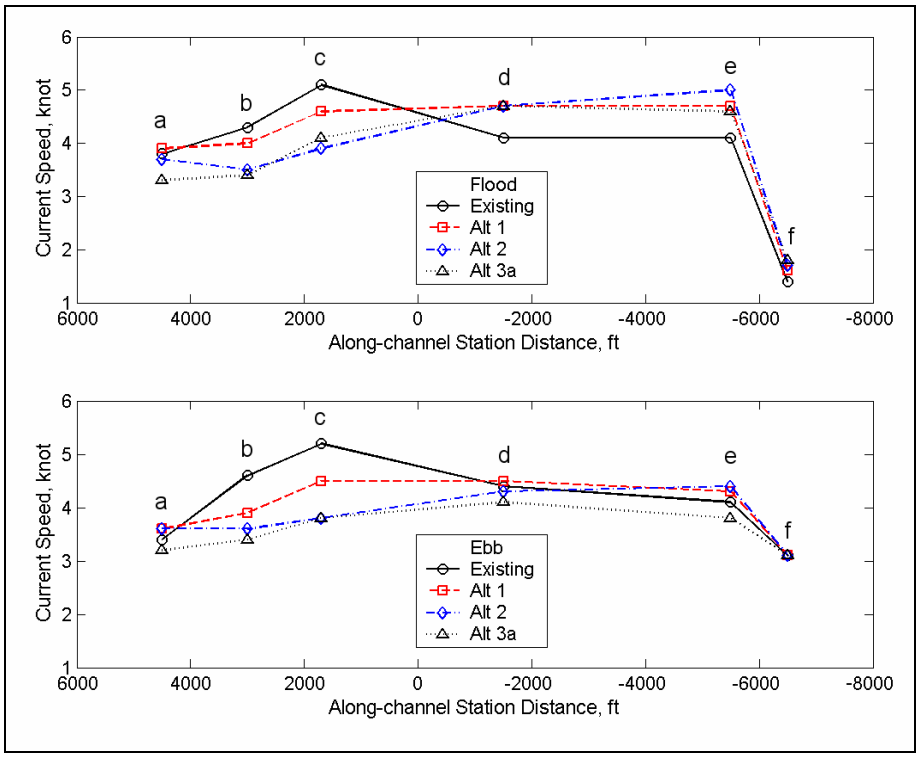

Figure 65b. Maximum current speed along center of MSC entrance for existing condition and Alt 3a

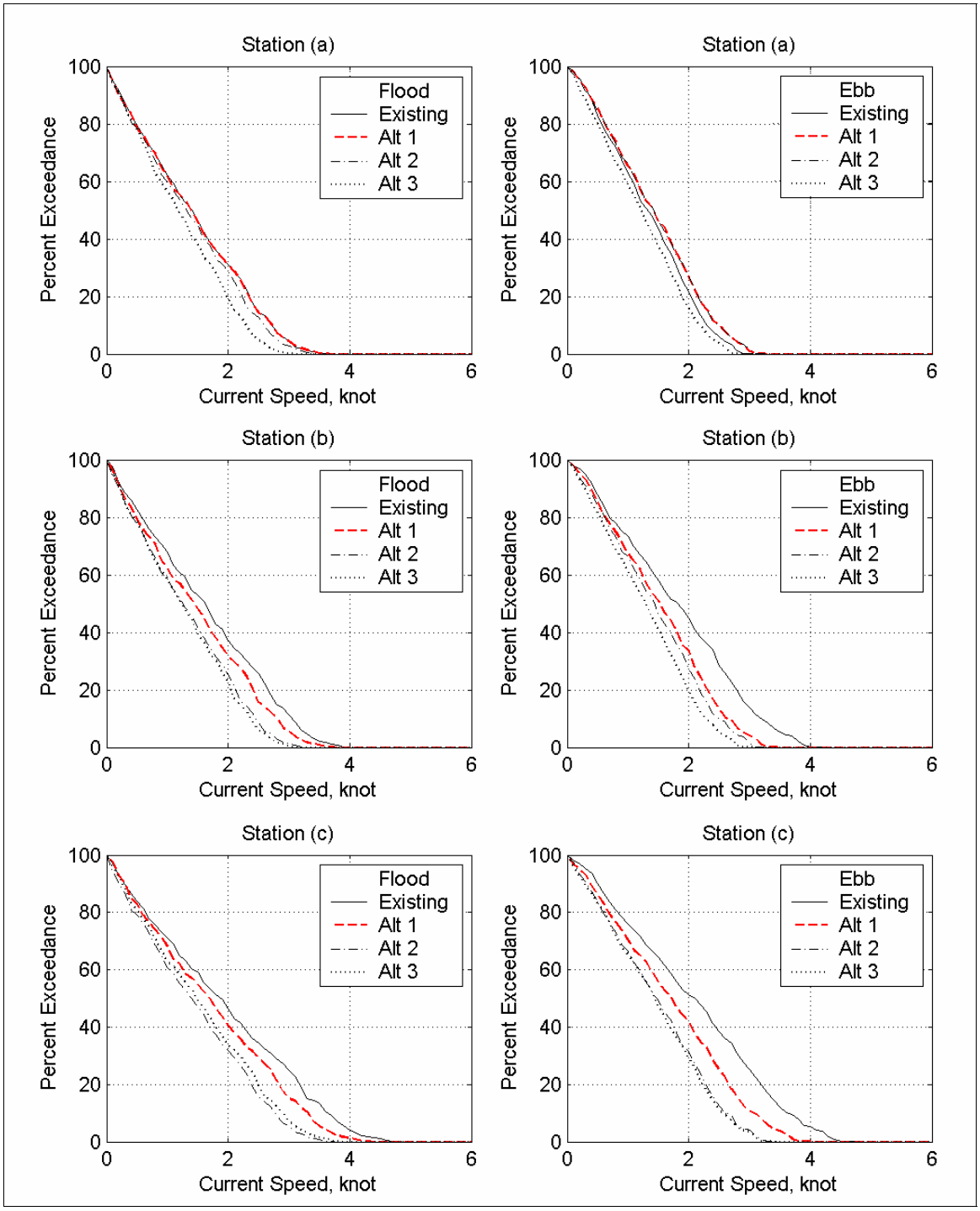

Figure 66. Percent exceedance diagrams for sta a, b, and c for January 2004

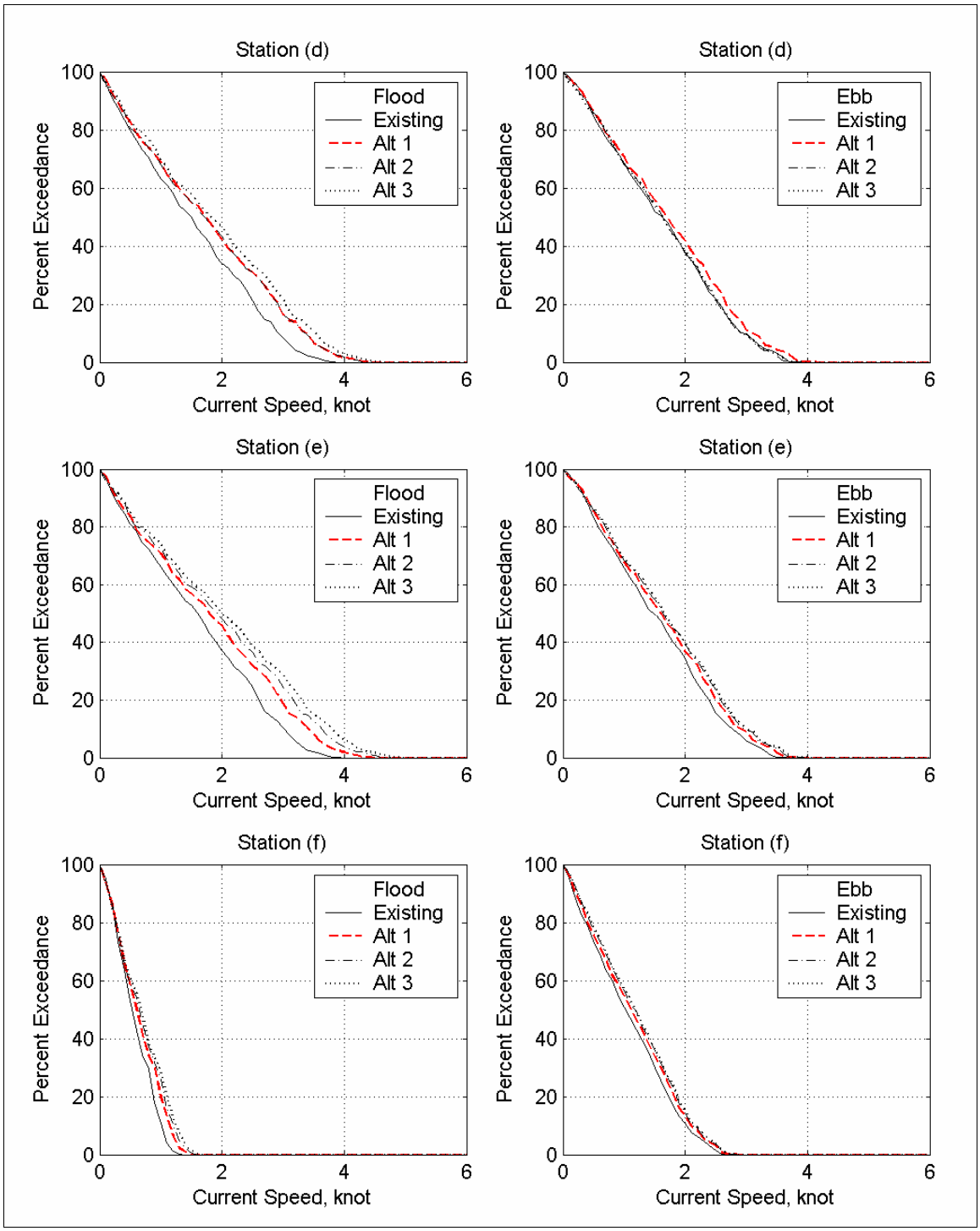

Figure 67. Percent exceedance diagrams for sta d, e, and f for January 2004

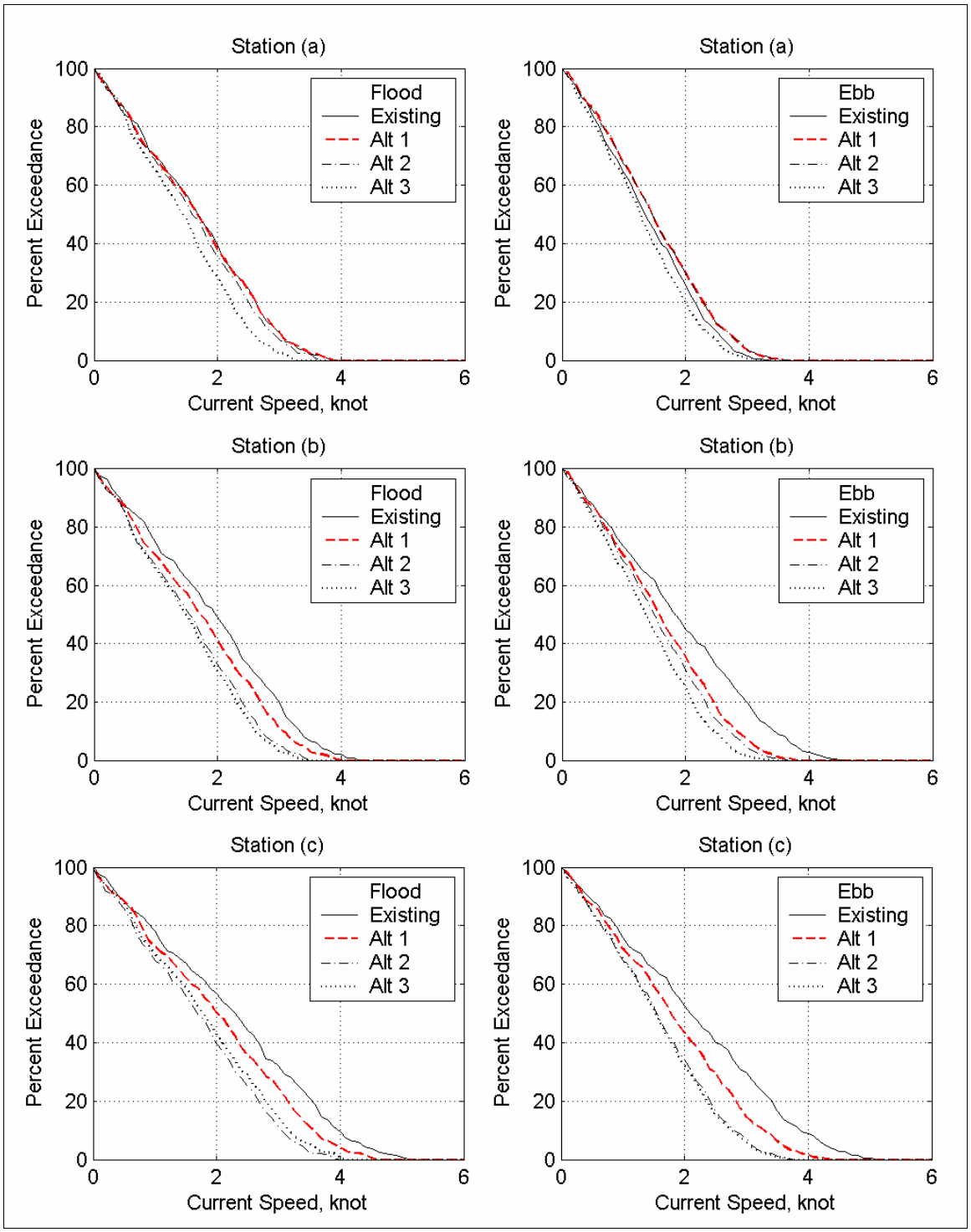

Figure 68. Percent exceedance diagrams for sta a, b, and c for 12 July to 10 August 2004

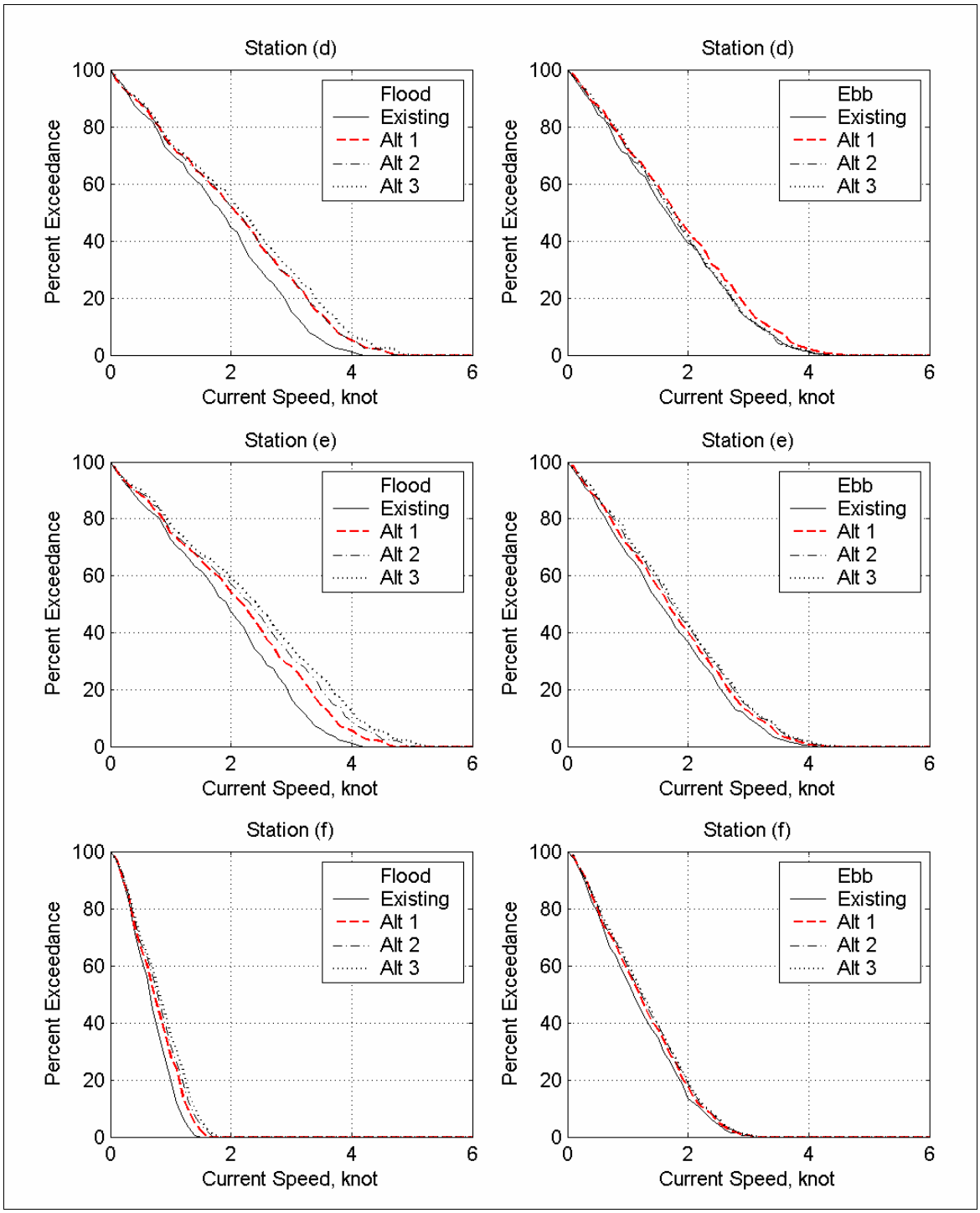

Figure 69. Percent exceedance diagrams for sta d, e, and f for 12 July to 10 August 2004

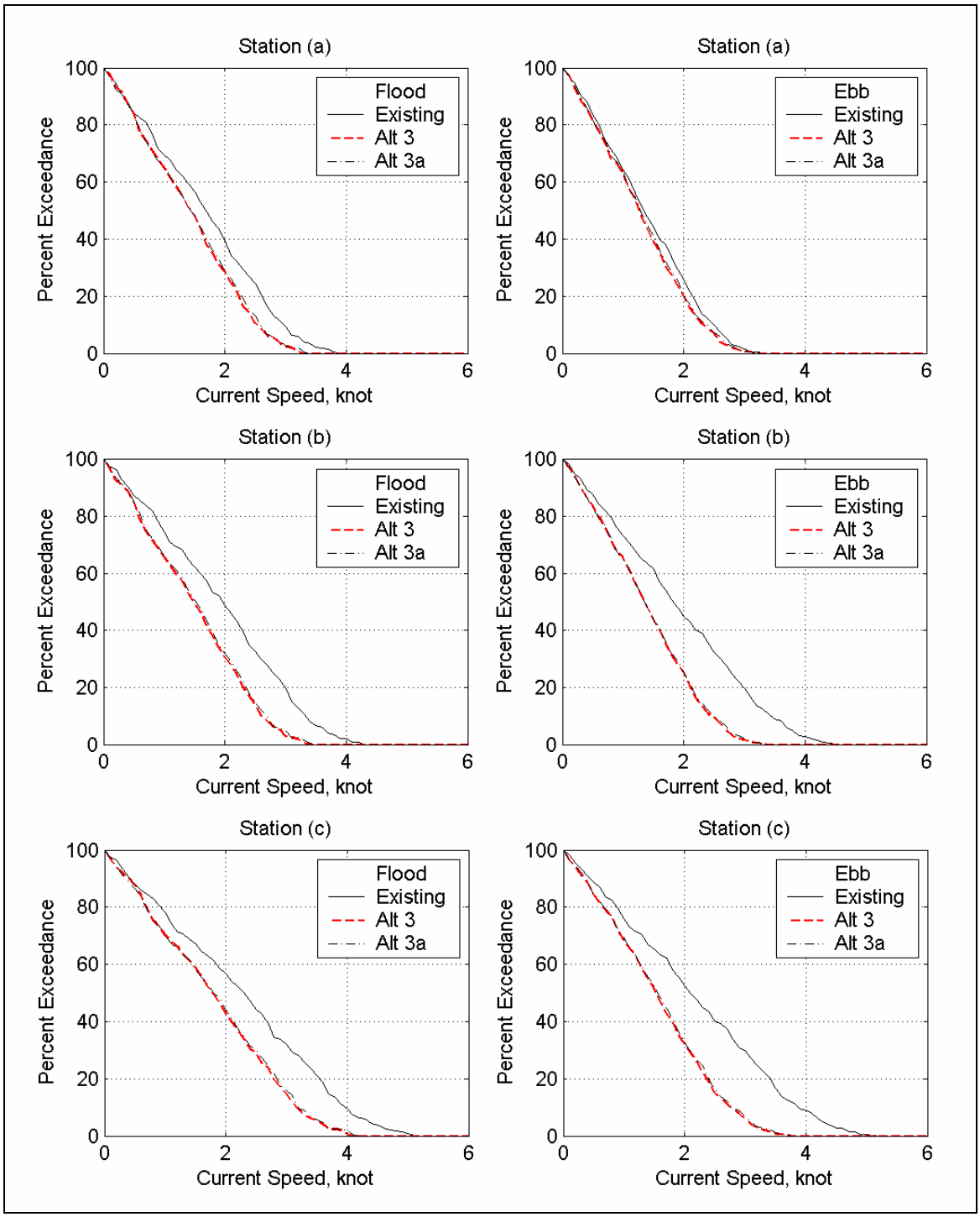

Figure 70. Percent exceedance diagrams for sta a, b, and c for January 2004, comparing Alt 3 and Alt 3a with existing condition

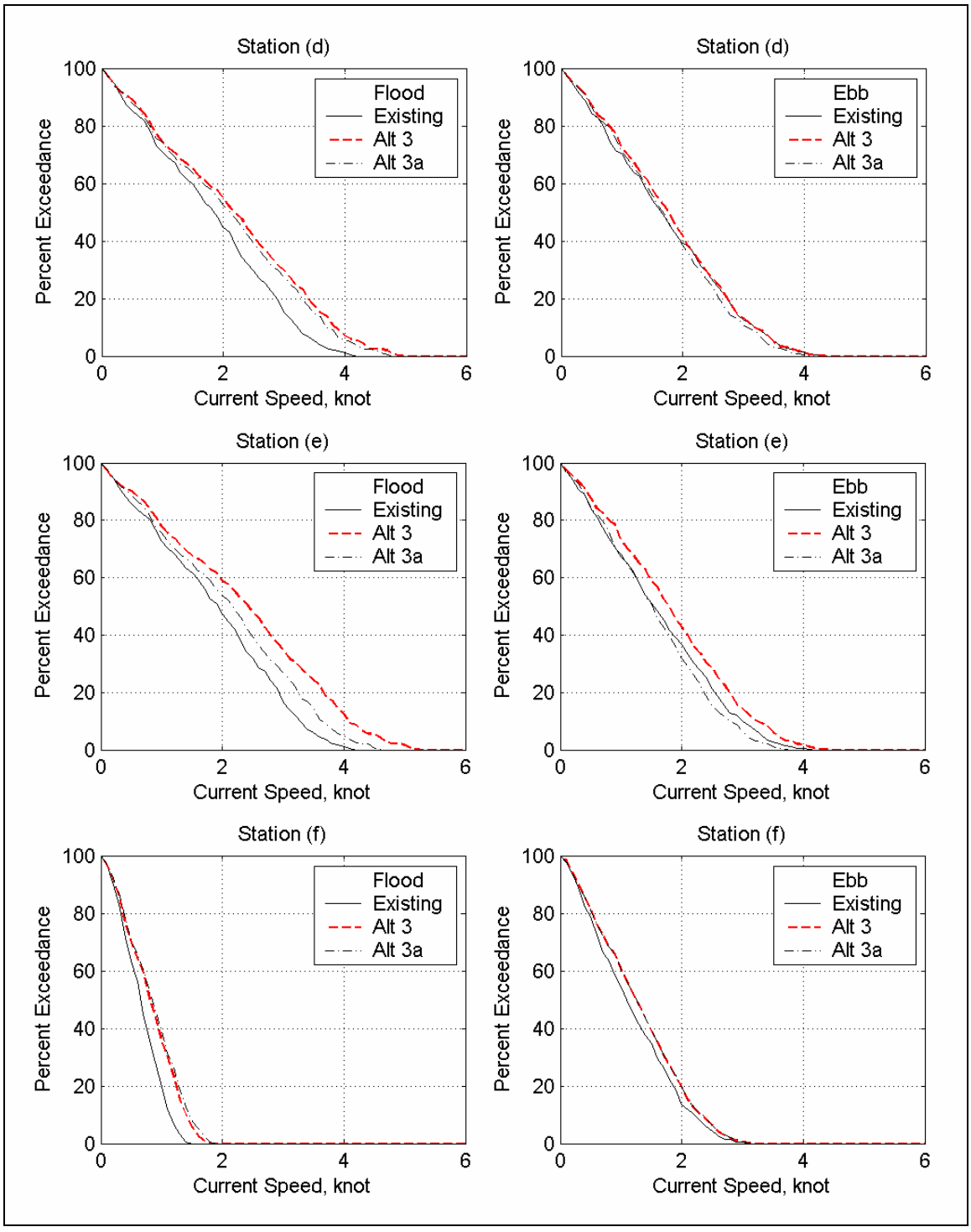

Figure 71. Percent exceedance diagrams for sta d, e, and f for January 2004, comparing Alt 3 and Alt 3a with existing condition

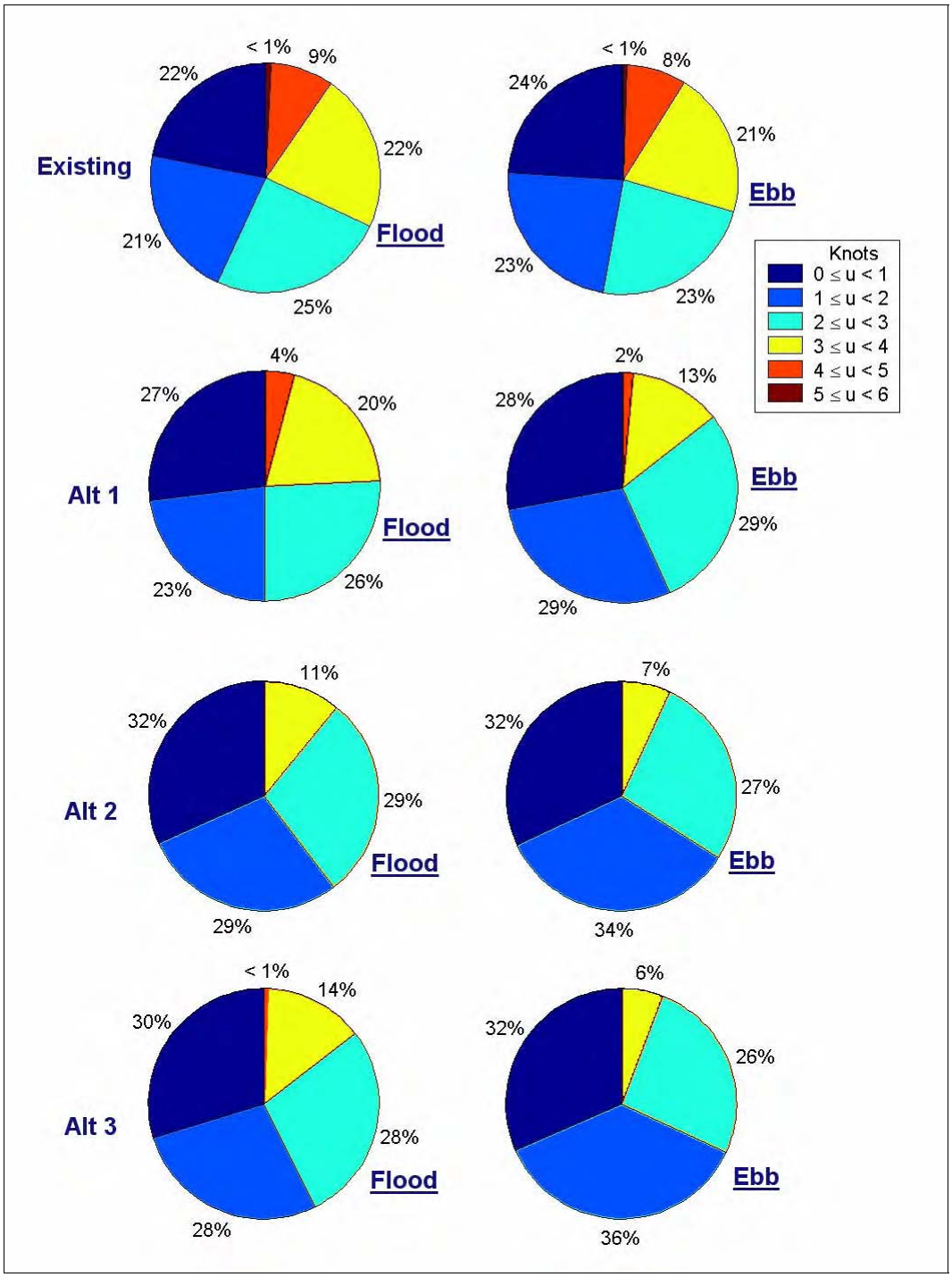

Figure 72. Current magnitude percent occurrence pie charts for sta c for January 2004

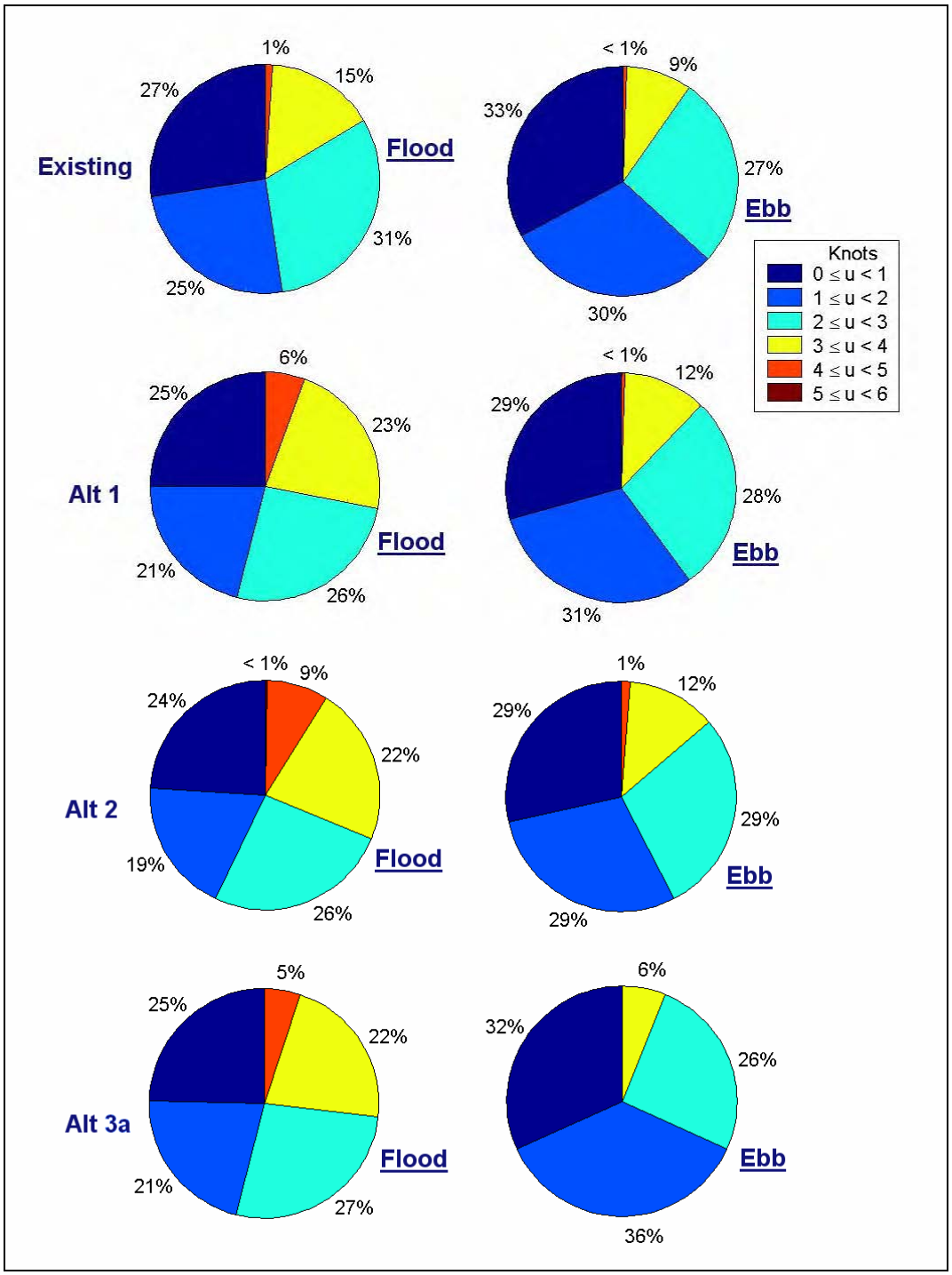

Figure 73. Current magnitude percent occurrence pie charts for sta e for January 2004, comparing Alt 1, Alt 2, and Alt 3A with existing condition

Table 17
Flood Current Speed (knots) at 20 Percent Exceedance, January 2004

Station	Existing	Alt 1*	Alt 2*	Alt 3*	Alt 3a*
a	2.6	2.6 (0%)	2.5 (-4%)	2.2 (-15%)	2.2 (-15%)
b	3.0	2.7 (-10%)	2.4 (-20%)	2.3 (-23%)	2.3 (-23%)
c	3.6	3.1 (-14%)	2.7 (-25%)	2.8 (-22%)	2.8 (-22%)
d	2.9	3.3 (14%)	3.3 (14%)	3.4 (17%)	3.3 (14%)
e	2.9	3.3 (14%)	3.5 (21%)	3.7 (28%)	3.3 (11%)
f	1.0	1.1 (10%)	1.2 (20%)	1.3 (30%)	1.3 (30%)

* Percent difference from existing condition shown in parentheses. Negative values indicate reduced magnitude, and positive values indicate increased magnitude.

Table 18
Ebb Current Speed (knots) at 20 Percent Exceedance, January 2004

Station	Existing	Alt 1*	Alt 2*	Alt 3*	Alt 3a*
a	2.1	2.3(10%)	2.3 (10%)	2.0 (-5%)	2.0 (-5%)
b	3.0	2.5 (-17%)	2.3 (-23%)	2.1 (-30%)	2.1 (-30%)
c	3.4	2.8 (-18%)	2.4 (-29%)	2.4 (-29%)	2.4 (-29%)
d	2.7	2.9 (7%)	2.8 (4%)	2.8 (4%)	2.6 (-4%)
e	2.6	2.7 (4%)	2.8 (8%)	2.8 (8%)	2.5 (-4%)
f	1.9	1.9 (0%)	2.0 (5%)	2.0 (5%)	2.0 (5%)

*Percent difference from existing condition shown in parentheses. Negative values indicate reduced magnitude, and positive values indicate increased magnitude.

Table 19
Flood Current Speed (knots) at 20 Percent Exceedance, 12 July to 10 August 2004

Station	Existing	Alt 1*	Alt 2*	Alt 3*
a	2.4	2.4 (0%)	2.2 (-8%)	2.0 (-17%)
b	2.7	2.4 (-11%)	2.1 (-22%)	2.0 (-26%)
c	3.2	2.8 (-13%)	2.4 (-25%)	2.5 (-22%)
d	2.5	2.9 (16%)	2.9 (16%)	3.0 (20%)
e	2.6	3.0 (15%)	3.2 (23%)	3.3 (27%)
f	0.9	1.0 (11%)	1.0 (11%)	1.1 (22%)

* Percent difference from existing condition shown in parentheses. Negative values indicate reduced magnitude, and positive values indicate increased magnitude.

Table 20
Ebb Current Speed (knots) at 20 Percent Exceedance, 12 July to 10 August 2004

Station	Existing	Alt 1*	Alt 2*	Alt 3*
a	2.1	2.1 (0%)	2.1 (0%)	1.9 (-10%)
b	2.8	2.3 (-18%)	2.2 (-21%)	2.0 (-29%)
c	3.2	2.7 (-16%)	2.3 (-28%)	2.2 (-31%)
d	2.6	2.7 (4%)	2.6 (0%)	2.6 (0%)
e	2.4	2.5 (4%)	2.6 (8%)	2.6 (8%)
f	1.7	1.8 (6%)	1.9 (12%)	1.9 (12%)

* Percent difference from existing condition shown in parentheses. Negative values indicate reduced magnitude, and positive values indicate increased magnitude.

Tables 21 and 22 present calculated mean flood and ebb flow discharges at the MSC and Pass Cavallo for the existing condition and three alternatives for the winter and summer month simulations. Discharges are greater in the winter than in the summer, mainly because the stronger wind in the winter drives more flow in and out of the bay. Both flood and ebb discharges through the MSC increase for the three alternatives because of partial or full removal of the bottleneck. With the bottleneck removed, the MSC becomes more efficient for flow exchange between the gulf and the bay. The change of flow discharge through Pass Cavallo is relatively small for the three alternatives.

Table 21
Calculated Mean Discharge (1,000 x cfs), January 2004

Location and Condition	Existing	Alt 1*	Alt 2*	Alt 3*	Alt 3a*
MSC, Flood	225	254 (13%)	269 (20%)	282 (25%)	286 (27%)
MSC, Ebb	211	231 (9%)	240 (14%)	244 (16%)	249 (18%)
Pass Cavallo, Flood	86	84 (-2%)	82 (-5%)	82 (-5%)	80 (-7%)
Pass Cavallo, Ebb	79	76 (-4%)	75 (-5%)	75 (-5%)	74 (-6%)

* Percent difference from existing condition shown in parentheses. Negative values indicate reduced magnitude, and positive values indicate increased magnitude.

Table 22
Calculated Mean Discharge (1,000 x cfs), 12 July to 10 August 2004

Location and Condition	Existing	Alt 1*	Alt 2*	Alt 3*
MSC, Flood	192	220 (15%)	232 (21%)	245 (28%)
MSC, Ebb	202	218 (8%)	225 (11%)	226 (12%)
Pass Cavallo, Flood	74	73 (-1%)	71 (-4%)	71 (-4%)
Pass Cavallo, Ebb	71	67 (-6%)	65 (-8%)	64 (-10%)

* Percent difference from existing condition shown in parentheses. Negative values indicate reduced magnitude, and positive values indicate increased magnitude.

Additional model simulations were conducted by coupling ADCIRC with the nearshore wave model STWAVE (Resio 1993; Smith et al. 2001) in the Inlet Modeling System to investigate the cross current induced by waves at the entrance of the MSC. Four additional modified jetty configurations were studied: (a) removal of the north bottleneck revetment, (b) widened bay entrance beyond that of Alt 3, in addition to the removal of the bottleneck, (c) Alt 2a - removed the north revetment at the bay entrance in addition to Alt 2, and (d) Alt 2b - shortened the south jetty at the Gulf entrance by 1,640 ft in addition to Alt 2a. It was found that the wave-induced contribution to the current was minimal at the jetty entrance of the MSC. Similarly, the four additional jetty relocations did not offer improvements over Alt 2 and Alt 3. For example, Figure 74 shows the maximum current speed during flood at 2100 GMT, 20 January, for Alt 2b. In this example, the flood current distribution is very asymmetrical at the Gulf entrance and maximum current speed is stronger along the north bottleneck revetment. This asymmetric flood flow pattern for unequal seaward jetties can cause further scouring adjacent to jetty toes and force navigation away from the channel centerline (Hughes 2000). Therefore, calculations from these extra simulations are not presented.

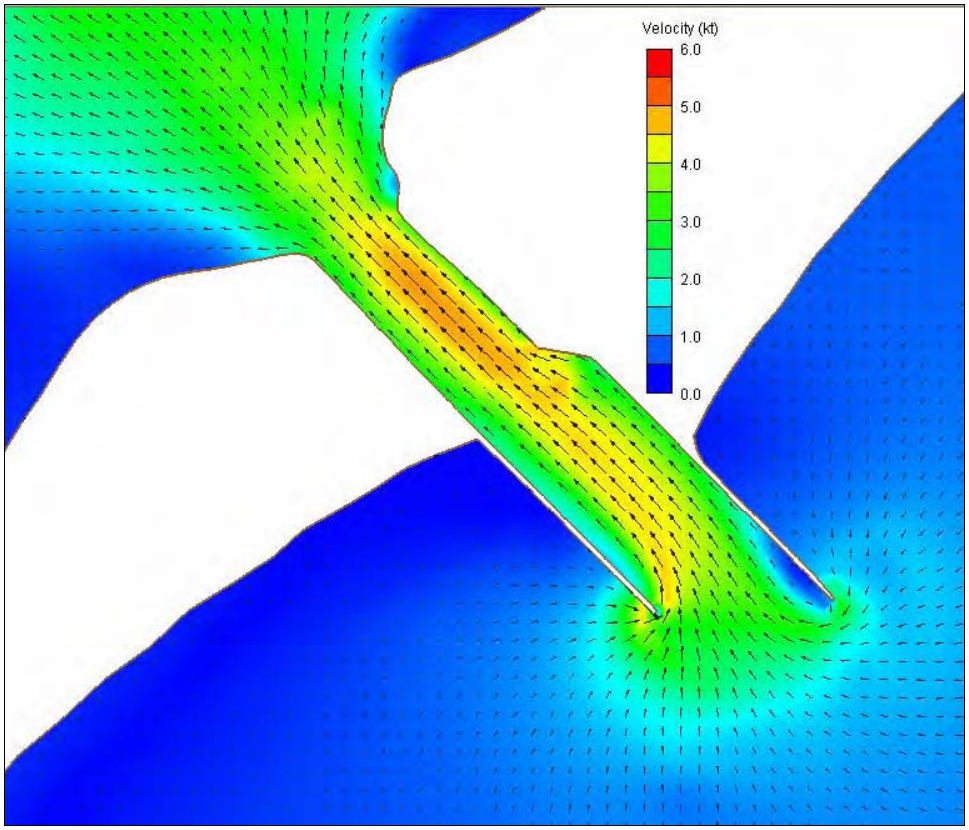

Figure 74. Calculated maximum current speed during flood at 2100 GMT, 20 January, for Alt 2b

Calculations with Pass Cavallo Closed

Pass Cavallo was the only permanent inlet connecting Matagorda Bay and the Gulf of Mexico before the MSC was opened in 1963 (Chapter 1). The width of Pass Cavallo decreased from more than 2.1 miles (11,500 ft) at its throat before 1965 to about 2,200 ft in 2003 (Chapter 2). The depth of Pass Cavallo also decreased substantially because of reduced current magnitude and flow rate in the inlet as a result of greater water exchange now between the bay and the gulf through the MSC than through Pass Cavallo. Measurements taken in 1997 (Kraus et al. 2000) indicate that three-fourths of the discharge, or tidal prism, passed through the MSC entrance at that time. Numerical model simulations conducted in the present study also show that the mean discharge through the MSC is about three times greater than through Pass Cavallo (Tables 21 and 22). The analysis presented in Chapter 2 suggests that Pass Cavallo may now be at or near equilibrium width, but the possibility exists that an extreme natural event, such as a hurricane, a tropical storm, turning winds of winter fronts, or an engineering action such as removal of the bottleneck at the MSC entrance, will lead to either temporary or permanent closure of Pass Cavallo. Closure of Pass Cavallo raises environmental concerns about the ecosystem in the Matagorda Bay, Espiritu Santo Bay, and the Gulf of Mexico nearshore. Also, the question arises as to the magnitude of increase in velocity and discharge through the MSC entrance should Pass Cavallo close.

Numerical simulations including the closure of Pass Cavallo were conducted for two alternatives: Pass Cavallo closed in the existing condition (Alt 4) and Pass Cavallo closed together with Alt 3, denoted as Alt 5. The purpose of these simulations was to evaluate the change in the current magnitude and discharge rate at the MSC entrance in response to the closure of Pass Cavallo. Tables 23 to 26 present the maximum flood and ebb current magnitudes at the MSC entrance for the existing condition, Alt 3, Alt 4, and Alt 5 for the two simulation cases of typical winter and summer months. Comparing Alt 4 to the existing condition indicates that both flood and ebb maximum current speeds in the MSC entrance increase by 7 to 10 percent at sta b and c in the bottleneck and by 8 to 17 percent at sta d and e in the wider channel between jetties. Comparing Alt 5 to Alt 3 indicates that both flood and ebb maximum current speeds are increased by 10 to 14 percent at sta b and c, and by 8 to 14 percent at sta d and e.

Tables 27 and 28 present calculated flood and ebb mean discharges at the MSC entrance for the existing condition, Alt 3, and the two alternatives with the closure of Pass Cavallo for simulations of January 2004 and 12 July to 10 August 2004, respectively. With Pass Cavallo closed, both flood and ebb mean discharges through the MSC entrance for Alt 4 and Alt 5 increase over the existing condition. Because stronger discharges indicate stronger currents, closure of Pass Cavallo is expected to increase channel scour and shore erosion around the bay perimeter in the vicinity of the MSC entrance.

Table 23
Maximum Flood Current Speed (knots) for Existing Condition and Alts 3, 4, and 5 at 2100 GMT, 20 January 2004

Station	Existing	Alt 3	Alt 4*	Alt 5**
a	3.8	3.3	4.3 (13%)	3.6 (9%)
b	4.3	3.3	4.7 (9%)	3.7 (12%)
c	5.1	4.1	5.6 (10%)	4.5 (10%)
d	4.1	4.9	4.5 (10%)	5.4 (10%)
e	4.1	5.2	4.5 (17%)	5.7 (10%)
f	1.4	1.7	1.5 (7%)	1.9 (12%)

* Percent difference from the existing condition shown in parentheses. Positive values indicate increased magnitude.
** Percent difference between Alt 5 and Alt 3.

Table 24
Maximum Ebb Current Speed (knots) for Existing Condition and Alts 3, 4, and 5 at 1300 GMT, 22 January 2004

Station	Existing	Alt 3	Alt 4*	Alt 5**
a	3.4	3.2	3.7 (9%)	3.5 (9%)
b	4.6	3.3	5.0 (8%)	3.7 (12%)
c	5.2	3.7	5.7 (10%)	4.2 (14%)
d	4.4	4.3	4.9 (11%)	4.8 (12%)
e	4.1	4.4	4.6 (12%)	5.0 (14%)
f	3.1	3.1	3.4 (10%)	3.5 (13%)

*Percent difference from the existing condition shown in parentheses. Positive values indicate increased magnitude.
** Percent difference between Alt 5 and Alt 3.

Table 25
Maximum Flood Current Speed (knots) for Existing Condition and Alts 3, 4, and 5 at 0800 GMT, 30 July 2004

Station	Existing	Alt 3	Alt 4*	Alt 5**
a	3.6	3.0	3.9 (8%)	3.3 (10%)
b	4.0	3.1	4.3 (7%)	3.4 (10%)
c	4.8	3.8	5.2 (8%)	4.2 (11%)
d	3.9	4.6	4.2 (8%)	5.0 (9%)
e	3.9	5.0	4.2 (8%)	5.4 (8%)
f	1.3	1.7	1.4 (8%)	1.8 (6%)

*Percent difference from the existing condition shown in parentheses. Positive values indicate increased magnitude.
** Percent difference between Alt 5 and Alt 3.

Table 26
Maximum Ebb Current Speed (knots) for Existing Condition and Alts 3, 4, and 5 at 0200 GMT, 2 August 2004

Station	Existing	Alt 3	Alt 4*	Alt 5**
a	3.1	2.9	3.4	3.2
b	4.2	3.0	4.6 (10%)	3.3 (10%)
c	4.8	3.4	5.3 (10%)	3.8 (12%)
d	4.0	3.9	4.4 (10%)	4.4 (13%)
e	3.7	4.0	4.2 (14%)	4.5 (13%)
f	2.8	2.9	3.1	3.3

*Percent difference from the existing condition shown in parentheses. Negative values indicate reduced magnitude, and positive values indicate increased magnitude.
** Percent difference between Alt 5 and Alt 3.

Table 27
Calculated Mean Discharge (1,000 x cfs) for Existing Condition and Alts 3, 4, and 5, January 2004

Location & Condition	Existing	Alt 3	Alt 4*	Alt 5**
MSC, Flood	225	282	243 (8%)	305 (8%)
MSC, Ebb	211	244	246 (17%)	283 (16%)
Pass Cavallo, Flood	86	82	0	0
Pass Cavallo, Ebb	79	75	0	0

* Percent difference to the existing condition shown in parentheses. Negative values indicate reduced magnitude, and positive values indicate increased magnitude.
** Percent difference between Alt 5 and Alt 3.

Table 28
Calculated Mean Discharge (1,000 x cfs) for Existing Condition and Alts 3, 4, and 5, 12 July to 10 August 2004

Location & Condition	Existing	Alt 3	Alt 4*	Alt 5**
MSC, Flood	192	245	216 (13%)	267 (9%)
MSC, Ebb	202	226	227 (12%)	264 (17%)
Pass Cavallo, Flood	74	71	0	0
Pass Cavallo, Ebb	71	64	0	0

* Percent difference to the existing condition shown in parentheses. Negative values indicate reduced magnitude, and positive values indicate increased magnitude.
** Percent difference between Alt 5 and Alt 3.

Summary

Three alternative modifications (Alt 1, Alt 2, and Alt 3; see Chapter 1) of the jetties at the MSC entrance were investigated for reducing the strong current through the entrance and compared to the existing condition. In addition, two hypothetical alternatives defined by closure of Pass Cavallo for the existing condition (Alt 4) and by closure of Pass Cavallo for Alt 3 (Alt 5) were examined. The channel cross section of Alt 3 was artificially increased to account for anticipated scour on the gulf side, and this variation was denoted as Alt 3a.

Simulations of water level and current were conducted for two different periods representing a typical winter month and a typical summer condition to evaluate the jetty alternatives. Calculation results were analyzed for flood and ebb current magnitudes and percent exceedance of current magnitude at six stations (sta a through f) in the MSC entrance.

Compared to the existing condition, simulations for Alt 2 and Alt 3 show reduced maximum current velocities in the bottleneck at sta b and c (bay side of entrance) by 19 to 27 percent for Alt 2 and by 20 to 29 percent for Alt 3. This reduction of current velocity for Alt 2 and Alt 3 is also shown in the percent exceedance current speed analysis. Compared to the existing condition, the current velocity corresponding to the 20 percent exceedance velocity at sta b and c is reduced 22 to 31 percent for Alt 3. These simulations show that the current magnitude for the existing condition is strong and unevenly distributed across the bay entrance channel, especially during ebb flow. A strong ebb current tends to generate eddies and cross currents that may be hazardous to navigation. On the other hand, the three alternatives would produce a more uniform current flow across the bay entrance channel. Among them, Alt 3 would produce the most uniform flow with the smallest current magnitude across the bay entrance. Therefore, a reduced cross current and fewer eddies at the bay entrance are expected for Alt 3.

Simulations for Alt 1, Alt 2, and Alt 3 indicate that the flood current speed would increase at sta d and e in the gulfward channel between jetties. It is probable that this increase of the flood current velocity would be smaller than the calculated value because the channel bottom is expected to be scoured under the strong current condition. To demonstrate this situation, a 60-ft channel (20 percent channel scour) was simulated between the jetties for January 2004 (denoted Alt 3a). The calculated flood current shows that the scour expected for Alt 3a would reduce the maximum current velocity at sta e from 5.2 to 4.6 knots (12 percent reduction) compared to 4.1 knots in the existing condition. For the current magnitude corresponding to 20 percent exceedance, the magnitude at sta e was reduced from 3.7 to 3.3 knots (11 percent reduction) compared to 2.9 knots for the existing condition.

Flood and ebb mean discharges at the MSC entrance and Pass Cavallo were calculated. Both the flood and ebb discharges through the MSC entrance would increase for Alt 1, Alt 2, and Alt 3 because of the partial or full removal of the bottleneck and improved hydraulic efficiency (less friction). In these simulations, the change in flow rate through Pass Cavallo was relatively small. The channel cross-sectional area of Pass Cavallo was held constant for these simulations. The ratio of discharges at Pass Cavallo and the MSC entrance is approximately 1:3 for these three alternatives (Tables 21 and 22).

If Pass Cavallo closes, the maximum current speed at the MSC entrance on flood and ebb is predicted to increase 7 to 17 percent for the existing condition. Comparing Alt 5 to Alt 3, the maximum current speed at the MSC entrance is predicted to increase 8 to 14 percent. A stronger current corresponds to a larger flow rate, so closure of Pass Cavallo would increase channel scour and shore erosion on the bay side of the MSC entrance. It is recommended to preserve Pass Cavallo, should that become necessary, to avoid an increase in discharge through the MSC, especially during storms.

5 Discussion and Conclusions

The objective of this study was to evaluate alternatives for improving jetty stability at the Gulf of Mexico entrance to the MSC by reducing the velocity of the current through it. In the existing condition, the current through the entrance regularly exceeds 3 knots and more than 5 knots on occasion. An inlet channel of stable cross-sectional area tends to support maximum tidal current velocities on the order of 2 knots, and inlet currents in the 2- to 3-knot range seem acceptable to ship pilots. The strong current through the MSC entrance results from the so-called bottleneck region in the land cut through Matagorda Peninsula, which constricts the flow, increasing the current velocity and producing a large and deep scour region on the bay side of the entrance. The goal of this study was to identify and evaluate alternatives to stabilize the jetties at the entrance to the MSC through reduction of the current velocity.

The strong current has produced a scour hole 90 to 100 ft deep in a channel authorized to 36-ft depth through the entrance. This scour hole is located on the bay side of the MSC entrance and is a consequence of both the strong along-channel current and the sharp turn in the ebb current around the narrow bay entrance. The scour hole is growing slowly and, if it approaches the south bank, failure of the revetment becomes a possibility. The strong current is also a concern to commercial navigation interests. Numerous navigation aid discrepancies are reported by the U.S. Coast Guard annually in the vicinity of the MSC-GIWW intersection, primarily because of the strong current through the MSC. Ships entering Matagorda Bay on strong flood current have diminished control until they are past the MSC-GIWW intersection. On strong ebb current, pilots report that cross-channel current velocity can cause concern for steerage through the bottleneck and jetties.

Components of this study to address jetty stability covered the following elements: review of the engineering and geology literatures, field data collection of water level and current, bathymetry surveys, engineering analysis, geomorphic analysis of local and regional trends in shoreline behavior, and numerical modeling of the circulation. A regional approach was taken in considering shoreline change on both the Gulf of Mexico and Matagorda Bay sides of the MSC entrance and in long-term morphologic behavior of Pass Cavallo.

Current Velocity and Jetty Stability

Numerical simulations were performed with a hydrodynamic model incorporating recent bathymetric surveys and calibrated against water elevation measured around Matagorda Bay and current velocity measured in the MSC entrance channel. Tidal forcing, wind, river discharges, and multiple inlets around Matagorda Bay were represented. Three alternatives and the existing condition were then evaluated for a representative winter month, when northerly weather fronts are strong and frequent, and a representative month-long period in summer, when sea breeze and southeast winds dominate. It was known from previous and the present work that a meteorological tide can dominate the astronomical tide on the Texas coast, where the wind is strong.

The current through the MSC entrance was analyzed at six stations, three on the bay side and three on the Gulf of Mexico side, for magnitude under the specified alternative. In addition, broad-area diagrams of maximum current speed were also produced to visualize general patterns. The following results were obtained:

a. Frequency-of-occurrence or percent-exceedance diagrams were developed as a means of quantifying the current through the MSC entrance and comparing alternatives. The concept is that an alternative does not have to reduce the current to an acceptable level all the time, but for a certain percent of the time. A 20 percent threshold was considered as an example.

b. Consideration was given to a reduction in the current magnitude at the bay entrance, a reduction in the percent exceedance, and the capability of training the ebb current toward the center of the channel (away from the jetties and more uniformly across the channel). Based on these criteria, widening the bottleneck to a nominal 2,000 ft and flanging the jetty revetment into the bay was judged to provide the best performance (Alt 3).

c. Alt 2, widening the bottleneck to a nominal 2,000 ft, had the second-best performance and was close to that of Alt 3, except that the current would not be trained to the center of the channel.

d. Although the discharge or tidal prism through the MSC entrance would increase for any of the alternatives, the decrease in discharge at Pass Cavallo, which would contribute to its further reduction in width, was small (on the order of 5 to 10 percent) because of wind setup in the southwest corner of the bay.

e. An extreme case of entrance widening (greater flanging of Alt 3) did not produce a notable decrease in current magnitude through the entrance, indicating that the alternatives explored in detail in this study are reasonable choices based on general considerations of the cost of dredging.

f. Alt 2 and Alt 3 would decrease the current magnitude on the bay side of the entrance and increase it on the Gulf of Mexico side. A moderate increase in along-channel current speed on the gulf side may provide a potential benefit by reducing sediment infilling by tip shoal development at the north jetty because of greater scouring action.

g. Scour anticipated in association with a strong flood current at the gulf side of the entrance for Alt 3 (denoted as Alt 3a) would reduce the increase in flood current to about 14 percent greater than for the existing condition (Table 17).

h. Alt 2 and Alt 3 are compatible with possible future plans for channel deepening and widening of the MSC.

i. A reduction in the flood current at the bay side of the MSC entrance is expected to reduce maintenance dredging requirements along the GIWW in the vicinity of Sundown Island, as well as decrease navigation discrepancies at the MSC-CIWW intersection.

j. The rationale for the existence of the bottleneck could not be fully ascertained. It is tentatively concluded that the designers did not expect a mile-long narrow land cut to grow to 2,000-ft width. Physical model tests performed for the original design employed land cuts through the entrance of various sizes approximately corresponding to channel widths. Extremely rapid growth in the channel width caused the land cut to be revetted in an expedient manner.

Regional Processes

Changes to coastal inlets can produce wide-ranging geomorphic responses. This section lists key regional findings of this study.

a. The regional long-term trend of shoreline change on the Gulf of Mexico side of Matagorda Peninsula is recession, attributable to relative sea-level rise, reduced river sediment input to the coast (by the Colorado, San Bernard, and Brazos Rivers), storms, and a reduction in supply from offshore deposits.

b. The gulf shoreline updrift and downdrift of the jetties initially advanced and receded, respectively, at a high rate. In recent years, the rate of shoreline change has decreased, but the trend for advance and recession north and south of the entrance, respectively, continues.

c. Pass Cavallo has transitioned through three eras of behavior in channel cross-sectional area (as judged primarily by inlet width). The first era, prior to about 1965 and the reduction in bay area by the growth of the Colorado River delta, was characterized by dynamic stability and a wide mouth (on the order of 10,000 ft). Era 2, from 1965 to about 1988, encompassed a time of rapid reduction in width of Pass Cavallo. Era 3, from 1988 to present, was characterized by dynamic stability, with an inlet mouth width of about 1,000 ft. A reduction in channel cross-sectional area followed a reduction in tidal prism caused by the growth of the Colorado River delta and the opening of the MSC entrance, for which the prism through Pass Cavallo decreased and the prism through the MSC entrance increased. The cross-sectional stability of Pass Cavallo results from the strong and frequent winds out of the southeast and northeast that produce setup in the southwest corner of Matagorda Bay.

d. Shoreline analysis indicated that both bay sides of the MSC entrance gained area through the placement of dredged material during new-work

dredging of the MSC. Although the shores have eroded since construction, except for a 0.25-mile reach southwest of the MSC, they are still located farther bayward than prior to the initiation of dredging of the MSC.

e. The extent of natural sand bypassing around the MSC entrance via the ebb shoal is unknown and warrants further study. Available bathymetry survey data indicate that the ebb shoal is growing at an annual rate of 165,000 cu yd/year. A stronger ebb current associated with the alternatives would push the ebb shoal farther offshore and temporarily decrease the bypassing rate.

f. Simulation of salinity change showed minimal impact (less than 1 ppt) for all alternatives.

Monitoring Recommendations

Whether or not construction proceeds with jetty stabilization measures at the MSC entrance, it is recommended that a minimum level of annual monitoring be conducted. Such monitoring would consist of the following three tasks:

a. High-resolution bathymetry surveys of the scour hole regions on the northwest side (bay side of south jetty), inside of the south jetty, and at the tips of both jetties. Comparisons to the previous years (difference maps) should be made to assess rates of change in depth and location.

b. Color vertical aerial photography of the MSC entrance and Pass Cavallo to assess changes in the general condition of the jetty, the positions of the shoreline for 2 miles adjacent to the jetties on both the gulf and bay sides of the entrance, and the width and geomorphology of Pass Cavallo.

c. Long-term measurements of water level and wind at Port Lavaca and Port O'Connor in continuation of TCOON support by the Galveston District.

References

Anders, F. J., and Byrnes, M. R. (1991). "Accuracy of shoreline change rates as determined from maps and aerial photographs," *Shore and Beach* 59(1), 17-26.

Bouma, A. H., and Bryant, W. R. (1969). "Rapid delta growth in Matagorda Bay, Texas," *Coastal Lagoons, a Symposium*, Univesidad Nacional Autónoma de México, 171-189.

Brown, C. A., and Kraus, N. C. (1997). "Environmental monitoring of dredging and processes in the lower Laguna Madre, Texas," Final Report, Year 1, contract report for the U.S. Army Engineer District, Galveston, Technical Report TAMU-CC-CBI-96-01, Conrad Blucher Institute for Surveying and Science, Texas A&M University-Corpus Christi, Corpus Christi, TX.

Brown, G. L., Sarruff, M. S., Fagerburg, T. L., and Raphelt, N. (2003). "Numerical model study of proposed navigation improvements at the Colorado River intersection with the Gulf Intra-Coastal waterway, TX," Draft Technical Report, U.S. Army Engineer Research and Development Center, Vicksburg, MS.

Bureau of Economic Geology. (2004). "Upper coast Gulf of Mexico vector shoreline data," Texas Bureau of Economic Geology, University of Texas at Austin, Austin, TX.

Collier, A., and Hedgpeth, J. W. (1950). "An introduction to the hydrography of tidal waters of Texas," *Publications of Insitute of Marine Science* 1(2), 125-194.

Committee on Tidal Hydraulics. (1964). "Problems in connection with Matagorda Ship Channel Project," U.S. Army Engineer Waterways Experiment Station, Vicksburg, MS, 4 p. plus two tables and three plates.

Dolan, R., Fenster, M. S., and Holme, S. J. (1991). "Temporal analysis of shoreline recession and accretion," *Journal of Coastal Research* 7(3), 723-744.

Foster, E. R., and Savage, R. J. (1989). "Methods of historical shoreline analysis," *Proceedings Coastal Zone'89*, ASCE, 4,434-4,448.

Gibeaut, J. C, White, W. A., Hepner, T., Gutierrez, R., Tremblay, T. A., Smyth, R., and Andrews, J. (2000). "Texas shoreline change project: Gulf of Mexico shoreline change from the Brazos River to Pass Cavallo," Texas Bureau of Economic Geology, The University of Texas at Austin, Austin, TX, 32 p.

Harwood, P. J. W. (1973). "Stability and geomorphology of Pass Cavallo and its flood delta since 1856, central Texas coast," M.A. thesis, The University of Texas at Austin, Austin, TX, 185 p.

Hoeke, R. K., Zarillo, G. A., and Synder, M. (2001). "A GIS based tool for extracting shoreline positions from aerial imagery (BeachTools)," Coastal and Hydraulics Engineering Technical Note CHETN IV-37, U.S. Army Engineer Research and Development Center, Vicksburg, MS, 12 p.

Hubertz, J. M., and Brooks, R. M. (1989). "Gulf of Mexico hindcast wave information." Wave Information Studies of U.S. Coastlines, WIS Report 18, U.S. Army Engineer Waterways Experiment Station, Vicksburg, MS.

Hughes, S. A. (2002). "Equilibrium cross-section area at tidal inlets," *Journal of Coastal Research* 18, 160-174.

Hughes, S. A. (2000). "Effect of Offset Jetties on Tidal Inlet Flood Flow," *Shore & Beach* 68(1), 31-38.

Jarrett, J. T. (1976). "Tidal prism-inlet area relationships," GITI Report 3, U.S. Army Engineer Waterways Experiment Station, Vicksburg, MS.

King, D. B., and Prickett, T. L. (1998). "Mouth of the Colorado River, Texas, monitoring program," Monitoring Completed Navigation Projects Program, Technical Report CHL-98-2, U.S. Army Engineer Waterways Experiment Station, Vicksburg, MS.

King, I. P. (1993). "RMA-10, a finite element model for three-dimensional density stratified flow," Department of Civil and Environmental Engineering, University of California, Davis, CA.

Kraus, N. C., and Heilman, D. J. (1997). "Packery Channel feasibility study: Inlet functional design and sand management. Report 1 of a two-part series," Technical Report TAMU-CC-CBI-96-06, Conrad Blucher Institute for Surveying and Science, Texas A&M University-Corpus Christi, Corpus Christi, TX.

Kraus, N. C., Mark, D. J., and Sarruff, S. (2000). "DMS: Diagnostic modeling system report 1, Reduction of sediment shoaling by relocation of the gulf Intracoastal Waterway, Matagorda Bay, Texas," ERDC/CHL TR-99-19, U.S. Army Engineer Research and Development Center, Coastal and Hydraulics Laboratory, Vicksburg, MS.

Kraus, N. C., and Militello, A. (1996). "Hydraulic feasibility of proposed Southwest Corner Cut, East Matagorda Bay, Texas," Technical Report TAMU-CC-CBI-96-03, Conrad Blucher Institute for Surveying and Science, Texas A&M University-Corpus Christi, Corpus Christi, TX.

Kraus, N .C., and Militello, A. (1999). "Hydraulic study of multiple inlet system: East Matagorda Bay, Texas," *Journal of Hydraulic Research* 125(3), 224-232.

Kraus, N. C., and Militello, A. (2001). "Analytical solution of one-dimensional bay forced by sea breeze," *Proceedings Waves 01*, ASCE, 1,644-1,653.

Kraus, N. C., and Rosati, J. D. (1997). "Interpretation of shoreline-position data for coastal engineering analysis," Coastal Engineering Technical Note CETN II-39, U.S. Army Engineer Research and Development Center, Vicksburg, MS, 16 pp.

Kraus, N. C., Thurlow, C. I., Heilman, D. J., Lindquist, A. L, and Earle, M. W. (1997). "Needs assessment for water-level gauging along the Texas coast for the U.S. Army Engineer District, Galveston," TR CHL-97-29, U.S. Army Engineer Waterways Experiment Station, Vicksburg, MS, 55 p. plus appendices.

LaRoi, L. M. (1997). "LaSalle's last voyage," *National Geographic* 191(5), 72-83.

Leatherman, S. P. (2003). "Shoreline change mapping and management along the U.S. east coast," *Journal of Coastal Research* SI(38), 5-13.

Lin, L., Kraus, N. C., and Barcak, R. G. (2001). "Predicting hydrodynamics of a proposed multiple-inlet system, Colorado River, Texas," *Proceedings 7th International Conference on Estuarine and Coastal Modeling,* ASCE, 837-851.

Luettich, R. A., Westerink, J. J., and Scheffner, N. W. (1992). "An advanced three-dimensional circulation model for shelves, coasts and estuaries, report 1: Theory and methodology of ADCIRC-2DDI and ADCIRC-3DL," Technical Report DRP-92-6, U.S. Army Engineer Waterways Experiment Station, Vicksburg, MS. 137 p.

Lyle, S. D., Hickman, L. E., Jr., and Debaugh, H. A., Jr. (1988). "Sea level variations for the United States 1855-1986," National Oceanic and Atmospheric Administration, National Ocean Service, Rockville, MD, 182 p.

Mason, C., and Sorensen, R. M. (1971). "Properties and stability of a Texas barrier beach inlet," Sea Grant Publication No. TAMU-SG-71-217, Oceanography and Civil Engineering Departments, Texas A&M University, College Station, TX.

Martin, L. R., and Rosati, J. D. (2003). "Authorities and policies supporting implementation of regional sediment management," Regional Sediment Management Demonstration Technical Note ERDC/RSM-TN-8, U.S. Army Engineer Research and Development Center, Vicksburg, MS, http://www.wes.army.mil/rsm/pubs/pdfs/rsm-tn-8.pdf.

Mathews, F. A., and Mueller, A. J. (1987). "Freshwater inflow requirements of a Texas estuary," *Proceedings Coastal Zone '87*, ASCE, 852-866.

McGowen, J. H., and Brewton, J. L. (1975). "Historical changes and related coastal processes, gulf and mainland shorelines, Matagorda Bay area, Texas," Bureau of Economic Geology, University of Texas at Austin, Austin, TX, 72 p.

Morton, R. A. (1977a). "Historical shoreline changes and their causes, Texas Gulf Coast," Geological Circular 77-6, Bureau of Economic Geology, University of Texas at Austin, Austin, TX.

Morton, R. A. (1977b). "Nearshore changes at jettied inlets, Texas coast," *Proceedings Coastal Sediments '77*, ASCE, 267-286.

Morton, R. A., Miller, T. L., and Moore, L. J. (2004). "National assessment of shoreline change: Part 1: Historical shoreline changes and associated coastal land loss along the U.S. Gulf of Mexico," U.S. Geologic Survey open file report, 2004-1043, 44 p.

Morton, R. A., Pieper, M. J., and McGowen, J. H. (1976). "Shoreline changes on Matagorda Peninsula (Brown Cedar Cut to Pass Cavallo), an analysis of historical changes on the Texas Gulf shoreline," Geological Circular 76-6, Bureau of Economic Geology, The Univesity of Texas at Austin, Austin, TX, 37 p.

National Oceanographic and Atmospheric Administration. (2000). "Tide and current glossary," U.S. Department of Commerce, National Oceanic and Atmospheric Administration, National Ocean Service, Center for Operational Oceanographic Products and Services, 29 p.

National Ocean Service. (2005). "Shoreline data rescue project of Matagorda Bay, Texas, vector shorelines," National Oceanographic and Atmopheric Administration, Silver Spring, MD.

Paine, J. G ., and Morton, R. A. (1989). "Shoreline and vegetation-line movement, Texas Gulf Coast, 1974 to 1982," Texas Bureau of Economic Geology, Geological Circular 89-1, The University of Texas at Austin, Austin, TX, 50 p.

Price, W. A. (1952). "Reduction of maintenance by proper orientation of ship channels through tidal inlets," *Proceedings 2nd Coastal Engineering Conference*, Council on Wave Research, 243-255.

Price, W. A. (1956). "Hurricanes affecting the coast of Texas from Galveston to the Rio Grande," Technical Memorandum 78, Department of the Army, Corps of Engineers, Beach Erosion Board, 17 p. plus appendices.

Price, W. A., and Parker, R. H. (1979). "Origins of permanent inlets separating barrier islands and influence of drowned valleys on tidal records along the gulf coast of Texas," *Transactions of the Gulf Coast Association of Geological Societies* 29, 371-385.

Resio, D. T. (1993). "STWAVE: Wave propagation simulation theory, testing, and application," Technical Report, Florida Institute of Technology, Melbourne, FL.

Rhodes, H. J., and Boland, R. A. (1963). "Contribution of Matagorda Bay model to design of Matagorda Bay deep draft navigation project," *Proceedings 8th Conference on Coastal Engineering*, ASCE, 598-615.

Shalowitz, A. L. (1964). *Shore and sea boundaries*. (Two vols.), Volume Two: Interpretation and Use of Coast and Geodetic Survey Data, Publication 10-1, U.S. Department of Commerce, Coast and Geodetic Survey, Washington, DC, 749 p.

Smith, J. M., Sherlock, A. R., and Resio, D. T. (2001). "STWAVE: Steady-state spectral wave model user's manual for STWAVE," Version 3.0, Special Report ERDC/CHL SR-01-1, U.S. Army Engineer Research and Development Center, Vicksburg, MS.

Simmons, H. B., and Rhodes, H. J. (1966). "Matagorda ship channel model study, Matagorda Bay, Texas; hydraulic model investigation," Technical Report No. 2-711, U.S. Army Engineer Waterways Experiment Station, Vicksburg, MS, 215 p.

Texas Natural Resources Information System. (1995). Digital orthophotograph quarter quadrangles, 1 meter resolution, 20 February 1995, URL: http://www.tnris.state.tx.us/digitaldata/1mdoqs.htm.

U.S. Army Corps of Engineers. (2000). "Planning guidance notebook," Engineer Regulation 1105-2-100, Headquarters, U.S. Army Corps of Engineers, Washington, DC.

U.S. Army Engineer District, Galveston. (1962). "Matagorda Ship Channel, Texas, Design Memorandum No. 5, Jetties, Appendix B: Engineering and Design," Galveston, TX, 8 p. plus exhibits and plates.

U.S. Army Engineer District, Galveston. (1971). "National shoreline study, Texas coast shores regional inventory report," U.S. Army Engineer District, Galveston, Galveston, TX, 13 p.

U.S. Army Engineer District, Galveston. (1985). "Galveston County shore erosion feasibility report and environmental impact statement," Volume 2, Galveston, TX.

U.S. Army Engineer District, Galveston. (1992). "Inlets along the Texas gulf coast," Section 22 Report, Planning Assistance to States Program, Galveston, TX, 56 p.

Van de Kreeke, J. (1985). "Stability of tidal inlets - Pass Cavallo, Texas," *Estuarine, Coastal and Shelf Science* 21, 33-43.

Van de Kreeke, J. (1990a). "Can multiple tidal inlets be stable?," *Estuarine, Coastal and Shelf Science* 30, 261-273.

Van de Kreeke, J. (1990b). "Stability analysis of a two-inlet system," *Coastal Engineering* 14, 481-497.

Wadsworth, A. H. (1966). "Historical deltation of the Colorado River, Texas," in *Deltas in their Geological Framework*, M. L. Shirley, ed., Houston Geological Society, 99-105.

Ward, G. H. (1982). "Pass Cavallo, Texas: Case study of tidal-prism capture," *Journal of Waterway, Port, Coastal and Ocean Division* 108(WW4), ASCE, 513-525.

Weiser, E. A., and Armstrong, J. (1963). "Design of deep draft navigation channel from Gulf of Mexico into Matagorda Bay, Texas," *Proceedings 8th Conference on Coastal Engineering*, ASCE, 578-597.

Westerink, J. J., Luettich, R. A., and Militello, A. (2001). "Leaky internal-barrier normal-flow boundaries in the ADCIRC coastal hydrodynamics code," Coastal and Hydraulics Laboratory Technical Note ERDC/CHL CHETN-IV-32, U.S. Army Engineer Research and Development Center, Vicksburg, MS.

Appendix A
Aerial Photographs, Matagorda Ship Channel Entrance

This appendix contains rectified aerial photographs of Matagorda Ship Channel at a scale of 1:40,000 ft.

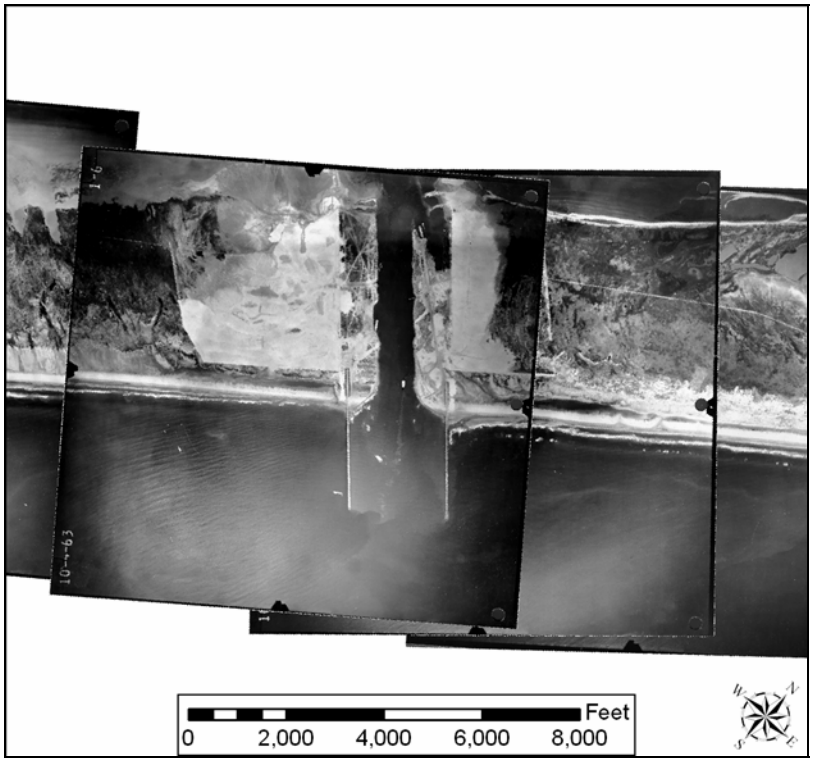

Figure A1. Matagorda Ship Channel Entrance, 4 October 1963

Figure A2. Matagorda Ship Channel Entrance, 22 October 1965

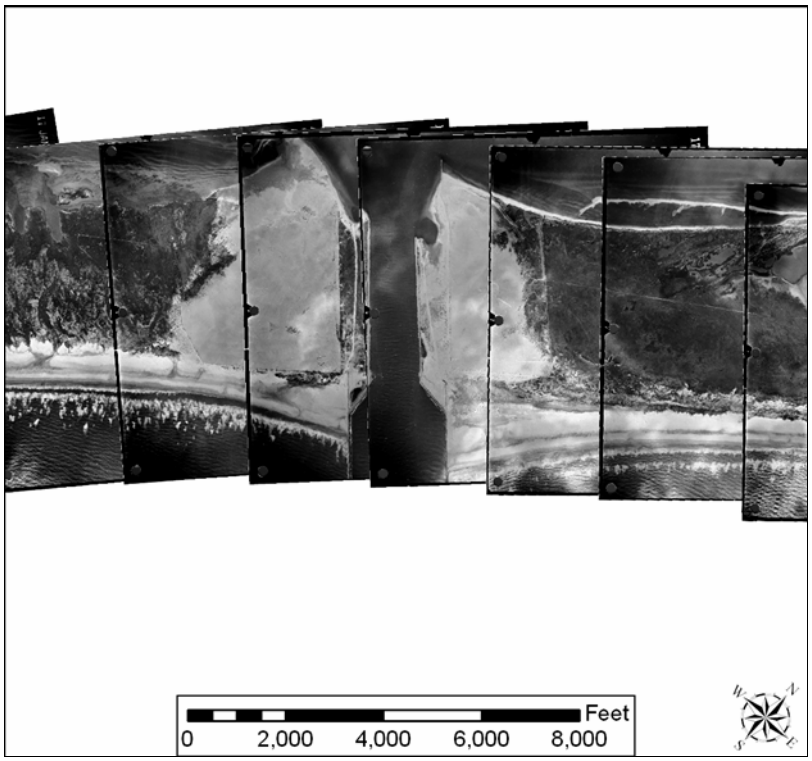

Figure A3. Matagorda Ship Channel Entrance, 17 January 1968

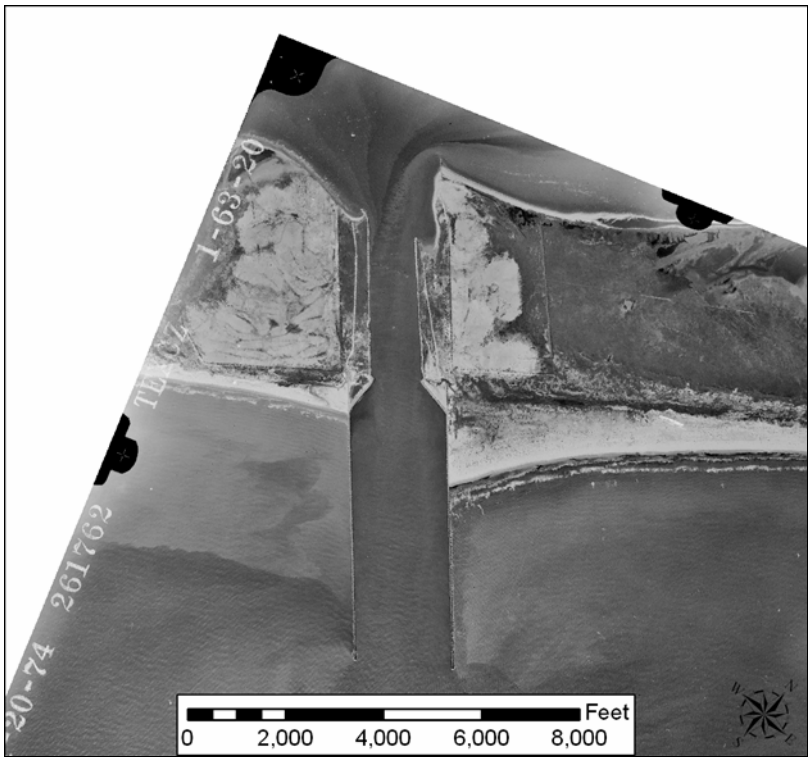

Figure A4. Matagorda Ship Channel Entrance, 20 November 1974

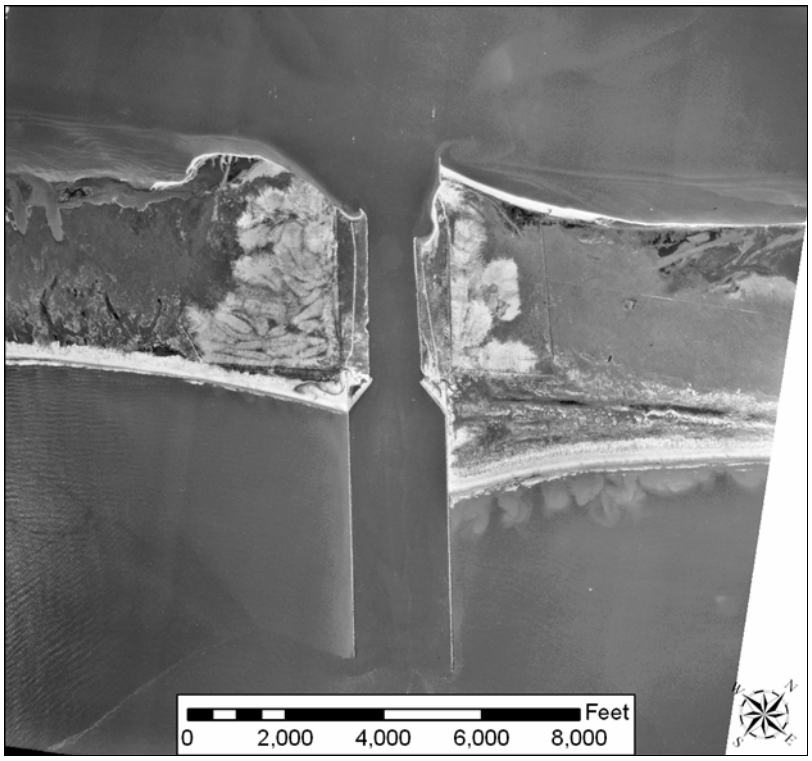

Figure A5. Matagorda Ship Channel Entrance, 30 November 1978

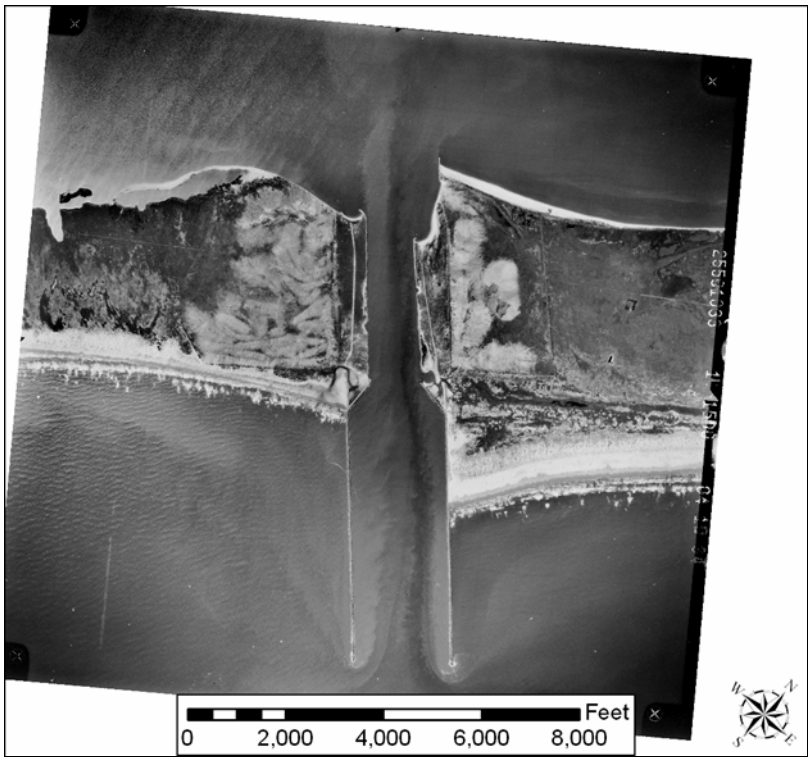

Figure A6. Matagorda Ship Channel Entrance, 10 April 1984

Figure A7. Matagorda Ship Channel Entrance, 17 October 1986

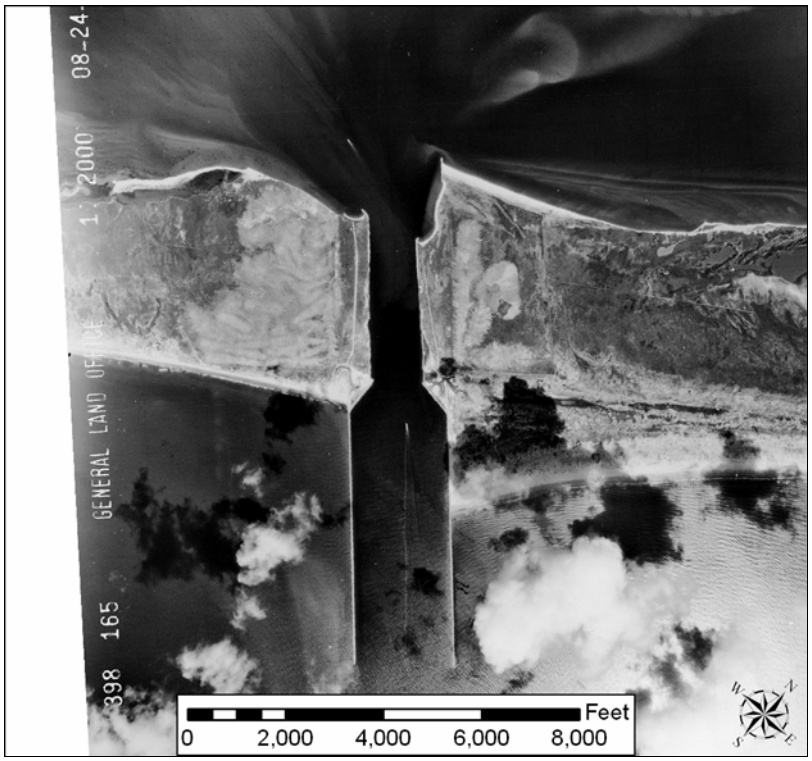

Figure A8. Matagorda Ship Channel Entrance, 24 August 1988

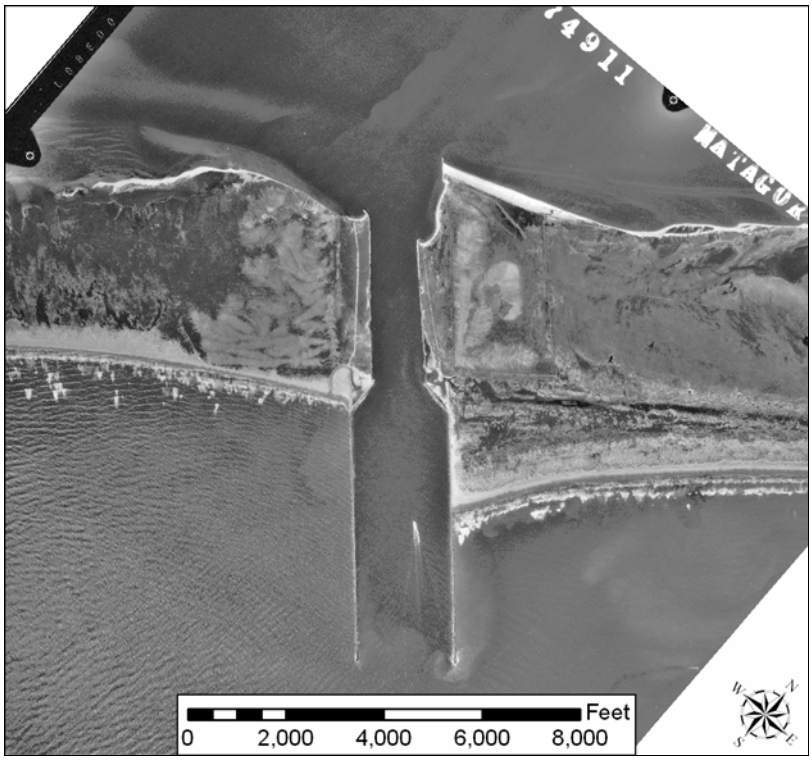

Figure A9. Matagorda Ship Channel Entrance, 1 March 1991

Figure A10. Matagorda Ship Channel Entrance, 20 February 1995

Figure A11. Matagorda Ship Channel Entrance, 26 September 2002

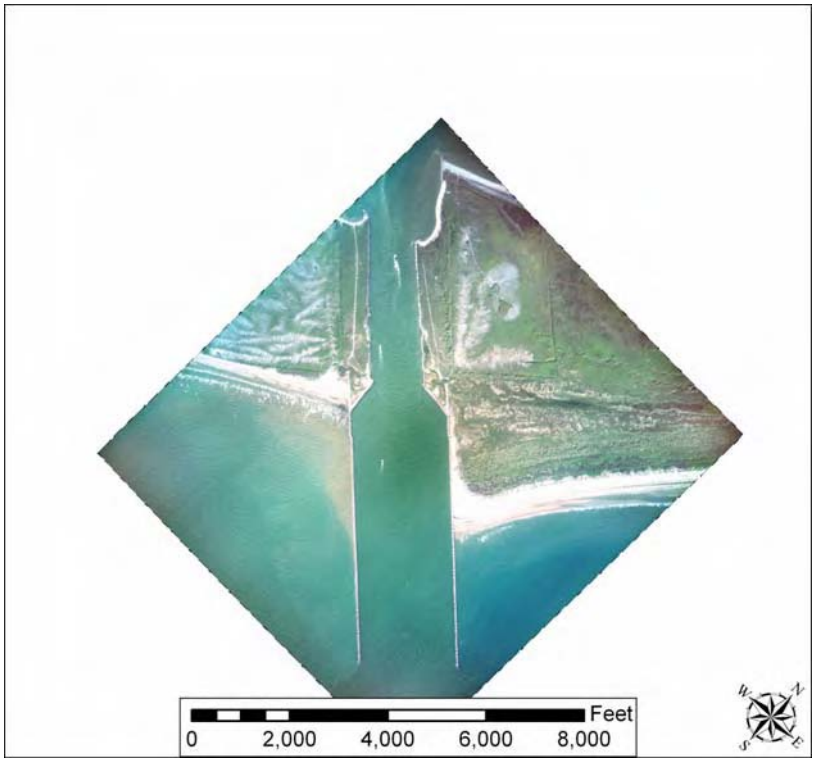

Figure A12. Matagorda Ship Channel Entrance, 7 August 2003

Appendix B
Aerial Photographs, Pass Cavallo

This appendix contains rectified aerial photographs of Pass Cavallo at a scale of 1:60,000 ft.

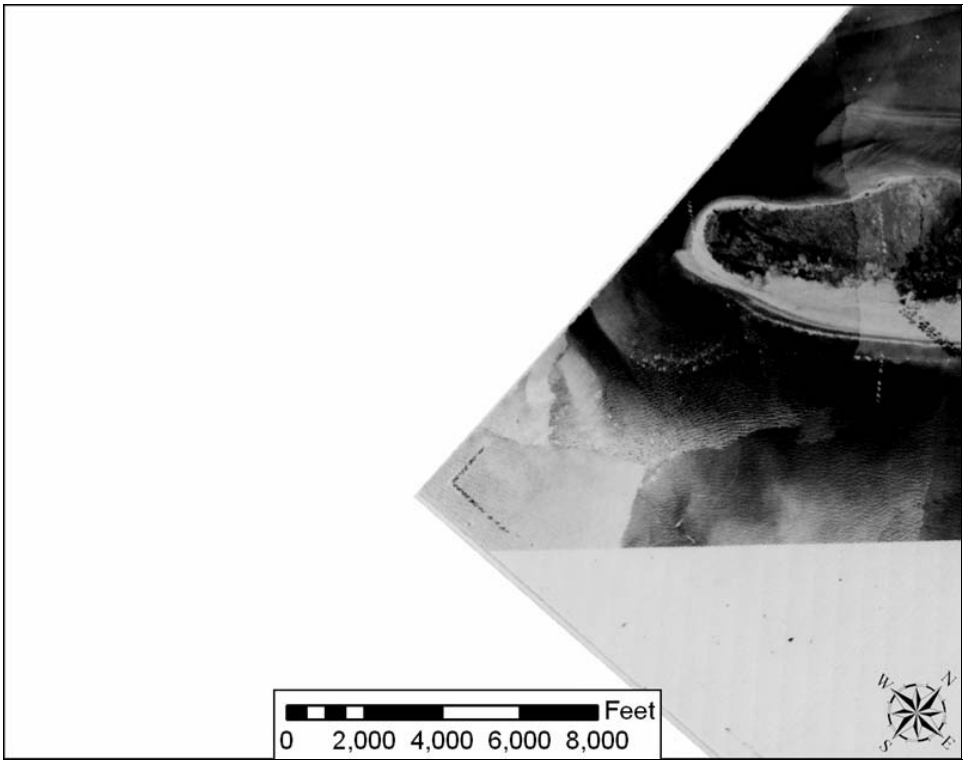

Figure B1. Pass Cavallo, Circa 1930

Figure B2. Pass Cavallo, 16 October 1943

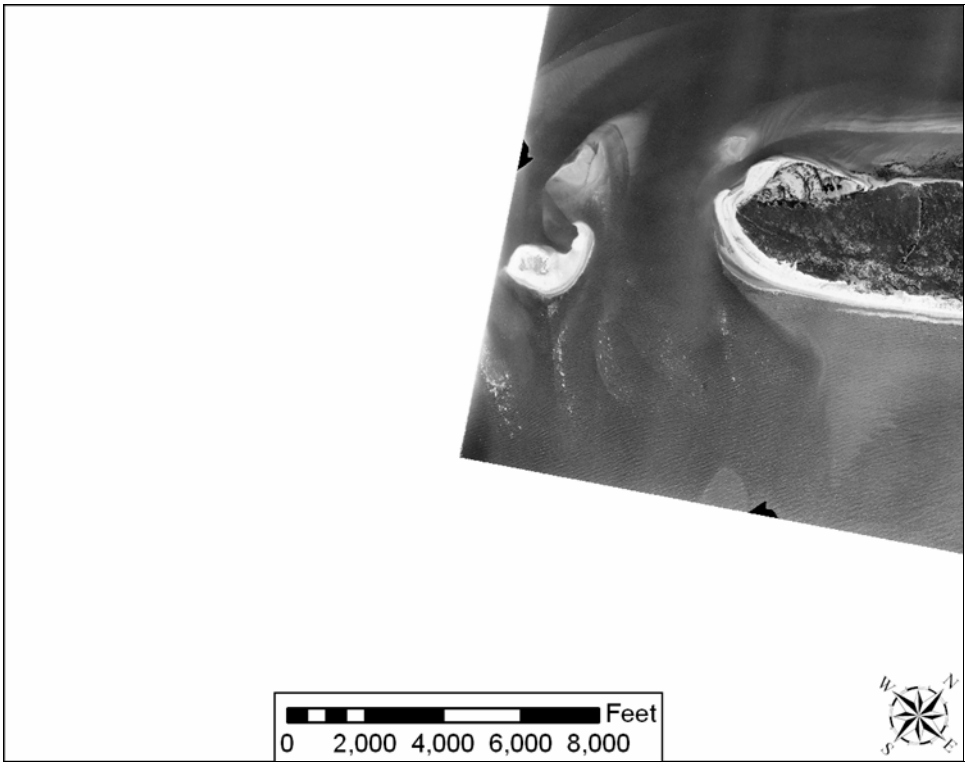

Figure B3. Pass Cavallo, Circa 1953

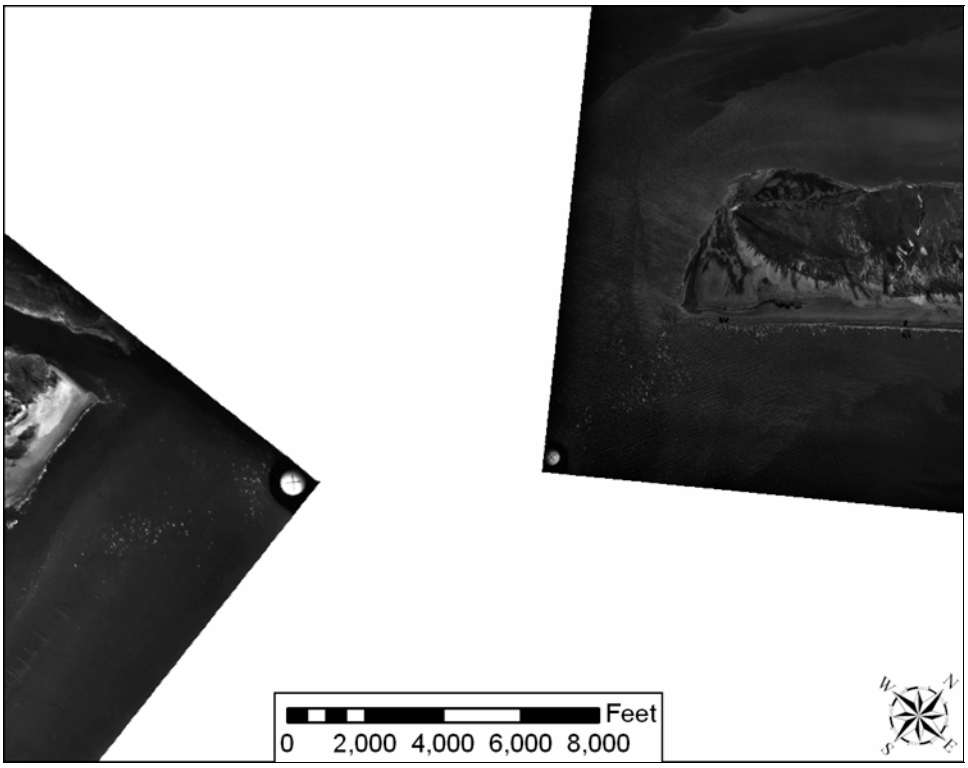

Figure B4. Pass Cavallo, 18 September 1961

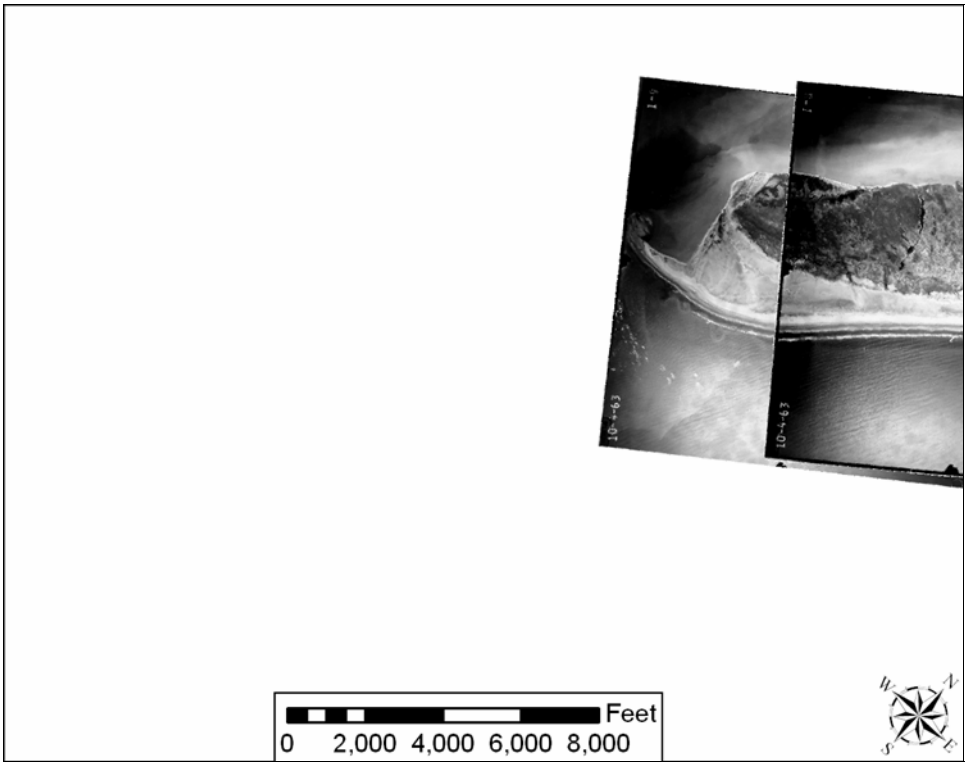

Figure B5. Pass Cavallo, 4 October 1963

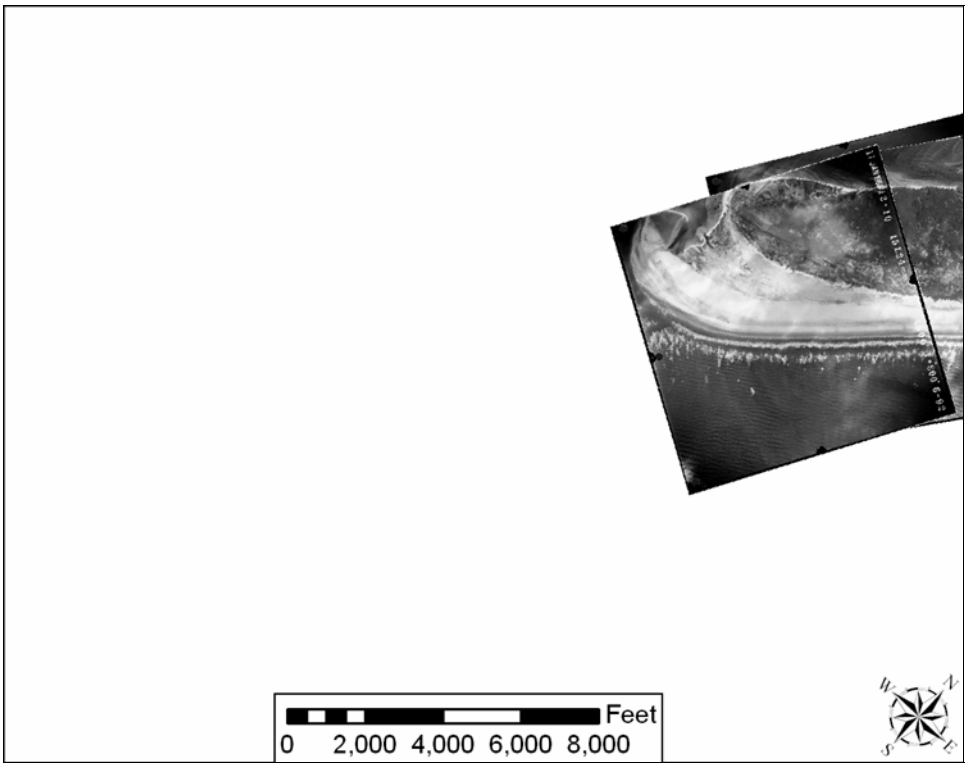

Figure B6. Pass Cavallo, 22 October 1965

Figure B7. Pass Cavallo, 17 January 1968

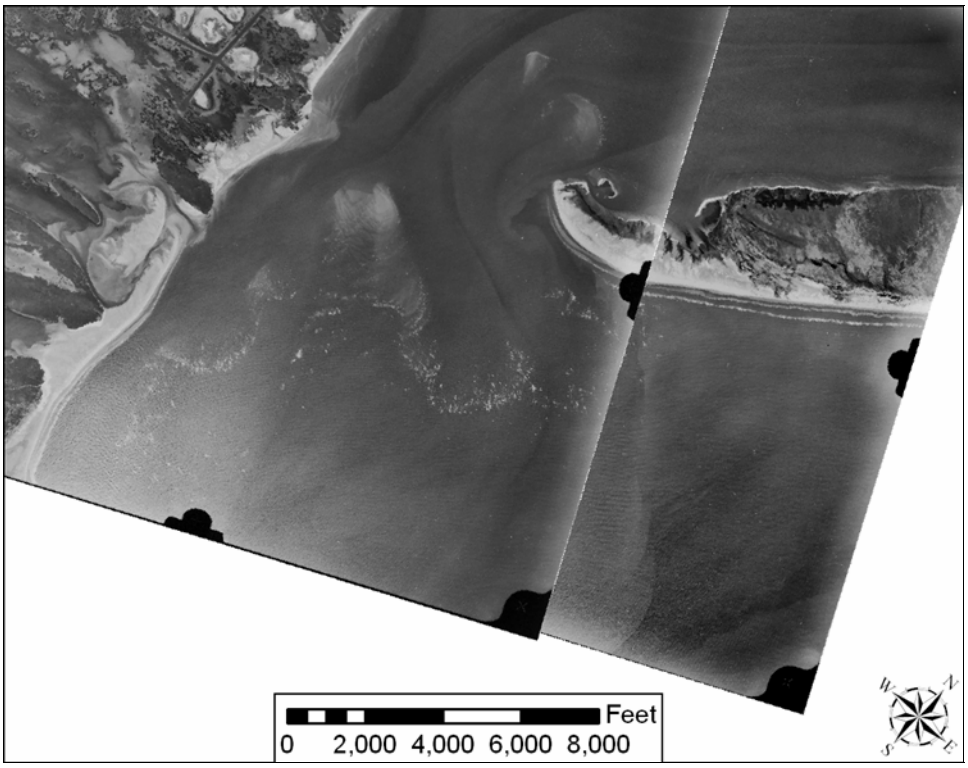

Figure B8. Pass Cavallo, 20 November 1974

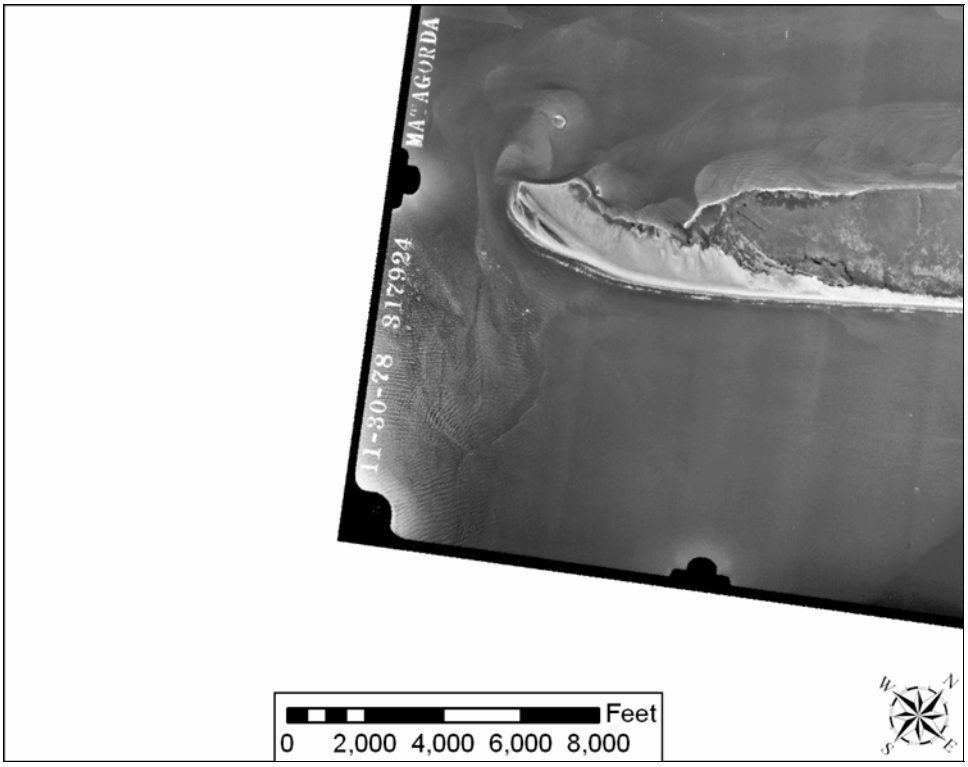

Figure B9. Pass Cavallo, 30 November 1978

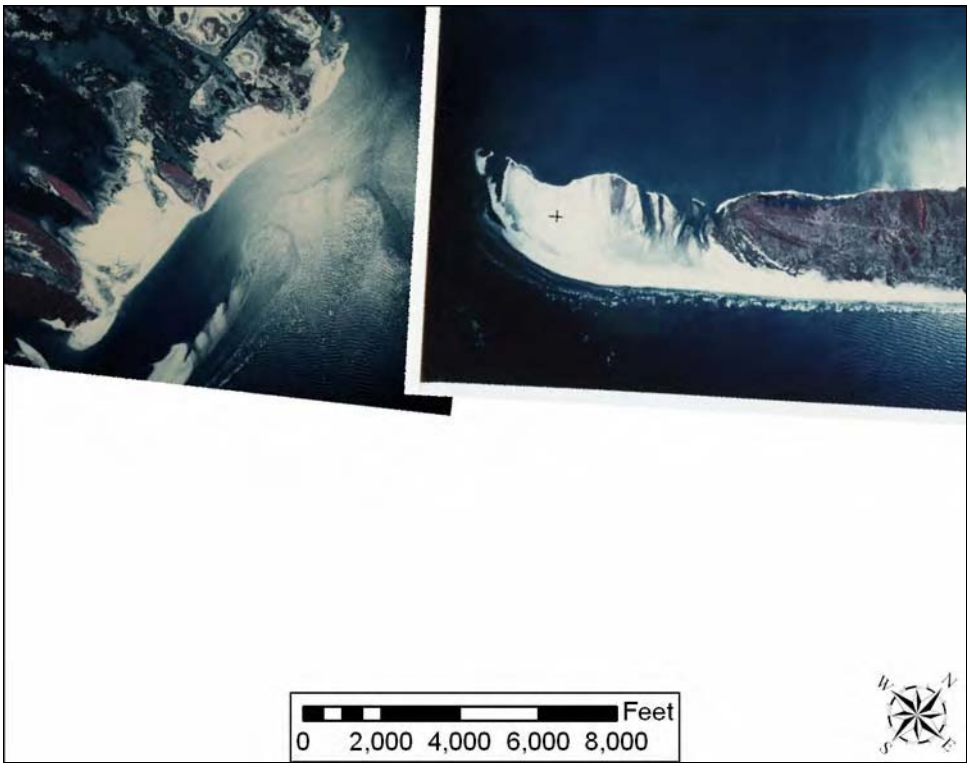

Figure B10. Pass Cavallo, Circa 1982

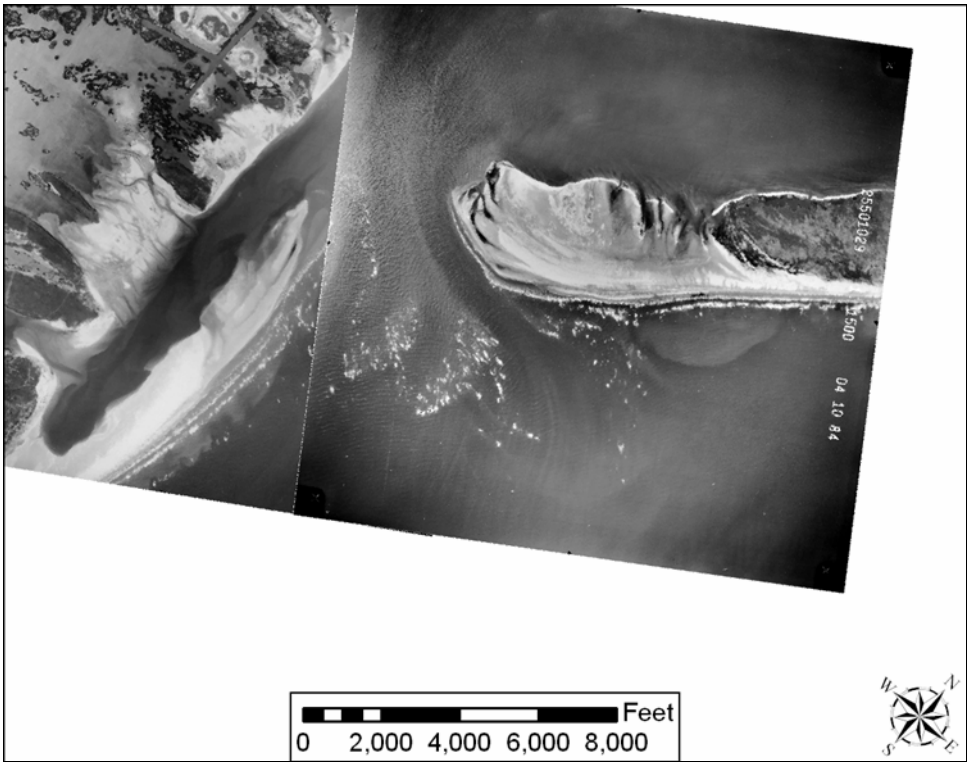

Figure B11. Pass Cavallo, 10 April 1984

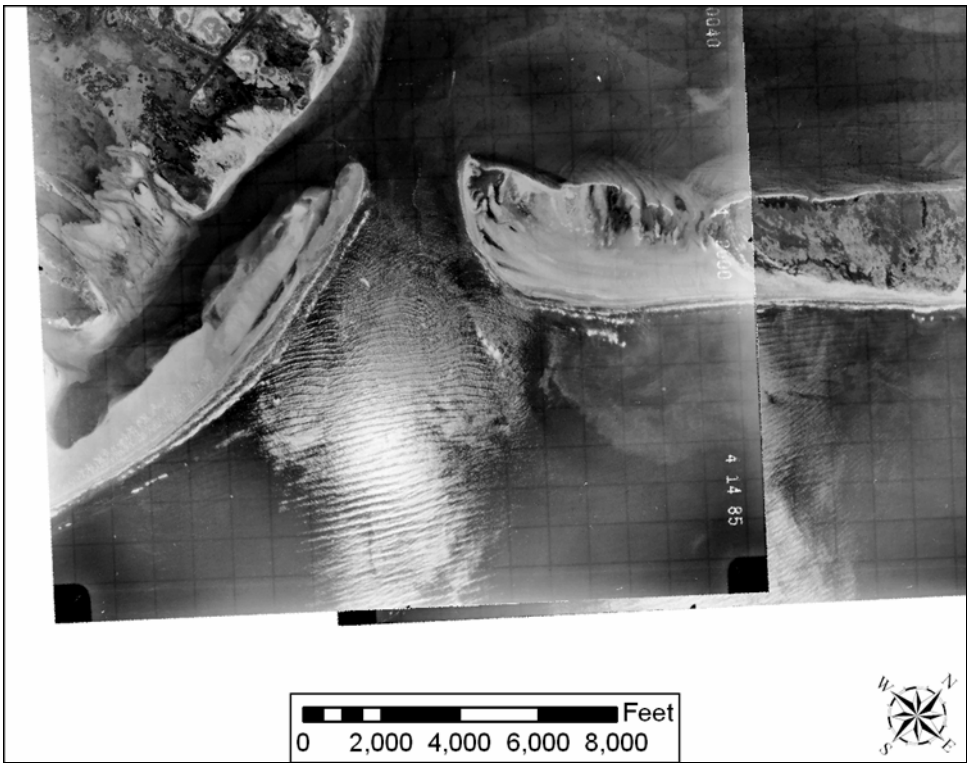

Figure B12. Pass Cavallo, 14 April 1985

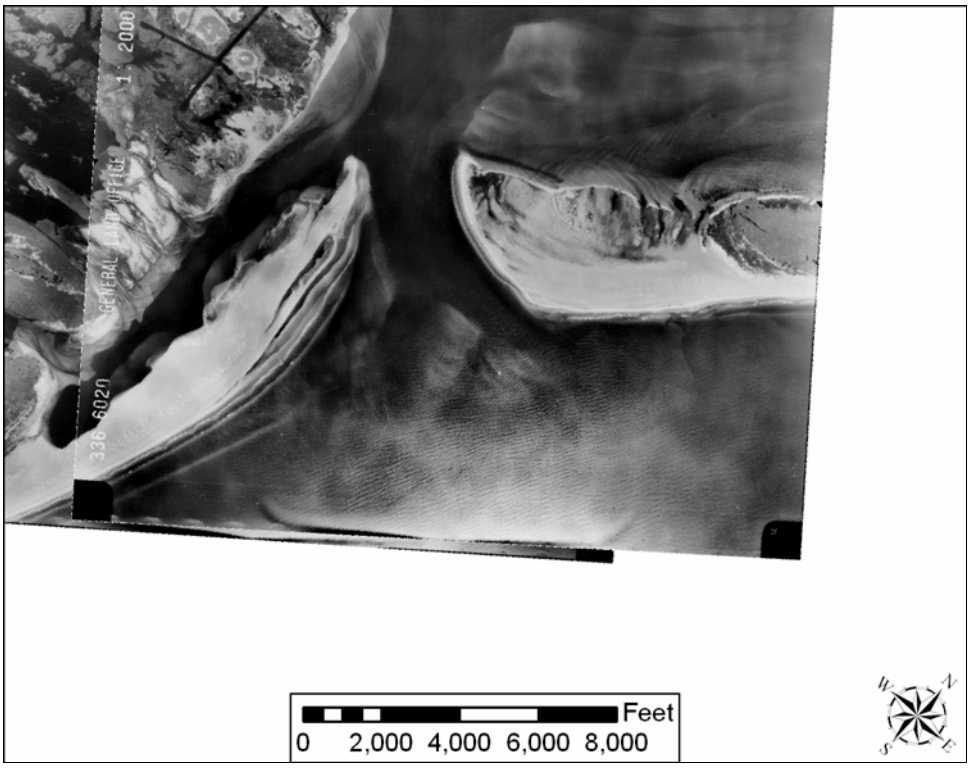

Figure B13. Pass Cavallo, 17 October 1986

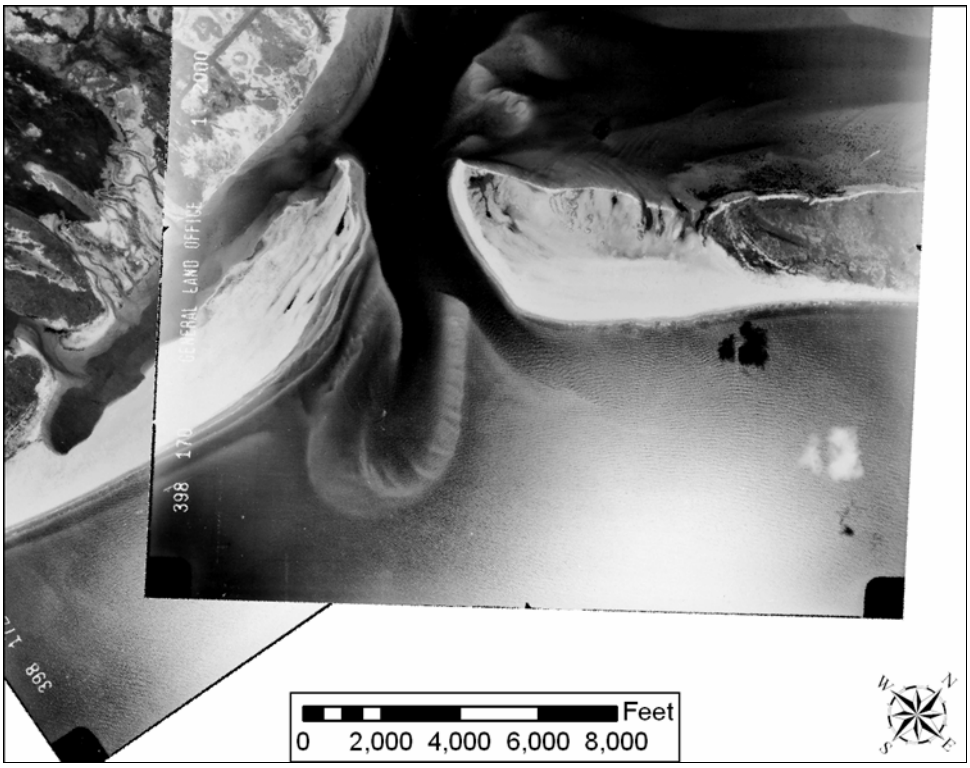

Figure B14. Pass Cavallo, 24 August 1988

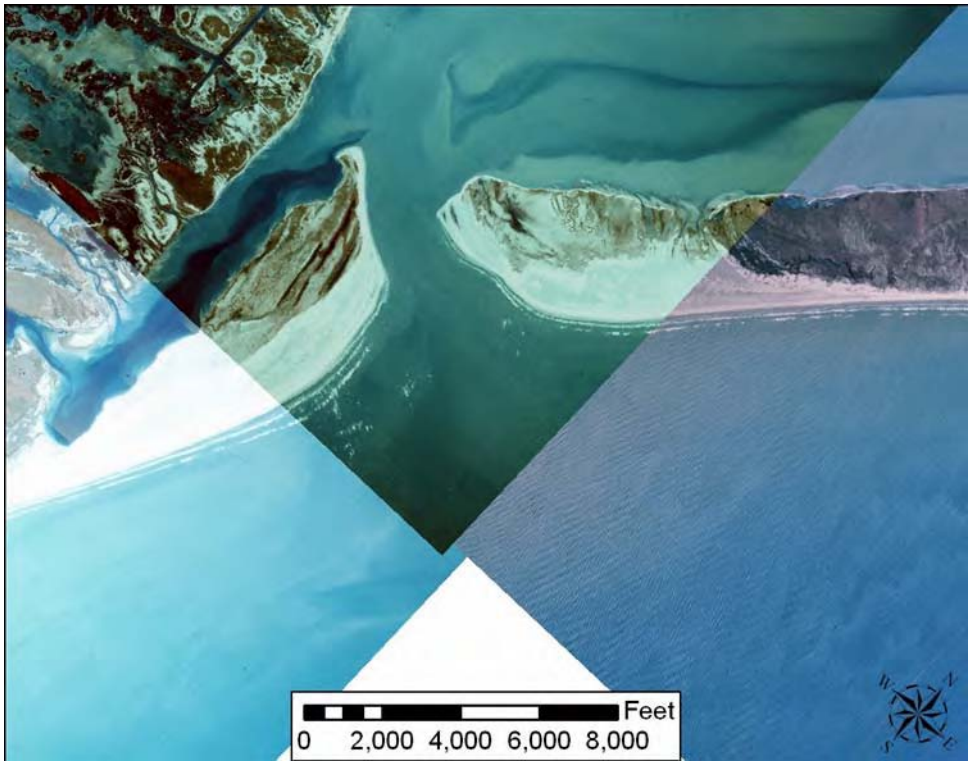

Figure B15. Pass Cavallo, 20 February 1995

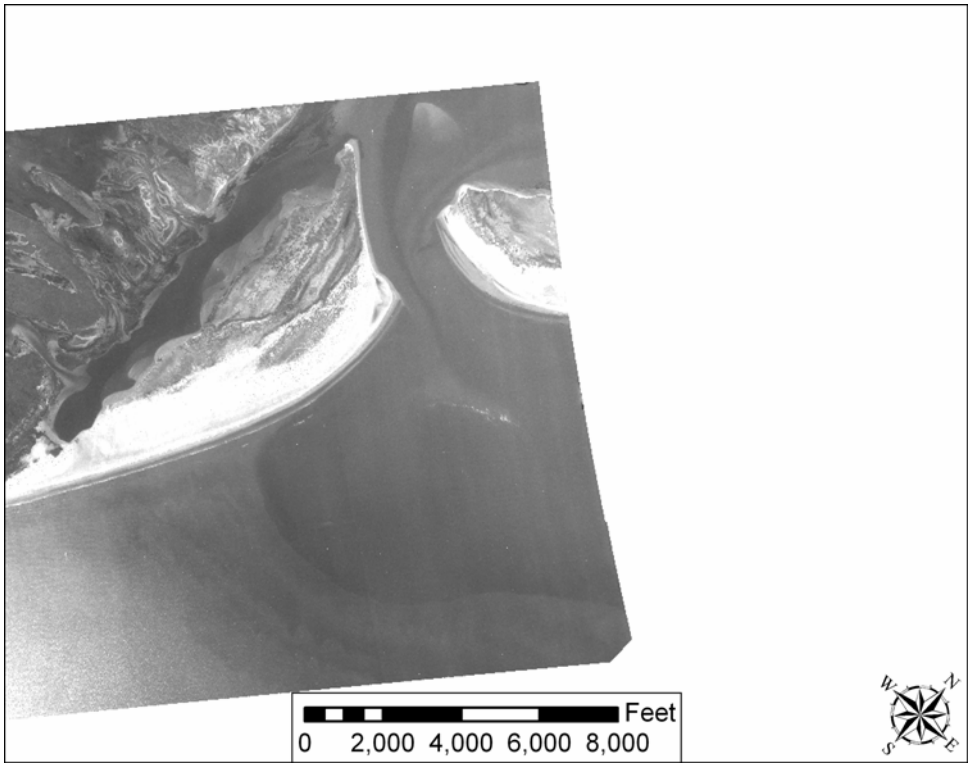

Figure B16. Pass Cavallo, 13 December 1999

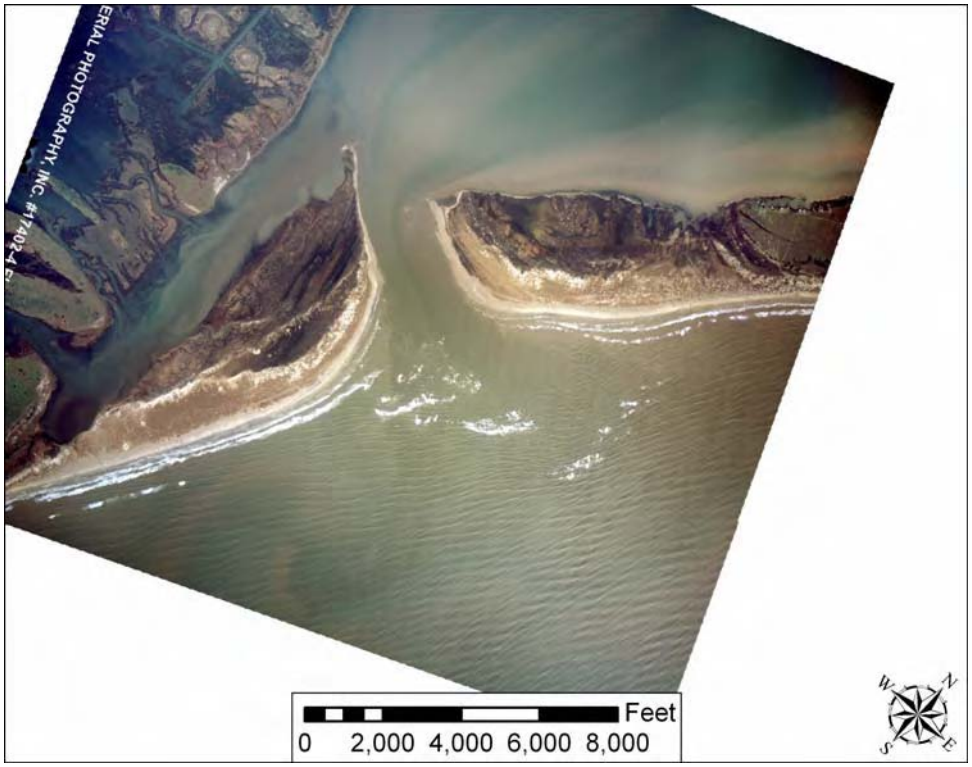

Figure B17. Pass Cavallo, 26 September 2002

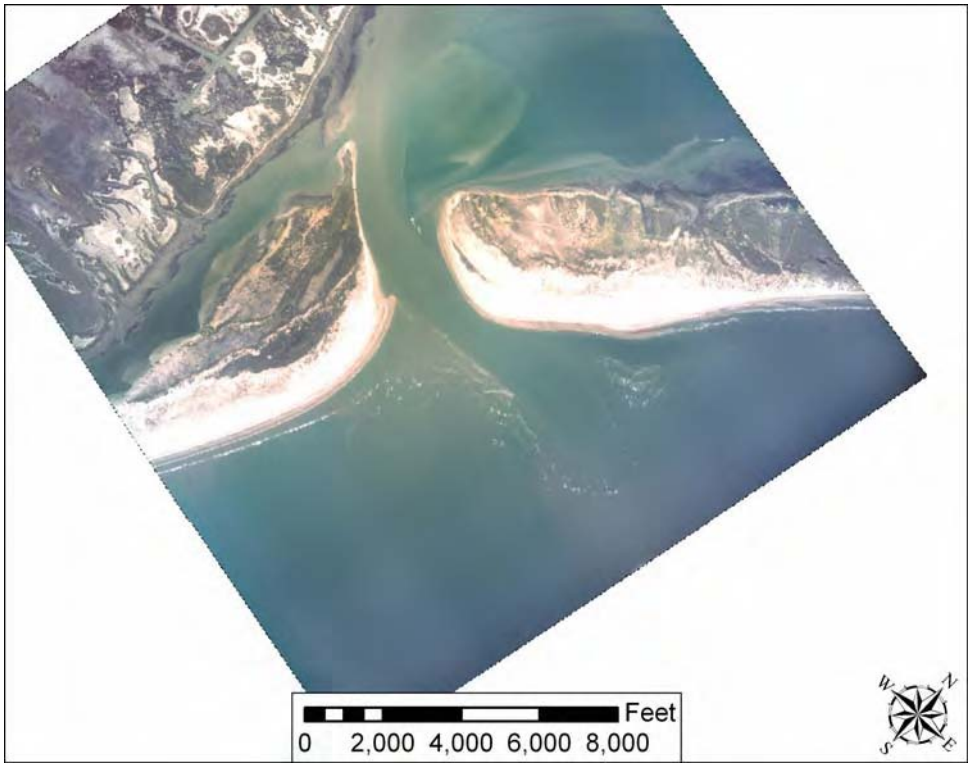

Figure B18. Pass Cavallo, 26 August 2003

Appendix C
Response of Salinity and Residence Time to MSC Alternatives

Purpose of Study

The U.S. Army Engineer District, Galveston, requested that the U.S. Army Engineer Research and Development Center (ERDC) apply an existing model to evaluate the extent of salinity intrusion to be expected in Matagorda Bay in response to the various alternatives for jetty stability described in the main text of this report. The Matagorda Ship Channel (MSC) entrance has been scouring over time, causing concern about the integrity of the existing jetties. The alternatives were developed to decrease current velocity through the entrance by widening the bottleneck region.

Matagorda Bay contains several areas that exhibit persistent mesohaline conditions and support a healthy estuarine habitat. These include the Colorado River delta (in the eastern arm of Matagorda Bay) and Lavaca Bay. The habitats in these areas are sensitive to changes in salinity.

This appendix documents the response of salinity and change in retention time in Matagorda Bay to the alternatives. The numerical model grid was modified to incorporate the entrance widening alternatives, increasing the resolution in areas of interest and in the entrance channel itself. The model was run using the same boundary conditions imposed in a previous study (Brown et al. 2003). Low, medium, and high river flow years were evaluated for each alternative.

Background of Model

ERDC performed and completed a numerical model study of hydrodynamics, including currents, salinity, and sediment changes associated with the plan to open Parker's Cut in Matagorda Bay and/or Southwest Cut in East Matagorda Bay, TX (Brown et al. 2003). The study investigated whether opening the cuts would provide more favorable currents for navigation at the Gulf Intracoastal Waterway (GIWW) intersection with the Mouth of Colorado River Bypass channel for the existing GIWW configuration. Attention was given to potential changes to salinity in Matagorda Bay and sedimentation in the area, especially at the old Colorado River channel and river delta, to assist the Galveston District in making environmental determinations. The consequence of

allowing some flow from the Colorado River to the old river channel near the diversion dam was also evaluated.

This two-dimensional model represented the intersection of the GIWW and the Colorado River, as well as an extensive area beyond it, including all of East Matagorda Bay and Matagorda Bay. The model was calibrated and verified successfully, which enabled evaluation of several proposed alternatives. (The report may be found at http://www.swg.usace.army.mil/Projects/GIWWColo/.)

Since completion of the project, the numerical model has been applied continually to evaluate new concerns involving areas of interest included in the model. During FY03, the model was modified to assess the effect different GIWW lock configurations would have on navigation along the intersection of the GIWW and the Colorado River.

Numerical Model

The TABS-MDS model of ERDC is used for computing hydrodynamics and salinity. The model was originally developed as RMA10 by Resource Management Associates (King 1993) and extensively modified by the ERDC staff into its present configuration. In agreement with the original author, the ERDC version of the code was given the name TABS-MDS to distinguish it from RMA10. It is a finite element model, which gives great flexibility in matching complex geometry. Through solution of equations of conservation of mass and horizontal momentum, as well as the convective-diffusion equation for transport of salinity and heat, the model accounts for forcing due to tides, freshwater inflows, wind, Coriolis effects (where applicable), and density gradients due to salinity and temperature. It also represents evaporation and precipitation to complete an accurate description of any system under study.

ERDC personnel have applied the code extensively over the last decade in a variety of field investigations with excellent results. Its proven effectiveness makes it well suited for this application.

Model Results

Mesh modifications and verification check

The model mesh was modified to improve resolution in the vicinity of the MSC entrance and also in the Colorado River delta, the eastern arm of Matagorda Bay. The original mesh contained 32,955 nodes and 10,351 elements, whereas the refined mesh (Figure C1) contains 39,081 nodes and 12,336 elements. Figure C2 shows the mesh in the vicinity of the MSC entrance. The blue portions of the mesh are solid boundaries in the existing condition, but they can be transformed into active elements for the various alternative evaluations.

The model was run with the verification boundary conditions from the original study, and the results were compared to the results obtained from that study. Figure C3 depicts the data collection locations in the original study, noting the locations of Gages 9 and 10 (these are the two gages located in Matagorda Bay). Figures C4 and C5 show statistical comparisons of the salinity verification results for both the original mesh and the refined

mesh. These statistics demonstrate that the refined mesh yields similar results, especially for the gages located in Matagorda Bay (Gages 9 and 10).

Model runs

The model was then run for four entrance channel configurations (see Chapter 1 of main text for more information):

a. Existing.

b. Alt 1. Removing the south bottleneck.

c. Alt 2. Removing the north and south bottlenecks

d. Alt 3. Removing the bottleneck and flanging the bay entrance.

These configurations are depicted in Figures C6-C9. Also shown are typical spring flood tide currents for each configuration.

Each entrance channel configuration was run for three flow years representing low, medium, and high flow conditions. The river inflow hydrographs of the Colorado River, Lavaca River, and Tres Palacios River for these years are given in Figures C10-C12.

Salinity

Figures C13-C24 depict the salinity change with respect to the existing condition for each of the proposed alternatives. Figures C13, C17, and C21 show the annual average salinity for the existing configuration for the low, medium, and high flow years, respectively. Figures C14-C16, Figures C18-C20, and Figures C22-C24 show the average annual salinity differences, computed as the salinity for the alternative minus the salinity for the existing condition.

These figures demonstrate that salinity change is minimal for all of the alternative configurations. The largest salinity increase is less than 1 ppt. This increase is seen in the Alt 3 runs, at a location just north of the MSC entrance. There is no observable salinity change in the eastern arm of Matagorda Bay for any of the alternatives.

There is a slight reduction in salinity observed in East Matagorda Bay. It appears that the changes to the MSC entrance cause a slight modification in the phasing and amplitude of the tide in Matagorda Bay, which in turn results in the diversion of some of the Colorado River flow from Matagorda Bay to East Matagorda Bay. However, this diversion is not large enough to significantly impact the salinity in the eastern arm of the Matagorda Bay.

There is a salinity reduction observed in Espiritu Santo Bay of approximately 1 ppt. However, because the model is truncated in this location and has no connection to the tide on the southern side, this reduction should not be considered a reliable prediction of the salinity impact in Espiritu Santo Bay.

Residence Time

The residence time was estimated by two independent analytical methods. The first method is an average flux method that can be used to generate a relationship between the

residence time and the average net outflow from the bay (the average net outflow is equal to the total freshwater inflow, plus or minus the net precipitation and evaporation). The second method is a tracer method that can be used to generate a relationship between the time-dependent total freshwater inflow to the bay and the resultant residence time of the bay.

The average flux method is computed as follows. The volumetric water flux through the inlet to the bay is measured over a specified duration. For this application, this flux is the total flux across both the MSC entrance and Pass Cavallo. The residence time is then estimated with the following equation:

$$t_R = \frac{\text{Average Tidal Prism}}{\text{Average Net Outflow}} = \frac{t_{HTS} \sum_{t=0}^{t=T} \left| Q_{\text{INLET}} \right|}{\sum_{t=0}^{t=T} Q_{\text{INLET}}} \qquad (1)$$

where

t_R =the residence time

t_{HTS} = the duration of a half tidal cycle (12.5 hr)

Q_{INLET} = the total volumetric water flux through the inlet(s)

T =the specified duration over which the fluxes are averaged.

This method is based on the assumption that there is no recirculation of the water flux between the MSC entrance and Pass Cavallo. It is also assumed that 100 percent of the net outflow that exits the model is lost to tide, i.e., none of the fresh water lost during an ebb cycle is pumped back into the bay during a subsequent flood cycle. Both of these assumptions tend to generate shorter duration predictions of the residence time.

The tracer method for estimating the residence time is computed as follows. A conservative tracer is placed throughout Matagorda Bay, at a uniform concentration. The model is then allowed to run, with a tracer concentration of 0 applied at all inflow points. The total mass of tracer in the bay is measured at each successive time step. The time required to remove half of the mass of tracer in the bay represents the average time required to replace a parcel of water in the bay. Hence, this time serves as an estimate of the residence time of the bay.

This method is based on the assumption that the efficiency of the offshore boundary with respect to removing tracer mass from the bay is known. This, in effect, assumes that the coastal currents are being modeled accurately, and investigation of the coastal current was beyond the scope of this study, but its influence is believed to be negligible. Typically, the model will underpredict this sweeping efficiency. Hence, the average flux method tends to generate longer duration predictions of the residence time.

Because the average flux method tends to underestimate the residence time, and the tracer method tends to overestimate the residence time, application of both methods to estimate the residence time effectively brackets the uncertainty in the results.

Figures C25 and C26 show the results of the residence time calculated by each method. Regardless of the method used, none of the proposed alternatives results in a significant change in the residence time calculated, except for the case of very low average inflow. There is some observable increase in the residence time for the alternatives in the average flux method calculation for low flows.

Conclusions

The analysis and change figures show that the salinity impact is minimal for all of the alternative configurations. The largest salinity increase is less than 1 ppt. This increase was found in the Alt 3 runs, just north of the MSC entrance. There is no observable salinity change in the eastern arm of Matagorda Bay for any of the alternatives.

The residence time was estimated using two independent methods: the average flux method and the tracer method. Regardless of the method, none of the proposed alternatives is predicted to produce a significant change in the residence time, except for the case of very low average river inflow. There is some observable increase in the residence time for the alternatives in the average flux method calculation for low flows.

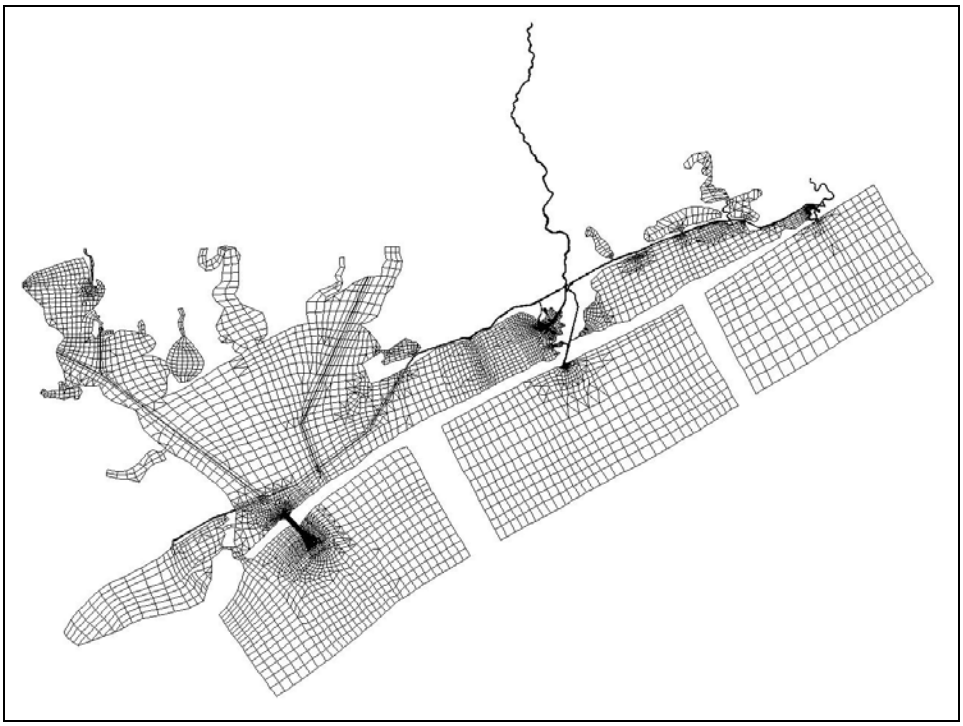

Figure C1. Entire model mesh

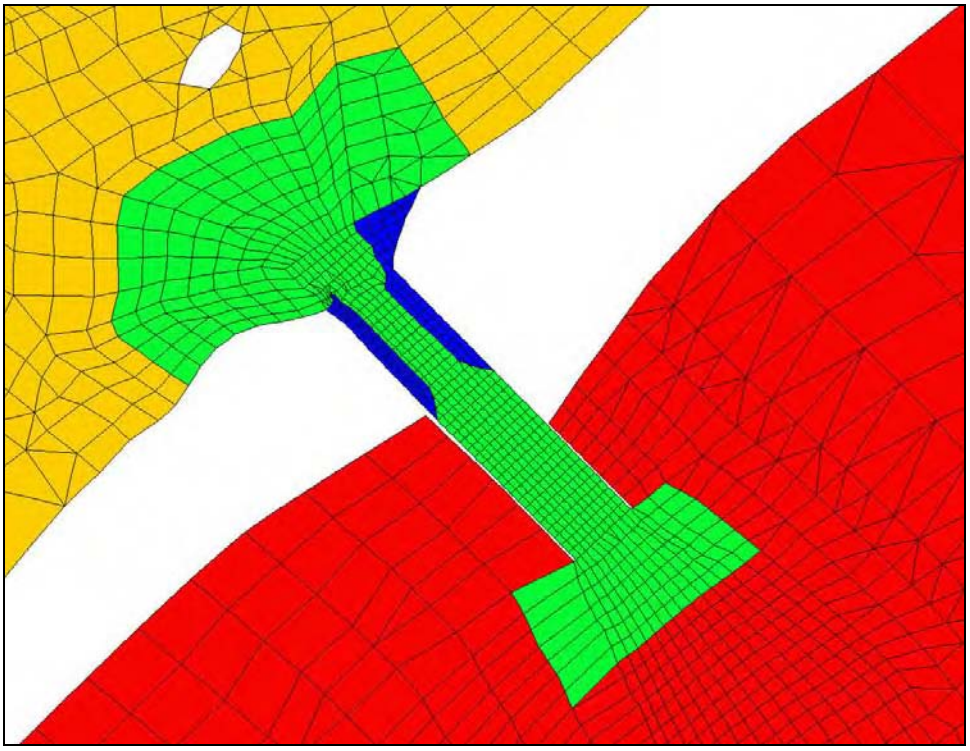

Figure C2. Model mesh at the MSC entrance

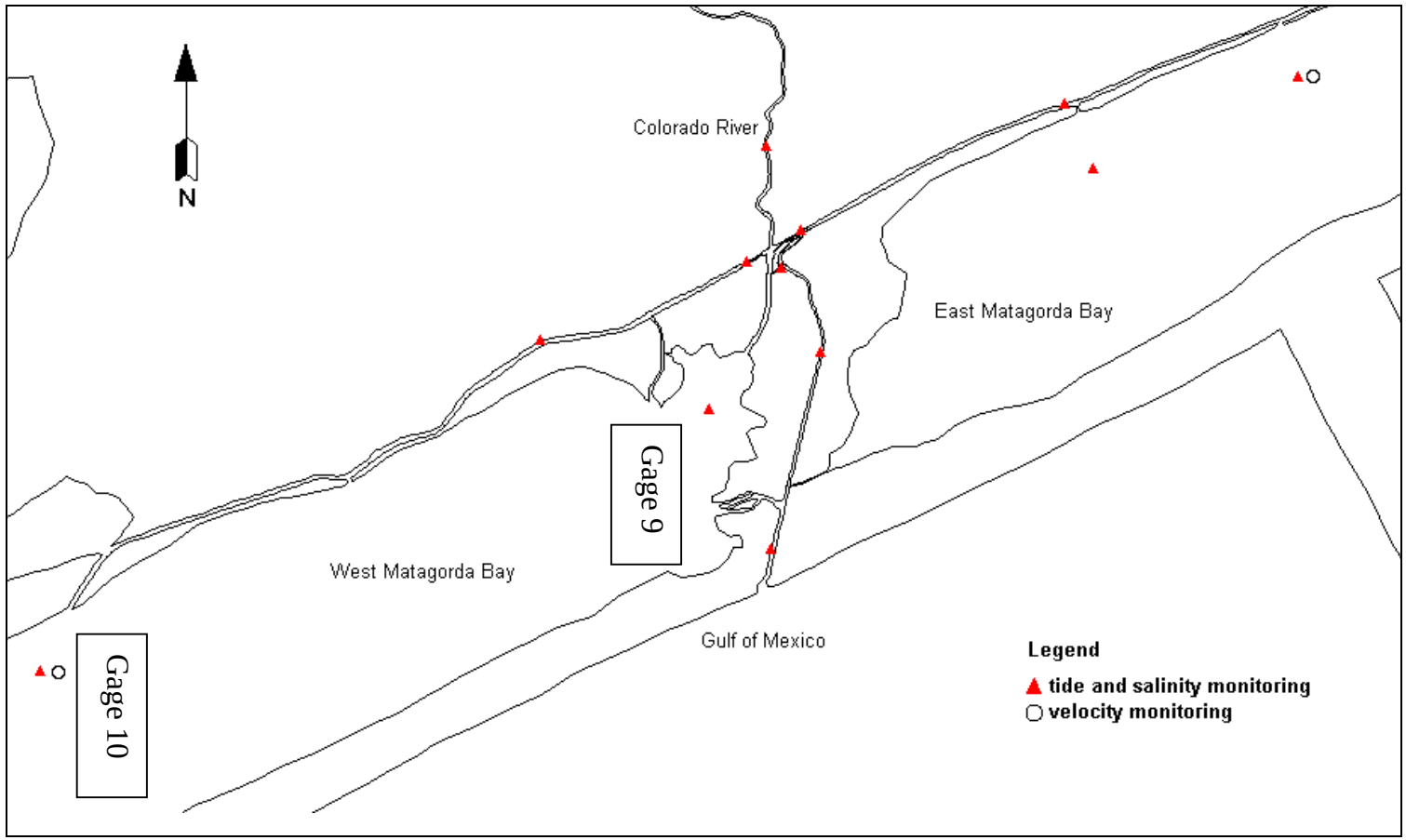

Figure C3. Data collection stations for original Mouth of Colorado Study

Figure C4. Salinity verification check for rms error

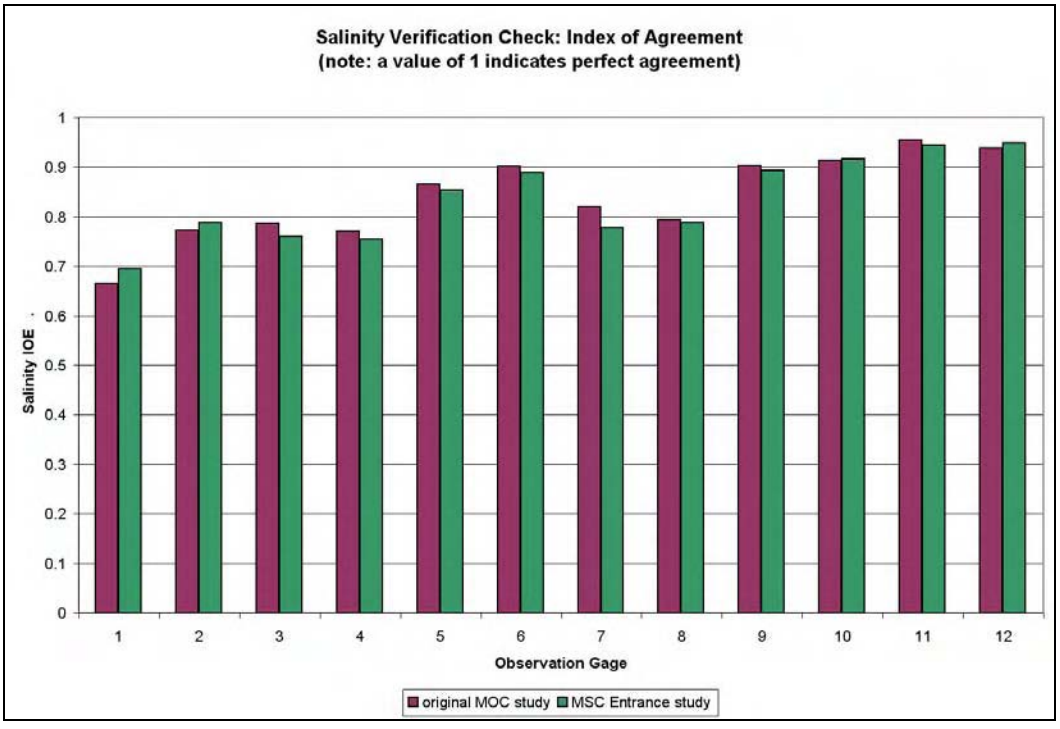

Figure C5. Salinity verification check for index of agreement

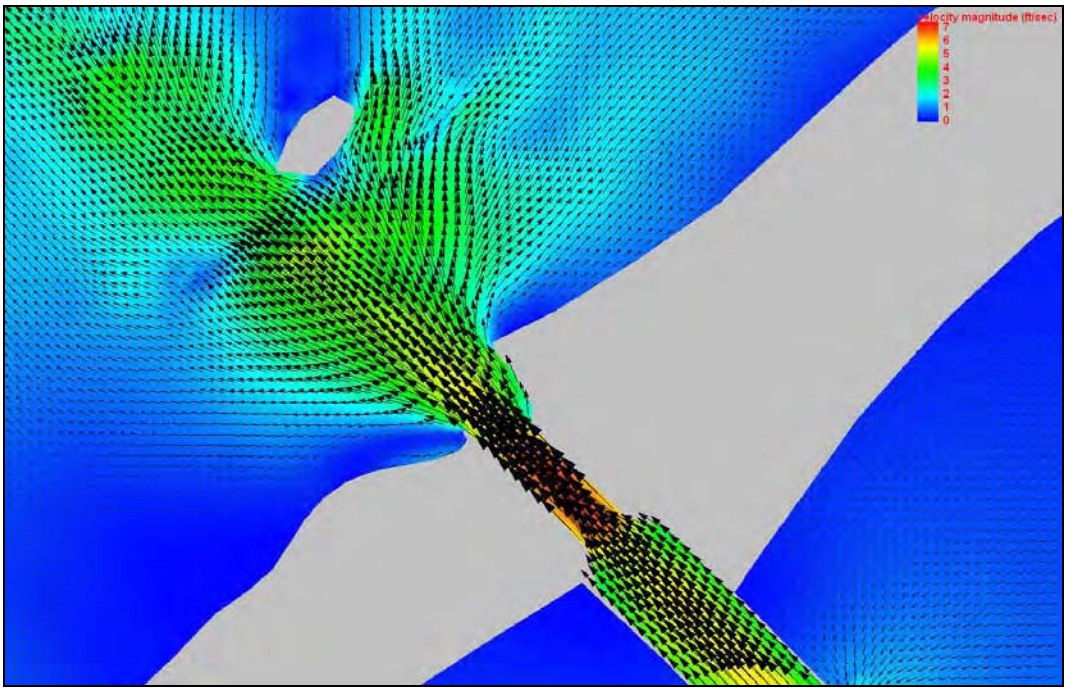

Figure C6. Flood tide currents for existing configuration

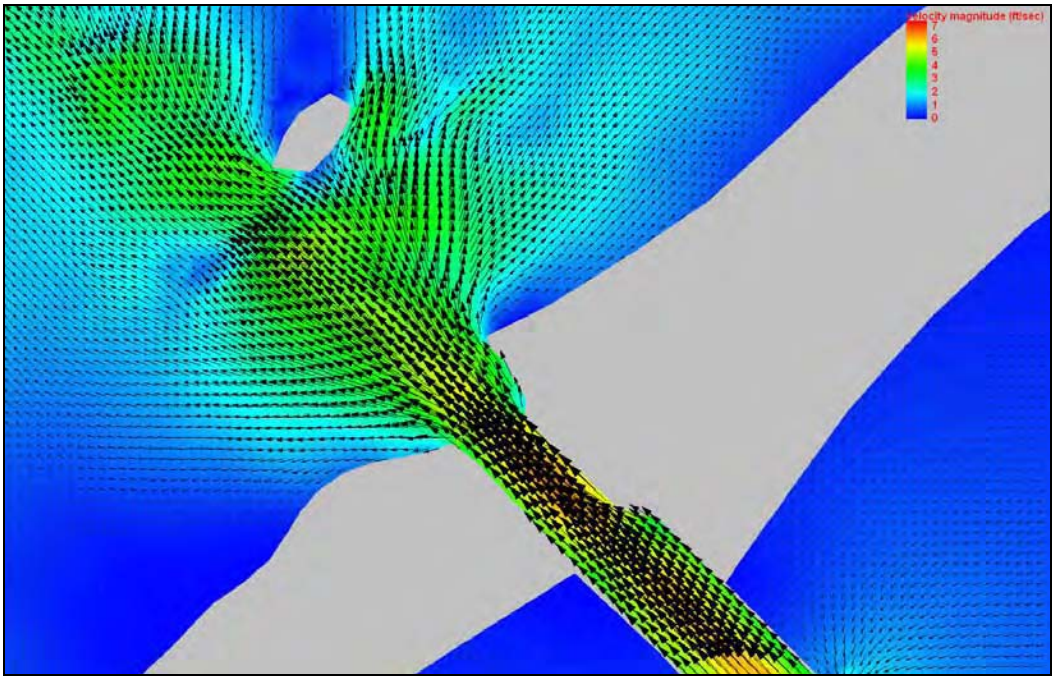

Figure C7. Flood tide currents for Alt 1

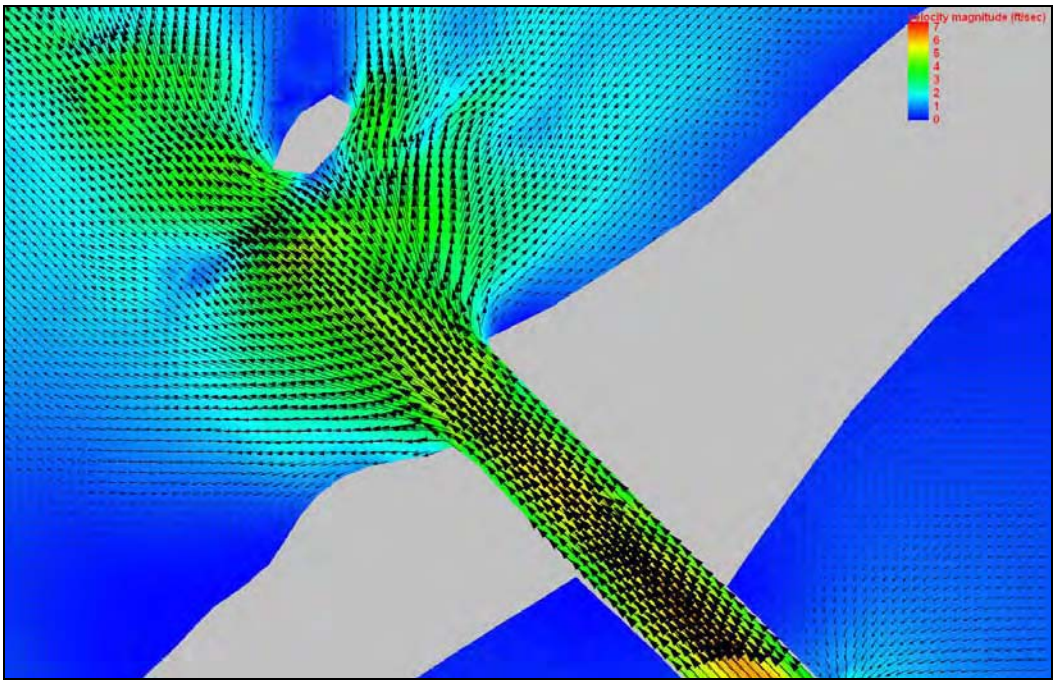

Figure C8. Flood tide currents for Alt 2

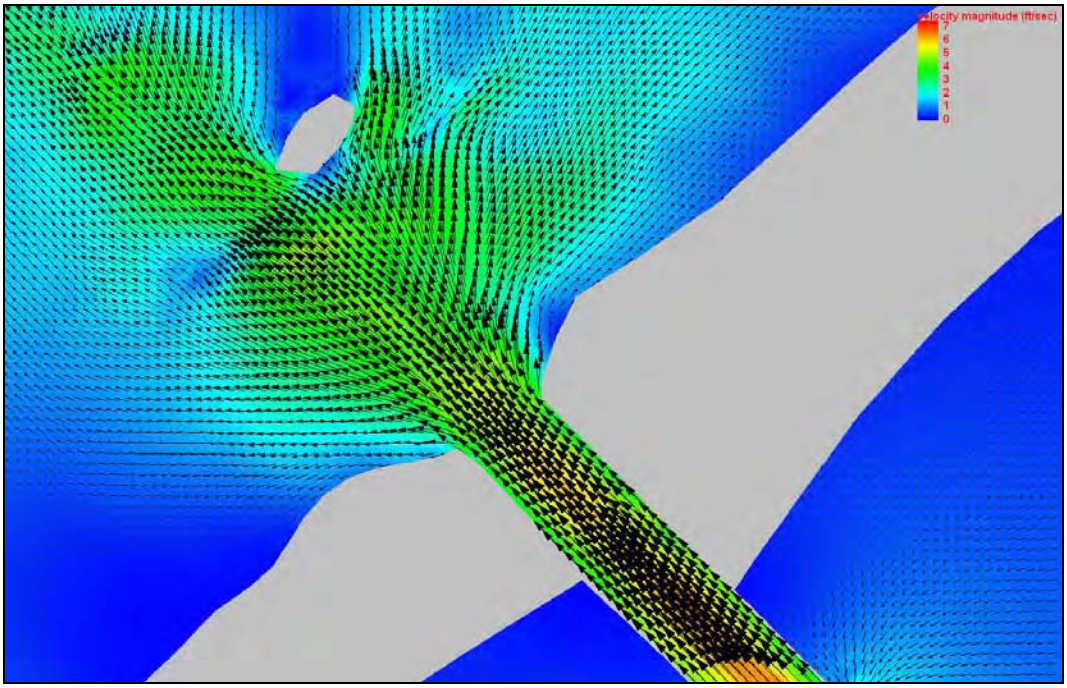

Figure C9. Flood tide currents for Alt 3

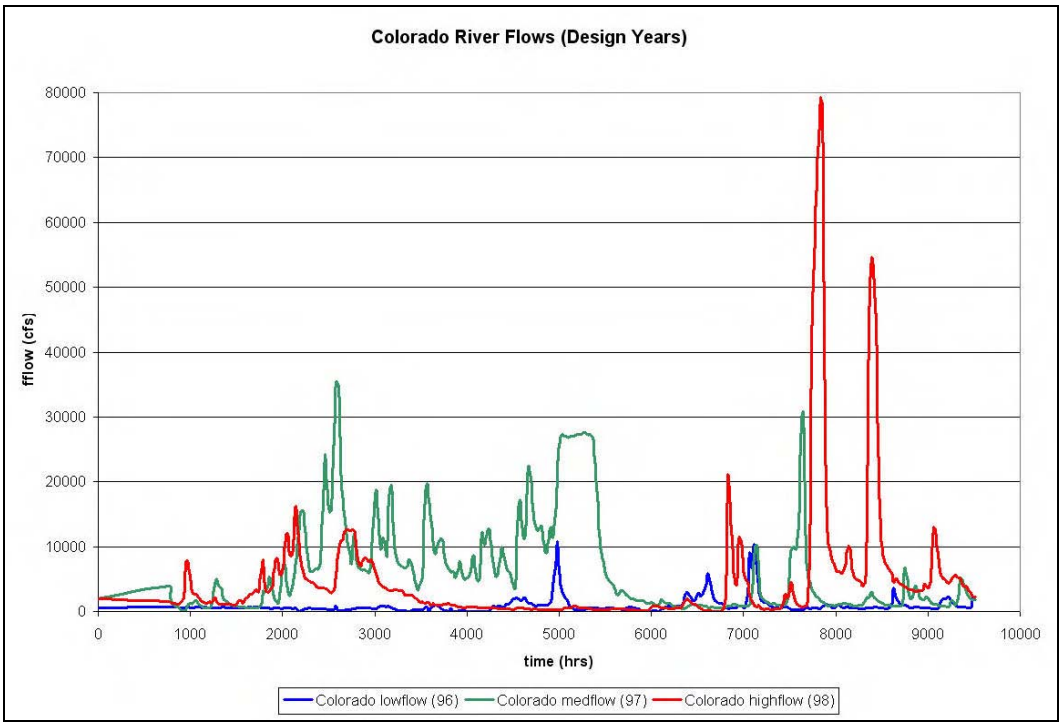

Figure C10. Design year flows for Colorado River

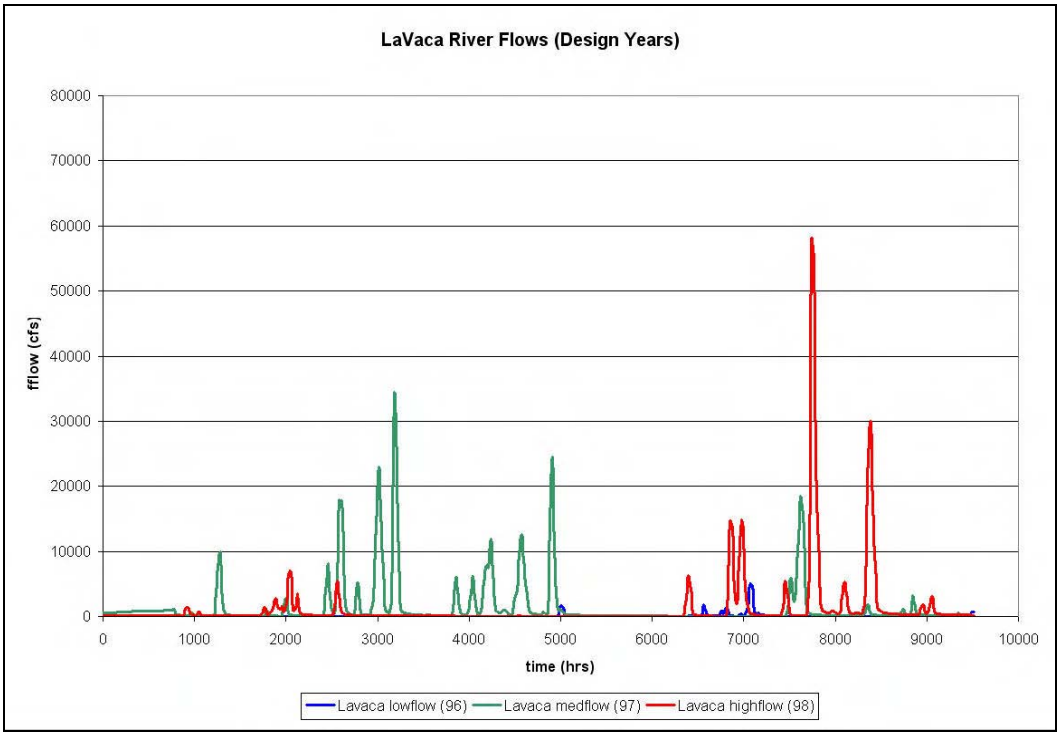

Figure C11. Design year flows for LaVaca River

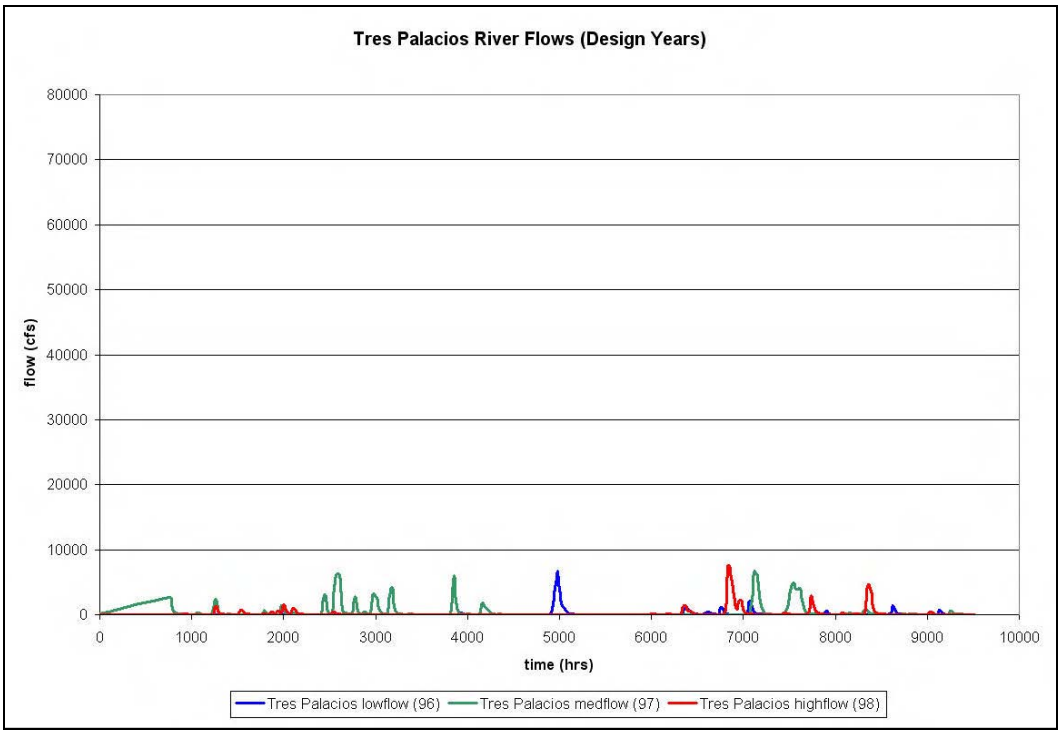

Figure C12. Design year flows for Tres Palacios River

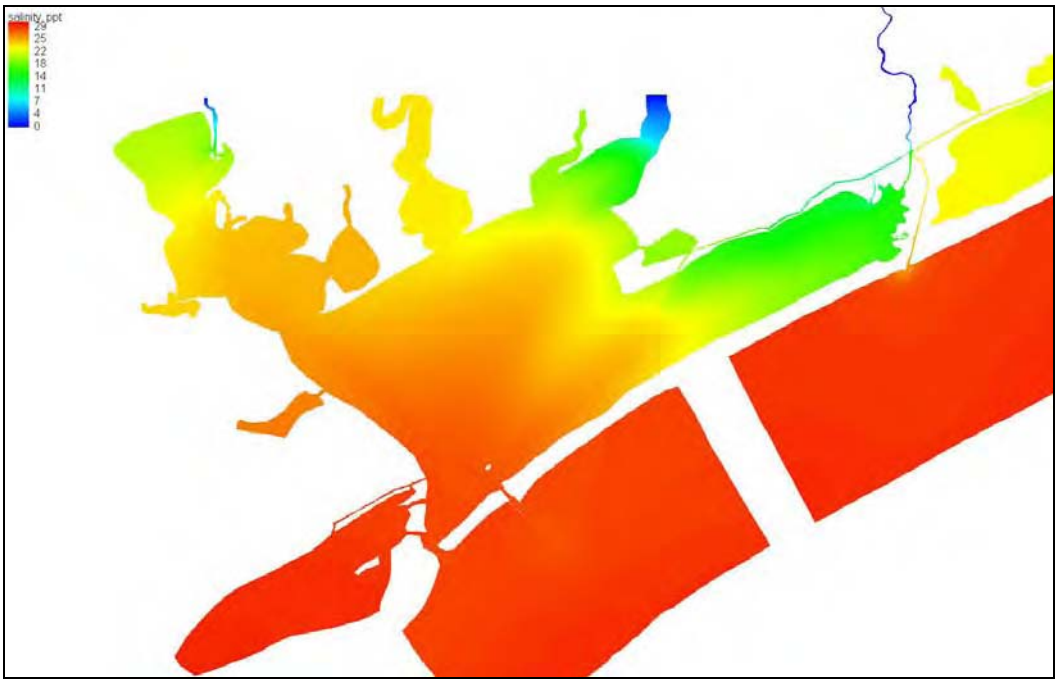

Figure C13. Annual average salinity for existing configuration, low flow scenario

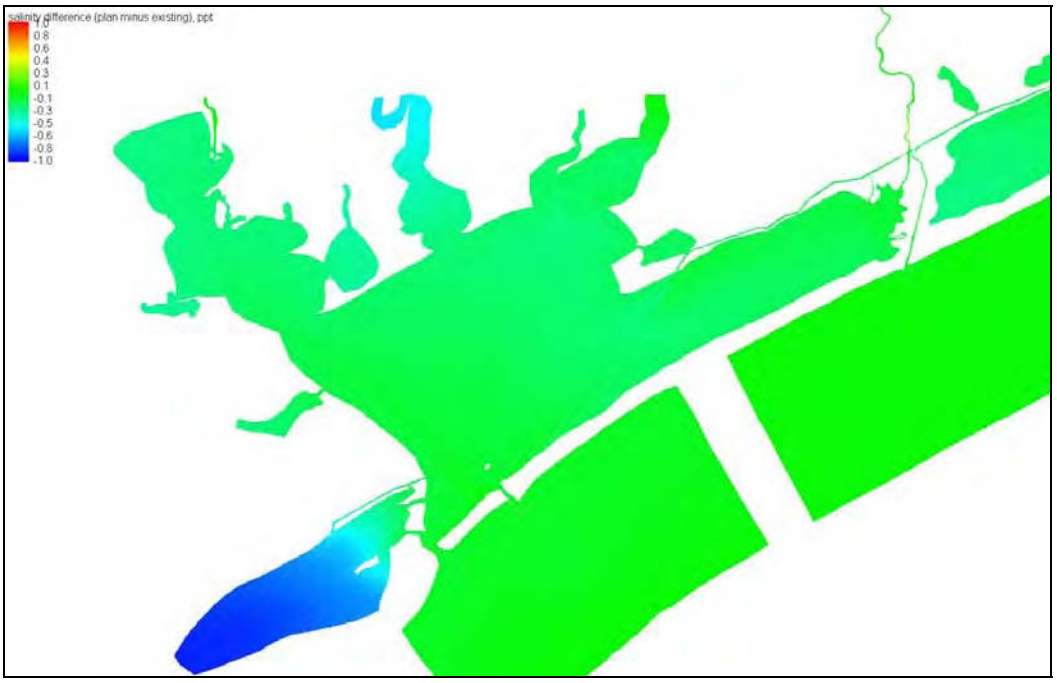

Figure C14. Annual average salinity difference for Alt 1, low flow scenario

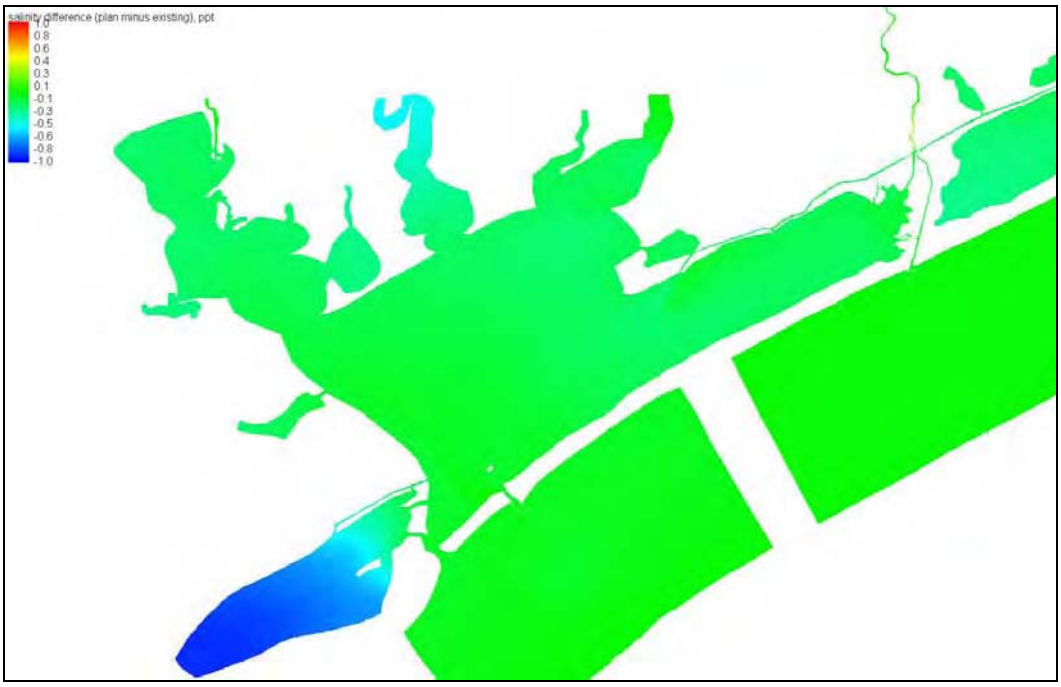

Figure C15. Annual average salinity difference for Alt 2, low flow scenario

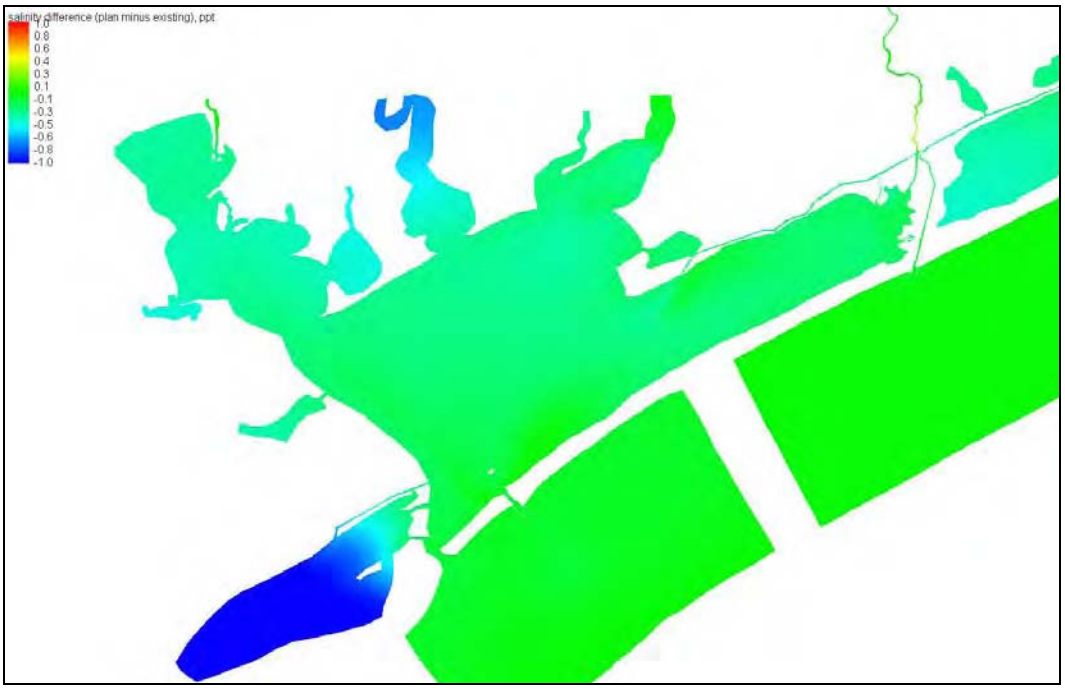

Figure C16. Annual average salinity difference for Alt 3, low flow scenario

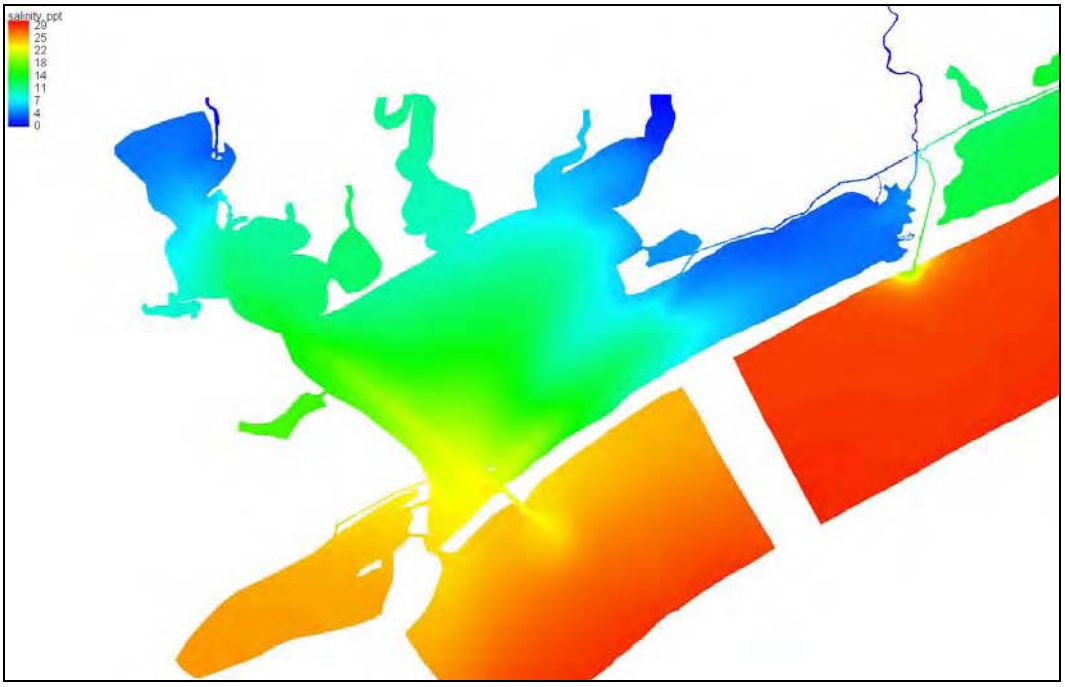

Figure C17. Annual average salinity for existing configuration, medium flow scenario

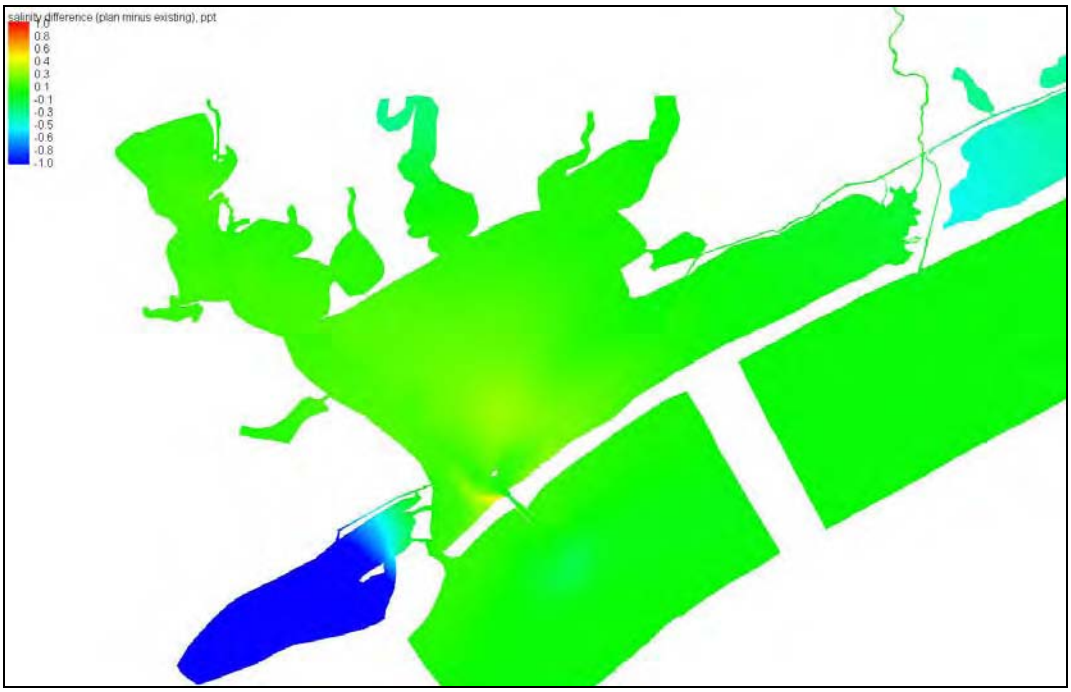

Figure C18. Annual average salinity difference for Alt 1, medium flow scenario

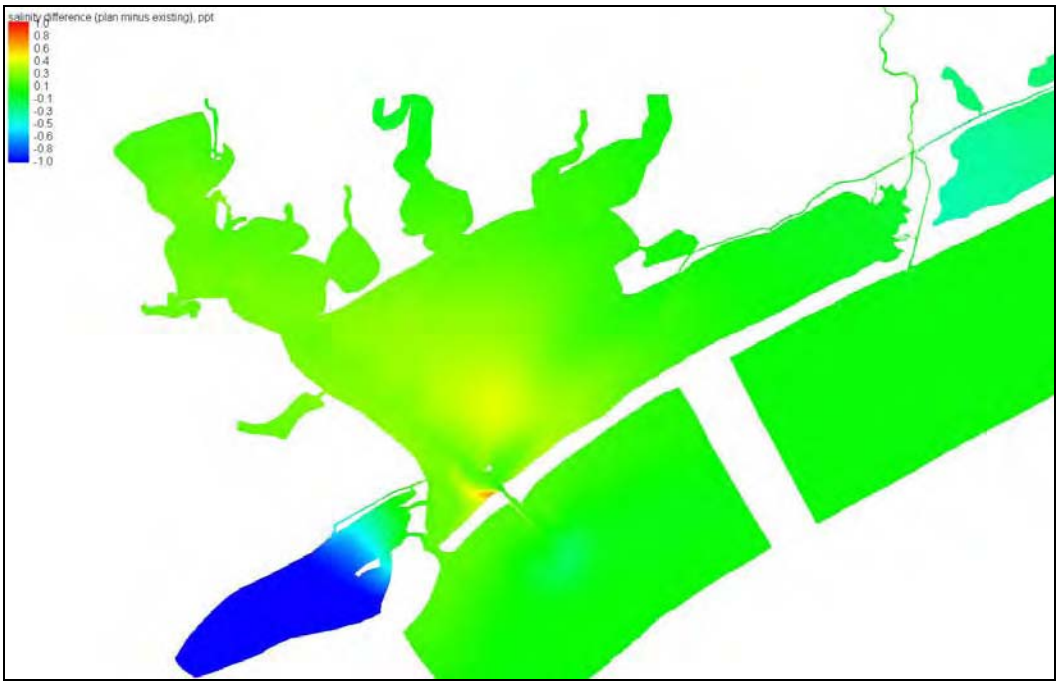

Figure C19. Annual average salinity difference for Alt 2, medium flow scenario

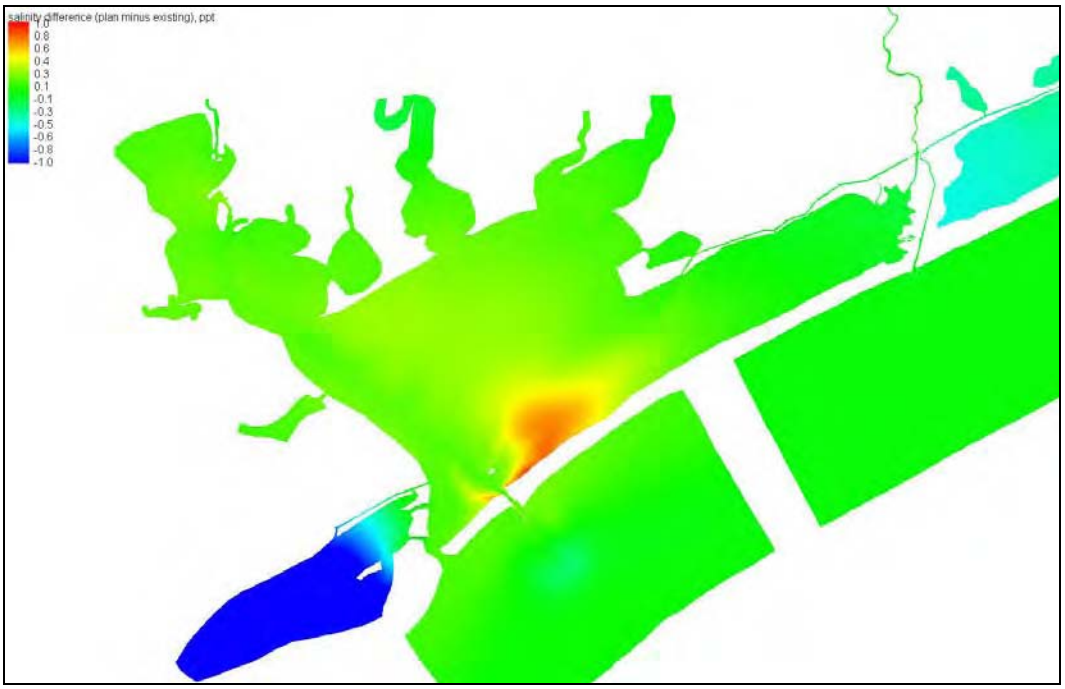

Figure C20. Annual average salinity difference for Alt 3, medium flow scenario

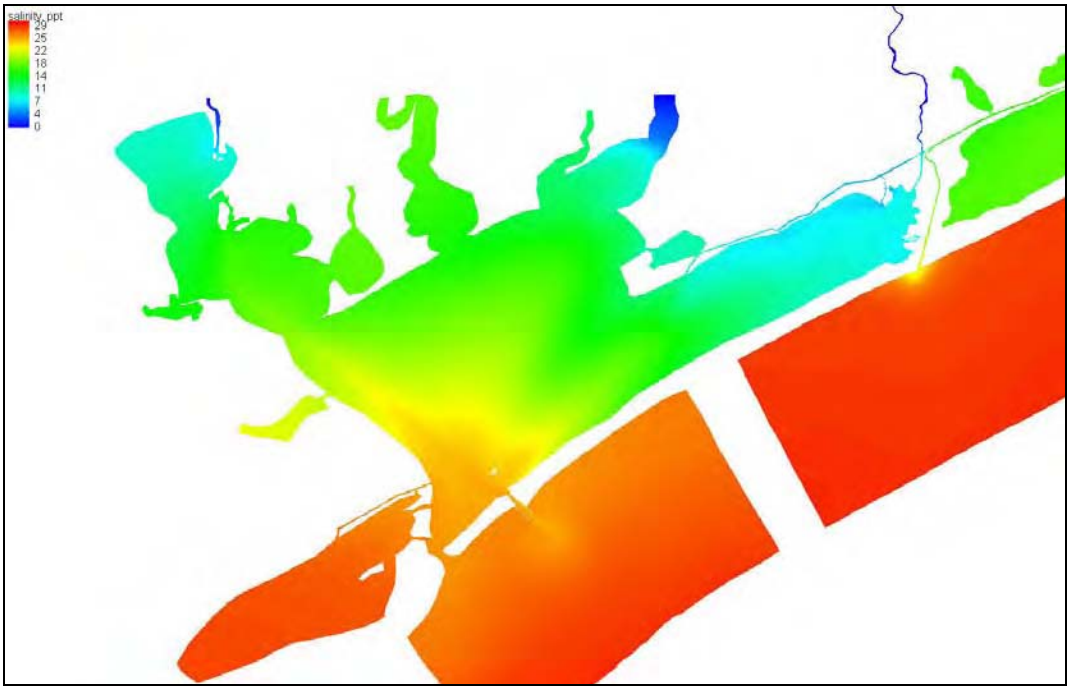

Figure C21. Annual average salinity for existing configuration, high flow scenario

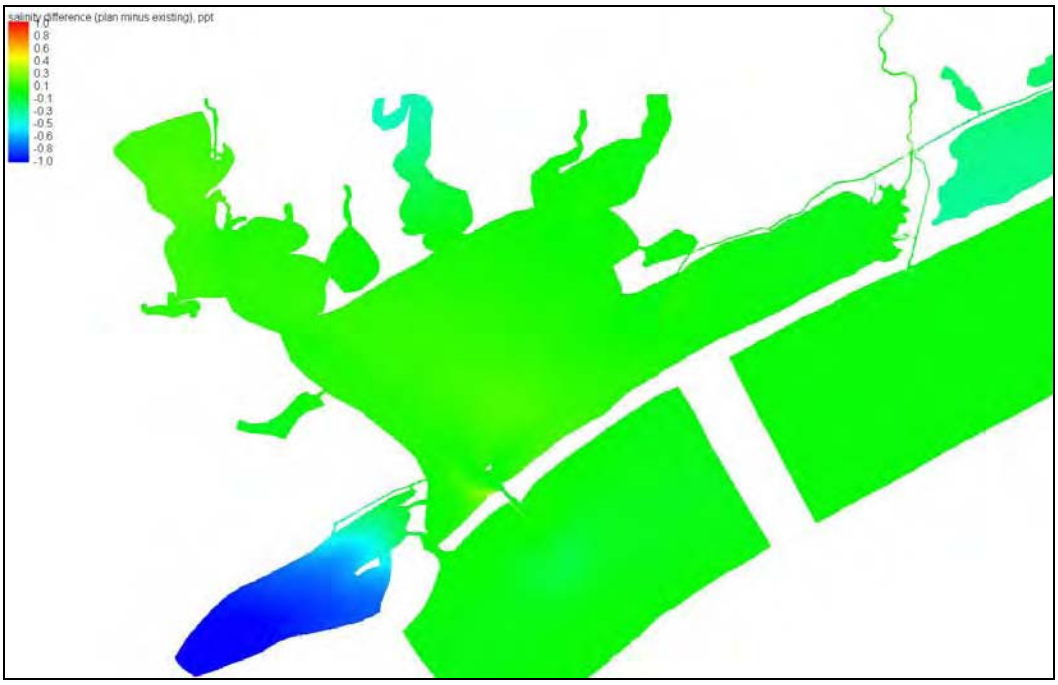

Figure C22. Annual average salinity difference for Alt 1, high flow scenario

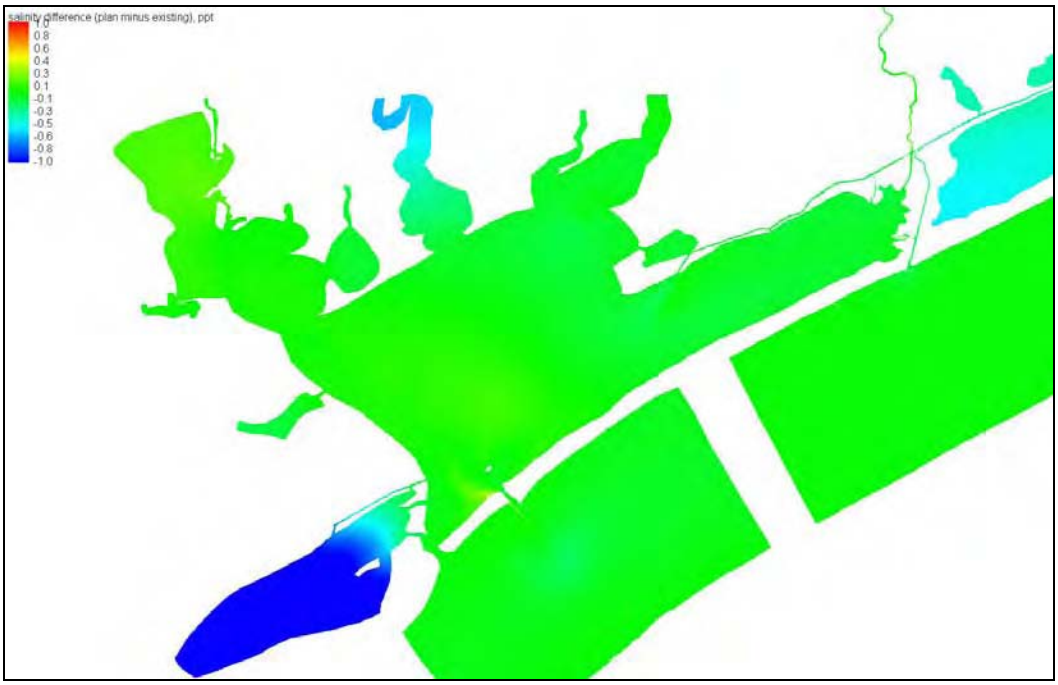

Figure 23: Annual average salinity difference for Alt 2, high flow scenario

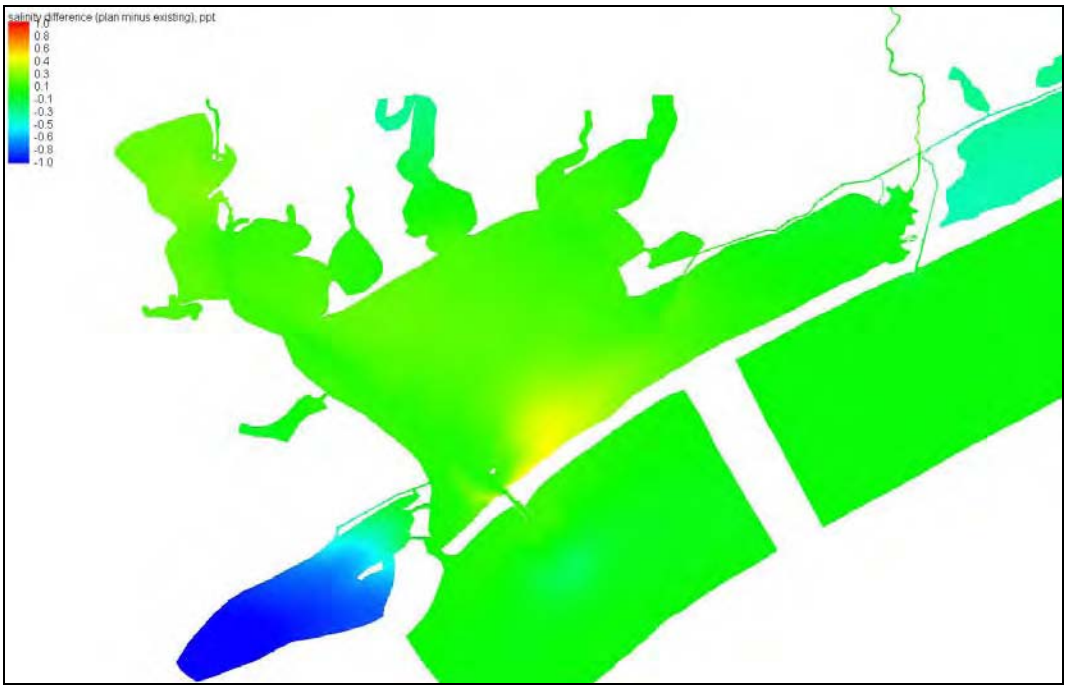

Figure C24. Annual average salinity difference for Alt 3, high flow scenario

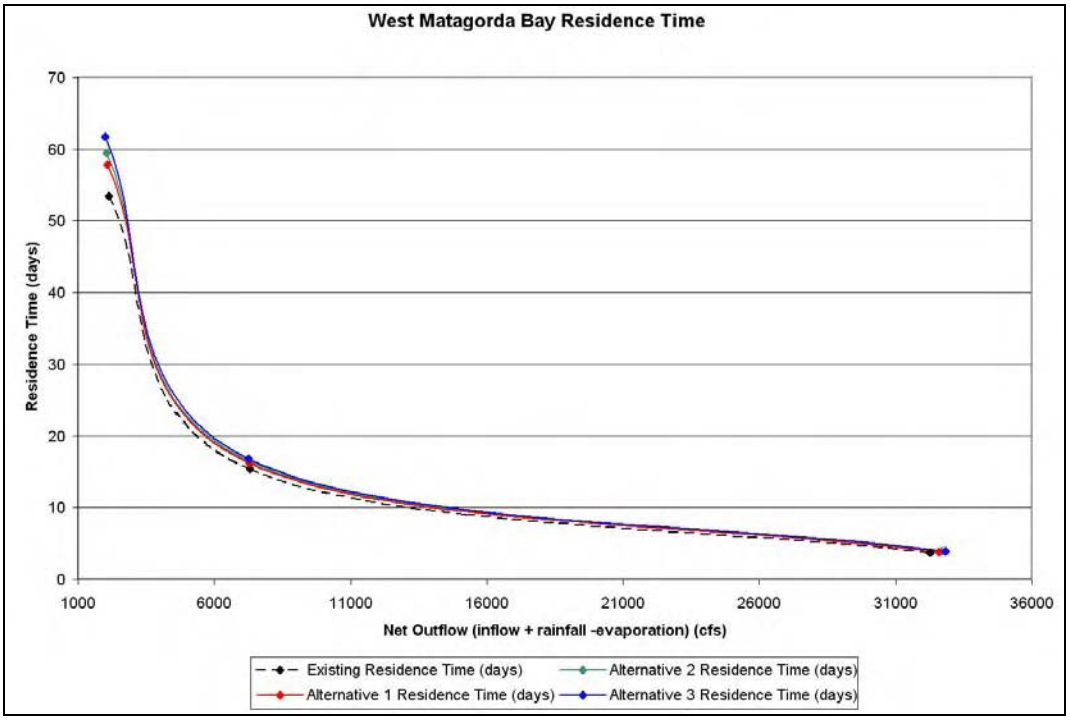

Figure C25. Residence time found by average flux method

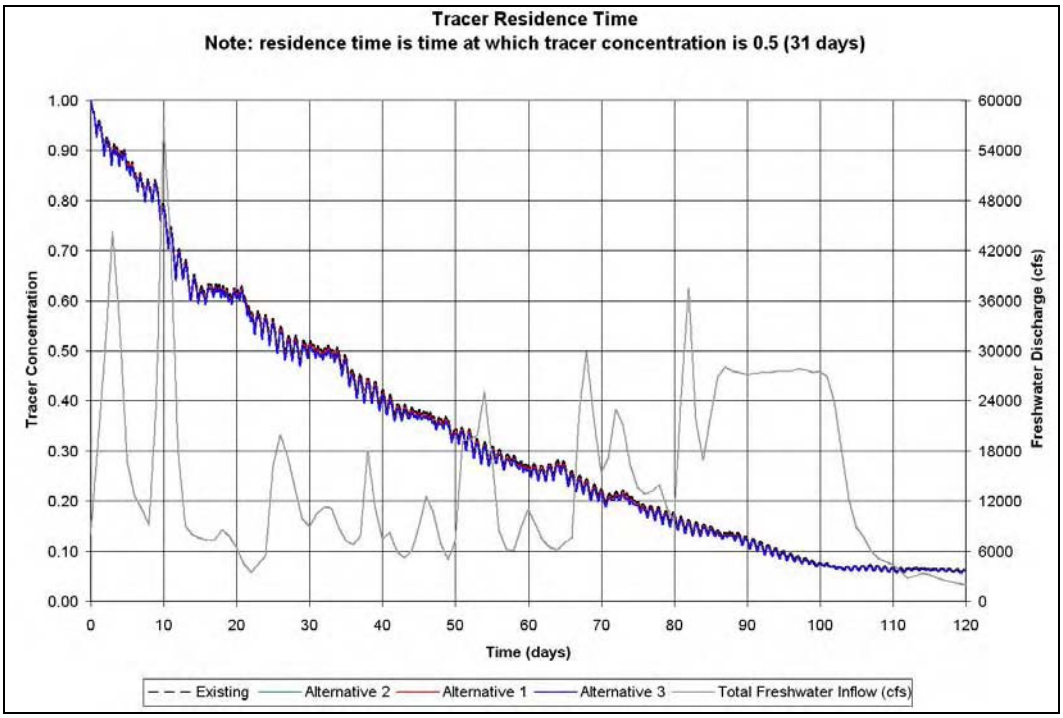

Figure C26. Residence time found by tracer method

REPORT DOCUMENTATION PAGE

Form Approved
OMB No. 0704-0188

1. REPORT DATE *(DD-MM-YYYY)*	2. REPORT TYPE	3. DATES COVERED *(From - To)*
August 2006		

4. TITLE AND SUBTITLE
Matagorda Ship Channel, Texas: Jetty Stability Study

5a. CONTRACT NUMBER

5b. GRANT NUMBER

5c. PROGRAM ELEMENT NUMBER

6. AUTHOR(S)
Nicholas C. Kraus, Lihwa Lin, Brian K. Batten, and Gary L. Brown

5d. PROJECT NUMBER

5e. TASK NUMBER

5f. WORK UNIT NUMBER

7. PERFORMING ORGANIZATION NAME(S) AND ADDRESS(ES)

Coastal and Hydraulics Laboratory
U.S. Army Engineer Research and Development Center
3909 Halls Ferry Road
Vicksburg, MS 39180-6199

8. PERFORMING ORGANIZATION REPORT NUMBER

ERDC/CHL TR-06-7

9. SPONSORING / MONITORING AGENCY NAME(S) AND ADDRESS(ES)
U.S. Army Engineer District, Galveston, 2000 Fort Pint Road, Galveston, TX 77550;
U.S. Army Corps of Engineers, Washington, DC 20314-1000

10. SPONSOR/MONITOR'S ACRONYM(S)

11. SPONSOR/MONITOR'S REPORT NUMBER(S)

12. DISTRIBUTION / AVAILABILITY STATEMENT
Approved for public release; distribution is unlimited.

13. SUPPLEMENTARY NOTES

14. ABSTRACT

The entrance of the Matagorda Ship Channel, connecting the Gulf of Mexico to Matagorda Bay, Texas, has experienced a strong currents since its construction in 1963-1964. Strong currents had been predicted in physical model experiments performed during design to determine the optimal location of the new inlet cut through Matagorda Peninsula and entrance configurations. The current has produced a large area of scour on the bay side of the inlet adjacent to the west jetty, and vessels encountering a strong along-channel and cross-channel current at the entrance experience difficulty in navigation. This study was performed to understand the hydrodynamics of the existing condition and evaluate alternatives for stabilizing the jetties to reduce the current velocity, thereby reducing the scour and improving navigation reliability. The interaction between the entrance and Pass Cavallo, the natural inlet to Matagorda Bay located southwest of the Matagorda Ship Channel entrance, was also examined in a regional approach. The study proceeded by review of the engineering and scientific literature, analysis of regional and local trends in the shoreline change at the entrance and at Pass Cavallo, field measurements of the water level and current, bathymetry surveys, and hydrodynamic numerical modeling of tidal circulation, including wind forcing and river discharges to the bay. Alternative configurations of the jetties were investigated with the hydrodynamic model. A frequency-of-occurrence methodology based on the current velocity magnitude was introduced to evaluate the alternatives. Possible changes in salinity were also investigated.

15. SUBJECT TERMS

Jetties	Navigation Channel	Pass Cavallo
Matagorda Bay	Numerical Model	Scour

16. SECURITY CLASSIFICATION OF:			17. LIMITATION OF ABSTRACT	18. NUMBER OF PAGES	19a. NAME OF RESPONSIBLE PERSON
a. REPORT	b. ABSTRACT	c. THIS PAGE			19b. TELEPHONE NUMBER *(include area code)*
UNCLASSIFIED	UNCLASSIFIED	UNCLASSIFIED		153	